



ISSN 2686-7575 (Online)

ТОНКИЕ ХИМИЧЕСКИЕ ТЕХНОЛОГИИ

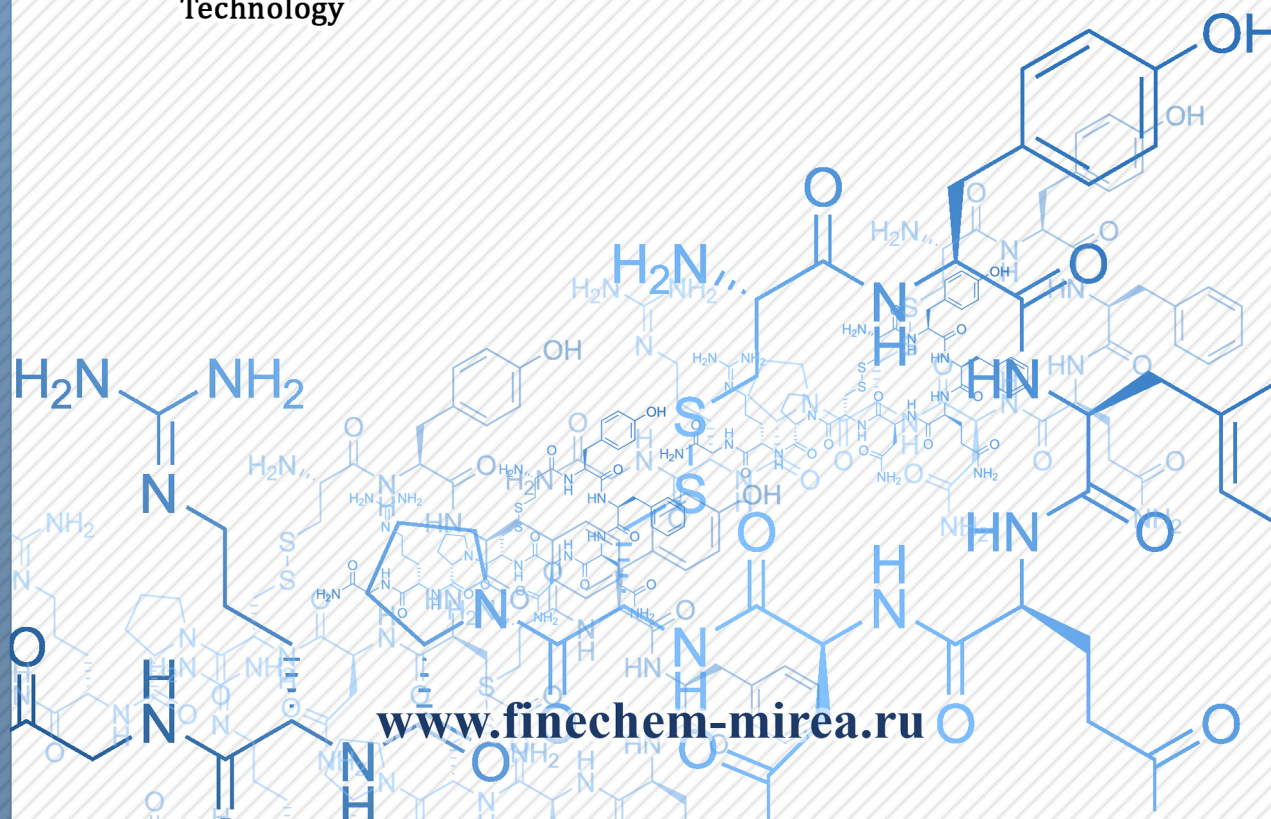
Fine Chemical Technologies

- | Theoretical Bases of Chemical Technology
- | Chemistry and Technology of Organic Substances
- | Chemistry and Technology of Medicinal Compounds and Biologically Active Substances
- | Biochemistry and Biotechnology
- | Synthesis and Processing of Polymers and Polymeric Composites
- | Chemistry and Technology of Inorganic Materials
- | Analytical Methods in Chemistry and Chemical Technology
- | Mathematical Methods and Information Systems in Chemical Technology

19(3)

2024

www.finechem-mirea.ru





ТОНКИЕ ХИМИЧЕСКИЕ ТЕХНОЛОГИИ

Fine Chemical Technologies

- | Theoretical Bases of Chemical Technology
- | Chemistry and Technology of Organic Substances
- | Chemistry and Technology of Medicinal Compounds and Biologically Active Substances
- | Biochemistry and Biotechnology
- | Synthesis and Processing of Polymers and Polymeric Composites
- | Chemistry and Technology of Inorganic Materials
- | Analytical Methods in Chemistry and Chemical Technology
- | Mathematical Methods and Information Systems in Chemical Technology

Tonkie Khimicheskie Tekhnologii =
Fine Chemical Technologies.
Vol. 19, No. 3, 2024

Тонкие химические технологии =
Fine Chemical Technologies.
Том 19, № 3, 2024

<https://doi.org/10.32362/2410-6593-2024-19-3>

www.finechem-mirea.ru

**Tonkie Khimicheskie Tekhnologii =
Fine Chemical Technologies
2024, Vol. 19, No. 3**

The peer-reviewed scientific and technical journal Fine Chemical Technologies highlights the modern achievements of fundamental and applied research in the field of fine chemical technologies, including theoretical bases of chemical technology, chemistry and technology of medicinal compounds and biologically active substances, organic substances and inorganic materials, biochemistry and biotechnology, synthesis and processing of polymers and polymeric composites, analytical and mathematical methods and information systems in chemistry and chemical technology.

Founder and Publisher

Federal State Budget
Educational Institution of Higher Education
“MIREA – Russian Technological University”
78, Vernadskogo pr., Moscow, 119454, Russian Federation.
Publication frequency: bimonthly.
The journal was founded in 2006. The name was Vestnik MITHT until 2015 (ISSN 1819-1487).

The journal is included into the List of peer-reviewed science press of the State Commission for Academic Degrees and Titles of the Russian Federation.

The journal is indexed: SCOPUS, DOAJ, Chemical Abstracts, Science Index, RSCI, Ulrich’s International Periodicals Directory

Editor-in-Chief:

Andrey V. Timoshenko – Dr. Sci. (Eng.), Cand. Sci. (Chem.), Professor, MIREA – Russian Technological University, Moscow, Russian Federation. Scopus Author ID 56576076700, ResearcherID Y-8709-2018, <https://orcid.org/0000-0002-6511-7440>, timoshenko@mirea.ru

Deputy Editor-in-Chief:

Valery V. Fomichev – Dr. Sci. (Chem.), Professor, MIREA – Russian Technological University, Moscow, Russian Federation. Scopus Author ID 57196028937, <http://orcid.org/0000-0003-4840-0655>, fomichev@mirea.ru

Executive Editor:

Sergey A. Durakov – Cand. Sci. (Chem.), Associate Professor, MIREA – Russian Technological University, Moscow, Russian Federation, Scopus Author ID 57194217518, ResearcherID AAS-6578-2020, <http://orcid.org/0000-0003-4842-3283>, durakov@mirea.ru

Editorial staff:

Managing Editor	Cand. Sci. (Eng.) Galina D. Seredina
Editor	Sofya M. Mazina
Science editors	Dr. Sci. (Chem.), Prof. Tatyana M. Buslaeva Dr. Sci. (Chem.), Prof. Anatolii A. Ischenko Dr. Sci. (Eng.), Prof. Anatolii V. Markov Dr. Sci. (Chem.), Prof. Vladimir A. Tverskoy
Desktop publishing	Sergey V. Trofimov

86, Vernadskogo pr., Moscow, 119571, Russian Federation.
Phone: +7 (499) 600-80-80 (#31288)
E-mail: seredina@mirea.ru

The registration number ПИ № ФС 77-74580 was issued in December 14, 2018 by the Federal Service for Supervision of Communications, Information Technology, and Mass Media of Russia

The subscription index of *Pressa Rossii*: **36924**

**Тонкие химические технологии =
Fine Chemical Technologies
2024, том 19, № 3**

Научно-технический рецензируемый журнал «Тонкие химические технологии» освещает современные достижения фундаментальных и прикладных исследований в области тонких химических технологий, включая теоретические основы химической технологии, химию и технологию лекарственных препаратов и биологически активных соединений, органических веществ и неорганических материалов, биохимию и биотехнологию, синтез и переработку полимеров и композитов на их основе, аналитические и математические методы и информационные системы в химии и химической технологии.

Учредитель и издатель

федеральное государственное бюджетное образовательное учреждение высшего образования «МИРЭА – Российский технологический университет» 119454, РФ, Москва, пр-т Вернадского, д. 78.
Периодичность: один раз в два месяца.
Журнал основан в 2006 году. До 2015 года издавался под названием «Вестник МИТХТ» (ISSN 1819-1487).

Журнал входит в Перечень ведущих рецензируемых научных журналов ВАК РФ.

Индексируется: SCOPUS, DOAJ, Chemical Abstracts, РИНЦ (Science Index), RSCI, Ulrich’s International Periodicals Directory

Главный редактор:

Тимошенко Андрей Всеволодович – д.т.н., к.х.н., профессор, МИРЭА – Российский технологический университет, Москва, Российская Федерация. Scopus Author ID 56576076700, ResearcherID Y-8709-2018, <https://orcid.org/0000-0002-6511-7440>, timoshenko@mirea.ru

Заместитель главного редактора:

Фомичёв Валерий Вячеславович – д.х.н., профессор, МИРЭА – Российский технологический университет, Москва, Российская Федерация. Scopus Author ID 57196028937, <http://orcid.org/0000-0003-4840-0655>, fomichev@mirea.ru

Выпускающий редактор:

Дураков Сергей Алексеевич – к.х.н., доцент, МИРЭА – Российский технологический университет, Москва, Российская Федерация, Scopus Author ID 57194217518, ResearcherID AAS-6578-2020, <http://orcid.org/0000-0003-4842-3283>, durakov@mirea.ru

Редакция:

Зав. редакцией	к.т.н. Г.Д. Середина
Редактор	С.М. Мазина
Научные редакторы	д.х.н., проф. Т.М. Буслаева д.х.н., проф. А.А. Ищенко д.т.н., проф. А.В. Марков д.х.н., проф. В.А. Тверской
Компьютерная верстка	С.В. Трофимов

119571, Москва, пр. Вернадского, 86, оф. Л-119.
Тел.: +7 (499) 600-80-80 (#31288)
E-mail: seredina@mirea.ru

Регистрационный номер и дата принятия решения о регистрации СМИ: ПИ № ФС 77-74580 от 14.12.2018 г. СМИ зарегистрировано Федеральной службой по надзору в сфере связи, информационных технологий и массовых коммуникаций (Роскомнадзор)

Индекс по Объединенному каталогу «Пресса России»: **36924**

EDITORIAL BOARD

Andrey V. Blokhin – Dr. Sci. (Chem.), Professor, Belarusian State University, Minsk, Belarus. Scopus Author ID 7101971167, ResearcherID AAF-8122-2019, <https://orcid.org/0000-0003-4778-5872>, blokhin@bsu.by.

Sergey P. Verevkin – Dr. Sci. (Eng.), Professor, University of Rostock, Rostock, Germany. Scopus Author ID 7006607848, ResearcherID G-3243-2011, <https://orcid.org/0000-0002-0957-5594>, Sergey.verevkin@uni-rostock.de.

Konstantin Yu. Zhizhin – Corresponding Member of the Russian Academy of Sciences (RAS), Dr. Sci. (Chem.), Professor, N.S. Kurnakov Institute of General and Inorganic Chemistry of the RAS, Moscow, Russian Federation. Scopus Author ID 6701495620, ResearcherID C-5681-2013, <http://orcid.org/0000-0002-4475-124X>, kyuzhizhin@igic.ras.ru.

Igor V. Ivanov – Dr. Sci. (Chem.), Professor, MIREA – Russian Technological University, Moscow, Russian Federation. Scopus Author ID 34770109800, ResearcherID I-5606-2016, <http://orcid.org/0000-0003-0543-2067>, ivanov_i@mirea.ru.

Carlos A. Cardona – PhD (Eng.), Professor, National University of Columbia, Manizales, Colombia. Scopus Author ID 7004278560, <http://orcid.org/0000-0002-0237-2313>, ccardonaal@unal.edu.co.

Elvira T. Krut'ko – Dr. Sci. (Eng.), Professor, Belarusian State Technological University, Minsk, Belarus. Scopus Author ID 6602297257, ela_krutko@mail.ru.

Anatolii I. Miroshnikov – Academician at the RAS, Dr. Sci. (Chem.), Professor, M.M. Shemyakin and Yu.A. Ovchinnikov Institute of Bioorganic Chemistry of the RAS, Member of the Presidium of the RAS, Chairman of the Presidium of the RAS Pushchino Research Center, Moscow, Russian Federation. Scopus Author ID 7006592304, ResearcherID G-5017-2017, aiv@ibch.ru.

Aziz M. Muzafarov – Academician at the RAS, Dr. Sci. (Chem.), Professor, A.N. Nesmeyanov Institute of Organoelement Compounds of the RAS, Moscow, Russian Federation. Scopus Author ID 7004472780, ResearcherID G-1644-2011, <https://orcid.org/0000-0002-3050-3253>, aziz@ineos.ac.ru.

РЕДАКЦИОННАЯ КОЛЛЕГИЯ

Блохин Андрей Викторович – д.х.н., профессор Белорусского государственного университета, Минск, Беларусь. Scopus Author ID 7101971167, ResearcherID AAF-8122-2019, <https://orcid.org/0000-0003-4778-5872>, blokhin@bsu.by.

Верёвкин Сергей Петрович – д.т.н., профессор Университета г. Росток, Росток, Германия. Scopus Author ID 7006607848, ResearcherID G-3243-2011, <https://orcid.org/0000-0002-0957-5594>, Sergey.verevkin@uni-rostock.de.

Жижин Константин Юрьевич – член-корр. Российской академии наук (РАН), д.х.н., профессор, Институт общей и неорганической химии им. Н.С. Курнакова РАН, Москва, Российская Федерация. Scopus Author ID 6701495620, ResearcherID C-5681-2013, <http://orcid.org/0000-0002-4475-124X>, kyuzhizhin@igic.ras.ru.

Иванов Игорь Владимирович – д.х.н., профессор, МИРЭА – Российский технологический университет, Москва, Российская Федерация. Scopus Author ID 34770109800, ResearcherID I-5606-2016, <http://orcid.org/0000-0003-0543-2067>, ivanov_i@mirea.ru.

Кардона Карлос Ариэль – PhD, профессор Национального университета Колумбии, Манизалес, Колумбия. Scopus Author ID 7004278560, <http://orcid.org/0000-0002-0237-2313>, ccardonaal@unal.edu.co.

Крутько Эльвира Тихоновна – д.т.н., профессор Белорусского государственного технологического университета, Минск, Беларусь. Scopus Author ID 6602297257, ela_krutko@mail.ru.

Мирошников Анатолий Иванович – академик РАН, д.х.н., профессор, Институт биоорганической химии им. академиков М.М. Шемякина и Ю.А. Овчинникова РАН, член Президиума РАН, председатель Президиума Пушкинского научного центра РАН, Москва, Российская Федерация. Scopus Author ID 7006592304, ResearcherID G-5017-2017, aiv@ibch.ru.

Музафаров Азиз Мансурович – академик РАН, д.х.н., профессор, Институт элементоорганических соединений им. А.Н. Несмеянова РАН, Москва, Российская Федерация. Scopus Author ID 7004472780, ResearcherID G-1644-2011, <https://orcid.org/0000-0002-3050-3253>, aziz@ineos.ac.ru.

Ivan A. Novakov – Academician at the RAS, Dr. Sci. (Chem.), Professor, President of the Volgograd State Technical University, Volgograd, Russian Federation.
Scopus Author ID 7003436556, ResearcherID I-4668-2015, <http://orcid.org/0000-0002-0980-6591>, president@vstu.ru.

Alexander N. Ozerin – Corresponding Member of the RAS, Dr. Sci. (Chem.), Professor, Enikolopov Institute of Synthetic Polymeric Materials of the RAS, Moscow, Russian Federation.
Scopus Author ID 7006188944, ResearcherID J-1866-2018, <https://orcid.org/0000-0001-7505-6090>, ozerin@ispm.ru.

Tapani A. Pakkanen – PhD, Professor, Department of Chemistry, University of Eastern Finland, Joensuu, Finland.
Scopus Author ID 7102310323, tapani.pakkanen@uef.fi.

Armando J.L. Pombeiro – Academician at the Academy of Sciences of Lisbon, PhD, Professor, President of the Center for Structural Chemistry of the Higher Technical Institute of the University of Lisbon, Lisbon, Portugal.
Scopus Author ID 7006067269, ResearcherID I-5945-2012, <https://orcid.org/0000-0001-8323-888X>, pombeiro@ist.utl.pt.

Dmitrii V. Pyshnyi – Corresponding Member of the RAS, Dr. Sci. (Chem.), Professor, Institute of Chemical Biology and Fundamental Medicine, Siberian Branch of the RAS, Novosibirsk, Russian Federation.
Scopus Author ID 7006677629, ResearcherID F-4729-2013, <https://orcid.org/0000-0002-2587-3719>, pyshnyi@niboch.nsc.ru.

Alexander S. Sigov – Academician at the RAS, Dr. Sci. (Phys. and Math.), Professor, President of MIREA – Russian Technological University, Moscow, Russian Federation.
Scopus Author ID 35557510600, ResearcherID L-4103-2017, sigov@mirea.ru.

Alexander M. Toikka – Dr. Sci. (Chem.), Professor, Institute of Chemistry, Saint Petersburg State University, St. Petersburg, Russian Federation.
Scopus Author ID 6603464176, ResearcherID A-5698-2010, <http://orcid.org/0000-0002-1863-5528>, a.toikka@spbu.ru.

Andrzej W. Trochimczuk – Dr. Sci. (Chem.), Professor, Faculty of Chemistry, Wrocław University of Science and Technology, Wrocław, Poland.
Scopus Author ID 7003604847, andrzej.trochimczuk@pwr.edu.pl.

Aslan Yu. Tsvadze – Academician at the RAS, Dr. Sci. (Chem.), Professor, A.N. Frumkin Institute of Physical Chemistry and Electrochemistry of the RAS, Moscow, Russian Federation.
Scopus Author ID 7004245066, ResearcherID G-7422-2014, tsiv@phyche.ac.ru.

Новаков Иван Александрович – академик РАН, д.х.н., профессор, президент Волгоградского государственного технического университета, Волгоград, Российская Федерация.
Scopus Author ID 7003436556, ResearcherID I-4668-2015, <http://orcid.org/0000-0002-0980-6591>, president@vstu.ru.

Озерин Александр Никифорович – член-корр. РАН, д.х.н., профессор, Институт синтетических полимерных материалов им. Н.С. Ениколопова РАН, Москва, Российская Федерация.
Scopus Author ID 7006188944, ResearcherID J-1866-2018, <https://orcid.org/0000-0001-7505-6090>, ozerin@ispm.ru.

Пакканен Тапани – PhD, профессор, Департамент химии, Университет Восточной Финляндии, Йоенсуу, Финляндия.
Scopus Author ID 7102310323, tapani.pakkanen@uef.fi.

Помбейро Армандо – академик Академии наук Лиссабона, PhD, профессор, президент Центра структурной химии Высшего технического института Университета Лиссабона, Португалия.
Scopus Author ID 7006067269, ResearcherID I-5945-2012, <https://orcid.org/0000-0001-8323-888X>, pombeiro@ist.utl.pt.

Пышный Дмитрий Владимирович – член-корр. РАН, д.х.н., профессор, Институт химической биологии и фундаментальной медицины Сибирского отделения РАН, Новосибирск, Российская Федерация.
Scopus Author ID 7006677629, ResearcherID F-4729-2013, <https://orcid.org/0000-0002-2587-3719>, pyshnyi@niboch.nsc.ru.

Сигов Александр Сергеевич – академик РАН, д.ф.-м.н., профессор, президент МИРЭА – Российского технологического университета, Москва, Российская Федерация.
Scopus Author ID 35557510600, ResearcherID L-4103-2017, sigov@mirea.ru.

Тойкка Александр Матвеевич – д.х.н., профессор, Институт химии, Санкт-Петербургский государственный университет, Санкт-Петербург, Российская Федерация.
Scopus Author ID 6603464176, ResearcherID A-5698-2010, <http://orcid.org/0000-0002-1863-5528>, a.toikka@spbu.ru.

Трохимчук Анджей – д.х.н., профессор, Химический факультет Вроцлавского политехнического университета, Вроцлав, Польша.
Scopus Author ID 7003604847, andrzej.trochimczuk@pwr.edu.pl.

Цивадзе Аслан Юсупович – академик РАН, д.х.н., профессор, Институт физической химии и электрохимии им. А.Н. Фрумкина РАН, Москва, Российская Федерация.
Scopus Author ID 7004245066, ResearcherID G-7422-2014, tsiv@phyche.ac.ru.

Contents

ANNIVERSARIES

- 181** | Congratulations to Academician Ivan Aleksandrovich Novakov on his 75th birthday!

THEORETICAL BASES OF CHEMICAL TECHNOLOGY

- 183** | *Victoria A. Gabrin, Tatiana E. Nikiforova, Vladimir A. Kozlov, Pavel B. Razgovorov*
Concentration of heavy metal ions from aqueous media under dynamic conditions using a composite sorbent based on chitosan and silica

CHEMISTRY AND TECHNOLOGY OF ORGANIC SUBSTANCES

- 192** | *Nadezhda T. Sevostyanova, Sergey A. Batashev, Anastasia S. Rodionova, Dar'ya K. Kozlenko*
Effect of 2-hexanol and methanol on the *one-pot* process of dehydration and alkoxyacylation for the synthesis of esters

CHEMISTRY AND TECHNOLOGY OF MEDICINAL COMPOUNDS AND BIOLOGICALLY ACTIVE SUBSTANCES

- 202** | *Tatyana G. Bodrova, Ulyana A. Budanova, Yury L. Sebyakin*
L-Ornithine derivatives with structural hetaryl and alkyl moiety: Synthesis and antibacterial activity

- 214** | *Maria A. Zakharova, Mikhail V. Chudinov*
PROTAC[®] technology and potential for its application in infection control

BIOCHEMISTRY AND BIOTECHNOLOGY

- 232** | *Vitaliy I. Loginov, Marina S. Gubenko, Alexey M. Burdenny, Irina V. Pronina, Pavel V. Postnikov, Yulia A. Efimova, Fedor V. Radus, Elena S. Mochalova, Tatyana P. Kazubskaya*
Methylation of a group of microRNA genes as a marker for the diagnosis and prognosis of non-small cell lung cancers

- 240** | *Dmitry S. Polyansky, Ekaterina I. Ryabova, Artem A. Derkaev, Nikita S. Starkov, Irina S. Kashapova, Dmitry V. Shcheblyakov, Andrey P. Karpov, Ilias B. Esmagambetov*
Development of technology for culturing a cell line producing a single-domain antibody fused with the Fc fragment of human IgG1

CHEMISTRY AND TECHNOLOGY OF INORGANIC MATERIALS

- 258** | *Ekaterina I. Efremova, Mikhail A. Lazov, Mikhail R. Kobrin, Valery V. Fomichev*
Solid solutions in disulfide systems $\text{Re(IV)S}_2\text{-Ti(IV)S}_2$, $\text{Re(IV)S}_2\text{-Mo(IV)S}_2$, and $\text{Re(IV)S}_2\text{-W(IV)S}_2$

СОДЕРЖАНИЕ

ЮБИЛЕИ

- 181** | Поздравляем академика Ивана Александровича Новакова с 75-летним юбилеем!

ТЕОРЕТИЧЕСКИЕ ОСНОВЫ ХИМИЧЕСКОЙ ТЕХНОЛОГИИ

- 183** | *В.А. Габрин, Т.Е. Никифорова, В.А. Козлов, П.Б. Разговоров*
Концентрирование ионов тяжелых металлов из водных сред в динамических условиях композиционным сорбентом на основе хитозана и диоксида кремния

ХИМИЯ И ТЕХНОЛОГИЯ ОРГАНИЧЕСКИХ ВЕЩЕСТВ

- 192** | *Н.Т. Севостьянова, С.А. Баташев, А.С. Родионова, Д.К. Козленко*
Влияние гексанола-2 и метанола на совмещенный процесс дегидратации и алкоксикарбонилирования для синтеза сложных эфиров

ХИМИЯ И ТЕХНОЛОГИЯ ЛЕКАРСТВЕННЫХ ПРЕПАРАТОВ И БИОЛОГИЧЕСКИ АКТИВНЫХ СОЕДИНЕНИЙ

- 202** | *Т.Г. Бодрова, У.А. Буданова, Ю.Л. Себякин*
Производные L-орнитина с гетарильными и алкильными фрагментами в структуре: синтез и антибактериальная активность

- 214** | *М.А. Захарова, М.В. Чудинов*
Технология PROTAC[®] и перспективы ее применения в борьбе с инфекциями

БИОХИМИЯ И БИОТЕХНОЛОГИЯ

- 232** | *В.И. Логинов, М.С. Губенко, А.М. Бурденный, И.В. Пронина, П.В. Постников, Ю.А. Ефимова, Ф.В. Радус, Е.С. Мочалова, Т.П. Казубская*
Метилирование группы генов микроРНК как маркер диагностики и прогноза немелкоклеточного рака легкого

- 240** | *Д.М. Полянский, Е.И. Рябова, А.А. Деркаев, Н.С. Старков, И.С. Кашапова, Д.В. Щепляков, А.П. Карпов, И.Б. Есмагамбетов*
Разработка технологии культивирования клеточной линии, продуцирующей однодоменное антитело, слитое с Fc-фрагментом IgG1 человека

ХИМИЯ И ТЕХНОЛОГИЯ НЕОРГАНИЧЕСКИХ МАТЕРИАЛОВ

- 258** | *Е.И. Ефремова, М.А. Лазов, М.Р. Кобрин, В.В. Фомичев*
Твердые растворы в системах дисульфидов $\text{Re(IV)S}_2\text{-Ti(IV)S}_2$, $\text{Re(IV)S}_2\text{-Mo(IV)S}_2$ и $\text{Re(IV)S}_2\text{-W(IV)S}_2$

Anniversaries

Юбилей

<https://doi.org/10.32362/2410-6593-2024-19-3-181-182>

EDN ZHWTCX



EDITORIAL ARTICLE

Congratulations to Academician Ivan Aleksandrovich Novakov on his 75th birthday!



Ivan Aleksandrovich Novakov, Honored Scientist of the Russian Federation, Academician of the Russian Academy of Sciences, Doctor of Chemical Sciences, and Member of the Editorial Board of our journal *Tonkie Khimicheskie Tekhnologii [Fine Chemical Technologies]*, marks his 75th anniversary on July 2, 2024.

Ivan Aleksandrovich's scientific, pedagogical, and organizational work is inextricably linked with the Volgograd State Technical University (VolgSTU). From 1988–2014, he served as rector of VolgSTU; from 2014 to the present, he has been its president. Since 1991, he has also been Head of the Department of Analytical and Physical Chemistry and Physico-Chemistry of Polymers.

Academician I.A. Novakov is the recipient of many well-deserved awards: Honorary Worker of Higher Professional Education of the Russian Federation (1998), Honored Scientist of the Russian Federation (2004), Honorary Worker of Science and Technology of the Russian Federation (2009). He was also awarded the Order “For Merit to the Fatherland” (III degree).

Academician I.A. Novakov is the author of more than 1500 scientific works, including 7 monographs and 262 patents. He is a member of the editorial boards of more than ten scientific journals, including *Polymer Science*, *Russian Journal of Applied Chemistry*, *Plasticheskie Massy*, *Tonkie Khimicheskie Tekhnologii [Fine Chemical Technologies]*. Academician I.A. Novakov is the Chairman of the Dissertation Council 24.2.282.01 on the basis of VolgSTU. Under his leadership, 56 dissertations for the Degree of Candidate of Sciences and 12 dissertations for the Degree of Doctor of Sciences have been successfully defended.

The wide-ranging fundamental research of Ivan Aleksandrovich Novakov has proven its relevance in many fields. In particular, he is responsible for the development of elastomeric materials from reactive oligomers by free-injection molding, which does not require the use of energy- and metal-intensive equipment in enclosed spaces. The results of his work have been implemented at over 3000 sports facilities. In 2004, I.A. Novakov and his colleagues were awarded the Hero City of Volgograd Prize in the field of science and technology.

Under his leadership, one of the priority areas of modern polymer chemistry related to the creation of heat-, thermo-, and chemically stable polymers based on frame structures has been developed. In 2007, I.A. Novakov and his colleagues were awarded the Lebedev Prize for a series of works in this field. In 2016, the team headed by I.A. Novakov was awarded the Prize of the Government of the Russian Federation in the field of science and technology.

The Editorial Board and the Editor-in-Chief of *Tonkie Khimicheskie Tekhnologii [Fine Chemical Technologies]* cordially congratulate Ivan Aleksandrovich on his 75th birthday, wishing him good health and new creative successes.

Best regards,
Editor-in-Chief

Andrey V. Timoshenko

РЕДАКЦИОННАЯ СТАТЬЯ

Поздравляем академика Ивана Александровича Новакова с 75-летним юбилеем!



2 июля 2024 г. исполняется 75 лет заслуженному деятелю науки Российской Федерации, академику Российской академии наук и члену редколлегии нашего журнала «Тонкие химические технологии = *Fine Chemical Technologies*» доктору химических наук Ивану Александровичу Новакову.

Научная, педагогическая и организационная работа Ивана Александровича неразрывно связана с Волгоградским государственным техническим университетом (ВолГГТУ). В период с 1988 по 2014 гг. И.А. Новаков являлся ректором, а с 2014 г. по настоящее время он — президент ВолГГТУ. С 1991 г. он возглавляет кафедру аналитической, физической химии и физико-химии полимеров.

Академик И.А. Новаков имеет заслуженные награды: почетный работник высшего профессионального образования Российской Федерации (1998 г.), Заслуженный деятель науки Российской Федерации (2004 г.), почетный работник науки и техники Российской Федерации (2009 г.). Награжден орденом «За заслуги перед Отечеством» III степени.

Академик И.А. Новаков является автором более 1500 научных работ, включая 7 монографий и 262 патентов. И.А. Новаков — член редколлегии более десяти научных изданий, среди которых журналы «Высокомолекулярные соединения», «Журнал прикладной химии», «Пластические массы», «Тонкие химические технологии = *Fine Chemical Technologies*» и др.

И.А. Новаков является председателем диссертационного совета 24.2.282.01 на базе ВолГГТУ. Под его руководством успешно защищены 56 диссертаций на соискание ученой степени кандидата наук и 12 диссертаций — на соискание ученой степени доктора наук.

Фундаментальные исследования Ивана Александровича Новакова разноплановы и актуальны. Им разработаны эластомерные материалы из реакционноспособных олигомеров методом свободно-литьевого формования, не требующем применения энергоемкого и металлоемкого оборудования в закрытых помещениях. Результаты работ внедрены более чем на 3000 спортивных объектах. В 2004 г. И.А. Новаков с коллегами удостоен «Премии города-героя Волгограда» в области науки и техники.

Под руководством И.А. Новакова развито одно из приоритетных направлений современной химии полимеров, связанное с созданием тепло-, термо- и химически устойчивых полимеров на основе каркасных структур. В 2007 г. за серию работ в этом направлении И.А. Новаков с коллегами удостоен премии имени С.В. Лебедева. В 2016 г. коллектив, возглавляемый И.А. Новаковым, удостоен премии Правительства Российской Федерации в области науки и техники.

Редакционная коллегия и главный редактор журнала «Тонкие химические технологии = *Fine Chemical Technologies*» сердечно поздравляют Ивана Александровича с 75-летием и желают ему крепкого здоровья и новых творческих успехов.

С наилучшими пожеланиями
Главный редактор

А.В. Тимошенко

Theoretical bases of chemical technology
Теоретические основы химической технологии

UDC 544.723:546.302:547.458.5

<https://doi.org/10.32362/2410-6593-2024-19-3-183-191>

EDN UAXSVB



RESEARCH ARTICLE

Concentration of heavy metal ions from aqueous media under dynamic conditions using a composite sorbent based on chitosan and silica

Victoria A. Gabrin¹✉, Tatiana E. Nikiforova¹, Vladimir A. Kozlov¹, Pavel B. Razgovorov²

¹Ivanovo State University of Chemistry and Technology, Ivanovo, 153000 Russia

²Yaroslavl State Technical University, Yaroslavl, 150023 Russia

✉ Corresponding author; e-mail: gabrinvictoria@gmail.com

Abstract

Objectives. The study set out to investigate the sorption, toxicological, and regeneration properties of a composite sorbent based on chitosan hydrogel and unsuspended silicon dioxide (chitosan–colloidal silica), which manifest themselves under dynamic conditions of purification of aqueous solutions, as a means of removing heavy metal ions.

Methods. The total dynamic exchange capacity of a chitosan–colloidal silica composite sorbent was evaluated under dynamic sorption conditions by passing solutions containing Zn(II), Cd(II), Cu(II), and Cr(III) ions having a concentration of 240–251 mg/L through a fixed sorption bed. The method for determining acute toxicity using daphnia (*Daphnia magna* Straus) is based on the direct calculation of the mortality of daphnia exposed to toxic substances contained in the test aqueous extract in comparison with a reference culture in samples that do not contain toxic substances. The regeneration ability of the sorbent was assessed by counting the number of sorption–desorption cycles using 0.1 M NaOH and 0.1 M NaHCO₃ eluents, as well as aqueous solutions of H₂O₂ (1 and 3%).

Results. The effectiveness of the chitosan–colloidal silica composite sorbent in the process of dynamic purification of aqueous media to remove Cu(II), Zn(II), Cd(II), and Cr(III) ions was established. After determining the times of ion breakthrough and saturation of the developed sorbent, its dynamic exchange capacity was calculated by processing the kinetic curves of sorption of heavy metal ions under dynamic conditions. The results of regeneration of the sorbent were presented in the context of the possibility of its reuse. It is shown that the sorbent can withstand up to five sorption–desorption cycles while maintaining a level copper cation extraction above 90%.

Conclusions. Analysis of the kinetic curves demonstrated that the driving force behind the removal of heavy metals from aqueous media by means of the obtained sorbent is the external diffusion mass transfer of ions from the mobile phase of the solution. Biotesting of samples showed that the developed chitosan-based sorbent does not have acute toxicity.

Keywords

heavy metals, adsorption, composites, chitosan, biotesting, regeneration

Submitted: 11.07.2023

Revised: 13.10.2023

Accepted: 14.03.2024

For citation

Gabrin V.A., Nikiforova T.E., Kozlov V.A., Razgovorov P.B. Concentration of heavy metal ions from aqueous media under dynamic conditions using a composite sorbent based on chitosan and silica. *Tonk. Khim. Tekhnol. = Fine Chem. Technol.* 2024;19(3):183–191. <https://doi.org/10.32362/2410-6593-2024-19-3-183-191>

НАУЧНАЯ СТАТЬЯ

Концентрирование ионов тяжелых металлов из водных сред в динамических условиях композиционным сорбентом на основе хитозана и диоксида кремния

В.А. Габрин¹✉, Т.Е. Никифорова¹, В.А. Козлов¹, П.Б. Разговоров²

¹ Ивановский государственный химико-технологический университет, Иваново, 153000 Россия

² Ярославский государственный технический университет, Ярославль, 155023 Россия

✉ Автор для переписки, e-mail: gabrinvictoria@gmail.com

Аннотация

Цели. Изучение сорбционных, токсикологических и регенерационных свойств композиционного сорбента на основе гидрогеля хитозана и несуспENDEDиРОВАННОГО диоксида кремния («хитозан–коллоидный кремнезем»), проявляющихся в динамических условиях очистки водных растворов от ионов тяжелых металлов.

Методы. Полную динамическую обменную емкость композиционного сорбента «хитозан–коллоидный кремнезем» оценивали в условиях динамической сорбции, пропуская через неподвижный сорбционный слой растворы, содержащие ионы Zn(II), Cd(II), Cu(II) и Cr(III) с концентрацией 240–251 мг/л. Метод определения острой токсичности с использованием дафний (*Daphnia magna* Straus) основан на прямом счете процента смертности дафний при воздействии токсических веществ, присутствующих в исследуемой водной вытяжке, по сравнению с контрольной культурой в пробах, не содержащих токсических веществ. Оценку регенерационной способности сорбента определяли фиксированием количества циклов сорбции–десорбции с использованием элюентов — 0.1 М NaOH, 0.1 М NaHCO₃, а также водных растворов H₂O₂ (1 и 3%).

Результаты. Установлена эффективность работы композиционного сорбента «хитозан–коллоидный кремнезем» в процессе динамической очистки водных сред от ионов Cu(II), Zn(II), Cd(II) и Cr(III). Определены времена проскока ионов и насыщения разработанного сорбента и рассчитана его динамическая обменная емкость путем обработки кинетических кривых сорбции ионов тяжелых металлов, снятых при осуществлении сорбции в динамических условиях. Представлены результаты регенерации и возможность повторного использования сорбента, который способен выдерживать до пяти циклов сорбции–десорбции с сохранением степени извлечения катионов меди выше 90%.

Выводы. Анализ кинетических кривых показал, что движущей силой динамической очистки водных сред от тяжелых металлов полученным сорбентом является внешнедиффузионный массоперенос ионов из подвижной фазы раствора. Биотестирование образцов показало, что разработанный сорбент на основе хитозана не обладает острой токсичностью.

Ключевые слова

адсорбция, тяжелые металлы, хитозан, композиты, биотестирование, регенерация

Поступила: 11.07.2023

Доработана: 13.10.2023

Принята в печать: 14.03.2024

Для цитирования

Габрин В.А., Никифорова Т.Е., Козлов В.А., Разговоров П.Б. Концентрирование ионов тяжелых металлов из водных сред в динамических условиях композиционным сорбентом на основе хитозана и диоксида кремния. *Тонкие химические технологии*. 2024;19(3):183–191. <https://doi.org/10.32362/2410-6593-2024-19-3-183-191>

INTRODUCTION

The need to improve the quality of water, representing a major technological and life resource, continues to present challenges [1–3]. Current improvements in wastewater treatment methods are mainly achieved by improving previously introduced methods, including those based on ion exchange-, electrolysis-, membrane separation-, ultrafiltration-, reverse osmosis-, catalysis-, sedimentation-, coagulation- (flocculation), and

adsorption approaches [4–6]. Due to its low energy intensity and high efficiency, the last of these methods is considered optimal for the removal of hazardous pollutants, including heavy metals [7–9]. Adsorption water treatment methods use a variety of materials: silica gel, activated carbon, resins, clays, and polymers. In terms of their economic feasibility and environmental significance, carbohydrate biopolymers (cellulose, alginate, and chitosan) have received increased attention as efficient alternative adsorbents over the past twenty years. This is

mainly due to their key advantages—natural abundance, environmental friendliness, biodegradability, ease of modification, and relatively low production cost [10]. Among the abovementioned carbohydrate biopolymers, chitosan is the most environmentally friendly due to its improved target sorption characteristics [11].

The main advantages of chitosan-based adsorbents are their high absorption capacity for heavy and rare earth metal ions. However, a key disadvantage of chitosan is its insolubility in aqueous solutions with $\text{pH} < 6.5$. In this regard, the development of chitosan-containing sorbents that are stable in acidic media was studied in numerous works. Attempts to solve the problem include the use of crosslinking agents: glutaraldehyde, epichlorohydrin, ethylene glycol diglycidyl ether, etc. [12].

The possibility of using chitosan adsorbents to obtain products of any shape (in the form of powder, microspheres, fibers, or membranes) dramatically expands its potential for wastewater treatment and in modern medicine. Chitosan can be used as a matrix to obtain composite sorbents, representing relatively inexpensive and effective materials with a developed surface. The fillers of this matrix can be zeolites, diatomite, silica, titania, montmorillonite, cellulose, etc. Although the introduction of such fillers into the chitosan matrix does not always lead to a significant increase in sorption capacity, the development of the scientific foundations and technology for creating new composite chitosan-containing sorbents based on its structural and mechanical characteristics represents a very promising direction in the development of industrial ecology [1, 7, 13].

The present work set out to investigate the sorption, toxicological, and regeneration properties of a composite sorbent based on chitosan hydrogel and unsuspended silicon dioxide (“chitosan–colloidal silica”), manifested under dynamic conditions of purification of aqueous solutions, as a means of removing heavy metal ions.

EXPERIMENTAL

Materials

Chitosan (*Bioprogress*, Russia; degree of deacetylation, 88%; molar mass, 220 kDa); epichlorohydrin (*Sigma-Aldrich*, USA; >98.0%); colloidal silica (silicon dioxide) (*Ekokremnii*, Russia; Kovelos 35/05; $r = 3\text{--}5\ \mu\text{m}$); sulfates of copper ($\text{CuSO}_4 \cdot 5\text{H}_2\text{O}$); zinc ($\text{ZnSO}_4 \cdot 7\text{H}_2\text{O}$); cadmium ($\text{CdSO}_4 \cdot 8\text{H}_2\text{O}$); chromium ($\text{Cr}_2(\text{SO}_4)_3 \cdot 6\text{H}_2\text{O}$); sodium hydroxide; acetic acid (50 vol %); sodium bicarbonate; hydrogen peroxide (aqueous) (*LenReaktiv*, Russia). These reagents were used without additional purification.

Along with sorbent regeneration efficiency and acute toxicity of aqueous extracts, the dynamic sorption characteristics of a chitosan–colloidal silica composite sorbent obtained according to the previously

published procedure were studied [13]. The obtained physicochemical and structural-mechanical characteristics, as well as the static sorption of copper ions, agree with the previous results [13].

Equipment and research methods

The total dynamic exchange capacity (TDEC) of the chitosan–colloidal silica composite sorbent was assessed under dynamic sorption conditions by passing solutions containing Zn(II), Cd(II), Cu(II), and Cr(III) ions at concentrations of 240–251 $\text{mg} \cdot \text{L}^{-1}$ through a fixed sorption bed. In a dynamic experiment, the sorbent (0.2 g on chitosan basis) was placed in a laboratory column in the sorption plant (Fig. 1). Every 10 min, the metal salt solution passing through the column was collected to determine its cation concentration with a 210 VGP atomic absorption spectrometer (*Buck Scientific*, USA).

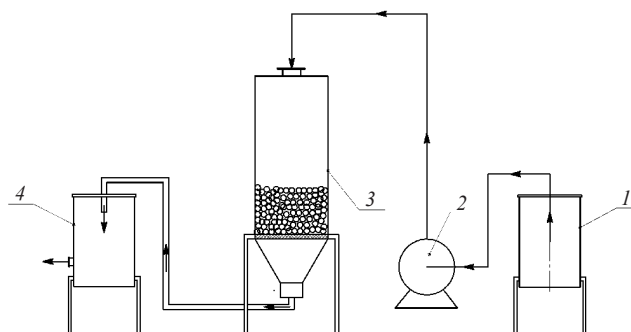


Fig. 1. Plant for studying dynamic sorption characteristics: (1) container with metal salt solution (electrolyte), (2) pump, (3) fixed-bed column with a sorbent, and (4) receiving container

The TDEC value was determined by analyzing the obtained dynamic curves by calculating the area above the output sorption curve:

$$S = C_{\text{in}} \times \Delta\tau_1 + \frac{C_{\text{in}} \times \Delta\tau_2}{2}, \quad (1)$$

$$\text{TDEC} = \frac{S \times Q}{m_{\text{sorb}}}, \quad (2)$$

where Q is the flow rate of the solution, $\text{L} \cdot \text{s}^{-1}$; m_{sorb} is the mass of the sorbent placed in the ion-exchange column, g; $\Delta\tau_1$ and $\Delta\tau_2$ are the times of breakthrough and saturation, respectively, s; and C_{in} is the concentration of copper ions at the inlet, $\text{mg} \cdot \text{L}^{-1}$.

Determination of the acute toxicity of the sorption material

The acute toxicity of the aqueous extract was determined using daphnia (*Daphnia magna* Straus) as a test object.

The method is based on direct calculation of the mortality percentage of daphnia exposed to toxic substances contained in the studied aqueous extract in comparison with a reference culture in the form of samples that do not contain toxic substances.

The acute toxicity A (%) of the aqueous extract was determined by the formula

$$A = \frac{X_{\text{ref}} - X_{\text{test}}}{X_{\text{ref}}} \times 100, \quad (3)$$

where X_{ref} is the number of surviving daphnia in the reference culture and X_{test} is the number of surviving daphnia in the water extract.

The preparation of cultivation water and dilutions of aqueous extracts for biotesting, and the biotesting itself were carried out according to the published method [14] for water samples obtained after contact with the studied modified sorbent. The biotesting was performed as follows. After growing daphnia cultures in a climatostat maintaining a 12-h photoperiod at room temperature ($25 \pm 0.1^\circ\text{C}$), ten age-synchronized daphnia cultures were placed for 1 day into each of the test tubes with test solutions pre-aerated for 30 min. The experimental conditions corresponded to the conditions for daphnia cultivation: $T = (20 \pm 2)^\circ\text{C}$, pH 7.0–8.2, and time 48 h.

Determination of the number of sorption–desorption cycles

In order to evaluate the possibility of reusing a composite sorbent without losing its effectiveness against heavy metal ions, desorption-based approaches can be used. Desorption of heavy metal ions was carried out using the suitable eluents 0.1 M NaOH and 0.1 M NaHCO_3 , as well as aqueous solutions of H_2O_2 (1 and 3%). The spent sorbent containing 0.1 g of dry chitosan was placed in 10 mL of a desorbing eluent solution and kept for 10 min. Following desorption, the chitosan–colloidal silica sorbent was washed with distilled water. When determining the number of sorption–desorption cycles, the sorbent regenerated in this way was reused to extract Cu(II) ions.

Regeneration efficiency was selected as a characteristic parameter of the recovery of spent sorbent. The regeneration efficiency RE (%) of the sorbent was calculated by the formula

$$RE = \frac{A_r}{A_0} \times 100, \quad (4)$$

where A_r and A_0 are the sorption after regeneration and the initial sorption of the sorbent, $\text{mg} \cdot \text{g}^{-1}$, respectively.

RESULTS AND DISCUSSION

The chitosan–colloidal silica composite sorbent was tested under dynamic conditions of sorption of various heavy metals (Fig. 2). The ion breakthrough time and sorbent saturation time were determined along with the TDEC (Table 1). In the experiment, the height of the packed sorbent bed ($5 \cdot 10^{-2}$ m) and the diameter of the column ($4 \cdot 10^{-2}$ m) remained unchanged. When calculating the total dynamic exchange capacity, the mass of the sorbent and the time consumption of the model wastewater solution were taken into account.

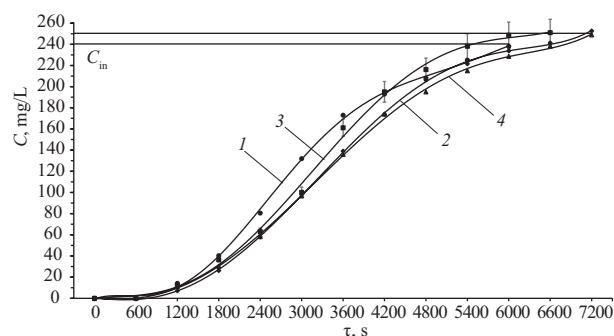


Fig. 2. Kinetic curves of sorption of (1) Cu(II), (2) Cd(II), (3) Zn(II), and (4) Cr(III) under dynamic conditions by the chitosan–colloidal silica sorbent at pH 5.9, $T = 298$ K, $m_{\text{sorb}} = 0.2$ g, and $Q = 0.15$ L · h⁻¹

The shape of the kinetic curves of sorption under dynamic conditions suggests that the sorption of Cu(II), Cd(II), Zn(II), and Cr(III) ions predominantly occurs by the external diffusion mechanism of mass transfer of ions

Table 1. TDEC of the sorbent and variables determined under dynamic conditions

Metal	$C_{\text{in}}, \text{mg} \cdot \text{L}^{-1}$	$m_{\text{sorb}}, \text{h}$	τ_1, s	τ_2, s	TDEC	
					$\text{mg} \cdot \text{g}^{-1}$	$\text{mol} \cdot \text{kg}^{-1}$
Cu(II)	240	0.2	900	5400	180	2.8
Cd(II)	250		1050	6200	216	2.0
Zn(II)	251		1000	5800	204	3.0
Cr(III)	248		1100	6300	219	4.2

Table 2. Acute toxicity of aqueous extract after contact with the chitosan–colloidal silica sorbent

Sorbent	Dilution ratio (aqueous extract content), %	Number of surviving daphnia		Mortality of daphnia in test, %
		Test	Reference	
Biotesting time: 48 h				
Chitosan–silica composite	10 (10)	10	10	0
	3 (33.3)	10	10	0
	1 (89)	10	10	0

from the mobile phase of the solution to the fixed sorbent bed. This may be due to the value of the crystallographic radius of the ion. Under both dynamic and static sorption conditions, sorbate–sorbate interactions are not excluded, leading to the formation of electrostatically bound ionic clusters. In a constant flow of liquid, such clusters do not significantly penetrate into the bulk phase through pore channels, but are mainly retained on the surface [15].

Further dynamic experiments will be aimed at identifying optimal process parameters and increasing the efficiency of using the chitosan–colloidal silica sorbent. Taking into account the increased sorption (sorption capacity) of the resulting material under static conditions, this primarily concerns the dosage of the sorbent and the dimensions of the column (8–10 mol/kg) [13].

Biotesting of the aqueous extract demonstrated the absence of an acute toxic effect at $A \leq 10\%$ (Table 2),

whereas in the case of $A \geq 50\%$, the previously shown acute toxic effect on living organisms is confirmed [14].

The biotesting of the water extract showed that, in the tested water after 48 h, the mortality of daphnia was less than 10%, which indicates the nontoxicity of the sorbent.

Figure 3 illustrates the change in the efficiency of regeneration of the chitosan–colloidal silica sorbent with an increasing number of sorption–desorption cycles using different eluents.

As noted earlier, a very important characteristic of sorbents is their regeneration ability. The developed chitosan–colloidal silica sorbent can maintain its efficient extraction of copper ions after five sorption–desorption cycles. The most efficient eluent is an H_2O_2 solution; here, the efficiency of using a 1% solution is comparable to that of a 3% solution. After five sorption–desorption cycles, the sorption capacity can be restored by more than 90%. When using sodium bicarbonate, the reduction

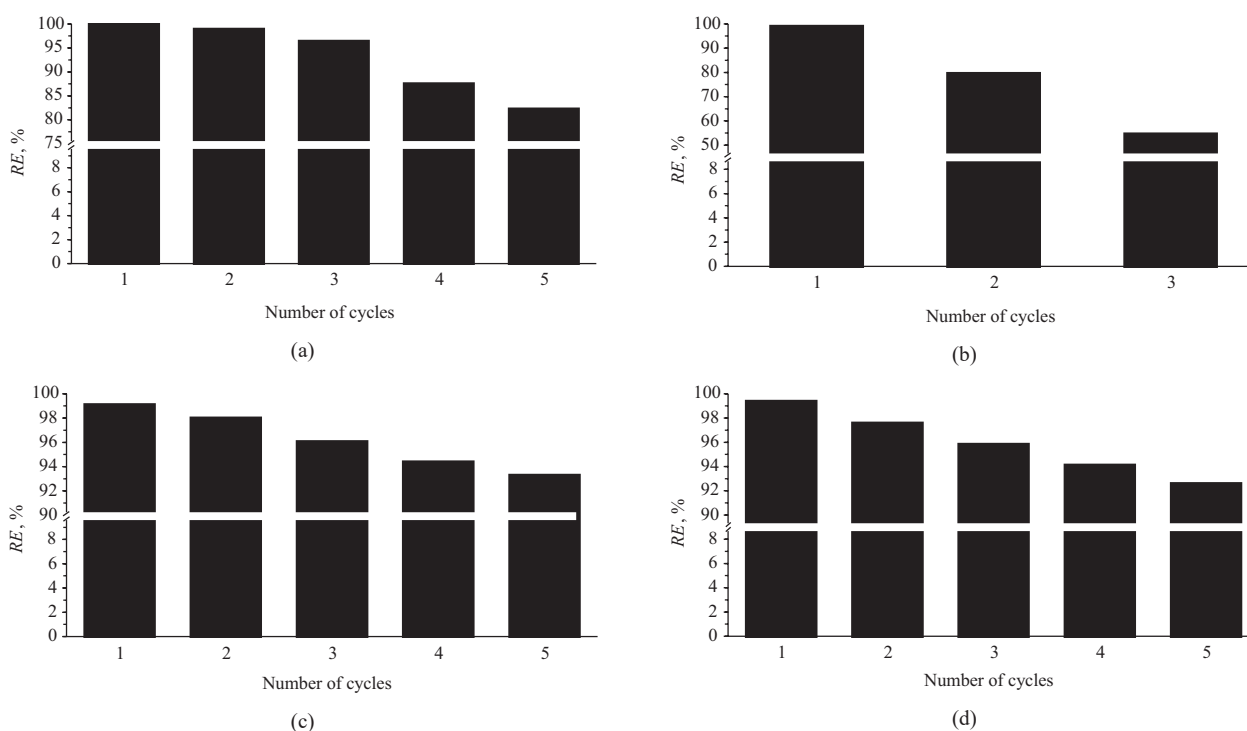


Fig. 3. Change in the efficiency of regeneration of the chitosan–colloidal silica sorbent with increasing number of sorption–desorption cycles. Eluents: (a) 0.1 M NaOH, (b) 0.1 M $NaHCO_3$, (c) 3% H_2O_2 , and (d) 1% H_2O_2

Table 3. Effect of the contact time of the spent sorbent with the eluent on the efficiency of sorbent regeneration and its mass loss in the first sorption–desorption cycle

0.1 M NaOH			0.1 M NaHCO ₃			3% H ₂ O ₂			1% H ₂ O ₂		
Contact time, min	Sorbent mass loss, %	RE, %	Contact time, min	Sorbent mass loss, %	RE, %	Contact time, min	Sorbent mass loss, %	RE, %	Contact time, min	Sorbent mass loss, %	RE, %
$V_{\text{solution}} = 10 \text{ mL}$											
1	0	15	1	0	10	1	0	2	1	0	1
3	1	45	3	0	30	3	0	20	3	0	25
5	2	70	5	0	59	5	0	80	5	0	86
10	5	97	10	0.5	92	10	0	97	10	0	98
15	8	96	15	2	93	15	1	95	15	0.5	97

in regeneration efficiency to 47% after three cycles makes further testing impractical. The optimal contact time of the sorbent and eluent was determined to be 10 min (Table 3).

A further increase in the contact time between the sorbent and the eluent did not provide more efficient regeneration. In addition, an increase in regeneration time was accompanied by a significant (up to 8% in the first cycle) sorbent mass loss in comparison with the initial mass of the sorbent.

Thus, crosslinked chitosan granules bulk-modified with colloidal silica, which have valuable properties in terms of permitting their reuse, can serve as an economical and effective sorbent for the extraction of heavy metal ions from aqueous media.

CONCLUSIONS

Dynamic parameters of the extraction of heavy metal ions by the chitosan–colloidal silica composite sorbent were obtained. It is shown that the column sorption of Cu(II), Cd(II), Zn(II), and Cr(III) ions from aqueous media predominately occurs by the external diffusion mechanism of mass transfer of ions from the mobile phase of the solution to the fixed bed of the sorbent. The conditions for the regeneration of the spent composite sorbent are identified. It is determined that the use of a 1% hydrogen peroxide solution as a reducing eluent allows the obtained sorbent to be used in five sorption–desorption cycles while maintaining the degree of extraction of metal ions above 90%. The biotesting method established the absence of acute toxicity for

living organisms of the aqueous extract of the solution in contact with the sorbent. In the future, the developed sorbent based on chitosan and silicon dioxide will be tested under conditions of purification of aqueous media similar to industrial conditions in order to evaluate the quality of purification of aqueous solutions for removing heavy metal ions used in electroplating and hydrocarbon processing (oil refining). This will help to improve effectiveness of natural water protection systems and reduce anthropogenic impacts on the environment.

Acknowledgments

The study was carried out within Research State Program (No. FZZW-2024-0004) using the resources of the Center for Shared Use of Scientific Equipment of Ivanovo State University of Chemistry and Technology (with the support of the Ministry of Science and Higher Education of Russian Federation, grant No. 075-15-2021-671).

Authors' contributions

V.A. Gabrin—formulating the aim of the study, planning and conducting experiments, processing experimental data, and writing the text of the article.

T.E. Nikiforova—correcting the aim of the study, research methodology, discussion of the results, and editing the content of the article.

V.A. Kozlov—correcting the research methodology, scientific consulting.

P.B. Razgovorov—general management and discussion of the results.

The authors declare no conflicts of interest.

REFERENCES

1. Dinu M.V., Humelnicu D., Lazar M.M. Analysis of Copper(II), Cobalt(II) and Iron(III) Sorption in Binary and Ternary Systems by Chitosan-Based Composite Sponges Obtained by Ice-Segregation Approach. *Gels*. 2021;7(3):103. <https://doi.org/10.3390/gels7030103>
2. Velasco-Garduño O. Martínez M.E., Gimeno M., Tecante A., Beristain-Cardoso R., Shirai K. Copper removal from wastewater by a chitosan-based biodegradable composite. *Environ. Sci. Pollut. Res.* 2020;27(4):28527–28535. <https://doi.org/10.1007/s11356-019-07560-2>
3. Kunin A.V., Ilyin A.A., Morozov L.N., Smirnov N.N., Nikiforova T.E., Prozorov D.A., Rumyantsev R.N., Afineevskiy A.V., Borisova O.A., Grishin I.S., Veres K.A., Kumikova A.A., Gabrin V.A., Gordina N.E. Catalysts and adsorbents for conversion of natural gas, fertilizers production, purification of technological liquids. *Izv. Vyssh. Uchebn. Zaved. Khim. Khim. Tekhnol. = ChemChemTech* (in Russ.). 2023;66(7):132–150. <https://doi.org/10.6060/ivkkt.20236607.6849j>
4. Omer A.M., Dey R., Eltaweil A.S., Abd El-Monaem E.M. Insights into recent advances of chitosan-based adsorbents for sustainable removal of heavy metals and anions. *Arabian J. Chem.* 2022;15(2):103543. <http://doi.org/10.1016/j.arabjc.2021.103543>
5. Chakraborty R., Asthana A., Singh A.K., Jain B., Susan A.B.H. Adsorption of heavy metal ions by various low-cost adsorbents: a review. *International Journal of Environmental Analytical Chemistry*. 2020:1–38. <https://doi.org/10.1080/03067319.2020.1722811>
6. Arora R. Adsorption of Heavy Metals — A Review. *Materials Today: Proceedings*. 2019;18:4745–4750. <https://doi.org/10.1016/j.matpr.2019.07.462>
7. Brião G.V., de Andrade J.R., da Silva M.G.C., Vieira M.G.A. Removal of toxic metals from water using chitosan-based magnetic adsorbents. A review. *Environ. Chem. Lett.* 2020;18(4):1145–1168. <http://doi.org/10.1007/s10311-020-01003-y>
8. Politaeva N., Yakovlev A., Yakovleva E., et al. Graphene oxide-chitosan composites for water treatment from copper cations. *Water*. 2022;14(9):1430. <https://doi.org/10.3390/w14091430>
9. Zhang W., An Y., Li S., Liu Z., Chen Z., Ren Y., Wang X. Enhanced heavy metal removal from an aqueous environment using an eco-friendly and sustainable adsorbent. *Sci. Rep.* 2020;10(1):16453. <https://doi.org/10.1038/s41598-020-73570-7>
10. Nikiforova T.E., Gabrin V.A., Razgovorov P.B. Peculiarities of Sorption of Heavy-Metal Ions by Polysaccharide and Polyamide Biopolymers. *Prot. Met. Phys. Chem. Surf.* 2023;59(3):313–324. <https://doi.org/10.1134/S2070205123700363>
[Original Russian Text: Nikiforova T.E., Gabrin V.A., Razgovorov P.B. Peculiarities of Sorption of Heavy-Metal Ions by Polysaccharide and Polyamide Biopolymers. *Fizikokhimiya poverkhnosti i zashchita materialov*. 2023;59(3):231–243 (in Russ.). <https://doi.org/10.31857/S0044185623700298>]
11. Soliman N.K., Moustafa A.F. Industrial solid waste for heavy metals adsorption features and challenges; a review. *J. Mat. Res. Technol.* 2020;9(5):10235–10253. <https://doi.org/10.1016/j.jmrt.2020.07.045>
12. Ghiorghita C.-A., Dinu M.V., Lazar M.M., Dragan E.S. Polysaccharide-Based Composite Hydrogels as Sustainable Materials for Removal of Pollutants from Wastewater. *Molecules*. 2022;27(23):8574. <https://doi.org/10.3390/molecules27238574>
13. Fufaeva V.A., Nikiforova T.E., Razgovorov P.B., Ignatyev A.A. Kinetic Characteristics of Extraction of Copper(II) Cations from Aqueous Media by Chitosan–Silicon Dioxide Hydrogel Sorbent. *Ekologiya i promyshlennost' Rossii = Ecology and Industry of Russia*. 2022;26(12):22–27 (in Russ.). <https://doi.org/10.18412/1816-0395-2022-12-22-27>

СПИСОК ЛИТЕРАТУРЫ

1. Dinu M.V., Humelnicu D., Lazar M.M. Analysis of Copper(II), Cobalt(II) and Iron(III) Sorption in Binary and Ternary Systems by Chitosan-Based Composite Sponges Obtained by Ice-Segregation Approach. *Gels*. 2021;7(3):103. <https://doi.org/10.3390/gels7030103>
2. Velasco-Garduño O. Martínez M.E., Gimeno M., Tecante A., Beristain-Cardoso R., Shirai K. Copper removal from wastewater by a chitosan-based biodegradable composite. *Environ. Sci. Pollut. Res.* 2020;27(4):28527–28535. <https://doi.org/10.1007/s11356-019-07560-2>
3. Кунин А.В., Ильин А.А., Морозов Л.Н., Смирнов Н.Н., Никифорова Т.Е., Прозоров Д.А., Румянцев Р.Н., Афинеевский А.В., Борисова О.А., Гришин И.С., Верес К.А., Курникова А.А., Габрин В.А., Гордина Н.Е. Катализаторы и адсорбенты для переработки природного газа, производства минеральных удобрений, очистки технологических жидкостей. *Известия вызов. Химия и хим. технология*. 2023;66(7):132–150. <https://doi.org/10.6060/ivkkt.20236607.6849j>
4. Omer A.M., Dey R., Eltaweil A.S., Abd El-Monaem E.M. Insights into recent advances of chitosan-based adsorbents for sustainable removal of heavy metals and anions. *Arabian J. Chem.* 2022;15(2):103543. <http://doi.org/10.1016/j.arabjc.2021.103543>
5. Chakraborty R., Asthana A., Singh A.K., Jain B., Susan A.B.H. Adsorption of heavy metal ions by various low-cost adsorbents: a review. *Int. J. Environ. Anal. Chem.* 2022;100(2):342–379. <https://doi.org/10.1080/03067319.2020.1722811>
6. Arora R. Adsorption of Heavy Metals — A Review. *Materials Today: Proceedings*. 2019;18:4745–4750. <https://doi.org/10.1016/j.matpr.2019.07.462>
7. Brião G.V., de Andrade J.R., da Silva M.G.C., Vieira M.G.A. Removal of toxic metals from water using chitosan-based magnetic adsorbents. A review. *Environ. Chem. Lett.* 2020;18(4):1145–1168. <http://doi.org/10.1007/s10311-020-01003-y>
8. Politaeva N., Yakovlev A., Yakovleva E., et al. Graphene oxide-chitosan composites for water treatment from copper cations. *Water*. 2022;14(9):1430. <https://doi.org/10.3390/w14091430>
9. Zhang W., An Y., Li S., Liu Z., Chen Z., Ren Y., Wang X. Enhanced heavy metal removal from an aqueous environment using an eco-friendly and sustainable adsorbent. *Sci. Rep.* 2020;10(1):16453. <https://doi.org/10.1038/s41598-020-73570-7>
10. Никифорова Т.Е., Габрин В.А., Разговоров П.Б. Особенности сорбции тяжелых металлов биополимерами полисахаридной и полиамидной природы. *Физикохимия поверхности и защита материалов*. 2023;59(3):231–243. <https://doi.org/10.31857/S0044185623700298>
11. Soliman N.K., Moustafa A.F. Industrial solid waste for heavy metals adsorption features and challenges; a review. *J. Mat. Res. Technol.* 2020;9(5):10235–10253. <https://doi.org/10.1016/j.jmrt.2020.07.045>
12. Ghiorghita C.-A., Dinu M.V., Lazar M.M., Dragan E.S. Polysaccharide-Based Composite Hydrogels as Sustainable Materials for Removal of Pollutants from Wastewater. *Molecules*. 2022;27(23):8574. <https://doi.org/10.3390/molecules27238574>
13. Фуфаева В.А., Никифорова Т.Е., Разговоров П.Б., Игнатьев А.А. Кинетические характеристики извлечения катионов меди(II) из водных сред гидрогелевым сорбентом хитозан–диоксид кремния. *Экология и промышленность России*. 2022;26(12):22–27. <https://doi.org/10.18412/1816-0395-2022-12-22-27>
14. Григорьев Ю.С., Шашкова Т.Л. Методика определения токсичности воды и водных вытяжек из почв, осадков сточных вод и отходов, питьевой, сточной и природной воды по смертности тест-объекта *Daphnia magna Straus* (ПНД Ф Т 14.1:2.4.12 – 06; Т 16.1:2.3.3.9 – 06). Красноярск: КрасГУ; 2006. 47 с.

14. Grigor'ev Yu.S., Shashkova T.L. *Metodika opredeleniya toksichnosti vodnykh vytyazhek iz pochv, osadkov stochnykh vod i otkhodov, pit'evoi, stochnoi i prirodnoi vody po smertnosti test-ob'ekta Daphnia magna Straus (PND F T 14.1:2:4.12 – 06; T 16.1:2.3.3.9 – 06) (Method for Determining the Toxicity of Aqueous Extracts from Soils, Sewage Sludge and Waste, Drinking, Waste and Natural Water by the Mortality of the Test Object Daphnia Magna Straus (PND F T 14.1:2:4.12 – 06; T 16.1:2.3.3.9 – 06)*. Krasnoyarsk: KrasGU; 2006. 47 p. (in Russ.).
15. Slavinskaya G.V., Kurenkova O.V. Changes of physicochemical and technological characteristics of ion-exchange materials in natural water treatment system. *Sorbtsionnye i Khromatograficheskie Protssesy*. 2013;13(3):322–331 (in Russ.).
15. Славинская Г.В., Куренкова О.В. Изменение физико-химических и технологических характеристик ионообменных материалов в установках кондиционирования природных вод. *Сорбционные и хроматографические процессы*. 2013;13(3):322–331.

About the authors

Victoria A. Gabrin, Postgraduate Student, Department of Food Technology and Biotechnology, Ivanovo State University of Chemistry and Technology (ISUCT) (7, Sheremetevskii pr., Ivanovo, 153000, Russia). E-mail: gabrinvictoria@gmail.com. Scopus Author ID 58398403100, RSCI SPIN-code 6197-2268, <https://orcid.org/0000-0002-1712-9121>

Tatiana E. Nikiforova, Dr. Sci. (Chem.), Associate Professor, Department of Food Technology and Biotechnology, Ivanovo State University of Chemistry and Technology (ISUCT) (7, Sheremetevskii pr., Ivanovo, 153000, Russia). E-mail: tatianaenik@mail.ru. Scopus Author ID 7006694263, ResearcherID N-1026-2017, RSCI SPIN-code 4080-7735, <https://orcid.org/0000-0002-0817-9258>

Vladimir A. Kozlov, Dr. Sci. (Chem.), Full Professor, Department of Chemistry and Technology of Macromolecular Compounds, Ivanovo State University of Chemistry and Technology (ISUCT) (7, Sheremetevskii pr., Ivanovo, 153000, Russia). E-mail: kozlov@isuct.ru. Scopus Author ID 57196498026, RSCI SPIN-code 4805-4551, <https://orcid.org/0000-0002-1034-4339>

Pavel B. Razgovorov, Dr. Sci. (Eng.), Professor, Head of the Department for the Organization of Research and Intellectual Activities, Yaroslavl State Technical University (YSTU) (88, Moskovskii pr., Yaroslavl, 150023, Russia). E-mail: razgovorovpb@ystu.ru. Scopus Author ID 17344647700, RSCI SPIN-code 2735-1209, <https://orcid.org/0000-0003-0514-5770>

Об авторах

Габрин Виктория Александровна, аспирант кафедры технологии пищевых продуктов и биотехнологии, ФГБОУ ВО «Ивановский государственный химико-технологический университет» (ИГХТУ) (153000, Россия, г. Иваново, Шереметевский пр-т, д. 7). E-mail: gabrinvictoria@gmail.com. Scopus Author ID 58398403100, SPIN-код РИНЦ 6197-2268, <https://orcid.org/0000-0002-1712-9121>

Никифорова Татьяна Евгеньевна, д.х.н., доцент кафедры технологии пищевых продуктов и биотехнологии ФГБОУ ВО «Ивановский государственный химико-технологический университет» (ИГХТУ) (153000, Россия, г. Иваново, Шереметевский пр-т, д. 7). E-mail: tatianaenik@mail.ru. Scopus Author ID 7006694263, ResearcherID N-1026-2017, SPIN-код РИНЦ 4080-7735, <https://orcid.org/0000-0002-0817-9258>

Козлов Владимир Александрович, д.х.н., профессор кафедры химии и технологии высокомолекулярных соединений ФГБОУ ВО «Ивановский государственный химико-технологический университет» (ИГХТУ) (153000, Россия, г. Иваново, Шереметевский пр-т, д. 7). E-mail: kozlov@isuct.ru. Scopus Author ID 57196498026, SPIN-код РИНЦ 4805-4551, <https://orcid.org/0000-0002-1034-4339>

Разговоров Павел Борисович, д.т.н., профессор, начальник управления организации научно-исследовательской и интеллектуальной деятельности ФГБОУ ВО «Ярославский государственный технический университет» (ЯГТУ) (150023, Россия, г. Ярославль, Московский пр-т, д. 88). E-mail: razgovorovpb@ystu.ru. Scopus Author ID 17344647700, SPIN-код РИНЦ 2735-1209, <https://orcid.org/0000-0003-0514-5770>

Translated from Russian into English by V. Glyanchenko

Edited for English language and spelling by Thomas A. Beavitt

UDC 66.095.62+547.295.3+544.47+544.478.1

<https://doi.org/10.32362/2410-6593-2024-19-3-192-201>

EDN SYTFBD



RESEARCH ARTICLE

Effect of 2-hexanol and methanol on the *one-pot* process of dehydration and alkoxy carbonylation for the synthesis of esters

Nadezhda T. Sevostyanova[✉], Sergey A. Batashev, Anastasia S. Rodionova, Dar'ya K. Kozlenko

Tula State Lev Tolstoy Pedagogical University, Tula, 300026 Russia

[✉]Corresponding author, e-mail: sevostyanova.nt@gmail.com

Abstract

Objectives. To study the possibility of *one-pot* synthesis (combination of two processes in one reactor) for the following pairs of processes: (1) dehydration of 2-hexanol and isomerizing alkoxy carbonylation of the resulting 2-hexene, in order to obtain 2-hexyl heptanoate, and (2) dehydration of 2-hexanol and isomerizing methoxy carbonylation of the resulting 2-hexene, in order to obtain methyl esters of C₇ carboxylic acids. To investigate the effect of the concentrations of 2-hexanol and methanol on the rate of the *one-pot* synthesis.

Methods. *One-pot* synthesis was studied in a toluene medium in a steel batch reactor designed to operate at elevated pressure and equipped with a glass insert, a magnetic stirrer, a sampler, and gas input and discharge devices. Samples of the reaction mass were taken during the combined process and were analyzed by means of gas–liquid chromatography with a flame ionization detector.

Results. The possibility of *one-pot* combination was demonstrated for 2-hexanol dehydration catalyzed by methanesulfonic acid, as well as for the isomerizing alkoxy carbonylation of the resulting 2-hexene with 2-hexanol and CO, catalyzed by the Pd(PPh₃)₂Cl₂–XANTPHOS–methanesulfonic acid system. The dependencies of the rates of the dehydration of 2-hexanol and the formation of esters of C₇ carboxylic acids on the concentration of 2-hexanol were shown to pass through a maximum. The possibility of the *one-pot* process was proved for the synthesis of esters from 2-hexanol, methanol, and CO with the predominant formation of heptanoic acid esters in the presence of the above catalytic system. The rates of dehydration of 2-hexanol and the formation of 2-hexyl esters of C₇ carboxylic acids were found to decrease with increasing the concentration of methanol in the reaction mass. Under mild conditions (temperature 115°C, CO pressure 3 MPa) with the addition of methanol, the total fraction of 2-hexyl and methyl heptanoic acid esters among C₇ carboxylic acid esters was determined to be 85.5%.

Conclusions. The reactions of intramolecular acid–catalytic dehydration of 2-hexanol and isomerizing alkoxy carbonylation of the resulting 2-hexene, catalyzed by the Pd(PPh₃)₂Cl₂–XANTPHOS–methanesulfonic acid system, can be performed as a *one-pot* process. Methanesulfonic acid simultaneously functions as a catalyst for the dehydration of 2-hexanol and a cocatalyst for the palladium–phosphine system for the alkoxy carbonylation of hexenes. In the presence of the Pd(PPh₃)₂Cl₂–XANTPHOS–methanesulfonic acid catalytic system, processes for the synthesis of heptanoic acid esters from 2-hexanol, methanol, and CO can be combined within one reactor. An increase in the methanol concentration negatively affects the rate of the dehydration of 2-hexanol and the formation of 2-hexyl esters of C₇ carboxylic acids. A small amount of methanol in the reaction mass leads to an increase in the fraction of heptanoic acid esters among C₇ carboxylic acid esters.

Keywords

one-pot synthesis, ester synthesis, alcohol dehydration, isomerizing alkoxy carbonylation, 2-hexanol, methanol, palladium catalyst, XANTPHOS diphosphine, methanesulfonic acid

Submitted: 07.09.2023

Revised: 30.01.2024

Accepted: 17.04.2024

For citation

Sevostyanova N.T., Batashev S.A., Rodionova A.S., Kozlenko D.K. Effect of 2-hexanol and methanol on the *one-pot* process of dehydration and alkoxy carbonylation for the synthesis of esters. *Tonk. Khim. Tekhnol. = Fine Chem. Technol.* 2024;19(3):192–201. <https://doi.org/10.32362/2410-6593-2024-19-3-192-201>

НАУЧНАЯ СТАТЬЯ

Влияние гексанола-2 и метанола на совмещенный процесс дегидратации и алкоксикарбонилирования для синтеза сложных эфиров

Н.Т. Севостьянова✉, С.А. Баташев, А.С. Родионова, Д.К. Козленко

Тульский государственный педагогический университет им. Л.Н. Толстого, Тула, 300026 Россия

✉ Автор для переписки, e-mail: sevostyanova.nt@gmail.com

Аннотация

Цели. Изучить возможности совмещения в одном реакторе процессов: 1) дегидратации гексанола-2 и изомеризирующего алкоксикарбонилирования образующегося гексена-2 для получения 2-гексилгептаноата; 2) дегидратации гексанола-2 и изомеризирующего метоксикарбонилирования образующегося гексена-2 для получения метиловых эфиров карбоновых кислот C_7 . Исследовать закономерности влияния концентрации гексанола-2 и метанола на скорость совмещенного процесса.

Методы. Совмещенный процесс изучали в среде толуола в периодическом стальном реакторе, рассчитанном на работу при повышенном давлении, снабженном стеклянной вставкой, магнитной мешалкой, пробоотборником, устройствами ввода и сброса газов. Отбираемые в ходе совмещенного процесса пробы реакционной массы анализировали методом газо-жидкостной хроматографии с пламенно-ионизационным детектором.

Результаты. Показана возможность совмещения в одном реакторе дегидратации гексанола-2, катализируемой метансульфо-кислотой, и изомеризирующего алкоксикарбонилирования образующегося гексена-2 гексанолом-2 и CO, катализируемого системой $Pd(PPh_3)_2Cl_2$ -XANTPHOS-метансульфо-кислота. Установлены экстремальные зависимости скоростей дегидратации гексанола-2 и образования сложных эфиров карбоновых кислот C_7 от концентрации гексанола-2. Показана возможность реализации совмещенного в одном реакторе процесса синтеза сложных эфиров из гексанола-2, метанола и CO с преимущественным образованием сложных эфиров гептановой кислоты в присутствии указанной каталитической системы. Обнаружено снижение скоростей дегидратации гексанола-2 и образования 2-гексильных эфиров карбоновых кислот C_7 с увеличением концентрации метанола в реакционной массе. В мягких условиях (температура 115°C, давление CO 3 МПа) в присутствии добавок метанола определена суммарная доля 2-гексильного и метилового эфиров гептановой кислоты среди сложных эфиров карбоновых кислот C_7 , которая составила 85.5%.

Выводы. Реакции внутримолекулярной кислотной-каталитической дегидратации гексанола-2 и изомеризирующего алкоксикарбонилирования образующегося гексена-2, катализируемого системой $Pd(PPh_3)_2Cl_2$ -XANTPHOS-метансульфо-кислота, могут быть совмещены в одном реакторе. Метансульфо-кислота одновременно выполняет функции катализатора дегидратации гексанола-2 и сокатализатора палладий-фосфиновой системы алкоксикарбонилирования гексенов. В присутствии каталитической системы $Pd(PPh_3)_2Cl_2$ -XANTPHOS-метансульфо-кислота могут быть реализованы в одном реакторе процессы синтеза сложных эфиров гептановой кислоты из гексанола-2, метанола и CO. Увеличение концентрации метанола негативно влияет на скорости дегидратации гексанола-2 и образование 2-гексильных эфиров карбоновых кислот C_7 . Небольшие количества метанола в реакционной массе приводят к увеличению доли сложных эфиров гептановой кислоты среди сложных эфиров карбоновых кислот C_7 .

Ключевые слова

совмещенный процесс, синтез сложного эфира, дегидратация спирта, изомеризирующее алкоксикарбонилирование, гексанол-2, метанол, палладиевый катализатор, дифосфин XANTPHOS, метансульфо-кислота

Поступила: 07.09.2023

Доработана: 30.01.2024

Принята в печать: 17.04.2024

Для цитирования

Севостьянова Н.Т., Баташев С.А., Родионова А.С., Козленко Д.К. Влияние гексанола-2 и метанола на совмещенный процесс дегидратации и алкоксикарбонилирования для синтеза сложных эфиров. *Тонкие химические технологии*. 2024;19(3):192–201. <https://doi.org/10.32362/2410-6593-2024-19-3-192-201>

INTRODUCTION

CO-based syntheses are used to obtain a wide range of organic products. For example, carbonylation of alcohols and alkoxy-carbonylation of unsaturated

compounds give esters. In the former case, it is mainly homogeneous catalysts based on rhodium and iridium compounds with the addition of iodides which are used, since not alcohols, but alkyl iodides are directly carbonylated [1, 2]. These processes primarily use

methanol and ethanol which produce carboxylic acids and esters as the main products, and hydrocarbons and ethers as by-products. In the latter case, the most active catalysts are considered to be homogeneous systems based on palladium compounds with organophosphine and H-acid promoters. In the presence of such systems, alkoxy-carbonylation yields only isomeric esters [3, 4]. The alkoxy-carbonylation of alkenes, which occurs with the cleavage of the C–C π bond, is energetically preferable to carbonylation of alcohol, which requires the cleavage of the C–O σ bond. However, some alcohols are more accessible than alkenes. Previously “*one-pot* synthesis” (combination of two processes in one reactor) was shown to be possible for the dehydration of (primary and secondary) alcohols and carbonylation of the resulting alkenes to form esters and carboxylic acids in the presence of homogeneous palladium catalysts and *p*-toluenesulfonic acid (TsOH) [5–8]. In particular, a *one-pot* process based on cyclohexanol and CO was carried out in the presence of homogeneous catalytic systems based on Pd(PPh₃)₂Cl₂ [6], PdCl₂ [7], and Pd(OAc)₂ [8] in combination with the promoting additive PPh₃ and TsOH. TsOH was a catalyst for the dehydration of cyclohexanol and a cocatalyst for the alkoxy-carbonylation of cyclohexene. However, of practical interest is the synthesis of esters of aliphatic acids, primarily, of a linear structure, which as a rule are of the greatest value. For example, heptanoates and decanoates

are components of hormonal drugs (testosterone preparations) [9]. High selectivities for esters of linear carboxylic acids are achieved in alkoxy-carbonylation catalyzed by means of palladium systems with some diphosphines, mainly *tert*-butyl-substituted diphosphines [10–16] and diphosphines of the XANTPHOS group¹ [17, 18]. These include in the case of alkenes with internal position of the C=C bond (isomerizing alkoxy-carbonylation). Isomerizing alkoxy-carbonylation consists of two stages: migration of a multiple bond from the internal position to the terminal position and subsequent alkoxy-carbonylation to form an ester with a mainly linear structure.

The purpose of this work was to study the possibility of *one-pot* combination of the following processes (Fig. 1): (1) dehydration of 2-hexanol (**1**) and isomerizing alkoxy-carbonylation of the resulting 2-hexene (**2**), in order to obtain 2-hexyl heptanoate (product **3a**, reactions (1), (2)); and (2) dehydration of alcohol **1** and isomerizing methoxy-carbonylation of alkene **2**, in order to form methyl esters of C₇ carboxylic acids (products **4a–4c**, reactions (1), (3)) aimed at increasing the rate of the process of obtaining esters; as well as to investigate the effect of the concentration of alcohol **1** and methanol on the rate of the *one-pot* process of ester synthesis.

The catalyst used in the *one-pot* processes being study was the Pd(PPh₃)₂Cl₂–XANTPHOS–methanesulfonic acid (MsOH) system. This catalytic precursor was chosen due to its highest level of activity in a model *one-pot*

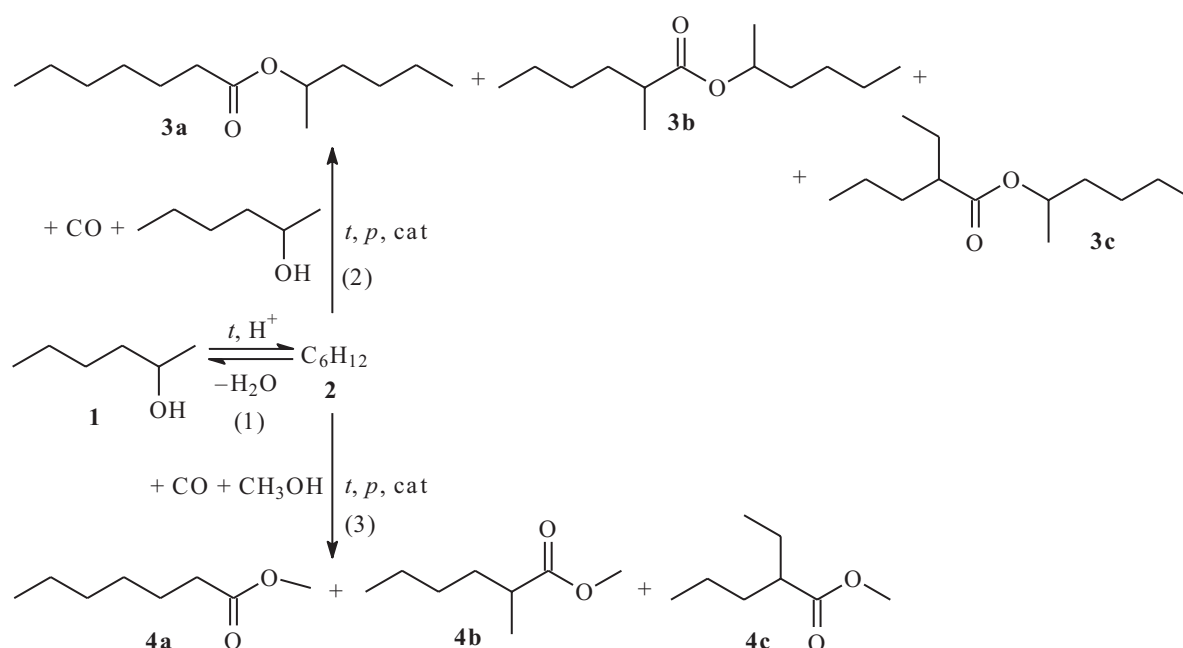


Fig. 1. Scheme of the *one-pot* synthesis of esters from 2-hexanol, methanol, and CO

¹ XANTPHOS is an organophosphorus compound C₃₉H₃₂OP₂ obtained from heterocyclic xanthene.

process based on cyclohexanol and CO in comparison with PdCl₂ and Pd(OAc)₂ [6–8]. XANTPHOS and MsOH were used as components of catalytic systems for isomerizing alkoxy-carbonylation [17, 18].

EXPERIMENTAL

The *one-pot* process was studied in a toluene medium (*Komponent-Reaktiv*, Russia) in a steel batch reactor (Russia) according to the published procedure [8]. During the experiments, the temperature was maintained at 115°C, and the pressure of a 1 : 1 mixture of CO (*BK Group*, Russia) and Ar (*Arton*, Russia) was 6.1 MPa. The concentrations of the components of the catalytic system were as follows, mol/L: $C(\text{Pd}(\text{PPh}_3)_2\text{Cl}_2) = 2.0 \cdot 10^{-3}$ (*TCl*, Japan), $C(\text{XANTPHOS}) = 2.5 \cdot 10^{-3}$ (*BIOSYNTH CARBOSYNTH*, USA), and $C(\text{MsOH}) = 0.16$ (*Sigma-Aldrich*, France).

Samples of the reaction mass were taken during each experiment and were analyzed by means of gas-liquid chromatography with a Crystallux-4000M chromatograph (*Meta-Chrom*, Russia) with a flame ionization detector and argon carrier gas. The carrier gas flow rate was 1.0 mL/min; and the flow splitting 1 : 60. The evaporator and detector temperatures were 300 and 320°C, respectively. The components of the reaction mass were separated in an Optima-5 capillary column (*MACHEREY-NAGEL*, Germany); 30 m × 0.32 mm; film thickness 0.35 μm; temperature programming mode: isothermal mode 80°C for 5 min, in the range 80–220°C at a heating rate of 20 deg/min, in the range 220–280°C at a heating rate of 8 deg/min, isothermal mode 280°C for 2.5 min. Peak areas were calculated using the NetChrom² program. The chromatogram peaks were identified by retention time by comparing them with the retention times of standard samples of substances.

The concentrations of substances 1–4 were calculated by the internal standard method and decane was used as an internal standard (*EKOS-I*, Russia). The internal standard was introduced at a constant concentration into the reaction solution in toluene before the start of the experiment. Toluene was chosen as a medium for the *one-pot* synthesis as the most commonly used solvent for alkoxy-carbonylation processes [6–8, 15, 19–22]. Insignificant (total yield of no more than 8%) amounts of ethers, heptanoic acid, and 2-methylhexanoic acid were formed as by-products.

RESULTS AND DISCUSSION

The possibility of the *one-pot* combination of the dehydration of alcohol 1 and the alkoxy-carbonylation of resulting alkene 2 was tested in experiments 1 and 2 (Table 1). The most reactive of all alcohols in alkoxy-carbonylation is known to be methanol [23]. In this regard, the *one-pot* synthesis was performed using both alcohol 1 and methanol (Table 1, experiments 3, 4). The yields of products 3a–3c were calculated by the formula:

$$\eta(3a-3c) = \frac{C(3a-3c)}{0.5C(1)} \cdot 100\%, \quad (A)$$

wherein $C(1)$ is the initial concentration of alcohol 1, mol/L; $C(3a-3c)$ are the concentrations of esters at the end of the process, mol/L.

The yields of products 4a–4c were calculated by the formula:

$$\eta(4a-4c) = \frac{C(4a-4c)}{C(\text{CH}_3\text{OH})} \cdot 100\%, \quad (B)$$

wherein $C(\text{CH}_3\text{OH})$ is the initial concentration of methanol, mol/L; $C(4a-4c)$ is the concentrations of esters at the end of the process, mol/L.

Table 1. Results of the study of *one-pot* processes based on alcohol 1 and CO (experiments 1 and 2), as well as alcohol 1, methanol, and CO (experiments 3 and 4); the time of the processes was 7 h

Exp. No.	$C(1)$, M	$C(\text{CH}_3\text{OH})$, M	Product yield, %				Conversion of alcohol 1, %
			3a	3(a+b+c)	4a	4(a+b+c)	1
1	0.500	–	36.1	60.3	–	–	94.7
2	1.000	–	10.4	20.0	–	–	39.5
3	0.250	0.250	10.7	13.7	13.9	15.6	66.4
4	0.500	0.500	5.4	7.2	5.1	6.1	42.3

² <https://www.meta-chrom.ru/catalog/soft/netchrom/>. Accessed February 28, 2024.

Table 2. Initial rates of alcohol **1** dehydration (r_1), formation of product **3a** (r_{3a}), and formation of the sum of products **3a+3b+3c** ($r_{3a+3b+3c}$) in experiments 1, 2, and 5–7

Exp. No.	$C(\mathbf{1})$, mol/L	$r_1 \cdot 10^2$, mol/(L·min)	$r_{3a} \cdot 10^4$, mol/(L·min)	$r_{3a+3b+3c} \cdot 10^4$, mol/(L·min)
1	0.500	1.70	2.2	3.0
2	1.000	0.85	0.9	1.3
5	0.150	0.26	0.6	0.7
6	0.300	1.21	2.5	3.5
7	0.750	1.01	1.6	2.2

The conversions of alcohol **1** and methanol were calculated by the formula:

$$\eta(\mathbf{1}, \text{CH}_3\text{OH}) = \frac{C'(\mathbf{1}, \text{CH}_3\text{OH})}{C(\mathbf{1}, \text{CH}_3\text{OH})} \cdot 100\%, \quad (\text{C})$$

wherein $C'(\mathbf{1}, \text{CH}_3\text{OH})$ is the concentration of alcohols at the end of the process, mol/L.

As the data in Table 1 shows, in the presence of methanol, the yields of products **3(a+b+c)** decreased, and the total yield of methyl and 2-hexyl esters was also lower when compared with experiments 1 and 2. The intermediate products in all experiments were 1-hexene and 2-hexene. The by-products were heptanoic acid, 2-methylhexanoic acid, and also ethers.

The effect of the concentration of alcohol **1** on the rate of the *one-pot* synthesis of ester products **3a–3c** was studied in a series of one-factor experiments (Table 2, experiments 1, 2, 5–7). This consisted of varying the concentration of alcohol **1** in a toluene medium and keeping other reaction conditions constant (in the absence of methanol). Table 2 presents the initial rates of the dehydration of alcohol **1** (r_1), the formation of product **3a** (r_{3a}), and the formation of the sum of products **3a+3b+3c** ($r_{3a+3b+3c}$) in the *one-pot* process.

Table 3. Initial rates of alcohol **1** dehydration in experiments 4 and 8–11 with the addition of methanol; in all experiments, $C(\mathbf{1}) = 0.500$ M

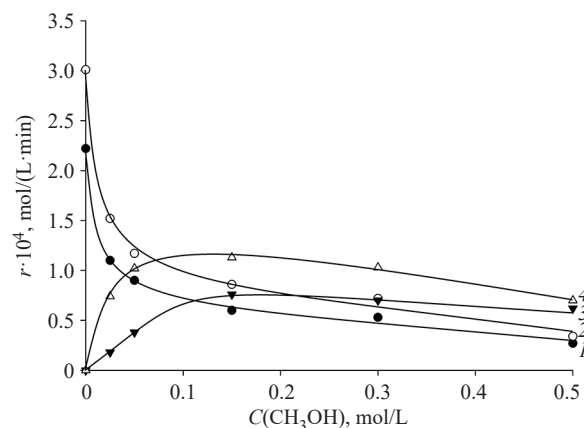
Exp. No.	$C(\text{CH}_3\text{OH})$, mol/L	$r_1 \cdot 10^2$, mol/(L·min)
8	0.025	1.48
9	0.050	1.29
10	0.150	1.10
11	0.300	0.90
4	0.500	0.78

Note: experiments are listed in order of increasing methanol concentration.

The rate r_1 was calculated from the slope of the initial portion of the curve for the total formation of free hexenes, esters, heptanoic acid, and 2-methylhexanoic acid. The rates of ester formation were calculated from the slopes of the initial portions of their accumulation curves.

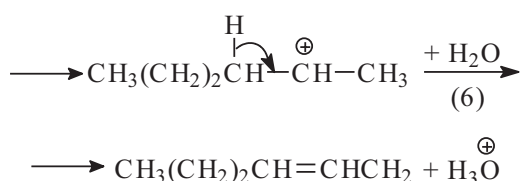
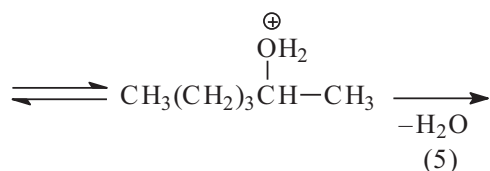
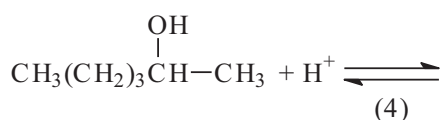
As the data in Table 2 shows, the dehydration rate reached its highest value at an alcohol **1** concentration of 0.500 mol/L. The rates of ester formation were the highest at $C(\mathbf{1}) = 0.300$ mol/L. The fraction of product **3a** among resulting esters **3a–3c** ranged from 57.5% at $C(\mathbf{1}) = 0.300$ M to 74.7% at $C(\mathbf{1}) = 0.15$ M. The conversion of alcohol **1** in the latter case reached 89.7%.

At the next stage of research, the effect of methanol on the *one-pot* process was studied in a series of one-factor experiments. This process simultaneously involved alcohol **1**, methanol, and CO. In these experiments (Table 3, experiments 4, 8–11), the concentration of methanol was varied, and the initial concentration of alcohol **1** was 0.500 M. Table 3 presents data on changes in the initial rate of the dehydration of alcohol **1**. Figure 2 illustrates the dependencies of the initial rates of the formation of products **3a–3c** and **4a–4c**.

**Fig. 2.** Dependencies of the rates of the formation of products (**1**) **3a**, (**2**) **3a+3b+3c**, (**3**) **4a**, and (**4**) **4a+4b+4c** in the *one-pot* process based on alcohol **1**, methanol, and CO

As the data in Table 3 (in comparison with the results of experiment 1, Table 2) and Fig. 2 shows, an increase in methanol concentration led to a decrease in the rates of the dehydration of alcohol **1**, the formation of product **3a**, and the formation of the sum of products **3a+3b+3c**. The dependencies of the rates of the formation of products **4a**, **4b**, and **4c** passed through a maximum. The total fraction of products **3a** and **4a** among the resulting esters ranged from 53.7% at $C(\text{CH}_3\text{OH})=0.025\text{ M}$ to 80.3% at $C(\text{CH}_3\text{OH})=0.50\text{ M}$. However, the conversion of alcohol **1** in the latter case was only 42.3%. In experiments 1–10, the fraction of products **3a+4a** among the various esters was the largest (85.5%) in experiment 3.

Liquid-phase dehydration of secondary alcohols under conditions of acid catalysis occurs by the *E1* mechanism [24]:

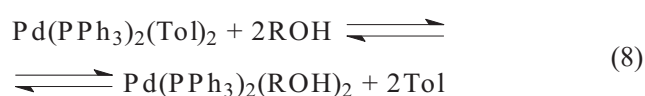


The dehydration of alcohols is known to be complicated by side reactions of the formation of ethers. In our studies, an increase in the concentration of alcohol **1** to 0.500 M led to an increase in the rate of dehydration. With a further increase in the concentration of alcohol **1**, solvation of the carbocation formed in reaction (5) by molecules of alcohol **1** apparently progressed, resulting in the formation of by-products (ethers) and a decrease in the rate of intramolecular dehydration. Under the action of methanol, these negative processes probably occur more actively, resulting in a decrease in the rate of the formation of hexenes as the methanol concentration is increased.

By-products of heptanoic and 2-methylhexanoic acids can be formed in two ways: by the hydrolysis of esters **3a**, **3b**, **4a**, and **4b** and the hydroxycarbonylation of 1-hexene and 2-hexene. This is similar to that described previously for the *one-pot* process based on cyclohexanol and CO [7, 8].

The established dependencies of the rates of the formation of products **3a–3c** in the *one-pot* process based on 2-hexanol and CO, as well as those of products **4a–4c**

in the *one-pot* process based on 2-hexanol, methanol, and CO, pass through a maximum. This is consistent with the data on the alkoxy-carbonylation of cyclohexene using cyclohexanol and methanol, catalyzed by the $\text{Pd}(\text{PPh}_3)_2\text{Cl}_2\text{-PPh}_3\text{-TsOH}$ system [21, 22]. The ascending branches of such dependencies are due to the participation of alcohols as co-reagents in alkoxy-carbonylation. The descending branches appear to be associated with the involvement of these components in ligand-exchange reactions leading to the formation of catalytically inactive palladium complexes (reactions (7), (8)) [21, 22].



The decrease in the rates of the formation of products **3a** and **3a+3b+3c** and the total rate of the formation of esters **3a+3b+3c+4a+4b+4c** in the presence of methanol is presumably a consequence of a decrease in the rate of the dehydration of alcohol **1**. At the same time the addition of methanol leads to an increase in the fraction of linear esters.

CONCLUSIONS

The possibility of *one-pot* combination was determined for the intramolecular acid-catalytic dehydration of alcohol **1** and the isomerizing alkoxy-carbonylation of the resulting 2-hexene, catalyzed by the $\text{Pd}(\text{PPh}_3)_2\text{Cl}_2\text{-XANTPHOS-MsOH}$ system. MsOH simultaneously served as a catalyst for the dehydration of 2-hexanol and a cocatalyst for the palladium–phosphine system of alkoxy-carbonylation of hexenes. The dependencies of the rates of the dehydration of alcohol **1** and the formation of 2-hexyl esters of C_7 carboxylic acids on concentration of alcohol **1** were shown to pass through a maximum. The main product of the *one-pot* process was 2-hexyl heptanoate. The rates of the dehydration of alcohol **1** and the formation of 2-hexyl esters of C_7 carboxylic acids were found to decrease with increasing methanol concentration. The dependencies of the rates of the formation of methyl esters of C_7 carboxylic acids on the concentration of methanol were demonstrated to pass through a maximum. The highest selectivities for heptanoic acid esters (up to 85.5%) were obtained at a molar ratio of 2-hexanol : $\text{CH}_3\text{OH} = 1 : 1$. Thus, further studies of the *one-pot* process based on 2-hexanol and CO with the addition of methanol should be aimed at finding optimal conditions, in order to ensure high yields of heptanoic acid esters.

Acknowledgments

The study was supported by the Russian Science Foundation (grant No. 22-23-00102), <https://rscf.ru/project/22-23-00102/>.

Authors' contributions

N.T. Sevostyanova—the idea of organizing the *one-pot* process, analysis and interpretation of the received data, and writing the text of the article.

S.A. Batashev—chromatographic analysis of the reaction mass, analysis and interpretation of the received data, and participation in writing the article.

A.S. Rodionova—experimental studies of the *one-pot* process with sampling of the reaction mass, calculations based on the experimental results, and participation in writing the article.

D.K. Kozlenko—experimental studies of the *one-pot* process with sampling of the reaction mass, calculations based on the experimental results, and participation in writing the article.

The authors N.T. Sevostyanova, S.A. Batashev, A.S. Rodionova, and D.K. Kozlenko confirm that there is no real or potential conflict of interest in relation to this article.

REFERENCES

1. Kalck P., Le C., Serp B.P. Recent advances in the methanol carbonylation reaction into acetic acid. *Coord. Chem. Rev.* 2020;402:213078. <https://doi.org/10.1016/j.ccr.2019.213078>
2. Sevostyanova N.T., Batashev S.A. Catalysts for Carbonylation of Alcohols to Obtain Carboxylic Acids and Esters. *Russ. J. Appl. Chem.* 2022;95(8):1085–1106. <https://doi.org/10.1134/S107042722208002X>
[Original Russian Text: Sevostyanova N.T., Batashev S.A. Catalysts for Carbonylation of Alcohols to Obtain Carboxylic Acids and Esters. *Zhurnal Prikladnoi Khimii.* 2022;95(8):947–970 (in Russ.). <https://doi.org/10.31857/S0044461822080011>]
3. Sevostyanova N.T., Batashev S.A. Alkoxy-carbonylation of unsaturated phytogenic substrates using palladium catalysts as a way for obtaining ester products. *Kataliz v Promyshlennosti.* 2023;23(1):37–55 (in Russ). <https://doi.org/10.18412/1816-0387-2023-1-37-55>
4. Liang W.-Y., Liu L., Zhou Q., Yang D., Lu Y., Liu Y. Pd-catalyzed alkoxy-carbonylation of alkenes promoted by H₂O free of auxiliary acid additive. *Mol. Catal.* 2020;482:110221. <https://doi.org/10.1016/j.mcat.2018.10.016>
5. Eliseev O.L., Bondarenko T.N., Stepin N.N., Lapidus A.L. Carbonylation of alcohols in the Pd(OAc)₂/TsOH/molten salt system. *Mendeleev Commun.* 2006;16(2):107–109. <https://doi.org/10.1070/MC2006v016n02ABEH002232>
6. Sevostyanova N.T., Batashev S.A. Effects of the *p*-toluenesulfonic acid concentration and temperature on the combined process of dehydration and hydrocarboxylation. *Bulleten' nauki i praktiki = Bulletin of Science and Practice.* 2016;7:8–13 (in Russ.). <https://www.bulletennauki.ru/gallery/%D0%91%D0%9D%D0%9F%20%E2%84%967%202016.pdf>
7. Sevostyanova N.T., Batashev S.A., Rodionova A.S. *One-pot* process involving dehydration of cyclohexanol and alkoxy-carbonylation of cyclohexene in the presence of catalytic system PdCl₂-PPh₃-*p*-toluenesulfonic acid. *Russ. Chem. Bull.* 2023;72(8):1936–1939. <https://doi.org/10.1007/s11172-023-3980-1>
[Original Russian Text: Sevostyanova N.T., Batashev S.A., Rodionova A.S. *One-pot* process involving dehydration of cyclohexanol and alkoxy-carbonylation of cyclohexene in the presence of catalytic system PdCl₂-PPh₃-*p*-toluenesulfonic acid. *Izvestiya Akademii Nauk. Seriya Khimicheskaya.* 2023;72(8):1936–1939 (in Russ.).]
8. Sevostyanova N.T., Batashev S.A., Rodionova A.S. Combined process of cyclohexyl cyclohexanecarboxylate synthesis from cyclohexanol and CO catalyzed by the Pd(OAc)₂-PPh₃-*p*-toluenesulfonic acid system. *Tonk. Khim. Tekhnol. = Fine Chem. Technol.* 2023;18(1):29–37 (in Russ.). <https://doi.org/10.32362/2410-6593-2023-18-1-29-37>

СПИСОК ЛИТЕРАТУРЫ

1. Kalck P., Le C., Serp B.P. Recent advances in the methanol carbonylation reaction into acetic acid. *Coord. Chem. Rev.* 2020;402:213078. <https://doi.org/10.1016/j.ccr.2019.213078>
2. Севостьянова Н.Т., Баташев С.А. Катализаторы карбонилирования спиртов для получения карбоновых кислот и сложных эфиров (обзор). *Журн. прикладной химии.* 2022;95(8):947–970. <https://doi.org/10.31857/S0044461822080011>
3. Севостьянова Н.Т., Баташев С.А. Алкоксикарбонилирование ненасыщенных субстратов растительного происхождения с использованием палладиевых катализаторов как путь к получению сложноэфирных продуктов. *Катализ в промышленности.* 2023;23(1):37–55. <https://doi.org/10.18412/1816-0387-2023-1-37-55>
4. Liang W.-Y., Liu L., Zhou Q., Yang D., Lu Y., Liu Y. Pd-catalyzed alkoxy-carbonylation of alkenes promoted by H₂O free of auxiliary acid additive. *Mol. Catal.* 2020;482:110221. <https://doi.org/10.1016/j.mcat.2018.10.016>
5. Eliseev O.L., Bondarenko T.N., Stepin N.N., Lapidus A.L. Carbonylation of alcohols in the Pd(OAc)₂/TsOH/molten salt system. *Mendeleev Commun.* 2006;16(2):107–109. <https://doi.org/10.1070/MC2006v016n02ABEH002232>
6. Севостьянова Н.Т., Баташев С.А. Влияние концентрации *n*-толуолсульфокислоты и температуры на совмещенный процесс дегидратации и гидрокарбалкоксилирования. *Бюллетень науки и практики.* 2016;7:8–13. <https://www.bulletennauki.ru/gallery/%D0%91%D0%9D%D0%9F%20%E2%84%967%202016.pdf>
7. Севостьянова Н.Т., Баташев С.А., Родионова А.С. Одно-реакторный совмещенный процесс дегидратации циклогексанола и алкоксикарбонилирования циклогексена в присутствии каталитической системы PdCl₂-PPh₃-*n*-толуолсульфокислота. *Изв. АН. Сер. хим.* 2023;72(8):1936–1939.
8. Севостьянова Н.Т., Баташев С.А., Родионова А.С. Совмещенный процесс синтеза циклогексилциклогексанкарбоксилата из циклогексанола и СО, катализируемый системой Pd(OAc)₂-PPh₃-*n*-толуолсульфокислота. *Тонкие химические технологии.* 2023;18(1):29–37. <https://doi.org/10.32362/2410-6593-2023-18-1-29-37>
9. Elks J., Ganellin C.R. (Eds.). *Dictionary of Drugs.* Boston: Springer; 1990. 2062 p. <https://doi.org/10.1007/978-1-4757-2085-3>
10. Herrmann N., Köhnke K., Seidensticker T. Selective product crystallization for concurrent product separation and catalyst recycling in the isomerizing methoxycarbonylation of methyl oleate. *ACS Sustainable Chem. Eng.* 2020;8(29):10633–10638. <https://doi.org/10.1021/acssuschemeng.0c03432>

9. Elks J., Ganellin C.R. (Eds.). *Dictionary of Drugs*. Boston: Springer; 1990. 2062 p. <https://doi.org/10.1007/978-1-4757-2085-3>
10. Herrmann N., Köhnke K., Seidensticker T. Selective product crystallization for concurrent product separation and catalyst recycling in the isomerizing methoxycarbonylation of methyl oleate. *ACS Sustainable Chem. Eng.* 2020;8(29):10633–10638. <https://doi.org/10.1021/acssuschemeng.0c03432>
11. Roesle P., Stempfle F., Hess S.K., Zimmerer J., Río Bártulos C., Lepetit B., Eckert A., Kroth P.G., Mecking S. Synthetic Polyester from Algae Oil. *Angew. Chem. Int. Ed.* 2014;53(26):6800–6804. <https://doi.org/10.1002/anie.201403991>
12. Quinzler D., Mecking S. Linear semicrystalline polyesters from fatty acids by complete feedstock molecule utilization. *Angew. Chem.* 2010;122(25):4402–4404. <https://doi.org/10.1002/ange.201001510>
13. Stempfle F., Ritter B.S., Mülhaupt R., Mecking S. Long-chain aliphatic polyesters from plant oils for injection molding, film extrusion and electrospinning. *Green Chem.* 2014;16(4):2008–2014. <https://doi.org/10.1039/C4GC00114A>
14. Dong K., Sang R., Wei Z., Liu J., Dühren R., Spannenberg A., Jiao H., Neumann H., Jackstell R., Franke R., Beller M. Cooperative catalytic methoxycarbonylation of alkenes: uncovering the role of palladium complexes with hemilabile ligands. *Chem. Sci.* 2018;9(9):2510–2516. <https://doi.org/10.1039/C7SC02964K>
15. Yang J., Liu J., Ge Y., Huang W., Ferretti F., Neumann H., Jiao H., Franke R., Jackstell R., Beller M. Efficient palladium-catalyzed carbonylation of 1,3-dienes: selective synthesis of adipates and other aliphatic diesters. *Angew. Chem. Int. Ed.* 2021;60(17):9527–9533. <https://doi.org/10.1002/anie.202015329>
16. Stempfle F., Quinzler D., Heckler I., Mecking S. Long-chain linear C₁₉ and C₂₃ monomers and polycondensates from unsaturated fatty acid esters. *Macromolecules.* 2011;44(11):4159–4166. <https://doi.org/10.1021/ma200627e>
17. Illner M., Schmidt M., Pogrzeba T., Urban C., Esche E., Schomaecker R., Repke J.-U. Palladium-catalyzed methoxycarbonylation of 1-dodecene in a two phase system: the path towards a continuous process. *Ind. Eng. Chem. Res.* 2018;57(27):8884–8894. <https://doi.org/10.1021/acs.iecr.8b01537>
18. Behr A., Vorholt A.J., Rentmeister N. Recyclable homogeneous catalyst for the hydroesterification of methyl oleate in thermomorphic solvent systems. *Chem. Eng. Sci.* 2013;99:38–43. <https://doi.org/10.1016/j.ces.2013.05.040>
19. Nifant'ev I.E., Sevostyanova N.T., Averyanov V.A., Batashev S.A., Vorobiev A.A., Toloraya S.A., Bagrov V.V., Tavtorkin A.N. The concentration effects of reactants and components in the Pd(OAc)₂/*p*-toluenesulfonic acid/trans-2,3-bis(diphenylphosphinomethyl)-norbornane catalytic system on the rate of cyclohexene hydrocarbomethoxylation. *Appl. Catal. A: Gen.* 2012;449:145–152. <https://doi.org/10.1016/j.apcata.2012.09.020>
20. Vavasori A., Toniolo L., Cavinato G. Hydroesterification of cyclohexene using the complex Pd(PPh₃)₂(TsO)₂ as catalyst precursor. Effect of a hydrogen source (TsOH, H₂O) on the TOF and a kinetic study (TsOH: *p*-toluenesulfonic acid). *J. Mol. Catal. A: Chem.* 2003;191(1):9–21. [https://doi.org/10.1016/S1381-1169\(02\)00358-8](https://doi.org/10.1016/S1381-1169(02)00358-8)
21. Aver'yanov V.A., Sevost'yanova N.T., Batashev S.A. Kinetics of cyclohexene hydrocarbalkoxylation with cyclohexanol catalyzed by the Pd(PPh₃)₂Cl₂-PPh₃-*p*-toluenesulfonic acid system. *Pet. Chem.* 2008;48(4):287–295. <https://doi.org/10.1134/S0965544108040063>
[Original Russian Text: Aver'yanov V.A., Sevost'yanova N.T., Batashev S.A. Kinetics of cyclohexene hydrocarbalkoxylation with cyclohexanol catalyzed by the Pd(PPh₃)₂Cl₂-PPh₃-*p*-toluenesulfonic acid system. *Нефтехимия.* 2008;48(4):286–294 (in Russ.).]
22. Roesle P., Stempfle F., Hess S.K., Zimmerer J., Río Bártulos C., Lepetit B., Eckert A., Kroth P.G., Mecking S. Synthetic polyester from algae oil. *Angew. Chem. Int. Ed.* 2014;53(26):6800–6804. <https://doi.org/10.1002/anie.201403991>
23. Quinzler D., Mecking S. Linear semicrystalline polyesters from fatty acids by complete feedstock molecule utilization. *Angew. Chem.* 2010;122(25):4402–4404. <https://doi.org/10.1002/ange.201001510>
24. Stempfle F., Ritter B.S., Mülhaupt R., Mecking S. Long-chain aliphatic polyesters from plant oils for injection molding, film extrusion and electrospinning. *Green Chem.* 2014;16(4):2008–2014. <https://doi.org/10.1039/C4GC00114A>
25. Dong K., Sang R., Wei Z., Liu J., Dühren R., Spannenberg A., Jiao H., Neumann H., Jackstell R., Franke R., Beller M. Cooperative catalytic methoxycarbonylation of alkenes: uncovering the role of palladium complexes with hemilabile ligands. *Chem. Sci.* 2018;9(9):2510–2516. <https://doi.org/10.1039/C7SC02964K>
26. Yang J., Liu J., Ge Y., Huang W., Ferretti F., Neumann H., Jiao H., Franke R., Jackstell R., Beller M. Efficient palladium-catalyzed carbonylation of 1,3-dienes: selective synthesis of adipates and other aliphatic diesters. *Angew. Chem. Int. Ed.* 2021;60(17):9527–9533. <https://doi.org/10.1002/anie.202015329>
27. Stempfle F., Quinzler D., Heckler I., Mecking S. Long-chain linear C₁₉ and C₂₃ monomers and polycondensates from unsaturated fatty acid esters. *Macromolecules.* 2011;44(11):4159–4166. <https://doi.org/10.1021/ma200627e>
28. Illner M., Schmidt M., Pogrzeba T., Urban C., Esche E., Schomaecker R., Repke J.-U. Palladium-catalyzed methoxycarbonylation of 1-dodecene in a two phase system: the path towards a continuous process. *Ind. Eng. Chem. Res.* 2018;57(27):8884–8894. <https://doi.org/10.1021/acs.iecr.8b01537>
29. Behr A., Vorholt A.J., Rentmeister N. Recyclable homogeneous catalyst for the hydroesterification of methyl oleate in thermomorphic solvent systems. *Chem. Eng. Sci.* 2013;99:38–43. <https://doi.org/10.1016/j.ces.2013.05.040>
30. Nifant'ev I.E., Sevostyanova N.T., Averyanov V.A., Batashev S.A., Vorobiev A.A., Toloraya S.A., Bagrov V.V., Tavtorkin A.N. The concentration effects of reactants and components in the Pd(OAc)₂/*p*-toluenesulfonic acid/trans-2,3-bis(diphenylphosphinomethyl)-norbornane catalytic system on the rate of cyclohexene hydrocarbomethoxylation. *Appl. Catal. A: Gen.* 2012;449:145–152. <https://doi.org/10.1016/j.apcata.2012.09.020>
31. Vavasori A., Toniolo L., Cavinato G. Hydroesterification of cyclohexene using the complex Pd(PPh₃)₂(TsO)₂ as catalyst precursor. Effect of a hydrogen source (TsOH, H₂O) on the TOF and a kinetic study (TsOH: *p*-toluenesulfonic acid). *J. Mol. Catal. A: Chem.* 2003;191(1):9–21. [https://doi.org/10.1016/S1381-1169\(02\)00358-8](https://doi.org/10.1016/S1381-1169(02)00358-8)
32. Аверьянов В.А., Севостьянова Н.Т., Баташев С.А. Кинетические закономерности гидрокарбоалкоксилирования циклогексена циклогексанолом, катализируемого системой Pd(PPh₃)₂Cl₂ – PPh₃ – *n*-толуолсульфокислота. *Нефтехимия.* 2008;48(4):286–294.
33. Аверьянов В.А., Баташев С.А., Севостьянова Н.Т., Носова Н.М. Кинетика и механизм катализируемого комплексом Pd(II) гидрокарбометоксилирования циклогексена. *Кинетика и катализ.* 2006;47(3):381–390.
34. Петров Э.С. Фосфиновые комплексы палладия в катализе реакций карбонилирования олефинов. *Журн. физ. химии.* 1988;62(10):2858–2868.
35. Белобородов В.Л., Зурабян С.Э., Лузин А.П., Тюкавкина Н.А. *Органическая химия*. М.: ГЭОТАР-Медиа; 2019. Кн. 1. 640 с.

22. Aver'yanov V.A., Batashev S.A., Sevost'yanova N.T., Nosova N.M. Kinetics and mechanism of cyclohexene hydroxymethoxylation catalyzed by a Pd(II) complex. *Kinet. Catal.* 2006;47(3):375–383. <https://doi.org/10.1134/S0023158406030086>
[Original Russian Text: Aver'yanov V.A., Batashev S.A., Sevost'yanova N.T., Nosova N.M. Kinetics and mechanism of cyclohexene hydroxymethoxylation catalyzed by a Pd(II) complex. *Kinetika i Kataliz.* 2006;47(3):381–390 (in Russ.).]
23. Petrov E.S. Phosphine complexes of palladium in the catalysis of olefin carbonylation reactions. *Zhurnal Fizicheskoi Khimii.* 1988;62(10):2858–2868 (in Russ.).
24. Beloborodov V.L., Zurabyan S.E., Luzin A.P., Tyukavkina N.A. *Organicheskaya khimiya (Organic Chemistry)*. Moscow: GEOTAR-Media; 2019. V. 1. 640 p. (in Russ.).

About the authors

Nadezhda T. Sevostyanova, Cand. Sci. (Chem.), Associate Professor, Senior Researcher, Head, Research and Production Center Himreaktivdiagnostika, Tula State Lev Tolstoy Pedagogical University (125, Lenina pr., Tula, 300026, Russia). E-mail: sevostyanova.nt@gmail.com. Scopus Author ID 25643582900, ResearcherID M-8567-2014, RSCI SPIN-code 9239-7136, <https://orcid.org/0000-0002-3499-2226>

Sergey A. Batashev, Cand. Sci. (Chem.), Associate Professor, Senior Researcher, Research and Production Center Himreaktivdiagnostika, Tula State Lev Tolstoy Pedagogical University (125, Lenina pr., Tula, 300026, Russia). E-mail: tulapharma@gmail.com. Scopus Author ID 14071256200, ResearcherID N-1405-2018, RSCI SPIN-code 8241-9789, <https://orcid.org/0000-0001-7537-7740>

Anastasia S. Rodionova, Researcher, Tula State Lev Tolstoy Pedagogical University (125, Lenina pr., Tula, 300026, Russia). E-mail: rodionova.nastia@ya.ru. Scopus Author ID 57189375048, <https://orcid.org/0000-0002-0896-5208>

Dar'ya K. Kozlenko, Researcher, Tula State Lev Tolstoy Pedagogical University (125, Lenina pr., Tula, 300026, Russia). E-mail: dk.reshetnikova@yandex.ru. Scopus Author ID 58600613300, <https://orcid.org/0009-0009-7166-8415>

Об авторах

Севостьянова Надежда Тенгизовна, к.х.н., доцент, старший научный сотрудник, руководитель научно-производственного центра «Химреактивдиагностика», ФГБОУ ВО «Тульский государственный педагогический университет им. Л.Н. Толстого» (300026, Россия, г. Тула, пр-т Ленина, д. 125). E-mail: sevostyanova.nt@gmail.com. Scopus Author ID 25643582900, ResearcherID M-8567-2014, SPIN-код РИНЦ 9239-7136, <https://orcid.org/0000-0002-3499-2226>

Баташев Сергей Александрович, к.х.н., доцент, старший научный сотрудник научно-производственного центра «Химреактив-диагностика», ФГБОУ ВО «Тульский государственный педагогический университет им. Л.Н. Толстого» (300026, Россия, г. Тула, пр-т Ленина, д. 125). E-mail: tulapharma@gmail.com. Scopus Author ID 14071256200, ResearcherID N-1405-2018, SPIN-код РИНЦ 8241-9789, <https://orcid.org/0000-0001-7537-7740>

Родионова Анастасия Сергеевна, исполнитель по гражданско-правовому договору реализации гранта Российского научного фонда, ФГБОУ ВО «Тульский государственный педагогический университет им. Л.Н. Толстого» (300026, Россия, г. Тула, пр-т Ленина, д. 125). E-mail: rodionova.nastia@ya.ru. Scopus Author ID 57189375048, <https://orcid.org/0000-0002-0896-5208>

Козленко Дарья Константиновна, исполнитель по гражданско-правовому договору реализации гранта Российского научного фонда, ФГБОУ ВО «Тульский государственный педагогический университет им. Л.Н. Толстого» (300026, Россия, г. Тула, пр-т Ленина, д. 125). E-mail: dk.reshetnikova@yandex.ru. Scopus Author ID 58600613300, <https://orcid.org/0009-0009-7166-8415>

Translated from Russian into English by V. Glyanchenko

Edited for English language and spelling by Dr. David Mossop

Chemistry and technology of medicinal compounds
and biologically active substances

Химия и технология лекарственных препаратов
и биологически активных соединений

UDC 577.112.345

<https://doi.org/10.32362/2410-6593-2024-19-3-202-213>

EDN FORUND



RESEARCH ARTICLE

L-Ornithine derivatives with structural hetaryl and alkyl moiety: Synthesis and antibacterial activity

Tatyana G. Bodrova, Ulyana A. Budanova✉, Yury L. Sebyakin

MIREA — Russian Technological University (M.V. Lomonosov Institute of Fine Chemical Technologies), Moscow, 119571 Russia

✉ Corresponding author, e-mail: c-221@yandex.ru

Abstract

Objectives. Cationic amphiphiles and antimicrobial peptidomimetics are widely investigated as antibacterial agents due to their membrane-active mechanism of action. Particular attention is focused on the rational design of compounds in this class to achieve high antimicrobial activity. The aim of the present work is to synthesize bivalent cationic amphiphiles with L-ornithine as a branching element and evaluate the effectiveness of their antibacterial action. The compounds differ in terms of hydrophobicity due to the variation of *N*-terminal aliphatic amino acids in the polar block and alternation of dialkyl and alkyl-hetaryl radicals in the lipophilic block.

Methods. For the synthesis of nonpolar fragments of amphiphiles, methods for the alkylation of amines with alkyl bromides in the presence of carbonate salts were used. The formation of amide bonds of L-ornithine derivatives with amino acids was carried out using the carbodiimide method. For the reaction products recovery from the reaction mixture, column chromatography on silica gel and aluminum oxide activated Brockmann grade II was used. The antimicrobial activity of the synthesized compounds against gram-positive *B. subtilis* 534 and gram-negative *E. coli* M17 bacterial strains was evaluated. Minimum inhibitory concentration (MIC) values were recorded using a serial microdilution method in a nutrient medium.

Results. Developed schemes for the preparation of bivalent cationic amphiphiles based on L-ornithine derivatives are presented. Differences in the structure of aliphatic amino acids (glycine, β -alanine, γ -aminobutyric acid (GABA)), in the length of alkyl radicals (C_8 , C_{12}), or in the presence of an indole moiety, were used in the design of target compounds. The high antibacterial activity of the synthesized compounds was demonstrated. The most active compounds were lipoamino acids with terminal GABA residues and asymmetrical non-polar block (tryptamyl–dodecylamine). The MIC values were 0.39 $\mu\text{g/mL}$ for gram-positive bacteria and 1.56 $\mu\text{g/mL}$ for gram-negative bacteria. A GABA derivative with a symmetrical lipophilic moiety based on dioctylamine demonstrated activity with an MIC of 0.78 $\mu\text{g/mL}$ against *B. subtilis* and 3.12 $\mu\text{g/mL}$ against *E. coli*.

Conclusions. Nine new lipoamino acid cationic bivalent amphiphiles based on L-ornithine were synthesized. The structure of the obtained compounds was confirmed by nuclear magnetic resonance ^1H spectroscopy and mass spectrometry data. Leading compounds in antimicrobial activity against both gram-positive and gram-negative strains of bacteria were determined. The influence of the degree of lipophilicity in the asymmetric nonpolar block on the level of exhibited antimicrobial activity is demonstrated.

Keywords

peptidomimetics, cationic amphiphiles, L-ornithine derivatives, minimum inhibitory concentration, antibacterial activity

Submitted: 03.07.2023

Revised: 07.11.2023

Accepted: 15.04.2024

For citation

Bodrova T.G., Budanova U.A., Sebyakin Yu.L. L-Ornithine derivatives with structural hetaryl and alkyl moiety: Synthesis and antibacterial activity. *Tonk. Khim. Tekhnol. = Fine Chem. Technol.* 2024;19(3):202–213. <https://doi.org/10.32362/2410-6593-2024-19-3-202-213>

НАУЧНАЯ СТАТЬЯ

Производные L-орнитина с гетарильными и алкильными фрагментами в структуре: синтез и антибактериальная активность

Т.Г. Бодрова, У.А. Буданова✉, Ю.Л. Себякин

МИРЭА — Российский технологический университет (Институт тонких химических технологий им. М.В. Ломоносова), Москва, 119571 Россия

✉ Автор для переписки, e-mail: c-221@yandex.ru

Аннотация

Цели. Катионные амфифилы и антимикробные пептидомиметики широко исследуются в качестве антибактериальных средств в связи с их мембрано-активным механизмом действия. Особое внимание уделяется рациональному дизайну данных соединений для достижения высокой антимикробной активности. Целью данной работы является синтез и определение эффективности антибактериального действия бивалентных катионных амфифилов с L-орнитином в качестве разветвителя. Соединения отличаются степенью гидрофобности за счет варьирования N-концевых алифатических аминокислот в полярном блоке и чередованием диалкильного и алкил-гетарильного радикалов в липофильном блоке.

Методы. Для синтеза неполярных фрагментов амфифилов использованы методы алкилирования аминов алкилбромидами в присутствии карбонатных солей. Формирование амидных связей производных L-орнитина с аминокислотами осуществлялось карбодиимидным методом. Для выделения продуктов реакции из реакционной смеси использовалась колоночная хроматография на силикагеле и окиси алюминия II степени активности по Брокману. Определена антимикробная активность синтезированных соединений по отношению к грамположительным *B. subtilis* 534 и грамотрицательным *E. coli* M17 штаммов бактерий. Значения минимальной ингибирующей концентрации (МИК) фиксировались с помощью метода серийных микроразбавлений в питательной среде.

Результаты. Разработаны схемы получения бивалентных катионных амфифилов на основе производных L-орнитина. В дизайне целевых соединений использовались различия в структуре алифатических аминокислот (глицин, β-аланин, γ-аминомасляная кислота (ГАМК)), в длине алкильных радикалов (C₈, C₁₂) или в наличии индольного фрагмента. Показана высокая антибактериальная активность синтезированных соединений. Наиболее активными оказались липоаминокислоты с терминальными остатками ГАМК и несимметричным неполярным блоком (триптамил–додециламин). Значения МИК составили 0.39 мкг/мл в отношении грамположительных бактерий и 1.56 мкг/мл для грамотрицательных бактерий. Производное ГАМК с симметричным липофильным фрагментом на основе диоксиламина продемонстрировало активность с МИК 0.78 мкг/мл в отношении *B. subtilis* и 3.12 мкг/мл в отношении *E. coli*.

Выводы. Синтезировано девять новых липоаминокислотных катионных бивалентных амфифилов на основе L-орнитина. Структура полученных соединений подтверждена данными спектроскопии ядерного магнитного резонанса ¹H и масс-спектрометрии. Определены соединения-лидеры по антимикробной активности как по отношению к грамположительным, так и по отношению к грамотрицательным штаммам бактерий. Показано влияние степени липофильности в асимметричном неполярном блоке на уровень проявляемой антимикробной активности.

Ключевые слова

пептидомиметики, катионные амфифилы, производные L-орнитина, минимальная ингибирующая концентрация, антибактериальная активность

Поступила: 03.07.2023

Доработана: 07.11.2023

Принята в печать: 15.04.2024

Для цитирования

Бодрова Т.Г., Буданова У.А., Себякин Ю.Л. Производные L-орнитина с гетарильными и алкильными фрагментами в структуре: синтез и антибактериальная активность. *Тонкие химические технологии*. 2024;19(3):202–213. <https://doi.org/10.32362/2410-6593-2024-19-3-202-213>

INTRODUCTION

The increasing number of antibiotic-resistant bacterial infections represents a major public health concern [1]. This can lead to longer hospital stays, the need for more outpatient follow-up, and higher costs of new drugs needed for treatment [2]. While hospital-acquired

infections have long been accompanied by high antibiotic resistance, there has also been a gradual increase in out-of-hospital infections in recent years. With the ever more rapid spread of bacterial genes due to globalization, multidrug-resistant strains are burgeoning worldwide [3].

To date, no antibiotic has entered clinical trials for which no cases of resistance have been reported [4]. This may be explained in terms of the tendency for existing antibiotics to inhibit processes necessary for bacterial survival, thus stimulating evolution by encouraging drug-resistant mutations [5–6].

Cationic amphiphiles and antimicrobial peptidomimetics are widely investigated as antibacterial agents due to their membrane-active mechanism of action, to which it is more difficult for bacteria to develop resistance [7, 8]. However, most of these compounds are limited in terms of practical application due to their low biocompatibility. For this reason, special attention is paid to the rational design of these compounds to achieve effective antimicrobial activity at minimal doses while maintaining low toxic side effects [9–12].

Indole derivatives are known to exhibit a variety of biological properties including antibacterial [13–15], antifungal [16], antiviral [17–18], antitumor [19], anti-inflammatory [20] and other activities. In this regard, the incorporation of the indole cycle into the structure of peptidomimetics seems to be a promising approach.

The aim of this study was to synthesize and determine the antibacterial efficacy of bivalent cationic amphiphiles with L-ornithine as a splitter. The compounds differ in the degree of hydrophobicity due to the variation of *N*-terminal aliphatic amino acids in the polar block and alternation of dialkyl and alkyl-hetaryl radicals in the lipophilic block (Fig.).

EXPERIMENTAL

Materials and methods

The experiments used the following commercially available chemicals and reagents without further purification: di-*tert*-butyl dicarbonate, *N,N'*-dicyclohexylcarbodiimide (DCC), 4-dimethylaminopyridine (DMAP), 1-hydroxybenzotriazole, L-lysine monohydrochloride, L-ornithine monohydrochloride, glycine, tryptophan, L-phenylalanine, γ -aminobutyric acid (GABA) (*Sigma-Aldrich*, Germany); β -alanine, tryptamine, 1-bromooctane, 1-bromododecane (*Acros Organics*, Belgium); potassium carbonic acid, sodium carbonic acid, sodium sulfuric acid anhydrous (*Chimmed*, Russia), trifluoroacetic acid (TFA) (*Biochem*, France).

The spectra obtained by ^1H nuclear magnetic resonance (NMR) spectroscopy were recorded in deuterated solvents (*Solvex-D*, Russia) deuterated chloroform (CDCl_3), dimethyl sulfoxide- d_6 ($\text{DMSO-}d_6$) on a Bruker DPX-300 NMR spectrometer (*Bruker BioSpin*, Germany) with an operating frequency of 300 MHz. The internal standard was hexamethyldisiloxane (*Sigma-Aldrich*, Germany). Mass

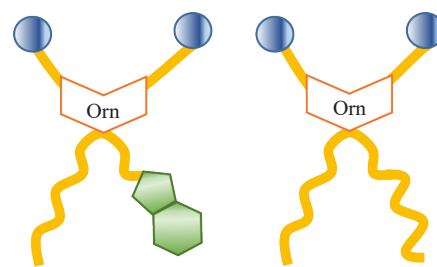


Fig. Schematic representation of target structures;
Orn — L-ornithine

spectra were recorded on a VISION 2000 time-of-flight mass spectrometer (*Thermo BioAnalysis*, United Kingdom) by MALDI (matrix assisted laser desorption/ionization), 2,4-dihydroxybenzoic acid (*Sigma-Aldrich*, Germany) was used as a matrix.

Thin-layer chromatography (TLC) was performed on Sorbfil plates (*IMID*, Russia) in solvent systems (*Component-Reactiv*, Russia): (A) chloroform-methanol 1 : 1, (B) methylene chloride-methanol 1 : 1, (C) toluene-ethyl acetate 2 : 1, (D) methylene chloride-methanol 20 : 1, (E) toluene-acetonitrile 1 : 25, (F) toluene-ethyl acetate 1 : 1, (G) toluene-ethyl acetate 7 : 1, (H) methylene chloride-methanol 25 : 1.

Column chromatography was performed on Merck 0.040–0.063 mm silica gel (*Merck*, Germany) and Brockmann L40/250 grade II aluminum oxide (*Chemapol*, Czech Republic). Detection of stains of substances by TLC was carried out by heating over a spirit flame. Substances containing double bonds were detected by aqueous potassium permanganate solution (*Chimmed*, Russia). Substances containing free amino group were detected by 5% ninhydrin solution (*Acros Organics*, Belgium) followed by heating to 55–75°C. Substances containing secondary or tertiary amino groups were detected in Dragendorff's reagent solution [21].

N-Tryptamyl-octylamine (**3a**)

We dissolved 0.50 g (3.12 mmol) of tryptamine **2**, 0.30 g (1.56 mmol) of 1-bromooctane and 0.51 g (1.56 mmol) of cesium carbonate (*Chimmed*, Russia) in 60 mL of acetonitrile. The reaction was carried out under stirring for 6 h at 25°C. Following completion of the reaction and solvent evaporation, 30 mL of distilled water was added to the reaction mixture and extracted with ethyl acetate (3 × 40 mL). The organic phase was dried over Na_2SO_4 , filtered, and evaporated using a rotary evaporator (*IKA*, Germany). The reaction was monitored by TLC in system (A). The product was isolated by column chromatography on aluminum oxide in system (E); 0.33 g (44%) of product **3a** was obtained with a retention factor $R_f(\text{A})$ of 0.38.

^1H NMR spectrum (CDCl_3 , δ , ppm): 0.87 (3H, t, CH_3); 1.25 (10H, m, $-\text{CH}_2-$); 1.5 (2H, m, $\text{CH}_2-\text{CH}_2-\text{NH}$); 2.35 (2H, s, $\text{CH}_2-\text{CH}_2-\text{NH}$ (ar)); 2.70 (2H, t, $\text{CH}_2-\text{CH}_2-\text{NH}$); 3.0 (2H, m, $\text{CH}_2-\text{CH}_2-\text{NH}$ (ar)); 3.75 (1H, qu., $-\text{NH}$); 7.15 (1H, m, ar- CH^5-); 7.20 (1H, dt, ar- CH^6-); 7.40 (2H, d, ar- CH^7-), 7.71 (1H, d, ar- CH^4-); 8.10 (1H, s, ar- NH).

N-Tryptamyl-dodecylamine (3b)

We dissolved 2.50 g (15.6 mmol) of tryptamine **2** and 3.12 g (12.5 mmol) of dodecyl bromide in tetrahydrofuran (*Component-Reaktiv*, Russia), then we added 2.60 g (18.8 mmol) of K_2CO_3 and KI (*Chimmed*, Russia) in catalytic amount. The reaction was carried out at room temperature (25°C) and under vigorous stirring for 6 h. The precipitate was then filtered off, the solvent was distilled off, and the remaining reaction mass was dissolved in ethyl acetate and washed with H_2O (3×50 mL). The organic phase was dried over Na_2SO_4 , filtered, and evaporated using a rotary evaporator. The product was isolated by column chromatography on aluminum oxide in system (H); 0.89 g (36%) of compound **3b** was obtained, $R_f(\text{B})$ 0.36.

^1H NMR spectrum (CDCl_3 , δ , ppm): 0.87 (3H, t, CH_3); 1.25 (18H, m, $-\text{CH}_2-$); 1.5 (2H, m, $\text{CH}_2-\text{CH}_2-\text{NH}$); 2.35 (2H, s, $\text{CH}_2-\text{CH}_2-\text{NH}$ (ar)); 2.70 (2H, t, $\text{CH}_2-\text{CH}_2-\text{NH}$); 3.00 (2H, m, $\text{CH}_2-\text{CH}_2-\text{NH}$ (ar)); 3.75 (1H, qu., $-\text{NH}$); 7.15 (1H, m, ar- CH^5-); 7.20 (1H, dt, ar- CH^6-); 7.42 (2H, d, ar- CH^7-), 7.72 (1H, d, ar- CH^4-); 8.10 (1H, s, ar- NH).

[α -N, δ -N-Bis-(*tert*-butoxycarbonyl)-L-ornithyl]-N'-tryptamyl octylamide (5a)

The reaction was carried out according to the described procedure [22]. From 0.93 g (2.31 mmol) of α -N, δ -N-bis-(*tert*-butoxycarbonyl)-L-ornithine (Boc_2Orn) **4** [22] and 0.63 g (2.31 mmol) of compound **3a**, 0.60 g (56%) of compound **5a** was obtained, $R_f(\text{F})$ 0.45.

^1H NMR spectrum (CDCl_3 , δ , ppm): 0.87 (3H, t, CH_3); 1.25 (10H, m, $-\text{CH}_2-$); 1.41 (18H, s, CCH_3), 1.60 (2H, m, $\text{CH}_2-\text{CH}_2-\text{NH}$ (Orn)); 1.69 (2H, m, β - CH_2); 1.90 (2H, m, ε - $\text{NH}-\text{CH}_2-\text{CH}_2-\text{CH}_2-$ (Orn)); 2.90 (2H, s, $\text{CH}_2-\text{CH}_2-\text{NH}$ (ar)); 3.13 (2H, m, $\text{CH}_2-\text{CH}_2-\text{NH}$ (Orn)); 3.24–3.41 (2H, m, α - CH_2); 3.49 (1H, s, ε - NH); 3.6–4.0 (2H, m, $\text{CH}_2-\text{CH}_2-\text{NH}$ (ar)); 4.50 (1H, α - NH (Orn)); 5.25 (1H, dd, $-\text{CH}-$ (Orn)); 7.05 (1H, d, ar- CH); 7.15 (1H, m, ar- CH^5-); 7.20 (1H, dt, ar- CH^6-); 7.43 (2H, d, ar- CH^7), 7.70 (1H, d, ar- CH^4-); 8.25 (1H, s, ar- NH).

[α -N, δ -N-Bis-(*tert*-butoxycarbonyl)-L-ornithyl]-N'-tryptamyl-dodecylamide (5b)

The reaction was carried out similarly to the preparation of compound **5a**. From 0.19 g (0.56 mmol) of

compound **4** and 0.19 g (0.56 mmol) of compound **3b**, 0.22 g (52%) of compound **5b** was obtained, $R_f(\text{F})$ 0.63.

^1H NMR spectrum (CDCl_3 , δ , ppm): 0.87 (3H, t, CH_3); 1.25 (18H, m, $-\text{CH}_2-$); 1.41 (18H, s, CCH_3), 1.60 (2H, m, $\text{CH}_2-\text{CH}_2-\text{NH}$ (Orn)); 1.71 (2H, m, β - CH_2); 1.90 (2H, m, ε - $\text{NH}-\text{CH}_2-\text{CH}_2-\text{CH}_2-$ (Orn)); 2.93 (2H, s, $\text{CH}_2-\text{CH}_2-\text{NH}$ (ar)); 3.11 (2H, m, $\text{CH}_2-\text{CH}_2-\text{NH}$ (Orn)); 3.2–3.4 (2H, m, α - CH_2); 3.49 (1H, s, ε - NH); 3.62–3.98 (2H, m, $\text{CH}_2-\text{CH}_2-\text{NH}$ (ar)); 4.50 (1H, s, α - NH (Orn)); 5.25 (1H, dd, $-\text{CH}-$ (Orn)); 7.05 (1H, d, ar- CH); 7.15 (1H, m, ar- CH^5-); 7.21 (1H, dt, ar- CH^6-); 7.40 (2H, d, ar- CH^7-), 7.72 (1H, d, ar- CH^4-); 8.25 (1H, s, ar- NH).

L-Ornithyl-N-tryptamyl octylamide (6a)

We added 650 μL (8.60 mmol) of TFA to 0.51 g (0.86 mmol) of compound **5a** in methylene chloride and stirred for 3 h. The reaction was monitored by TLC data in system (D). Following completion of the reaction, the solvent was distilled off in vacuo. The residue was dissolved in 40 mL ethyl acetate, washed with 5% NaHCO_3 solution (2×30 mL), then with H_2O (30 mL) to pH 7. The organic phase was dried over Na_2SO_4 , and the solvent was distilled off using a rotary evaporator. 15 mg (45%) of compound **6a** was obtained, $R_f(\text{A})$ 0.15. MALDI-TOF (matrix-assisted laser desorption/ionization time-of-flight) (m/z): 425 $[\text{M}+\text{K}]^+$, 409 $[\text{M}+\text{Na}]^+$.

L-Ornithyl-N-tryptamyl-dodecylamide (6b)

The reaction was carried out similarly to the preparation of compound **6a**. From 0.22 g (0.35 mmol) of compound **5b**, 68 mg (44.3%) of product **6b** was obtained, $R_f(\text{A})$ 0.23.

[α -N, δ -N-Bis-((*N*-*tert*-butoxycarbonyl)-glycyl)-ornithyl]-N'-tryptamyl octylamide (8a)

The reaction was carried out similarly to the preparation of compound **5a**. From 45 mg (0.26 mmol) of *N*-*tert*-butoxycarbonylglycine (Boc-Gly) **7c** [22] and 40 mg (0.10 mmol) of compound **6a**, 25 mg (33.5%) of compound **8a** was obtained, $R_f(\text{D})$ 0.49.

^1H NMR spectrum (CDCl_3 , δ , ppm): 0.87 (3H, t, CH_3); 1.25 (10H, m, $-\text{CH}_2-$); 1.45 (18H, s, CCH_3), 1.57 (2H, br., $\text{CH}_2-\text{CH}_2-\text{NH}$ (Orn)); 1.61 (2H, br., β - CH_2); 1.75 (2H, m, δ - $\text{NH}-\text{CH}_2-\text{CH}_2-\text{CH}_2-$ (Orn)); 2.60 (2H, s, $\text{CH}_2-\text{CH}_2-\text{NH}$ (ar)); 3.22 (2H, m, $\text{CH}_2-\text{CH}_2-\text{NH}$ (Orn)); 3.35–3.55 (2H, m, α - CH_2); 3.95 (2H, br., $-\text{CH}_2-$ (Gly)); 4.10 (2H, m, $\text{CH}_2-\text{CH}_2-\text{NH}$ (ar)); 4.51 (1H, α - NH (Orn)); 5.40 (1H, dd, $-\text{CH}-$ (Orn)); 7.05 (1H, d, ar- CH); 7.08–7.19 (1H, m, ar- CH^5-); 7.22 (1H, dt, ar- CH^6-); 7.40 (2H, d, ar- CH^7), 7.71 (1H, d, ar- CH^4-); 8.25 (1H, s, ar- NH).

[α -*N*, δ -*N*-Bis-((*N*-*t*-ret-butoxycarbonyl)- β -alanyl)-ornithyl]-*N'*-tryptamyl octylamide (**8b**)

The reaction was carried out similarly to the preparation of compound **5a**. From 68 mg (0.36 mmol) of *N*-*t*-ret-butoxycarbonyl- β -alanine (Boc- β -Ala) **7d** [22], and 55 mg (0.14 mmol) of compound **6a**, 41 mg (35%) of compound **8b** was obtained, R_f (G) 0.49.

^1H NMR spectrum (CDCl_3 , δ , ppm): 0.87 (3H, t, CH_3); 1.25 (10H, m, $-\text{CH}_2-$); 1.43 (18H, s, CCH_3), 1.62 (2H, m, $\text{CH}_2-\text{CH}_2-\text{NH}$ (Orn)); 1.73 (2H, m, $\beta-\text{CH}_2$); 1.90 (2H, m, $\delta-\text{NH}-\text{CH}_2-\text{CH}_2-\text{CH}_2-$ (Orn)); 2.25 (4H, br., $\beta-\text{CH}_2$ (β -Ala)), 2.90 (2H, s, $\text{CH}_2-\text{CH}_2-\text{NH}$ (ar)); 3.15 (2H, m, $\text{CH}_2-\text{CH}_2-\text{NH}$ (Orn)); 3.2–3.4 (2H, m, $\alpha-\text{CH}_2$); 3.35 (4H, br., $\alpha-\text{CH}_2$ (β -Ala)), 3.49 (1H, s, $\delta-\text{NH}$); 3.6–3.9 (2H, m, $\text{CH}_2-\text{CH}_2-\text{NH}$ (ar)); 4.32 (1H, br., $-\text{NH}$ (β -Ala)); 4.50 (1H, $\alpha-\text{NH}$ (Orn)); 5.25 (1H, dd, $-\text{CH}-$ (Orn)); 7.05 (1H, d, ar- $\text{CH}-$); 7.15 (1H, m, ar- CH^5-); 7.20 (1H, dt, ar- CH^6-); 7.41 (2H, d, ar- CH^7), 7.72 (1H, d, ar- CH^4-); 8.25 (1H, s, ar-NH).

[α -*N*, δ -*N*-Bis-((*N*-*t*-ret-butoxycarbonyl)-GABA)-L-ornithyl]-*N'*-tryptamyl octylamide (**8c**)

The reaction was carried out similarly to the preparation of compound **8a**. From 53 mg (0.26 mmol) of *N*-*t*-ret-butoxycarbonyl-GABA (Boc-GABA) **7e** [22] and 40 mg (0.10 mmol) of compound **6a**, 12 mg (34%) of compound **8c** was obtained, R_f (F) 0.35.

^1H NMR spectrum (CDCl_3 , δ , ppm): 0.87 (3H, t, CH_3); 1.25 (10H, m, $-\text{CH}_2-$); 1.41 (18H, s, CCH_3), 1.55–1.66 (2H, m, $\text{CH}_2-\text{CH}_2-\text{NH}$ (Orn)); 1.62–1.73 (2H, m, $\beta-\text{CH}_2$); 1.74–1.82 (4H, m, $-\text{CH}_2-\text{CH}_2-\text{CH}_2-\text{NH}$ (GABA)), 1.90 (2H, m, $\delta-\text{NH}-\text{CH}_2-\text{CH}_2-\text{CH}_2-$ (Orn)); 2.25 (4H, m, $-\text{CH}_2-\text{CH}_2-\text{CH}_2-\text{NH}$ (GABA)), 2.91 (2H, s, $\text{CH}_2-\text{CH}_2-\text{NH}$ (ar)); 3.00 (4H, m, $-\text{CH}_2-\text{CH}_2-\text{CH}_2-\text{NH}$ (GABA)), 3.12 (4H, m, $-\text{CH}_2-\text{CH}_2-\text{CH}_2-\text{NH}$ (GABA)), 3.15–3.19 (2H, m, $\text{CH}_2-\text{CH}_2-\text{NH}$ (Orn)); 3.2–3.4 (2H, m, $\alpha-\text{CH}_2$); 3.49 (1H, s, $\delta-\text{NH}$); 3.6–3.9 (2H, m, $\text{CH}_2-\text{CH}_2-\text{NH}$ (ar)); 4.02 (2H, m, $-\text{CH}_2-\text{CH}_2-\text{CH}_2-\text{NH}$ (GABA)), 4.50 (1H, $\alpha-\text{NH}$ (Orn)); 5.25 (1H, dd, $-\text{CH}-$ (Orn)); 7.05 (1H, d, ar- $\text{CH}-$); 7.15 (1H, m, ar- CH^5-); 7.20 (1H, dt, ar- CH^6-); 7.41 (2H, d, ar- CH^7); 7.71 (1H, d, ar- CH^4-); 8.25 (1H, s, ar-NH).

[α -*N*, δ -*N*-bis-((*N*-*t*-ret-butoxycarbonyl)-glycyl)-L-ornithyl]-*N'*-tryptamyl-dodecylamide (**8d**)

The reaction was carried out analogously to the preparation of compound **5a**. From 19 mg (0.11 mmol) of Boc-Gly **7c** and 20 mg (0.045 mmol) of compound **6b**, 19 mg (29%) of compound **8d** was obtained, R_f (D) 0.49.

^1H NMR spectrum (CDCl_3 , δ , ppm): 0.87 (3H, t, CH_3); 1.25 (18H, m, $-\text{CH}_2-$); 1.43 (18H, s, CCH_3), 1.50 (2H, br., $\beta-\text{CH}_2$ (alkyl)); 1.71 (2H, br., $\gamma-\text{CH}_2-$ (Orn)); 1.9–2.3 (2H, m, $\beta-\text{CH}_2-$ (Orn)); 3.11 (2H, br., $\text{CH}_2-\text{CH}_2-\text{NH}$ (ar)); 3.30 (2H, m, $\delta-\text{CH}_2-$ (Orn)); 3.40 (4H, br., $-\text{CH}_2-$ (Gly)), 3.7–3.9 (2H, m, $\alpha-\text{CH}_2-$ (ar)); 3.7–3.9 (2H, dm, $\alpha-\text{CH}_2-$ (alkyl)), 4.12 (1H, m, $-\text{CH}-$ (Orn)); 4.60 (1H, br., $\delta-\text{NH}$ (Orn)); 4.80 (2H, br., $-\text{NH}$ (Gly)); 5.11 (1H, br., $\alpha-\text{NH}$ (Orn)); 7.05 (1H, d, ar- $\text{CH}-$); 7.15 (1H, m, ar- CH^5-); 7.20 (1H, dt, ar- CH^6-); 7.41 (2H, d, ar- CH^7), 7.70 (1H, d, ar- CH^4-); 8.25 (1H, s, ar-NH).

[α -*N*, δ -*N*-Bis-((*N*-*t*-ret-butoxycarbonyl)- β -alanyl)-L-ornithyl]-*N'*-tryptamyl-dodecylamide (**8e**)

The reaction was carried out similarly to the preparation of compound **5a**. From 26 mg (0.015 mmol) of Boc- β -Ala **7d** and 27 mg (0.006 mmol) of compound **6b**, 16 mg (16%) of compound **8e** was obtained, R_f (D) 0.44.

^1H NMR spectrum (CDCl_3 , δ , ppm): 0.87 (3H, t, CH_3); 1.25 (18H, m, $-\text{CH}_2-$); 1.43 (18H, s, CCH_3), 1.49 (2H, br., $\beta-\text{CH}_2$ (alkyl)); 1.70 (2H, br., $\gamma-\text{CH}_2-$ (Orn)); 1.9–2.3 (2H, m, $\beta-\text{CH}_2-$ (Orn)); 3.03 (4H, br., $\beta-\text{CH}_2$ (β -Ala)), 3.10 (2H, br., $\text{CH}_2-\text{CH}_2-\text{NH}$ (ar)); 3.30 (2H, m, $\delta-\text{CH}_2-$ (Orn)); 3.51 (4H, br., $\alpha-\text{CH}_2$ (β -Ala)), 3.7–3.9 (2H, m, $\alpha-\text{CH}_2-$ (ar)); 3.7–3.9 (2H, m, $\alpha-\text{CH}_2-$ (alkyl)); 4.10 (1H, m, $-\text{CH}-$ (Orn)); 4.60 (1H, br., $\delta-\text{NH}$ (Orn)); 4.81 (2H, br., $-\text{NH}$ (β -Ala)); 5.08 (1H, br., $\alpha-\text{NH}$ (Orn)); 7.05 (1H, d, ar- $\text{CH}-$); 7.15 (1H, m, ar- CH^5-); 7.19 (1H, dt, ar- CH^6-); 7.40 (2H, d, ar- CH^7), 7.69 (1H, d, ar- CH^4-); 8.25 (1H, s, ar-NH).

[α -*N*, δ -*N*-Bis-((*N*-*t*-ret-butoxycarbonyl)-GABA)-L-ornithyl]-*N'*-tryptamyl-dodecylamide (**8f**)

The reaction was carried out similarly to the preparation of compound **5a**. From 28 mg (0.015 mmol) of Boc-gABA **7e** and 27 mg (0.006 mmol) of compound **6b**, 47 mg (24%) of compound **8f** was obtained, R_f (D) 0.44.

^1H NMR spectrum (CDCl_3 , δ , ppm): 0.87 (3H, t, CH_3); 1.25 (18H, m, $-\text{CH}_2-$); 1.41 (18H, s, CCH_3), 1.55 (2H, br., $\beta-\text{CH}_2$ (alkyl)); 1.70 (2H, m, $\gamma-\text{CH}_2-$ (Orn)); 1.89 (4H, m, $\gamma-\text{CH}_2-$ (GABA)), 2.21 (2H, m, $\beta-\text{CH}_2-$ (Orn)); 3.03 (4H, br., $\beta-\text{CH}_2$ (GABA)), 3.08 (2H, br., $\text{CH}_2-\text{CH}_2-\text{NH}$ (ar)); 3.29 (2H, m, $\delta-\text{CH}_2-$ (Orn)); 3.50 (4H, br., $\alpha-\text{CH}_2$ (GABA)), 3.7–3.9 (2H, m, $\alpha-\text{CH}_2-$ (ar)); 3.7–3.9 (2H, m, $\alpha-\text{CH}_2-$ (alkyl)), 4.10 (1H, m, $-\text{CH}-$ (Orn)); 4.58 (1H, br., $\delta-\text{NH}$ (Orn)); 4.77 (2H, br., $-\text{NH}$ (GABA)); 5.10 (1H, br., $\alpha-\text{NH}$ (Orn)); 7.05 (1H, d, ar- $\text{CH}-$); 7.15 (1H, m, ar- CH^5-); 7.18 (1H, dt, ar- CH^6-); 7.40 (2H, d, ar- CH^7), 7.71 (1H, d, ar- CH^4-); 8.25 (1H, s, ar-NH).

Trifluoroacetate salt
of [α -*N*, δ -*N*-bis-((*N*-*tert*-butoxycarbonyl)-
glycyl)-L-ornithyl]-*N'*-tryptamyl
octylamide (**9a**)

Compound **8a** 24 mg (0.033 mmol) was dissolved in anhydrous methylene chloride and cooled to 0°C. To the resulting solution 0.33 mmol TFA was added. The reaction mixture was stirred for 2 h at room temperature. The reaction was monitored by TLC data in system (D). The TFA and solvent were distilled off on a rotary evaporator; 23 mg (98%) of product **9a** was obtained. MALDI-TOF (*m/z*): 537 [M+K]⁺, 521 [M+Na]⁺.

Trifluoroacetate salt
of [α -*N*, δ -*N*-bis-((*N*-*tert*-butoxycarbonyl)-
 β -alanyl)-L-ornithyl]-*N'*-tryptamyl
octylamide (**9b**)

The reaction was carried out analogously to the preparation of compound **9a**. From 41 mg (0.059 mmol) of compound **8b**, 40 mg (99%) of product **9b** was obtained. MALDI-TOF (*m/z*): 567 [M+K]⁺, 551 [M+Na]⁺.

Trifluoroacetate salt
of [α -*N*, δ -*N*-bis-((*N*-*tert*-butoxycarbonyl)-
GABA)-L-ornithyl]-*N'*-tryptamyl
octylamide (**9c**)

The reaction was carried out analogously to the preparation of compound **9a**. From 12 mg (0.019 mmol) of compound **8c**, 11 mg (98%) of product **9c** was obtained. MALDI-TOF (*m/z*): 579 [M+K]⁺, 595 [M+Na]⁺.

Trifluoroacetate salt
of [α -*N*, δ -*N*-bis-((*N*-*tert*-butoxycarbonyl)-
glycyl)-L-ornithyl]-*N'*-tryptamyl-
dodecylamide (**9d**)

The reaction was carried out analogously to the preparation of compound **9a**. From 19 mg (0.026 mmol) of compound **8d**, 18 mg (99%) of product **9d** was obtained. MALDI-TOF (*m/z*): 595 [M+K]⁺, 579 [M+Na]⁺.

Trifluoroacetate salt
of [α -*N*, δ -*N*-bis-((*N*-*tert*-butoxycarbonyl)-
 β -alanyl)-L-ornithyl]-*N'*-tryptamyl-
dodecylamide (**9e**)

The reaction was carried out analogously to the preparation of compound **9a**. From 16 mg (0.021 mmol) of compound **8e**, 16 mg (99%) of product **9e** was obtained. MALDI-TOF (*m/z*): 623 [M+K]⁺, 607 [M+Na]⁺.

Trifluoroacetate salt
of [α -*N*, δ -*N*-di-((*N*-*tert*-butoxycarbonyl)-GABA)-
L-ornithyl]-*N'*-tryptamyl-dodecylamide (**9f**)

The reaction was carried out analogously to the preparation of compound **9a**. From 41 mg (0.053 mmol) of compound **8f**, 43.3 mg (99%) of product **9f** was obtained. MALDI-TOF (*m/z*): 651 [M+K]⁺, 635 [M+Na]⁺.

[α -*N*, δ -*N*-Bis-((*tert*-butoxycarbonyl)-L-ornithyl)-
N'-dioctylamide (**11**)

The reaction was carried out analogously to the preparation of compound **5a**. From 1.00 g (4.14 mmol) of Boc₂Orn **4**, 1.71 g (8.29 mmol) of DCC, and 1.66 g of dioctylamine **10**, 0.95 g (75%) of compound **11** was obtained, *R_f* (F) 0.64.

¹H NMR spectrum (CDCl₃, δ , ppm): 0.87 (6H, t, CH₃); 1.27 (20H, m, -CH₂-); 1.44 (18H, s, CCH₃), 1.55 (4H, br., -CH₂-CH₂-NH-CH₂-CH₂-); 1.73 (2H, m, CH₂-CH₂-NH (Orn)); 1.92 (2H, m, δ -NH-CH₂-CH₂-CH₂- (Orn)); 3.03–3.25 (2H, m, CH₂-CH₂-NH (Orn)); 3.50 (4H, m, CH₂-CH₂-NH-CH₂-CH₂-) 4.52 (1H, s, δ -NH); 5.01 (1H, α -NH (Orn)).

L-Ornithyl-*N*-dioctylamide (**12**)

The reaction was carried out similarly to the preparation of compound **6a**. From 0.95 g (1.69 mmol) of compound **11**, 0.30 g (49%) of compound **12** was obtained, *R_f* (A) 0.19.

[α -*N*, δ -*N*-Bis-((*N*-*tert*-butoxycarbonyl)-glycyl)-
L-ornithyl]-*N'*-dioctylamide (**13a**)

The reaction was carried out similarly to the preparation of compound **5a**. From 0.12 g (0.07 mmol) of Boc-Gly **7c** and 0.02 g (0.028 mmol) of compound **12**, 23 mg (29%) of compound **13a** was obtained, *R_f* (D) 0.57.

¹H NMR spectrum (CDCl₃, δ , ppm): 0.87 (6H, t, CH₃); 1.27 (20H, m, -CH₂-); 1.44 (18H, s, CCH₃); 1.55 (4H, br., -CH₂-CH₂-NH-CH₂-CH₂-); 1.59 (2H, m, CH₂-CH₂-NH (Orn)); 1.90 (2H, m, δ -NH-CH₂-CH₂-CH₂- (Orn)); 3.10–3.25 (2H, m, CH₂-CH₂-NH (Orn)); 3.20 (4H, m, -CH₂- (Gly)); 3.45 (4H, m, CH₂-CH₂-NH-CH₂-CH₂-); 3.81 (2H, br., -NH (Gly)); 4.81 (1H, s, δ -NH); 5.10 (1H, α -NH (Orn)).

[α -*N*, δ -*N*-Bis-((*N*-*tert*-butoxycarbonyl)-
 β -alanyl)-L-ornithyl]-*N'*-dioctylamide (**13b**)

The reaction was carried out similarly to the preparation of compound **5a**. From 0.12 g (0.063 mmol) of Boc- β -Ala **7d** and 0.10 g (0.028 mmol) of compound **12**, 19.5 mg (31%) of compound **13b** was obtained, *R_f* (H) 0.55.

^1H NMR spectrum (CDCl_3 , δ , ppm): 0.87 (6H, t, CH_3); 1.27 (20H, m, $-\text{CH}_2-$); 1.44 (18H, s, CCH_3); 1.55 (4H, br., $-\text{CH}_2-\text{CH}_2-\text{NH}-\text{CH}_2-\text{CH}_2-$); 1.60 (2H, m, $\text{CH}_2-\text{CH}_2-\text{NH}$ (Orn)); 1.89 (2H, m, $\delta\text{-NH}-\text{CH}_2-\text{CH}_2-\text{CH}_2-$ (Orn)); 3.00 (4H, br., $\beta\text{-CH}_2$ ($\beta\text{-Ala}$), 3.12–3.25 (2H, m, $\text{CH}_2-\text{CH}_2-\text{NH}$ (Orn)); 3.45 (4H, m, $\text{CH}_2-\text{CH}_2-\text{NH}-\text{CH}_2-\text{CH}_2$); 3.50 (4H, br., $\alpha\text{-CH}_2$ ($\beta\text{-Ala}$)); 4.80 (1H, s, $\delta\text{-NH}$); 5.10 (2H, br., $-\text{NH}$ ($\beta\text{-Ala}$)); 5.28 (1H, d, $\alpha\text{-NH}$ (Orn)).

[$\alpha\text{-N},\delta\text{-N}$ -Bis-((*N*-*tert*-butoxycarbonyl)-GABA)-L-ornithyl]-*N'*-dioctylamide (**13c**)

The reaction was carried out similarly to the preparation of compound **5a**. From 0.14 g (0.07 mmol) of Boc-gABA **7e** and 0.10 g (0.028 mmol) of compound **12**, 20 mg (27%) of compound **13c** was obtained, R_f (H) 0.60.

^1H NMR spectrum (CDCl_3 , δ , ppm): 0.87 (6H, t, CH_3); 1.27 (20H, m, $-\text{CH}_2-$); 1.44 (18H, s, CCH_3); 1.55 (4H, br., $-\text{CH}_2-\text{CH}_2-\text{NH}-\text{CH}_2-\text{CH}_2-$); 1.73 (2H, m, $\text{CH}_2-\text{CH}_2-\text{NH}$ (Orn)); 1.91 (4H, m, $\gamma\text{-CH}_2-$ (GABA)); 1.92 (2H, m, $\delta\text{-NH}-\text{CH}_2-\text{CH}_2-\text{CH}_2-$ (Orn)); 2.97 (4H, br., $\beta\text{-CH}_2$ (GABA)); 3.01–3.22 (2H, m, $\text{CH}_2-\text{CH}_2-\text{NH}$ (Orn)); 3.50 (4H, m, $\text{CH}_2-\text{CH}_2-\text{NH}-\text{CH}_2-\text{CH}_2$); 3.58 (4H, br., $\alpha\text{-CH}_2$ (GABA)); 4.50 (1H, s, $\delta\text{-NH}$); 4.77 (2H, br., $-\text{NH}$ (GABA)); 5.01 (1H, $\alpha\text{-NH}$ (Orn)).

Trifluoroacetate salt of [$\alpha\text{-N},\delta\text{-N}$ -bis-((*N*-*tert*-butoxycarbonyl)-glycyl)-L-ornithyl]-*N'*-dioctylamide (**14a**)

The reaction was carried out similarly to the preparation of compound **9a**. From 23 mg (0.033 mmol) of compound **13a**, 23 mg (99%) of product **14a** was obtained. MALDI-TOF (m/z): 508 [$\text{M}+\text{K}$] $^+$, 492 [$\text{M}+\text{Na}$] $^+$.

Trifluoroacetate salt of [$\alpha\text{-N},\delta\text{-N}$ -bis-((*N*-*tert*-butoxycarbonyl)- β -alanyl)-L-ornithyl]-*N'*-dioctylamide (**14b**)

The reaction was carried out similarly to the preparation of compound **9a**. From 19 mg (0.028 mmol) of compound **13b**, 20 mg (99%) of product **14b** was obtained. MALDI-TOF (m/z): 536 [$\text{M}+\text{K}$] $^+$, 520 [$\text{M}+\text{Na}$] $^+$.

Trifluoroacetate salt of [$\alpha\text{-N},\beta\text{-N}$ -bis-((*N*-*tert*-butoxycarbonyl)-GABA)-L-ornithyl]-*N'*-dioctylamide (**14c**)

The reaction was carried out similarly to the preparation of compound **9a**. From 20 mg (0.028 mmol) of compound **13c**, 21 mg (99%) of product **14c** was obtained. MALDI-TOF (m/z): 564 [$\text{M}+\text{K}$] $^+$, 548 [$\text{M}+\text{Na}$] $^+$.

Antibacterial activity

Antibacterial activity was studied by determining the minimum inhibitory concentration (MIC) by serial broth microdilution [23]. Suspensions of *B. Subtilis* 534 and *E. coli* M17 with a concentration of 1.5×10^8 CFU/mL and an optical density of 0.5 McFarland units were used as test microorganisms. The wells of a 96-well plate were filled with 50 μL each of the contaminated broth and appropriate amounts of the test compounds. The plates were incubated at $36 \pm 1^\circ\text{C}$ for 16–18 h. The MIC of the substances is taken as the first transparent well in the row when counting from the right-hand side.

RESULTS AND DISCUSSION

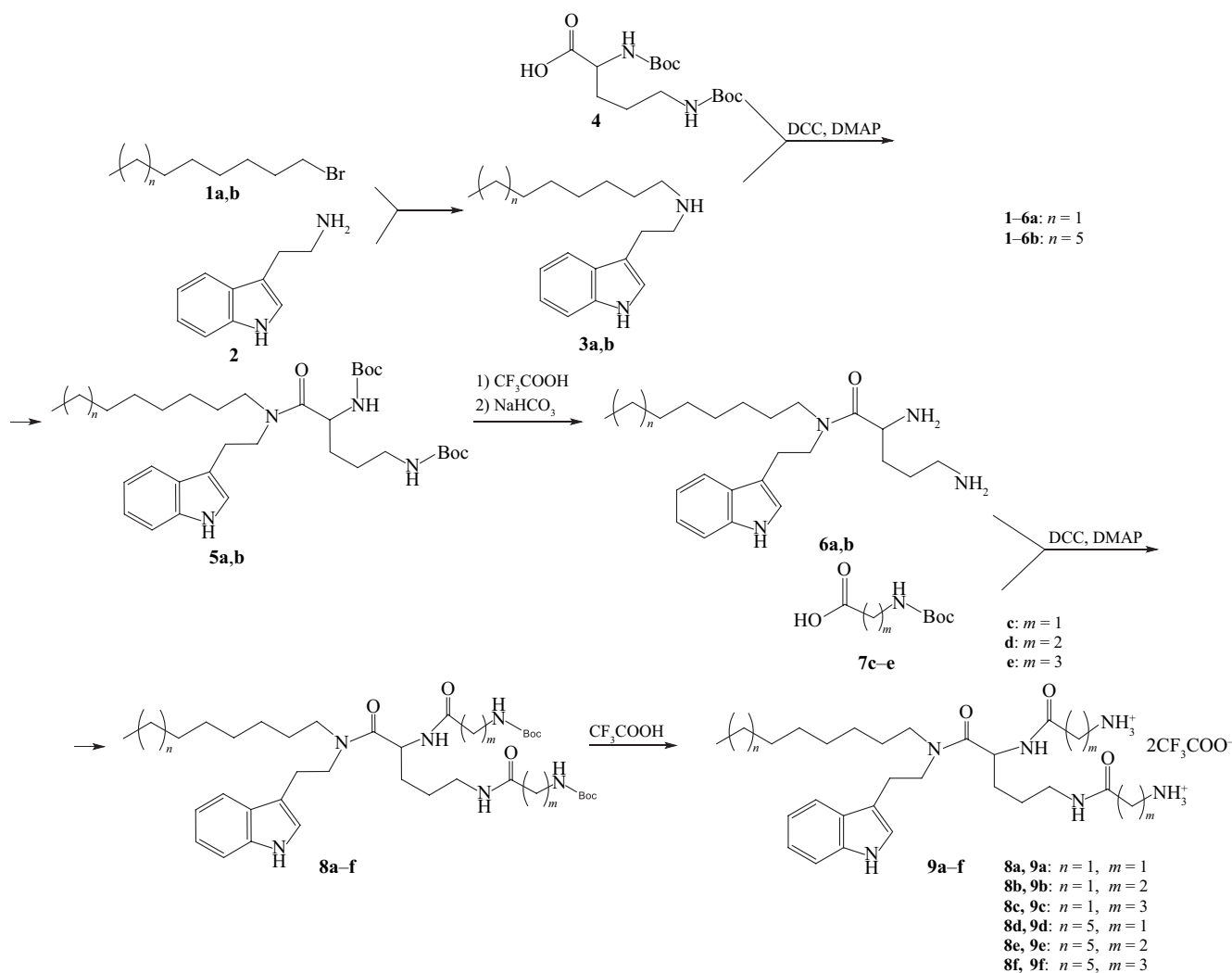
The design of target compounds was based on differences in the structure of aliphatic amino acids (glycine, β -alanine, GABA), in the length of alkyl radicals (C_8 , C_{12}), or in the presence of an indole fragment.

A developed scheme for the preparation of bivalent cationic amphiphiles based on L-ornithine derivatives containing a tryptamine residue was based on differences in the length of aliphatic chains C_8 and C_{12} (Scheme 1).

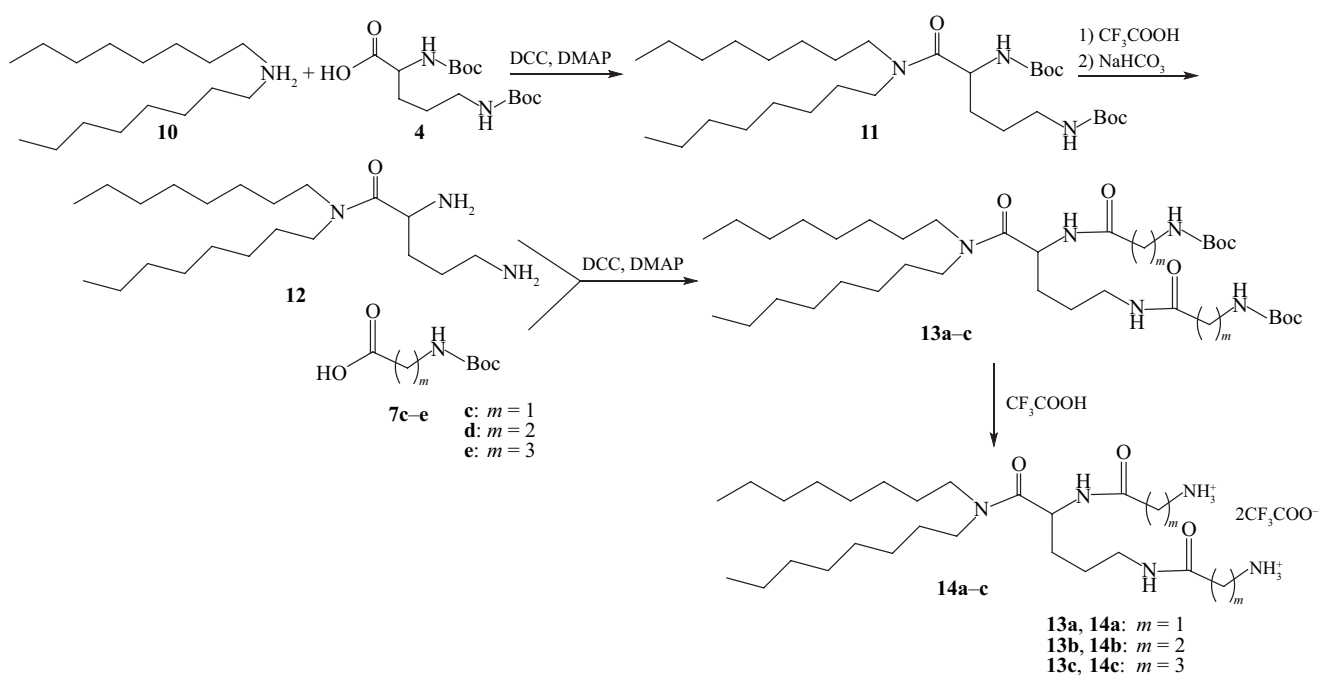
To obtain compound **3a**, the alkylation of tryptamine **2** was carried out with octyl bromide in the presence of potassium carbonate and potassium iodide in acetonitrile. The alkylation reaction with dodecyl bromide was carried out in tetrahydrofuran in the presence of cesium carbonate. The products were separated by column chromatography on aluminum oxide. Boc-protected L-ornithine was attached to the obtained tryptamine derivatives by carbodiimide method. The products were isolated by column chromatography on silica gel. To obtain compounds **6a,b** with free amino groups, **5a,b** was treated with a solution of TFA in methylene chloride (volume ratio 1 : 1) followed by treatment with 5% NaHCO_3 solution.

The addition of Boc-protected glycine, β -alanine and GABA residues to **6a,b** was carried out in the presence of DCC and DMAP. Protective groups were removed using the standard method to give trifluoroacetate salts of **9a–f**. The structure of the target and intermediate compounds was confirmed by ^1H NMR spectroscopy and mass spectrometry. The NMR spectra contained proton signals characteristic of aliphatic radicals in the hydrophobic block, aromatic rings of tryptamine residue, and the hydrocarbon skeleton of amino acids.

Scheme 2 was used to prepare L-ornithine derivatives with a symmetrical lipophilic fragment of two alkyl chains.

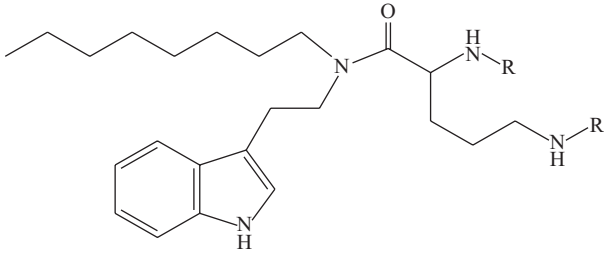
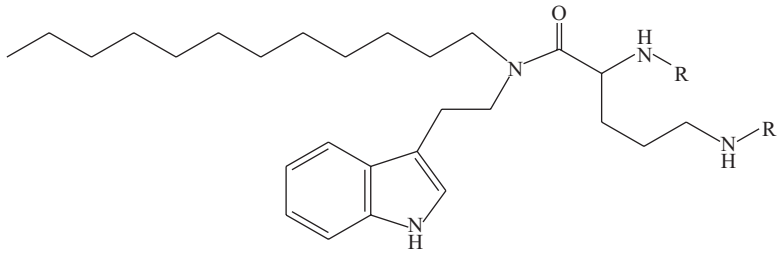
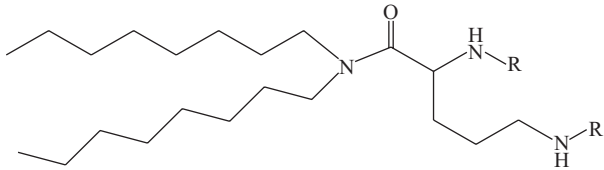


Scheme 1. Synthesis of amphiphiles with hetaryl moiety



Scheme 2. Synthesis of amphiphiles with dialkyl moiety

Table. Minimum inhibitory concentration of compounds **9a–f**, **14a–c** against gram-negative bacteria *E. coli* and gram-positive bacteria *B. subtilis*

Structures	Sample code	–R	MIC, µg/mL	
			<i>E. coli</i> M17	<i>B. subtilis</i> 534
	9a	Gly	3.12	6.25
	9b	β-Ala	3.12	1.56
	9c	GABA	1.56	1.56
	9d	Gly	6.25	3.12
	9e	β-Ala	3.12	0.39
	9f	GABA	1.56	0.39
	14a	Gly	6.25	6.25
	14b	β-Ala	6.25	1.56
	14c	GABA	3.12	0.78

Compound **11** was prepared similarly to **5a,b** from Boc-protected L-ornithine **4** and dioctylamine **10** by carbodiimide method. The reaction product was isolated by column chromatography on silica gel. Aliphatic amino acids were attached to free amino groups of L-ornithine **12** derivative with subsequent removal of Boc-protecting groups. The structure of the obtained compounds was confirmed by MALDI mass spectrometry. Molecular ion peaks were present in the mass spectra of compounds **14a–c**.

Antimicrobial activity was determined for the synthesized compounds against gram-positive *B. subtilis* and gram-negative *E. coli* bacterial strains. The MIC values were fixed using the method of serial broth microdilution (Table).

The most active compounds were lipoamino acids with terminal GABA residues and unsymmetrical nonpolar block (tryptamyl-dodecylamine). MIC values were 0.39 µg/mL against gram-positive bacteria and 1.56 µg/mL for gram-negative bacteria. A GABA derivative with a symmetric lipophilic moiety based on dioctylamine showed activity with MICs of 0.78 µg/mL against *B. subtilis* and 3.12 µg/mL against *E. coli*.

CONCLUSIONS

As a result of this work, the synthesis of nine new lipoaminoacid bivalent cationic amphiphiles based on L-ornithine was carried out. The structure of the obtained compounds was confirmed by ¹H NMR spectroscopy and mass spectrometry. High antibacterial activity of the synthesized compounds was demonstrated. The leading compounds with low MIC values both against gram-positive and gram-negative bacterial strains were revealed. The influence of the degree of lipophilicity in the asymmetric nonpolar block on the level of antimicrobial activity was demonstrated.

Acknowledgments

This work was performed using the equipment of the Shared Science and Training Center for Collective Use at the RTU MIREA and supported by the Ministry of Science and Higher Education of the Russian Federation within the framework of agreement No. 075-15-2021-689 dated September 01, 2021.

Authors' contributions

T.G. Bodrova—conducting research, collecting and providing material.

U.A. Budanova—carrying out individual stages of the study, writing the text of the article.

Yu.L. Sebyakin—development of the concept of scientific work, literature review, scientific editing of the article.

The authors declare no conflicts of interest.

REFERENCES

1. Francine P. Systems Biology: New Insight into Antibiotic Resistance. *Microorganisms*. 2022;10(12):2362. <https://doi.org/10.3390/microorganisms10122362>
2. Van Duin D., Paterson D.L. Multidrug-Resistant Bacteria in the Community: An Update. *Infect. Dis. Clin. North Am.* 2020;34(4):709–722. <https://doi.org/10.1016/j.idc.2020.08.002>
3. Mayegowda S.B., Ng M., Alghamdi S., Atwah B., Alhindi Z., Islam F. Role of Antimicrobial Drug in the Development of Potential Therapeutics. *Evid. Based Complement. Alternat. Med.* 2022;2022:2500613. <https://doi.org/10.1155/2022/2500613>
4. Bakka T.A., Strøm M.B., Andersen J.H., Gautun O.R. Synthesis and antimicrobial evaluation of cationic low molecular weight amphipathic 1, 2, 3-triazoles. *Bioorg. Med. Chem. Lett.* 2017;27(5):1119–1123. <https://doi.org/10.1016/j.bmcl.2017.01.092>
5. Taubes G. The bacteria fight back. *Science*. 2008;321(5887):356–361. <https://doi.org/10.1126/science.321.5887.356>
6. Bortolotti A., Troiano C., Bobone S., Konai M.M., Ghosh C., Bocchinfuso G., Acharya Y., Santucci V., Bonacorsi S., Di Stefano C., Haldar J., Stella L. Mechanism of lipid bilayer perturbation by bactericidal membrane-active small molecules. *Biochim. Biophys. Acta Biomembr.* 2023;1865(1):184079. <https://doi.org/10.1016/j.bbamem.2022.184079>
7. Kristiansson E., Fick J., Janzon A., Grabic R., Rutgersson C., Weijdegård B., Söderström H., Larsson D.G. Pyrosequencing of antibiotic-contaminated river sediments reveals high levels of resistance and gene transfer elements. *PLoS One*. 2011;6(2):e17038. <https://doi.org/10.1371/journal.pone.0017038>
8. Guo Y., Hou E., Wen T., Yan X., Han M., Bai L.P., Fu X., Liu J., Qin S. Development of Membrane-Active Honokiol/Magnolol Amphiphiles as Potent Antibacterial Agents against Methicillin-Resistant *Staphylococcus aureus* (MRSA). *J. Med. Chem.* 2021;64(17):12903–12916. <https://doi.org/10.1021/acs.jmedchem.1c01073>
9. Schweizer L., Ramirez D., Schweizer F. Effects of Lysine *N*- ζ -Methylation in Ultrashort Tetrabasic Lipopeptides (UTBLPs) on the Potentiation of Rifampicin, Novobiocin, and Niclosamide in Gram-Negative Bacteria. *Antibiotics*. 2022;11(3):335. <https://doi.org/10.3390/antibiotics11030335>
10. Neubauer D., Jaśkiewicz M., Bauer M., Gołacki K., Kamysz W. Ultrashort Cationic Lipopeptides—Effect of *N*-Terminal Amino Acid and Fatty Acid Type on Antimicrobial Activity and Hemolysis. *Molecules*. 2020;25(2):257. <https://doi.org/10.3390/molecules25020257>
11. Dawgul M.A., Greber K.E., Bartoszewska S., Baranska-Rybak W., Sawicki W., Kamysz W. *In Vitro* Evaluation of Cytotoxicity and Permeation Study on Lysine- and Arginine-Based Lipopeptides with Proven Antimicrobial Activity. *Molecules*. 2017;22(12):2173. <https://doi.org/10.3390/molecules22122173>
12. Wang M., Feng X., Gao R., Sang P., Pan X., Wei L., Lu C., Wu C., Cai J. Modular Design of Membrane-Active Antibiotics: From Macromolecular Antimicrobials to Small Scorpionlike Peptidomimetics. *J. Med. Chem.* 2021;64(14):9894–9905. <https://doi.org/10.1021/acs.jmedchem.1c00312>
13. Rehberg N., Sommer G.A., Drießen D., Kruppa M., Adeniyi E.T., Chen S., Wang L., Wolf K., Tasch B.O.A., Ioerger T.R., Zhu K., Müller T.J.J., Kalscheuer R. Nature-Inspired (di)Azine-Bridged Bisindole Alkaloids with Potent Antibacterial *in Vitro* and *in Vivo* Efficacy against Methicillin-Resistant *Staphylococcus aureus*. *J. Med. Chem.* 2020;63(21):12623–12641. <https://doi.org/10.1021/acs.jmedchem.0c00826>
14. Yu H.F., Qin X.J., Ding C.F., Wei X., Yang J., Luo J.R., Liu L., Khan A., Zhang L.C., Xia C.F., Luo X.D. Nepenthe-Like Indole Alkaloids with Antimicrobial Activity from *Ervatamia chinensis*. *Org. Lett.* 2018;20(13):4116–4120. <https://doi.org/10.1021/acs.orglett.8b01675>
15. Liu J., Li H., He Q., Chen K., Chen Y., Zhong R., Li H., Fang S., Liu S., Lin S. Design, synthesis, and biological evaluation of tetrahydroquinoline amphiphiles as membrane-targeting antimicrobials against pathogenic bacteria and fungi. *Eur. J. Med. Chem.* 2022;243:114734. <https://doi.org/10.1016/j.ejmech.2022.114734>
16. Lawrence C.L., Okoh A.O., Vishwapathi V., McKenna S.T., Critchley M.E., Smith R.B. *N*-alkylated linear heptamethine polyenes as potent non-azole leads against *Candida albicans* fungal infections. *Bioorg. Chem.* 2020;102:104070. <https://doi.org/10.1016/j.bioorg.2020.104070>
17. Whitby L.R., Boyle K.E., Cai L., Yu X., Gochin M., Boger D.L. Discovery of HIV fusion inhibitors targeting gp41 using a comprehensive α -helix mimetic library. *Bioorg. Med. Chem. Lett.* 2012;22(8):2861–2865. <https://doi.org/10.1016/j.bmcl.2012.02.062>
18. Lee W.G., Gallardo-Macias R., Frey K.M., Spasov K.A., Bollini M., Anderson K.S., Jorgensen W.L. Picomolar inhibitors of HIV reverse transcriptase featuring bicyclic replacement of a cyanovinylphenyl group. *J. Am. Chem. Soc.* 2013;135(44):16705–16713. <https://doi.org/10.1021/ja408917n>
19. Pape V.F., Tóth S., Füredi A., Szebényi K., Lovrics A., Szabó P., Wiese M., Szakács G. Design, synthesis and biological evaluation of thiosemicarbazones, hydrazinobenzothiazoles and arylhydrazones as anticancer agents with a potential to overcome multidrug resistance. *Eur. J. Med. Chem.* 2016;117:335–354. <https://doi.org/10.1016/j.ejmech.2016.03.078>
20. Özdemir A., Altıntop M.D., Turan-Zitouni G., Çiftçi G.A., Ertoran İ., Alataş Ö., Kaplancikli Z.A. Synthesis and evaluation of new indole-based chalcones as potential antiinflammatory agents. *Eur. J. Med. Chem.* 2015;89:304–309. <https://doi.org/10.1016/j.ejmech.2014.10.056>
21. Korotkin M.D., Filatova S.M., Denieva Z.G., Budanova U.A., Sebyakin Y.L. Synthesis of diethanolamine-based amino acid derivatives with symmetric and asymmetric radicals in their hydrophobic domain and potential antimicrobial activity. *Tonk. Khim. Tekhnol. = Fine Chem. Technol.* 2022;17(1):50–64 (Russ., Eng.). <https://doi.org/10.32362/2410-6593-2022-17-1-50-64>

22. Guseva M.K., Budanova U.A., Sebyakin Yu.L. Synthesis and evaluation of the antimicrobial activity of cationic amphiphiles based on bivalent diethylenetriamine derivatives. *Pharm. Chem. J.* 2023;56(12):1607–1612 <https://doi.org/10.1007/s11094-023-02834-z>

[Original Russian Text: Guseva M.K., Budanova U.A., Sebyakin Yu.L. Synthesis and evaluation of the antimicrobial activity of cationic amphiphiles based on bivalent diethylenetriamine derivatives. *Khimiko-Farmatsevticheskii Zhurnal.* 2023;56(12):38–43 (in Russ.). <https://doi.org/10.30906/0023-1134-2022-56-12-38-43>]

About the authors

Tatyana G. Bodrova, Master Student, Medicinal and Organic Chemistry, M.V. Lomonosov Institute of Fine Chemical Technologies, MIREA – Russian Technological University (86, Vernadskogo pr., Moscow, 119571, Russia). E-mail: btatg2014@yandex.ru

Ulyana A. Budanova, Cand. Sci. (Chem.), Associate Professor, N.A. Preobrazhensky Department of Chemistry and Technology of Biologically Active Compounds, Medical and Organic Chemistry, M.V. Lomonosov Institute of Fine Chemical Technologies, MIREA – Russian Technological University (86, Vernadskogo pr., Moscow, 119571, Russia). E-mail: c-221@yandex.ru. Scopus Author ID 14622352500, ResearcherID E-1659-2014, RSCI SPIN-code 3901-8710, <https://orcid.org/0000-0003-1702-9435>

Yury L. Sebyakin, Dr. Sci. (Chem.), Professor, N.A. Preobrazhensky Department of Chemistry and Technology of Biologically Active Compounds, Medical and Organic Chemistry, M.V. Lomonosov Institute of Fine Chemical Technologies, MIREA – Russian Technological University (86, Vernadskogo pr., Moscow, 119571, Russia). E-mail: c-221@yandex.ru. Scopus Author ID 6701455145, ResearcherID T-2835-2019, RSCI SPIN-code 3491-3514, <https://orcid.org/0000-0002-7027-378X>

Об авторах

Бодрова Татьяна Геннадьевна, магистрант, Институт тонких химических технологий им. М.В. Ломоносова, ФГБОУ ВО «МИРЭА – Российский технологический университет» (119571, Россия, Москва, пр-т Вернадского, д. 86). E-mail: btatg2014@yandex.ru

Буданова Ульяна Александровна, к.х.н., доцент кафедры химии и технологии биологически активных соединений, медицинской и органической химии им. Н.А. Преображенского, Институт тонких химических технологий им. М.В. Ломоносова, ФГБОУ ВО «МИРЭА – Российский технологический университет» (119571, Россия, Москва, пр-т Вернадского, д. 86). E-mail: c-221@yandex.ru. Scopus Author ID 14622352500, ResearcherID E-1659-2014, SPIN-код РИНЦ 3901-8710, <https://orcid.org/0000-0003-1702-9435>

Себякин Юрий Львович, д.х.н., профессор кафедры химии и технологии биологически активных соединений, медицинской и органической химии им. Н.А. Преображенского, Институт тонких химических технологий им. М.В. Ломоносова, ФГБОУ ВО «МИРЭА – Российский технологический университет» (119571, Россия, Москва, пр-т Вернадского, д. 86). E-mail: c-221@yandex.ru. Scopus Author ID 6701455145, ResearcherID T-2835-2019, SPIN-код РИНЦ 3491-3514, <https://orcid.org/0000-0002-7027-378X>

Translated from Russian into English by H. Moshkov

Edited for English language and spelling by Thomas A. Beavitt

Chemistry and technology of medicinal compounds
and biologically active substances

Химия и технология лекарственных препаратов
и биологически активных соединений

UDC 615.281.8, 544.165, 615.275.4

<https://doi.org/10.32362/2410-6593-2024-19-3-214-231>

EDN FUJWGT



REVIEW ARTICLE

PROTAC[®] technology and potential for its application in infection control

Maria A. Zakharova[✉], Mikhail V. Chudinov

MIREA — Russian Technological University (M.V. Lomonosov Institute of Fine Chemical Technologies), Moscow, 119571
Russia

[✉] Corresponding author, e-mail: matildafox@mail.ru

Abstract

Objectives. To describe the pharmaceutical technology of controlled degradation of protein molecules (PROTAC[®], Proteolysis Targeting Chimera), approaches to the design of the PROTAC[®] molecule, methods of ligand and linker selection and synthesis, as well as the application of this technology in dealing with a variety of diseases and the possible limitations of its use.

Results. The review covers 77 sources, mostly from 2020–2023. The review outlines the principle of PROTAC[®] technology: the construction of a chimeric molecule consisting of three fragments. One fragment specifically binds to the biotarget, another recruits the proteolytic system of the host cell, and the third binds them together. The main areas of the current development of the technology are described herein, as well as the opportunities and limitations of chimeric molecules in the fight against different types of infectious diseases.

Conclusion. The potential to use PROTAC[®] technology to combat cancer as well as neurodegenerative, autoimmune, and infectious diseases is shown.

Keywords

PROTAC, ubiquitin-proteasome system, E3 ligases, molecular design, antiviral drugs

Submitted: 30.08.2023

Revised: 03.11.2023

Accepted: 11.04.2024

For citation

Zakharova M.A., Chudinov M.V. PROTAC[®] technology and potential for its application in infection control. *Tonk. Khim. Tekhnol. = Fine Chem. Technol.* 2024;19(3):214–231. <https://doi.org/10.32362/2410-6593-2024-19-3-214-231>

ОБЗОРНАЯ СТАТЬЯ

Технология PROTAC® и перспективы ее применения в борьбе с инфекциями

М.А. Захарова✉, М.В. Чудинов

МИРЭА — Российский технологический университет (Институт тонких химических технологий им. М.В. Ломоносова),
Москва, 119571 Россия

✉ Автор для переписки, e-mail: matildafox@mail.ru

Аннотация

Цели. Описать фармацевтическую технологию направленной деградации белковых молекул (PROTAC®, PROTeolysis Targeting Chimera), подходы к конструированию молекулы PROTAC®, методы подбора и синтеза лигандов и линкера, а также применение данной технологии в борьбе с различными заболеваниями и возможные ограничения ее использования.

Результаты. Обзор охватывает 77 источников, в основном за 2020–2023 гг. В обзоре изложен принцип технологии PROTAC®, который заключается в конструировании химерной молекулы, состоящей из трех фрагментов. Один фрагмент специфически связывается с биомшенью, другой рекрутирует протеолитическую систему клетки-хозяина, а третий связывает их между собой. Описаны направления современного развития технологии, а также возможности и ограничения химерных молекул в борьбе с разными типами инфекционных заболеваний.

Выводы. Показаны перспективы использования технологии PROTAC® в борьбе с онкологическими, нейродегенеративными, аутоиммунными и инфекционными заболеваниями.

Ключевые слова

PROTAC, убиквитин-протеасомная система, лигазы E3, молекулярный дизайн, противовирусные препараты

Поступила: 30.08.2023

Доработана: 03.11.2023

Принята в печать: 11.04.2024

Для цитирования

Захарова М.А., Чудинов М.В. Технология PROTAC® и перспективы ее применения в борьбе с инфекциями. *Тонкие химические технологии*. 2024;19(3):214–231. <https://doi.org/10.32362/2410-6593-2024-19-3-214-231>

INTRODUCTION

Chimeric molecule technology used in the controlled degradation of proteins (PROTAC®, Proteolysis Targeting Chimeras) is one of the most promising developments in rational drug design. The concept of drugs based on controlled degradation of selected target proteins was proposed in 2001 [1], while active development started only a few years ago. In 2016, the PubMed¹ database contained references to only 13 publications with the PROTAC keyword. In 2022 there were already 479 of such references. Although, at the moment, no drug based on this technology has yet received FDA (U.S. Food and Drug Administration) approval, at least 15 such drugs, mostly antitumor drugs, are in various stages of clinical trials. The theoretical mechanism of the PROTAC®

molecule action is schematically presented in Fig. 1. The target molecule is constructed of 3 blocks: block 1 is responsible for binding to the target protein; block 2 is responsible for interaction with the enzyme ubiquitinligase E3 (EC 2.3.2.27)²; and block 3 binds them together. The PROTAC® molecule binds the first ligand fragment to the target protein, while the second fragment interacts with the E3 ligase. Thus, protein molecules are physically brought closer together. The main function of E3 ligases is to trigger the mechanism of labeling different proteins with the peptide fragment ubiquitin. This mechanism is mediated by another enzyme, E2 ligase, and carries out the destruction of unnecessary protein molecules in the cell by a special proteasomal enzyme complex [2]. As a result of PROTAC® molecule action, the target protein molecule

¹ <https://pubmed.ncbi.nlm.nih.gov/>. Accessed February 26, 2024.

² <https://www.brenda-enzymes.org/>. Accessed February 26, 2024.

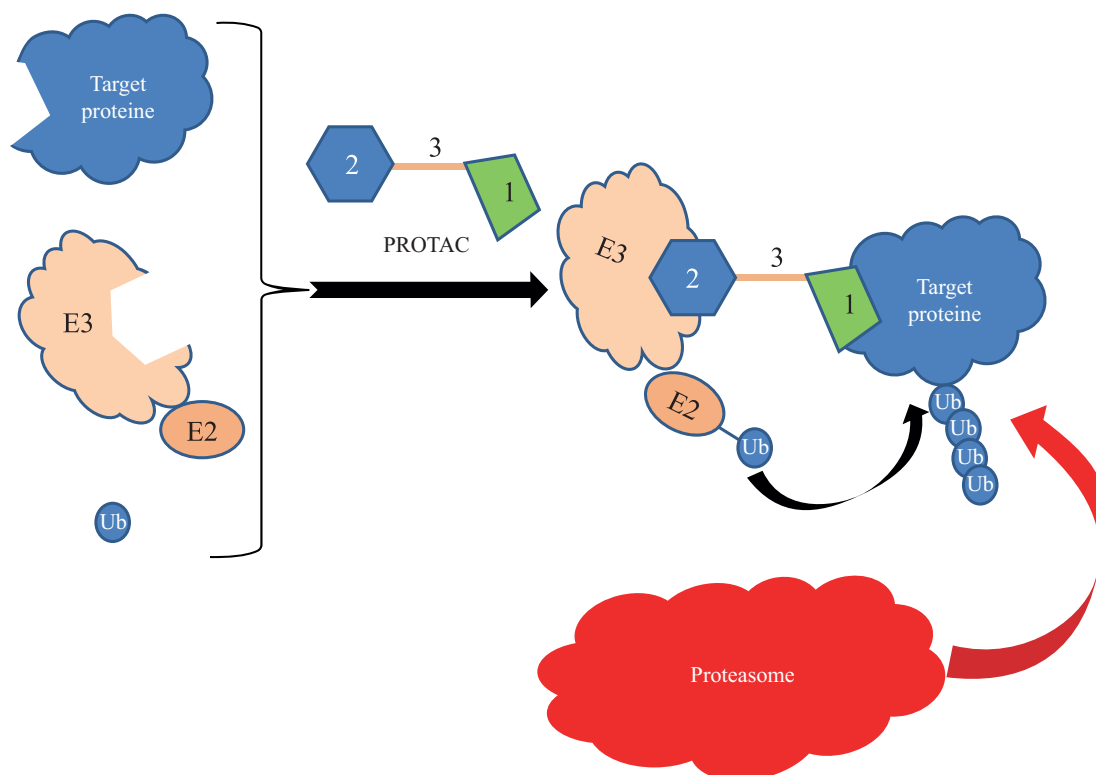


Fig. 1. PROTAC-induced degradation of the target protein by the ubiquitin-proteasome system (Ub — ubiquitin)

is tagged with a polyubiquitin chain and is attacked by the proteasome, resulting in its degradation.

The obvious field of application for the technology is in the treatment of cancer. Selective targeted destruction of tumor cell components is the main area for cancer chemotherapy. PROTAC® technology allows such targets that are inaccessible to conventional drugs to be attacked, i.e., suicide inhibitors. The technology can be used in neurodegenerative diseases such as Alzheimer's disease, autoimmune diseases and in all areas where specifically targeted drugs such as monoclonal antibodies are used. The undoubted advantage of PROTAC® is the relative simplicity and low cost of the active substance which is constructed from small molecules produced by conventional chemical synthesis.

Many reviews published in recent years [3–10] are devoted to the advantages and prospects of this technology. However, the simplicity of the idea hides many difficulties in its realization. This review is devoted to the achievements and problems in the design of chimeric molecules for selective degradation of target proteins, as well as the potential for the application of PROTAC® technology in the fight against infectious agents.

Construction of the PROTAC® molecule

The PROTAC® molecule consists of three structural components. Each of them is selected in accordance with the structure of the biotarget and, in turn, characterizes the pharmacodynamic and pharmacokinetic properties of the chimera. In terms of the design algorithm, well-studied ligands with a proven affinity to the target are chosen most often. A modification point is defined in the ligand structure, preferably at the periphery, where the pharmacophore will not be affected. At this point a linker group is attached to it. For the resulting intermediates, binding to the target is tested and, if successful, an E3 ligase selected from a set of known structures is attached to the other end of the linker. The construction of the PROTAC® molecule is complete, but its performance will depend on many nuances in the selection of all three components.

Selection of ligands to E3 ligase

The number of ubiquitin-transferring ligases in the human body is in excess of 600 [2]. However, only a few of them have low-molecular-weight ligands and are suitable for working with the PROTAC®

molecule. E3 ligase is an enzyme which performs the function of attaching ubiquitin to an arbitrary protein. In this sense there are almost no differences between different types of ligases. However, some of them have their own activator: a binding site for a low molecular weight ligand. Interaction with this ligand activates the enzyme. In fact, out of all the possible varieties, 3 ligases are normally used in practice: CRBN (cereblon), VHL (short for Von Hippel–Lindau) and cIAP (cellular inhibitor of apoptosis). They account for more than 95% of the described active PROTAC[®] chimeras, and more than half of them—for CRBN [6]. The known synthetic ligands to these three proteins are shown in Fig. 2.

Thalidomide **1** and its derivatives **2–5** are CRBN ligands. Their binding to CRBN is responsible for the antitumor activity of these compounds [12]. The ligands of other enzymes used are pseudo-peptide molecules containing non-natural amino acids. A comparison of

ligand structures explains the reasons for the popularity of CRBN: simplicity, synthetic availability and activity in racemic form. Another reason for this choice is that the activity of PROTAC[®] molecules targeting the same protein but designed for different ligases differs [3]. The most efficient chimeras are constructed on the basis of CRBN. However, the choice of ligase should be determined primarily by the biotarget, since the proteome has significant differences in different organs and tissues [13, 14].

Synthesis of ligands to CRBN

According to a review [11], the frequency of ligands to CRBN in successful PROTAC[®] molecules varies depending on the attachment point and linker type (Fig. 3).

The most common ligands **15–17** are based on the structure of pomalidomide **2**. The methods for

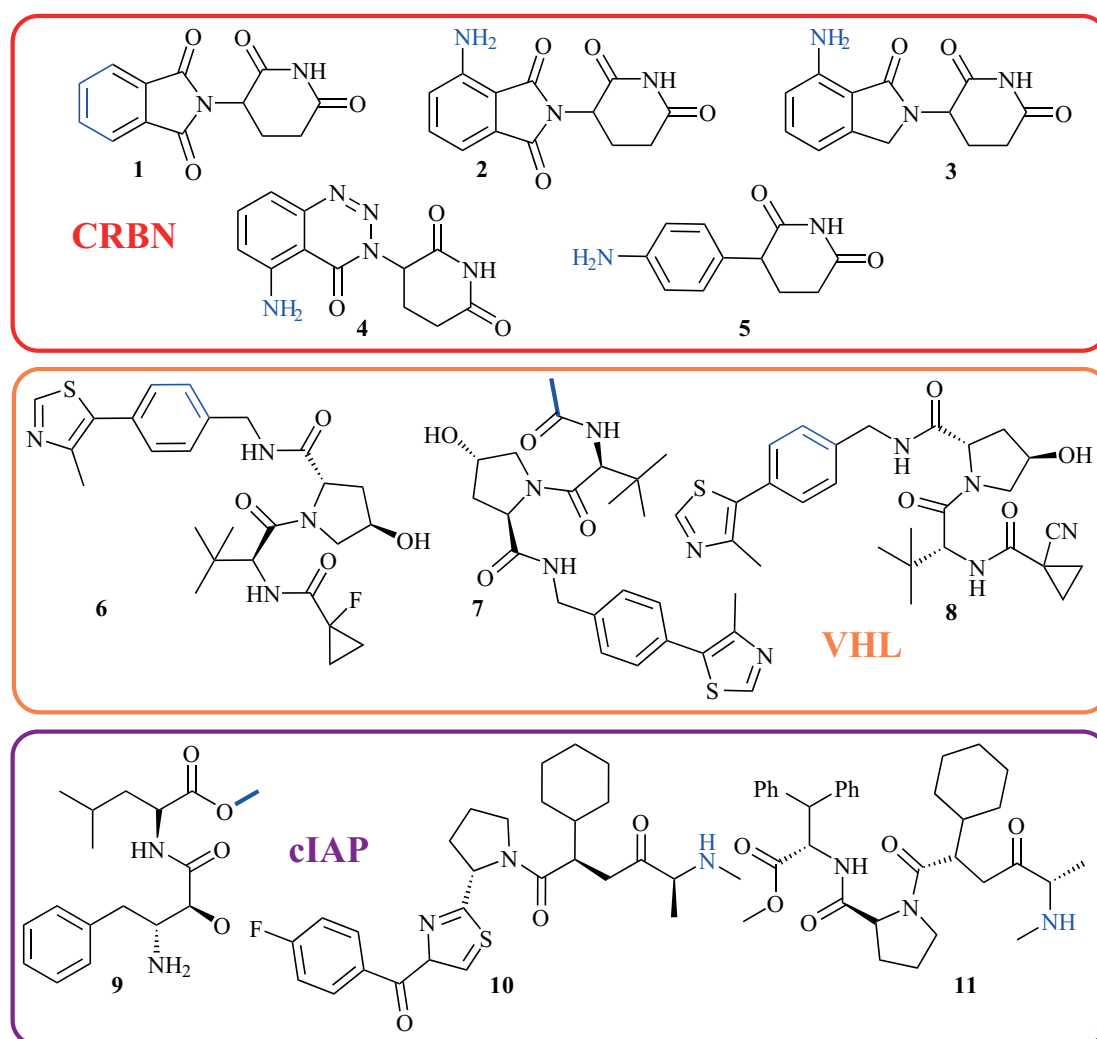


Fig. 2. Ligands of ligases E3. Possible modification points are marked in blue [11]

their synthesis are presented in Scheme 1. From the most available Boc-L-glutamine in the presence of a condensing agent (usually carbonyldiimidazole), a cyclic derivative **12** is obtained. After removal of the protecting group, it is acylated with 3-substituted phthalic anhydride. Linker groups are attached to the resulting derivatives **14**. This is achieved either by direct substitution of fluorine for amine **15**, or the nitro group of compound **14b** is first reduced to an amine, whereupon pomalidomide **2** is obtained. This is then acylated or alkylated at the amino group. Similarly, 4-hydroxyphthalimidomide **14c** is prepared from 3-hydroxyphthalic anhydride, which is alkylated on the phenolic hydroxyl to synthesize ligands of type **18**. Ligands of types **19–20**, in which the linker is attached via a carbon chain, are prepared by Pd-catalyzed cross-coupling with terminal acetylenes. There are a few alternative routes to these structures, but almost all are based on the condensation of substituted phthalic anhydride with glutamine, glutamic acid, or cyclic 3-aminopiperidine-2,6-dione **13**. The differences are mainly determined by the convenience of linker chain attachment and the overall yield of the synthetic scheme.

Similarly, derivatives substituted at the 4 position of the phenyl ring of phthalic anhydride are obtained. More details on the methods of synthesis of E3 ligands can be found in the review article by Bricelj *et al.* [11].

Selection of linker group and assembly of PROTAC® molecule

The efficiency of the chimeric molecule depends not only on the affinity of ligands to the target protein and E3 ligase, but also on the proper selection of the linker group binding them. A number of studies [15, 16] have shown that the length, flexibility, and structural features of the linker group play a critical role for the formation of the ternary complex “target protein–PROTAC–ligase E3.” Simple and relatively short hydrocarbon chains or polyethylene glycols are most often chosen as the initial linker which are gradually modified in the process of structure optimization. The attachment point of the linker to the ligands and the linker chain orientation should be selected in such a way as not to reduce the affinity of the ligands. Most often the selection is carried out by rational design methods, based on the established structure of the binding site. The main rules for selecting

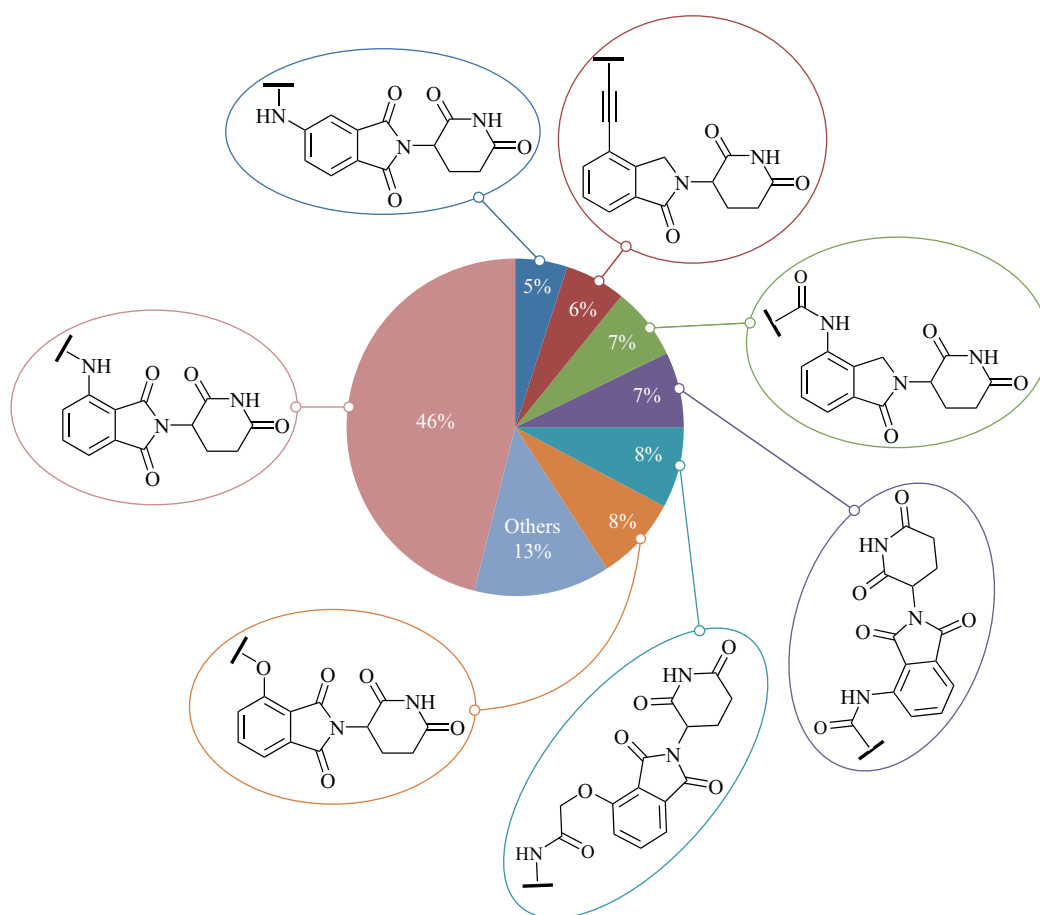
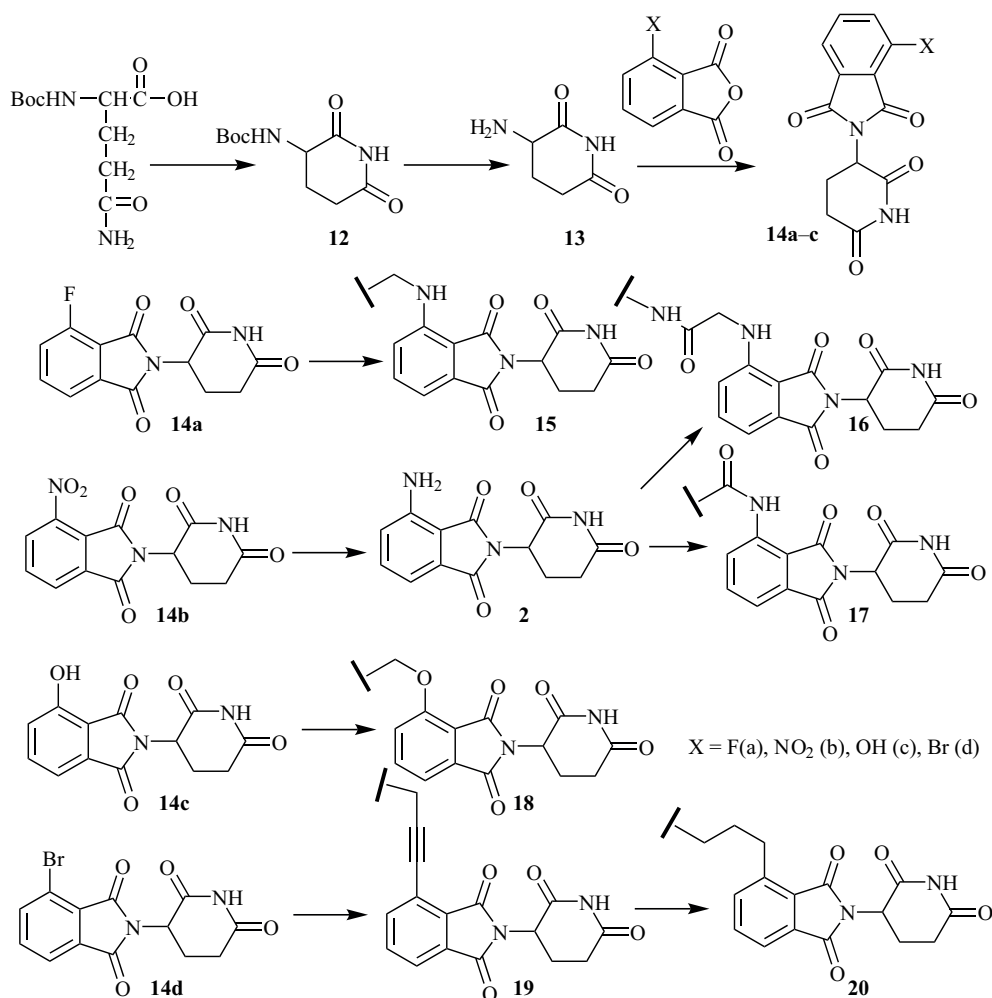


Fig. 3. Structures of synthetic ligands to CRBN in successful PROTAC® [11]



Scheme 1. Synthesis of CRBN ligands based on 3-substituted phthalic anhydride

the attachment point are as follows: (1) the molecular fragment of the ligand should not be changed significantly so as not to lose affinity; (2) the linker should enter the active center from the side available for solvation [6]. An example of the effect of linker on the activity of

a chimeric molecule is shown in Cao *et al.* [17] (Fig. 4). The chimeric molecule SK-575 **22** was designed to degrade the nuclear protein PARP1 (poly(ADP-ribose) polymerase), a validated cancer target, and was based on the structure of inhibitor **21** (Olaparib). It showed

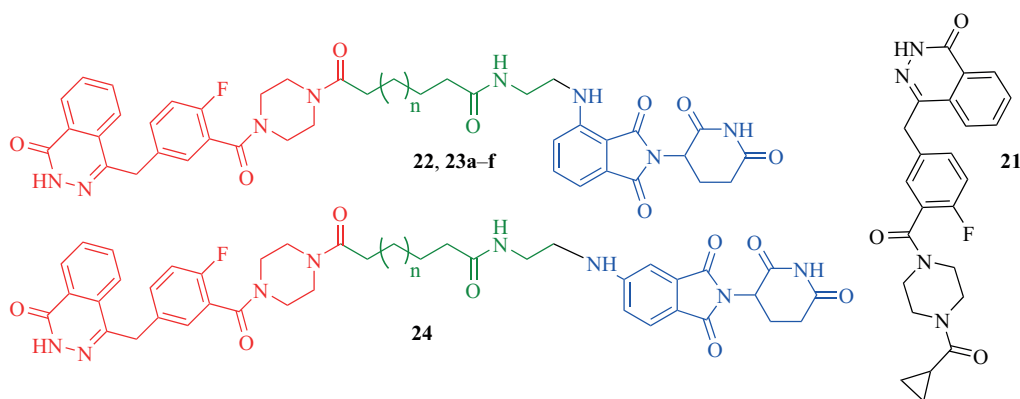


Fig. 4. Structures of PROTACs® for degradation of PARP1 (blue is the CRBN ligand, red is the ligand to PARP1, green is the spacer group) [17] and the initial inhibitor

Table. IC₅₀ (μM) value depending on linker length

Compound	22 <i>n</i> = 7	23a <i>n</i> = 1	23b <i>n</i> = 3	23c <i>n</i> = 5	23d <i>n</i> = 6	23e <i>n</i> = 8	23e <i>n</i> = 9	24 <i>n</i> = 7
IC ₅₀ , μM	0.019 ± 0.006*	>10	0.83 ± 0.26	0.123 ± 0.071	0.029 ± 0.008	0.021 ± 0.003	0.025 ± 0.004	0.035 ± 0.015

Note: *n* is the number of carbon groups in the chain. IC₅₀ (μM) is concentration of half-maximal inhibition.

* Parameters show the high efficiency of compound **22**.

efficient degradation of the target protein (>99%) at a concentration of 100 nM in a model cell system, although its homologs had lower activity. The **23c–e** homologs, which had 1–2 atoms different spacer chain lengths, were comparable in activity. Shorter or longer linkers markedly decreased the activity of the chimera. Isomer **24** at the same concentration degraded only 77% of the target protein. It can be assumed that the attachment point of the linker affects the stability of the ternary complex. To a large extent, the degradation efficiency of the target protein is influenced by the type of linker. Analogs of compound **22** with polyethylene glycol linkers were 3–5 times less active (Table).

The degree of the target protein destruction depends on many factors. Affinity to the target protein is not a direct indicator of PROTAC[®] molecule efficiency. Affinity is necessary for the PROTAC[®] molecule to work, but a high binding constant to the target protein does not guarantee its efficiency.

The sequence of work on the design of PROTAC[®] molecules to describe the experimental techniques and test systems used, is presented in the form of a protocol in Carmony and Kim [18]. The design principles of PROTAC[®] molecules with different targets are discussed in detail in [19, 20]. In most works, the design and assembly of the final molecule is described in a step-by-step sequence (ligand synthesis–spacer selection–chimera

assembly–activity studies). However, rapid synthesis of large libraries of target molecules for high-efficiency screening and optimization may be one of the directions of technological development. Examples of technological platforms for highly efficient synthesis of libraries of PROTAC[®] molecules are given in [21–23].

TARGET SELECTION AND PROSPECTS FOR TECHNOLOGY DEVELOPMENT

The choice of target protein is the main element when designing the PROTAC[®] molecule and this is determined by the therapeutic goal. The very concept of targeted protein degradation seems to be the most suitable for the fight against cancer [24–26]. Indeed, the first PROTAC[®] molecules to have passed phase I and II clinical trials target androgen (ARV-110, **25**) [27, 28] and estrogen (ARV-471, **26**) [29] receptors, and are designed to target prostate cancer and breast cancer, respectively (Fig. 5).

An important advantage of PROTAC[®] technology when compared to traditional drugs is that not only the active site of the target protein, but also any fragment thereof can be used for chimera binding. Thus, the spectrum of biotargets is expanded to include many previously inaccessible targets for therapy.

A focus on well-studied targets unites all successful examples of the development of chimeric

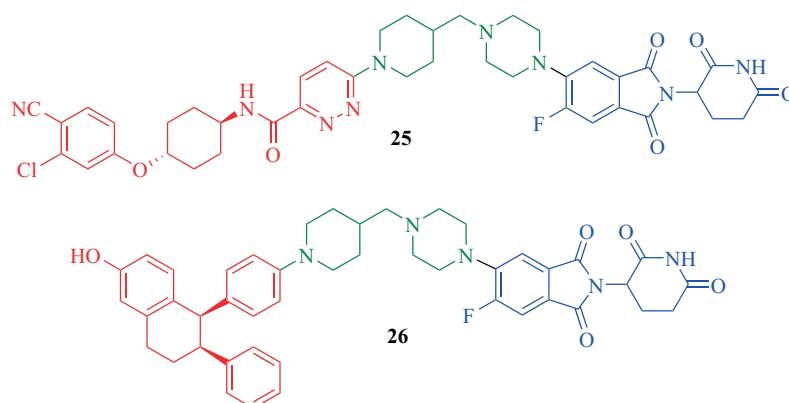


Fig. 5. The first clinically successful examples of PROTAC[®] technology application (blue is the CRBN ligand, red is the ligand to the target receptor, green is the spacer group)

molecules—protein disruptors. The targets for PROTAC[®] molecules are receptors [27, 29, 30], protein kinases [31], bromodomain-containing proteins and protein transducers [3], as well as many other proteins.

Like all successful innovations, PROTAC[®] technology has generated a whole range of new directions. They are all united by the idea of using the cell's own mechanisms to attack a biotarget. The first such direction was the use of alternative pathways for degradation of target proteins not mediated by the ubiquitin-proteasome system. Autophagy is another way in which cells divest themselves of unnecessary components [32]. Takahashi *et al.* [33] showed that it is possible to design molecules **27–28**, named by them as AUTAC (autophagy-targeted chimera) (Fig. 6), which utilize the autophagy mechanism to target protein degradation. Like the PROTAC[®] molecule, such a chimera acts inside the cell. AUTAC binds a “warhead” for the target protein to a guanine derivative which tags the protein for destruction by autophagy [34]. Targeted proteolysis can be induced by so-called heat shock proteins (HSPs). Chimeras which utilize binding to the HSP90 protein (HEMTAC) are described in a study by Li *et al.* [35]. About 40% of the proteins belong to

membrane or extracellular proteins. These targets are not accessible to the proteasome system and are not subject to autophagy. Many of them play an important role in the processes of carcinogenesis, age-related and autoimmune diseases [36]. The lysosomal degradation pathway can be involved against extracellular proteins [37, 38]. A number of structures, known as LYTAC (lysosome-targeted chimera), have been identified in which ligands to specific carrier proteins CI-M6PR [38] or ASGPR **29** [39, 40] are used to transport the extracellular target protein into the lysosome (Fig. 6). Monoclonal antibodies [39] or aptamers [40, 41] were used as ligands to the target protein.

An alternative to PROTAC[®] technology is the actively developing RIBOTAC (Ribonuclease Targeting Chimeras) technology: chimeric molecules targeting RNA degradation [42]. In this case, not only the method of degradation, but also the type of biotarget is changed. When the target is a nucleotide sequence, binding to it is usually by means of either an antisense oligonucleotide or small interfering RNA (siRNA). Using ligands of this type for chimera targeting means rejecting almost all the advantages of the new technology: simplicity and cheapness of synthesis, stability of the molecule, as well

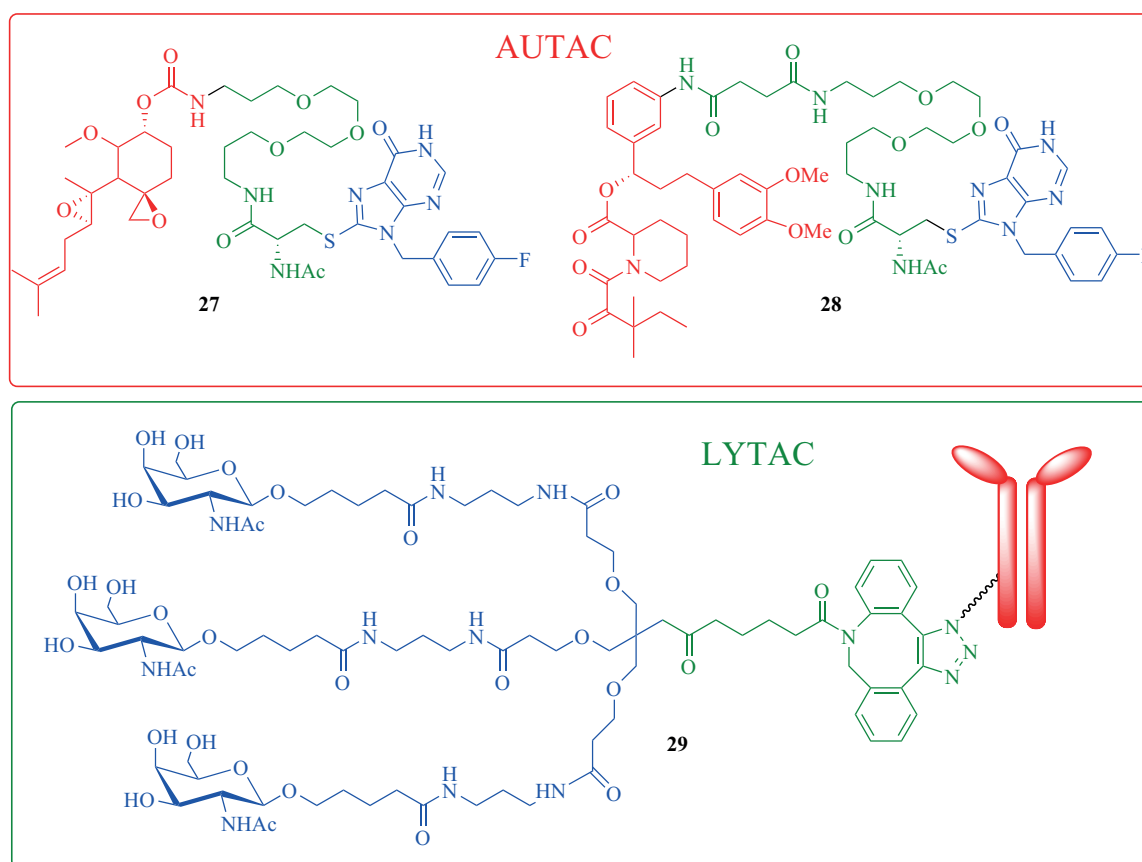


Fig. 6. The structures of AUTAC **27–28** (blue is a guanylate marker, red is a ligand to the target receptor, green is a spacer group) [33] and LYTAC **29** (blue is an ASGPR ligand, red is an antibody to the target protein, green is a spacer group) [39]

as the possibility to use enteral routes of administration into the body. Therefore, RIBOTAC technology uses small molecules which bind selectively to RNA, especially to those RNAs which form stable secondary and tertiary structures [43] (Fig. 7). The target disruptor is interferon-dependent ribonuclease L (EC 3.1.26), an enzyme involved in the immune system. It is activated by an oligoadenylate fragment responsible for binding to ribonuclease in the RIBOTAC structure. The search for ribonuclease ligands among other small molecules is described in [45].

Another alternative are chimeras in which different biopolymers, such as peptides, oligonucleotides, or antibodies (non-small molecule PROTACs or NSM-PROTAC), rather than small molecules act as ligands to the target protein [46]. Such constructs lose a number of advantages of the original technology, while instead gain more precise targeting of previously inaccessible targets.

TECHNOLOGY CHALLENGES AND SOLUTIONS

There exists a set of difficulties inherent in PROTAC[®] technology which have so far prevented it from attaining

a leading position in drug design [47]. The first such problem is the inherently poor pharmacological properties of most chimeric molecules. Almost all of them fall outside the accepted drug-likeness parameters due to their significant size and molecular weight. Low solubility also complicates the development of dosage forms for oral administration. This problem can be partly solved by conventional structure-based design methods [48, 49].

Another difficulty in the design of chimeric molecules is related to the relatively weak set of tools available for this work. While there is a huge variety of physicochemical methods and test systems for searching and optimizing traditional drugs, no such variety of approaches has yet been developed for the new technology. As mentioned earlier, the efficacy of PROTAC[®] molecule is not directly related to the easily measured affinity, but rather to the stability of the ternary complex and protein-protein interaction parameters. It is not yet fully understood what these values, as well as the selectivity of PROTAC[®] molecules, depend upon. Thus, it will be some time before the rational design of new chimeras becomes routine procedure. A review on tools and methods for the rational design of PROTAC[®] molecules is presented by Liu *et al.* [50].

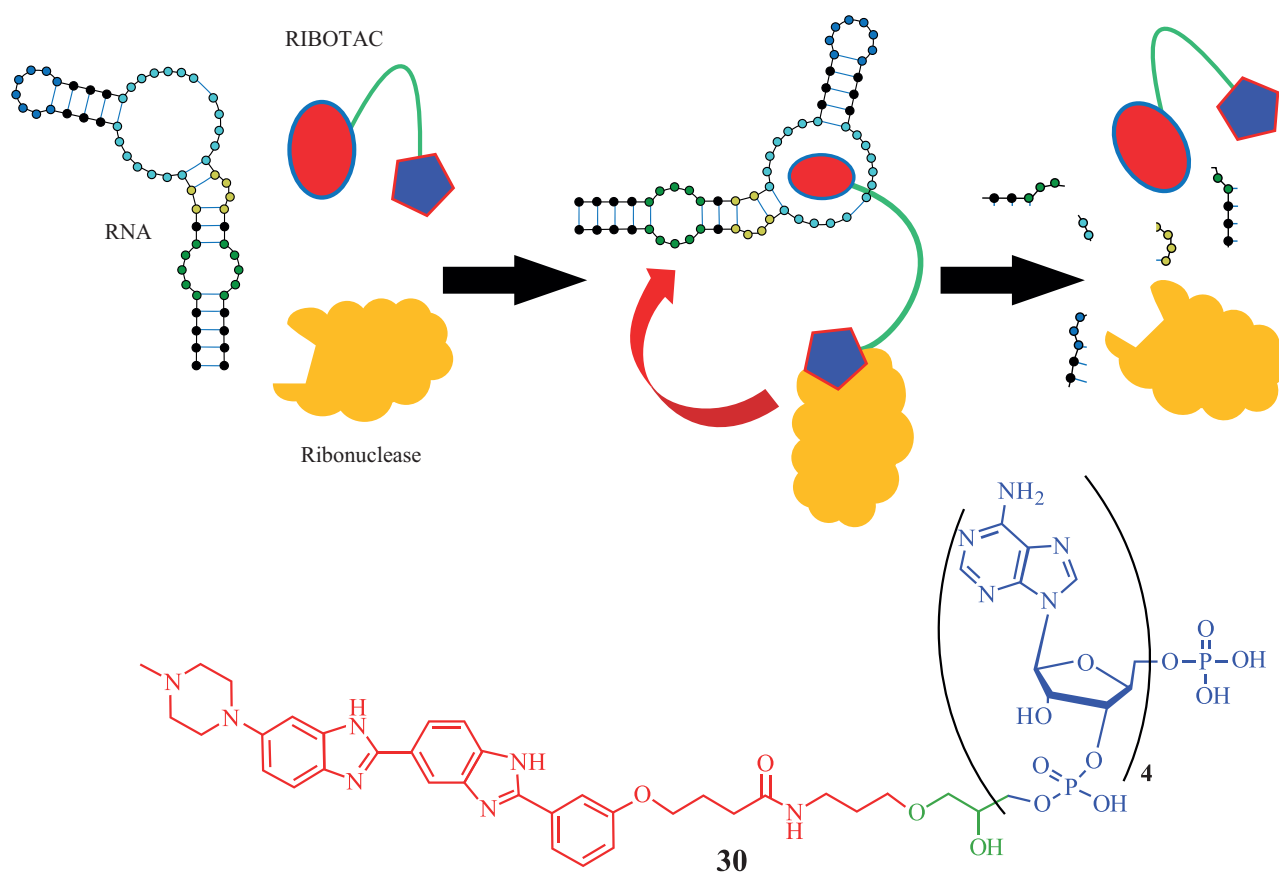


Fig. 7. RIBOTAC-induced degradation of RNA by ribonuclease L. MicroRNA-210 is a targeted chimeric molecule TGP-210-RL **30** [44] (blue is a ligand to ribonuclease L, red is a ligand to microRNA-210, green is a spacer group)

Another problem is related to the mechanism of action of PROTAC[®] molecules. When traditional suicide inhibitors enter the cell, each drug molecule “kills” only one target molecule (enzyme or receptor). Thus the drug action is directly related to concentration and affinity. However, PROTAC[®] recruits the cell’s own systems, and once the target protein is broken down, the chimera is incorporated into a new catalytic cycle. Thus, the action of the drug will continue until all PROTAC[®] molecules are completely eliminated or broken down. This opens the way to the highest level of efficacy on the one hand and uncontrollable side effects on the other. It is highly desirable to provide a chemical “switch” as a way of stopping or reactivating the effect of the disrupting molecule at the right moment.

This type of development is currently being carried out in the field of photopharmacology [52]. An example of a photoswitchable PROTAC[®] molecule is shown in Fig. 8. The initial structure is a chimeric molecule ARV-771 **31** targeting the oncomic target BRD-4. The spacer length is 11 Å, and if changed up or

down, the stability of the ternary complex is disturbed and PROTAC[®] stops working. In the structure of the photoswitchable molecule **32a**, the polyethylene glycol spacer is replaced by a fragment of substituted *trans*-azobenzene of equal length. Upon irradiation with 530 nm light, azobenzene is isomerized to the *cis*-form **32b**. Hereby the distance between the ligands is reduced to 8 Å and the substance loses activity. The reverse transition is initiated by irradiation at 415 nm.

The “switch” may also be purely chemical in nature. Variants of chimeric anticancer molecules utilizing the folate targeting system have been described [53]. In normal cells, folic acid receptors are present in low numbers when compared to many types of tumor cells which actively express these receptors. When the inactive prodrug **33** conjugated to folic acid is transported into cancer cells, the active substance, PROTAC[®] ARV-771 **31**, is released by the action of endogenous hydrolases (Fig. 9).

Another way to bring the pharmacodynamics of the PROTAC[®] molecule closer to conventional models is to

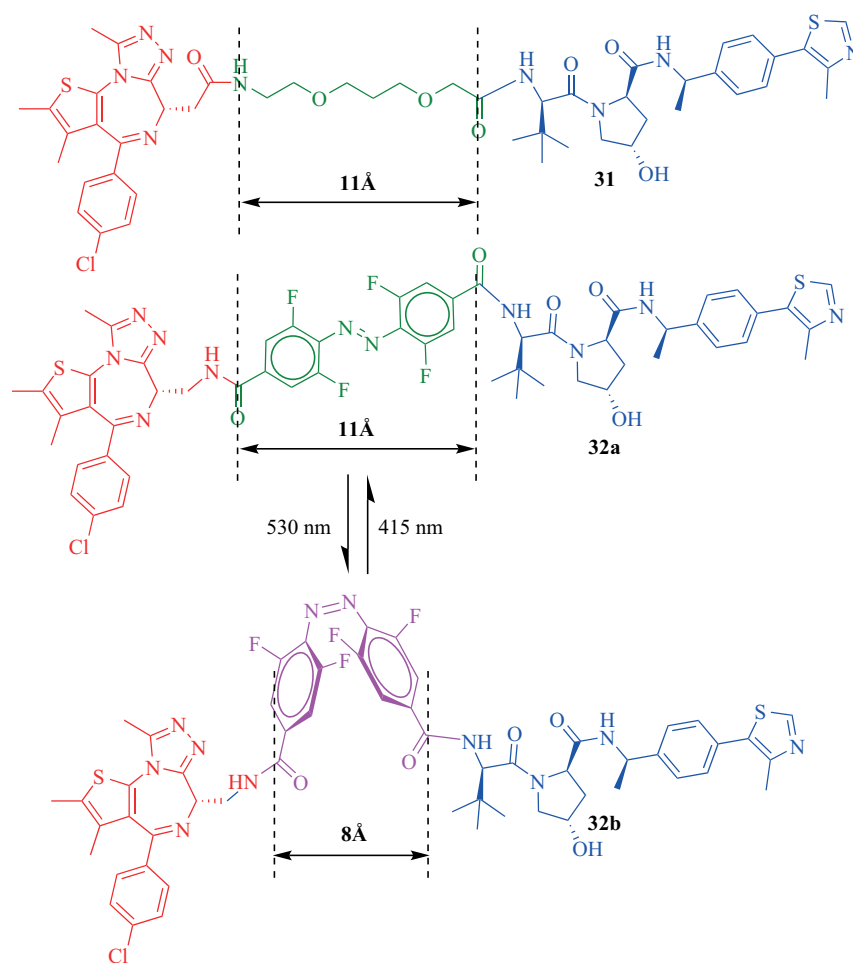


Fig. 8. Photoinduced switching PROTAC[®] (blue is ligand to the E3 VHL ligase, red is ligand to the target protein BRD4, and green is spacer groups) [51]

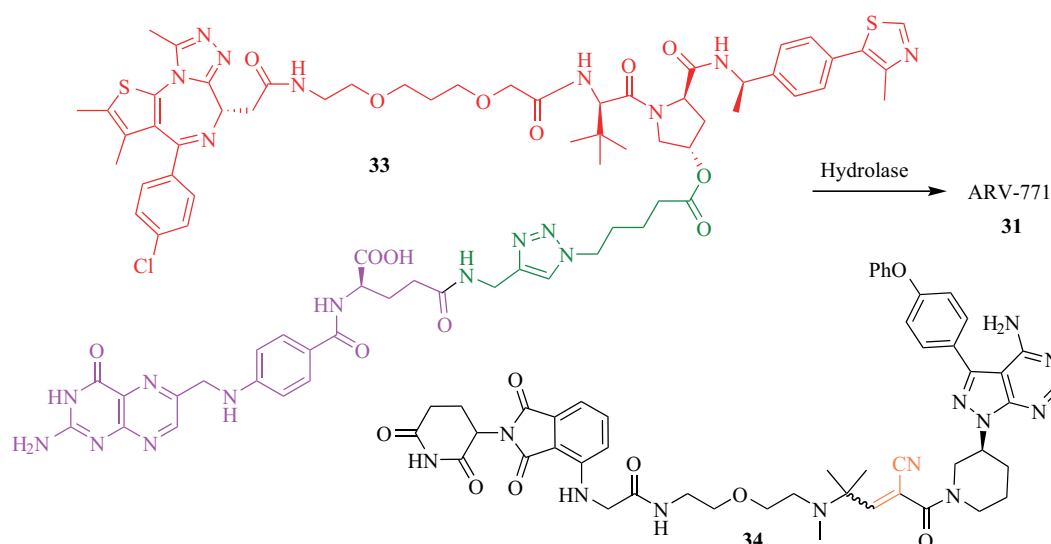


Fig. 9. PROTAC[®] **33** with folate delivery system to the tumor cell (the fragment of the initial active substance is highlighted in red, the folate group is highlighted in purple, the spacer fragment is highlighted in green) [53]; covalent PROTAC[®] (an orange fragment is an acrylamide group responsible for covalent binding to the target) [54]

use covalent inhibitors as a “warhead”. If the ligand in the chimera binds covalently to the target protein when the proteasome destroys the target, it releases the already spent molecule. It is then unable to re-enter the catalytic cycle. Thus, the PROTAC[®] molecule begins to function as a conventional suicide inhibitor, while retaining an advantage in the target spectrum. There are other design concepts for PROTAC[®] technology which utilize covalent binding, including reversible binding [55]. A study by Jin *et al.* [56] proposed controlling the degradation process of the target protein by introducing into the cell a substance which selectively binds the active PROTAC[®] molecule.

APPLICATION OF PROTAC[®] TECHNOLOGY IN INFECTION COMBAT: OPPORTUNITIES AND LIMITATIONS

At first glance, the use of the new technology against pathogens and viruses appears very promising. However, the number of publications describing antibacterial or antiviral PROTAC[®] molecules is still relatively small. Strategies for the application of directed protein degradation against bacterial, viral and protozoan infections should be considered separately due to the significant differences between the biotargets.

Strictly speaking, it is impossible to apply PROTAC[®] technology in its original form against prokaryotic cells, i.e., bacteria, since the ubiquitin-proteasome system exists only in eukaryotes. However, the very idea of directed degradation of target proteins through activation of the cell’s own systems may well be

extended to bacterial cells. In 2022, Morreale *et al.* [57] proposed the concept of BacPROTAC, based on the protease system of gram-positive bacteria and mycobacteria ClpCP, similar to the ubiquitin-proteasome system of eukaryotes. When compared to eukaryotic proteasomes, which recognize complex polyubiquitin chains, the activation mechanism of ClpCP is much simpler. A phosphate group bound to the arginine residue of the target protein serves as a degradation tag. As proof of concept viability, the researchers tested the degradation efficiency of a model protein (streptavidin) *in vitro* by coupling its ligand (biotin) to phosphorylated arginine via a linker in the BacPROTAC-1 **35** compound (Fig. 10).

Compound **35** at a concentration of 100 μ M degraded the target protein *in vitro* in the presence of ClpCP in *Bacillus subtilis*. However, the pharmacokinetics of BacPROTAC-1, based on phosphorylated arginine, is unsatisfactory and the guanidine phosphate group is unstable. The researchers proposed replacing the arginine-phosphate ligand with cyclic peptide molecules similar to cyclomarin A: an antibiotic isolated from a marine actinomycete that has significant affinity for ClpCP.

BacPROTAC is currently more of a fundamental concept than a technology. There are still many hurdles to be overcome before it can be applied in practice. The high selectivity of the PROTAC[®] molecule in the case of antibacterial therapy is rather a disadvantage. The countless variety of genetically variable pathogenic microorganisms makes it extremely difficult to select a target and a universal approach to chimera design.

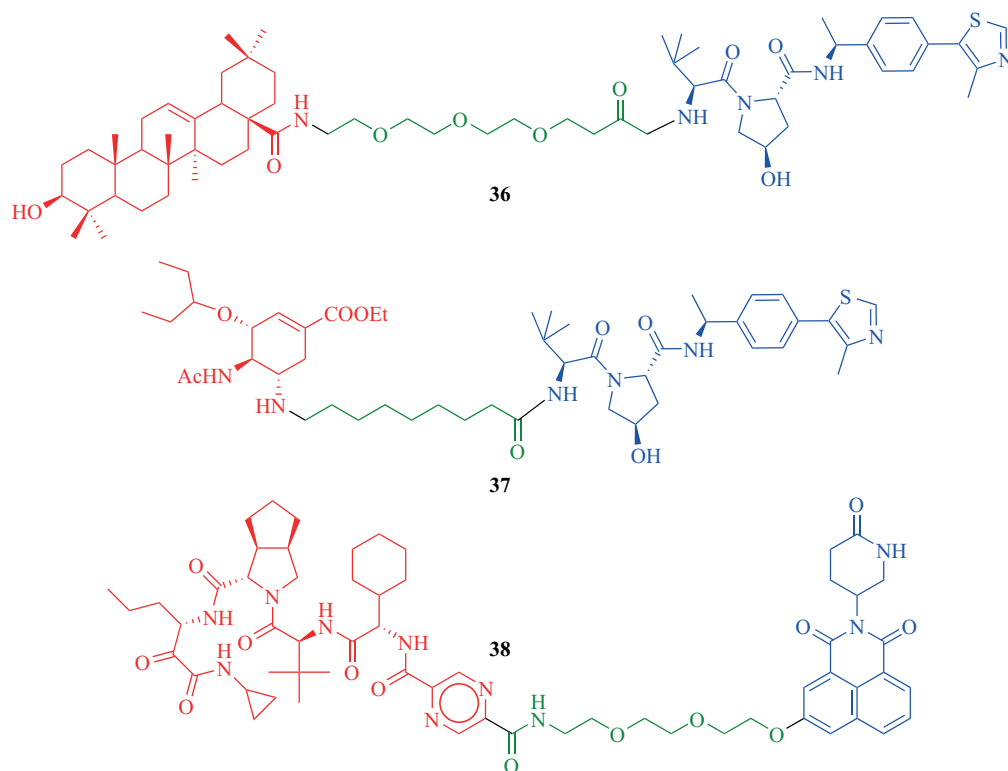


Fig. 11. Structures of PROTACs® aimed at various viral proteins (E3 ligands are blue, ligands to the target protein are red, linker groups are green)

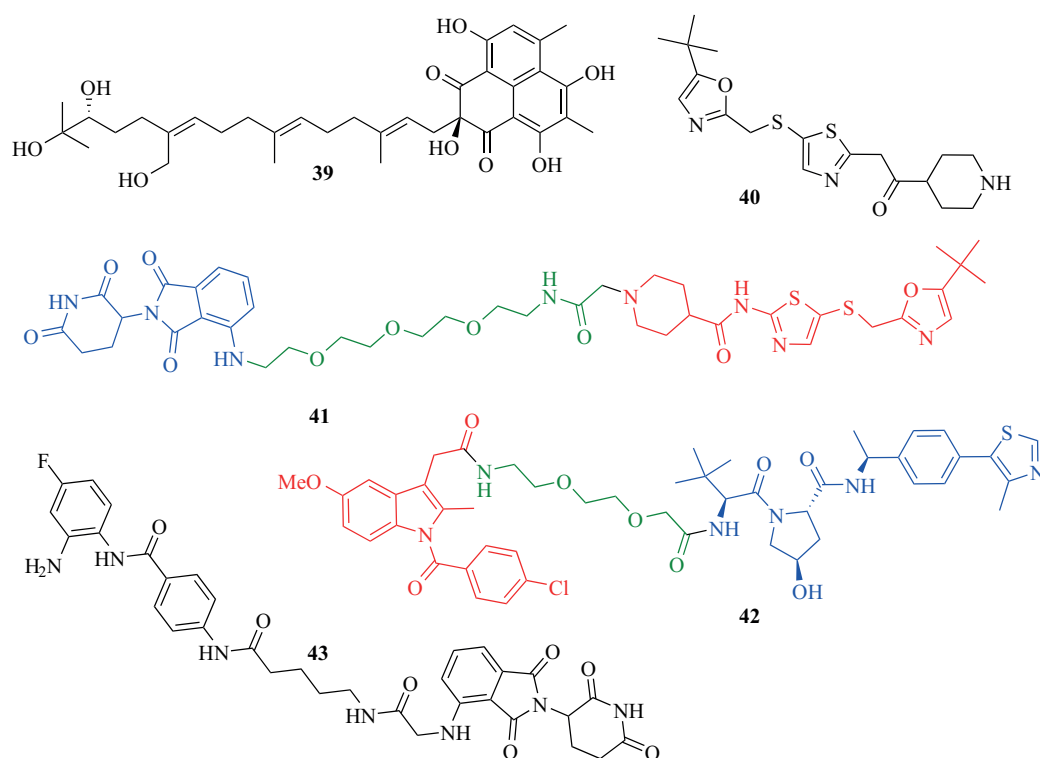


Fig. 12. Structures of antiviral PROTACs® (E3 ligands are blue, ligands to the target protein are red, linker groups are green)

effect against influenza A. This is due to the fact that it is a ligand of both virus polymerase and E3 ligase TRIM25 [72].

Another way of fighting viral infection is to inhibit the pathological cellular processes caused by the virus. In this case, the action of PROTAC[®] technology is more traditional. Infection caused by cytomegalovirus develops with the participation of cyclin-dependent protein kinases (CDK), inhibitors of which are being tested as antiviral drugs [73]. In particular, compound SNS-032 **40** from *Selleck* (USA), a selective CDK inhibitor, served as the basis for the antiviral PROTAC[®] drug **41** [74]. Compound **41** ($EC_{50} = 0.025 \pm 0.001 \mu\text{M}$) was almost four times as effective when compared with the original SNS-032 ($EC_{50} = 0.105 \pm 0.004 \mu\text{M}$).

In the search for an effective therapy for COVID-19 during the pandemic, many registered drugs from a wide variety of classes were retested. In particular, indomethacin, an old anti-inflammatory drug, was found to have some efficacy against coronavirus infection. Desantis *et al.* [75] developed several PROTAC[®] drugs which utilize the structure of indomethacin as a “warhead” targeting prostaglandin-E synthase 2 (PGE-2). This enzyme interacts with the coronavirus protein NSP7 which is required for SARS-CoV2 replication. The exact mechanism of the antiviral action of indomethacin is unclear, but destruction of PGE-2 suppresses replication. The most active compound **42** ($EC_{50} = 18.1 \mu\text{M}$) is 5 times more effective than indomethacin ($EC_{50} = 94.4 \mu\text{M}$). Interestingly, these PROTAC[®] compounds are also active against other types of coronaviruses, e.g., HCoV-OC43, while not exhibiting cytotoxicity against uninfected cells.

One reason for the high mortality rate of COVID-19 is the hyperactivation of the inflammatory response caused by histone deacetylases (HDACs). Inhibition of HDAC-3 reduces inflammation. HDAC-3-targeted chimeras for the treatment of COVID-19 were proposed by Zahid *et al.* [76] based on the anti-inflammatory drug PROTAC[®] HD-TAC7 **43** (*MedChemExpress*, USA). Computer analysis showed that the proposed molecules could theoretically be used to control inflammatory responses in COVID-19. However, the potential

practical applications were limited by unresolved pharmacokinetic problems. Molecular dynamic modeling and computational analysis have also been used in [77] to design possible PROTAC[®] molecules targeting the SARS-CoV-2 protease, another confirmed viral target. However, the results of the calculations have yet to be verified by chemical synthesis and activity studies on models and *in vivo* studies.

CONCLUSIONS

PROTAC[®], a targeted protein degradation technology, is based on the use of heterobifunctional molecules to recruit intracellular protein degradation mechanisms to an intracellular target protein of interest. This chemically induced affinity between the molecular mechanism of protein degradation and the target leads to polyubiquitinylation and proteasomal degradation of the target protein. The PROTAC[®] chimeric molecule is assembled from three parts: a ligand to the target protein; a ligand to the E3 ligase enzyme recruiting ubiquitin-proteasome system; and a linker that binds them together. The publicly available PROTAC-DB 2.0³ database contains information on 3270 engineered chimeras, 360 “warheads”, 1500 linkers and 80 E3 ligase ligands, as well as data on known crystal structures of ternary complexes.

Originally designed to target cancer and neurodegenerative diseases, this technology can also be directed against infections. New modifications suggest the use not only of the proteasome system, but also other defense mechanisms of the cell. Nucleic acids also act as a biological target. As of the end of 2022, at least 20 PROTAC[®] projects worldwide were in clinical trials and at least one had reached Phase III. The precise targeting of the body’s own defense systems, which is no less effective than monoclonal antibody technology but cheaper, opens the way to treating a wide variety of diseases.

Authors’ contribution

All authors equally contributed to the research work.

The authors declare no conflicts of interest.

³ <http://cadd.zju.edu.cn/protacdb/>. Accessed February 26, 2024.

REFERENCES

- Sakamoto K.M., Kim K.B., Kumagai A., Mercurio F., Crews C.M., Deshaies R.J. Protacs: chimeric molecules that target proteins to the Skp1-Cullin-F box complex for ubiquitination and degradation. *Proc. Natl. Acad. Sci. U S A.* 2001;98(15):8554–8559. <https://doi.org/10.1073/pnas.141230798>
- Kleiger G., Mayor T. Perilous journey: a tour of the ubiquitin-proteasome system. *Trends Cell Biol.* 2014;24(6):352–359. <https://doi.org/10.1016/j.tcb.2013.12.003>
- Bekes M., Langley D.R., Crews C.M. PROTAC targeted protein degraders: the past is prologue. *Nat. Rev. Drug Discov.* 2022;21(3):181–200. <https://doi.org/10.1038/s41573-021-00371-6>
- He M., Cao C., Ni Z., Liu Y., Song P., Hao S., et al. PROTACs: great opportunities for academia and industry (an update from 2020 to 2021). *Signal Transduct. Target. Ther.* 2022;7(1):181. <https://doi.org/10.1038/s41392-022-00999-9>
- Koroleva O.A., Dutikova Yu.V., Trubnikov A.V., et al. PROTAC: targeted drug strategy. Principles and limitations. *Russ. Chem. Bull.* <https://doi.org/10.1007/s11172-022-3659-z> [Original Russian Text: Koroleva O.A., Dutikova Yu.V., Trubnikov A.V., Zenov F.A., Manasova E.V., Shtil' A.A., Kurkin A.V. PROTAC: targeted drug strategy. Principles and limitations. *Izvestiya Akademii Nauk. Seriya khimicheskaya.* 2022;71(11):2310–2334 (in Russ.).]
- Cao C., He M., Wang L., He Y., Rao Y. Chemistries of bifunctional PROTAC degraders. *Chem. Soc. Rev.* 2022;51(16):7066–7114. <https://doi.org/10.1039/d2cs00220e>
- Liu Z., Hu M., Yang Y., Du C., Zhou H., Liu C., et al. An overview of PROTACs: a promising drug discovery paradigm. *Mol. Biomed.* 2022;3(1):46. <https://doi.org/10.1186/s43556-022-00112-0>
- Yang N., Kong B., Zhu Z., Huang F., Zhang L., Lu T., et al. Recent advances in targeted protein degraders as potential therapeutic agents. *Mol. Divers.* 2024;28:309–333. <https://doi.org/10.1007/s11030-023-10606-w>
- Li S., Chen T., Liu J., Zhang H., Li J., Wang Z., et al. PROTACs: Novel tools for improving immunotherapy in cancer. *Cancer Lett.* 2023;560:216128. <https://doi.org/10.1016/j.canlet.2023.216128>
- Guedeny N., Cornu M., Schwalen F., Kieffer C., Voisin-Chiret A.S. PROTAC technology: A new drug design for chemical biology with many challenges in drug discovery. *Drug Discov. Today.* 2023;28(1):103395. <https://doi.org/10.1016/j.drudis.2022.103395>
- Bricelj A., Steinebach C., Kuchta R., Gutschow M., Sosic I. E3 Ligase Ligands in Successful PROTACs: An Overview of Syntheses and Linker Attachment Points. *Front. Chem.* 2021;9:707317. <https://doi.org/10.3389/fchem.2021.707317>
- Chamberlain P.P., Lopez-Girona A., Miller K., Carmel G., Pagarigan B., Chie-Leon B., et al. Structure of the human Cereblon-DDB1-lenalidomide complex reveals basis for responsiveness to thalidomide analogs. *Nat. Struct. Mol. Biol.* 2014;21(9):803–809. <https://doi.org/10.1038/nsmb.2874>
- Simpson L.M., Glennie L., Brewer A., Zhao J.F., Crooks J., Shpiro N., et al. Target protein localization and its impact on PROTAC-mediated degradation. *Cell Chem. Biol.* 2022;29(10):1482–1504.e7. <https://doi.org/10.1016/j.chembiol.2022.08.004>
- Shah V.J., Đikić I. Localization matters in targeted protein degradation. *Cell Chem. Biol.* 2022;29(10):1465–1466. <https://doi.org/10.1016/j.chembiol.2022.09.006>
- Bemis T.A., La Clair J.J., Burkart M.D. Unraveling the Role of Linker Design in Proteolysis Targeting Chimeras. *J. Med. Chem.* 2021;64(12):8042–8052. <https://doi.org/10.1021/acs.jmedchem.1c00482>
- Gadd M.S., Testa A., Lucas X., Chan K.H., Chen W., Lamont D.J., et al. Structural basis of PROTAC cooperative recognition for selective protein degradation. *Nat. Chem. Biol.* 2017;13(5):514–521. <https://doi.org/10.1038/nchembio.2329>
- Cao C., Yang J., Chen Y., Zhou P., Wang Y., Du W., et al. Discovery of SK-575 as a Highly Potent and Efficacious Proteolysis-Targeting Chimera Degradator of PARP1 for Treating Cancers. *J. Med. Chem.* 2020;63(19):11012–11033. <https://doi.org/10.1021/acs.jmedchem.0c00821>
- Carmony K.C., Kim K.B. PROTAC-induced proteolytic targeting. In: Dohmen R., Scheffner M. (Eds.). *Ubiquitin Family Modifiers and the Proteasome.* Methods in Molecular Biology. Humana Press; 2012. V. 832. P. 627–638. https://doi.org/10.1007/978-1-61779-474-2_4419
- Bondeson D.P., Smith B.E., Burslem G.M., Buhimschi A.D., Hines J., Jaime-Figueroa S., et al. Lessons in PROTAC Design from Selective Degradation with a Promiscuous Warhead. *Cell Chem. Biol.* 2018;25(1):78–87.e5. <https://doi.org/10.1016/j.chembiol.2017.09.010>
- Paiva S.L., Crews C.M. Targeted protein degradation: elements of PROTAC design. *Curr. Opin. Chem. Biol.* 2019;50:111–119. <https://doi.org/10.1016/j.cbpa.2019.02.022>
- Rao Z., Li K., Hong J., Chen D., Ding B., Jiang L., et al. A practical “preTACs-cytoblot” platform accelerates the streamlined development of PROTAC-based protein degraders. *Eur. J. Med. Chem.* 2023;251:115248. <https://doi.org/10.1016/j.ejmech.2023.115248>
- Guo L., Zhou Y., Nie X., Zhang Z., Li C., et al. A platform for the rapid synthesis of proteolysis targeting chimeras (Rapid-TAC) under miniaturized conditions. *Eur. J. Med. Chem.* 2022;236:114317. <https://doi.org/10.1016/j.ejmech.2022.114317>
- Bhela I.P., Ranza A., Balestrero F.C., Serafini M., Aprile S., Di Martino R.M.C., et al. A Versatile and Sustainable Multicomponent Platform for the Synthesis of Protein Degradators: Proof-of-Concept Application to BRD4-Degrading PROTACs. *J. Med. Chem.* 2022;65(22):15282–15299. <https://doi.org/10.1021/acs.jmedchem.2c01218>
- Liu Z., Zhang Y., Xiang Y., Kang X. Small-Molecule PROTACs for Cancer Immunotherapy. *Molecules.* 2022;27(17):5439. <https://doi.org/10.3390/molecules27175439>
- Li J., Chen X., Lu A., Liang C. Targeted protein degradation in cancers: Orthodox PROTACs and beyond. *The Innovation.* 2023;4(3):100413. <https://doi.org/10.1016/j.xinn.2023.100413>
- Yedla P., Babalghith A.O., Andra V.V., Syed R. PROTACs in the Management of Prostate Cancer. *Molecules.* 2023;28(9):3698. <https://doi.org/10.3390/molecules28093698>
- Gao X., Burris Iii H.A., Vuky J., Dreicer R., Sartor A.O., Sternberg C.N., et al. Phase 1/2 study of ARV-110, an androgen receptor (AR) PROTAC degrader, in metastatic castration-resistant prostate cancer (mCRPC). *J. Clin. Oncol.* 2022;40(6_suppl):17–17. https://doi.org/10.1200/JCO.2022.40.6_suppl.017
- Ha S., Luo G., Xiang H. A Comprehensive Overview of Small-Molecule Androgen Receptor Degradators: Recent Progress and Future Perspectives. *J. Med. Chem.* 2022;65(24):16128–16154. <https://doi.org/10.1021/acs.jmedchem.2c01487>
- Hamilton E.P., Schott A.F., Nanda R., Lu H., Keung C.F., Gedrich R., et al. ARV-471, an estrogen receptor (ER) PROTACdegrader, combined with palbociclib in advanced ER+/human epidermal growth factor receptor 2–negative (HER2–) breast cancer: Phase 1b cohort (part C) of a phase 1/2 study. *J. Clin. Oncol.* 2022;40(16_suppl):TPS1120–TPS1120. https://doi.org/10.1200/JCO.2022.40.16_suppl.TPS1120

30. Xu H., Ohoka N., Yokoo H., Nemoto K., Ohtsuki T., Matsufuji H., *et al.* Development of Agonist-Based PROTACs Targeting Liver X Receptor. *Front. Chem.* 2021;9:674967. <https://doi.org/10.3389/fchem.2021.674967>
31. Yu F., Cai M., Shao L., Zhang J. Targeting Protein Kinases Degradation by PROTACs. *Front. Chem.* 2021;9:679120. <https://doi.org/10.3389/fchem.2021.679120>
32. Dikic I., Elazar Z. Mechanism and medical implications of mammalian autophagy. *Nat. Rev. Mol. Cell Biol.* 2018;19(6):349–364. <https://doi.org/10.1038/s41580-018-0003-4>
33. Takahashi D., Moriyama J., Nakamura T., Miki E., Takahashi E., Sato A., *et al.* AUTACs: Cargo-Specific Degradation Using Selective Autophagy. *Mol. Cell.* 2019;76(5):797–810.e10. <https://doi.org/10.1016/j.molcel.2019.09.009>
34. Li X., Liu Q., Xie X., Peng C., Pang Q., Liu B., *et al.* Application of Novel Degradation Employing Autophagy for Expediting Medicinal Research. *J. Med. Chem.* 2023;66(3):1700–1711. <https://doi.org/10.1021/acs.jmedchem.2c01712>
35. Li Z., Ma S., Zhang L., Zhang S., Ma Z., Du L., *et al.* Targeted Protein Degradation Induced by HEMTACs Based on HSP90. *J. Med. Chem.* 2023;66(1):733–751. <https://doi.org/10.1021/acs.jmedchem.2c01648>
36. Brown K.J., Seol H., Pillai D.K., Sankoorikal B.J., Formolo C.A., Mac J., *et al.* The human secretome atlas initiative: implications in health and disease conditions. *Biochim. Biophys. Acta.* 2013;1834(11):2454–2461. <https://doi.org/10.1016/j.bbapap.2013.04.007>
37. Banik S.M., Pedram K., Wisnovsky S., Ahn G., Riley N.M., Bertozzi C.R. Lysosome-targeting chimaeras for degradation of extracellular proteins. *Nature.* 2020;584(7820):291–297. <https://doi.org/10.1038/s41586-020-2545-9>
38. Caianiello D.F., Zhang M., Ray J.D., Howell R.A., Swartzel J.C., Branham E.M.J., *et al.* Bifunctional small molecules that mediate the degradation of extracellular proteins. *Nat. Chem. Biol.* 2021;17(9):947–953. <https://doi.org/10.1038/s41589-021-00851-1>
39. Ahn G., Banik S.M., Miller C.L., Riley N.M., Cochran J.R., Bertozzi C.R. LYTACs that engage the asialoglycoprotein receptor for targeted protein degradation. *Nat. Chem. Biol.* 2021;17(9):937–946. <https://doi.org/10.1038/s41589-021-00770-1>
40. Wu Y., Lin B., Lu Y., Li L., Deng K., Zhang S., *et al.* Aptamer-LYTACs for Targeted Degradation of Extracellular and Membrane Proteins. *Angew. Chem. Int. Ed. Engl.* 2023;62(15):e202218106. <https://doi.org/10.1002/anie.202218106>
41. Kong L., Meng F., Wu S., Zhou P., Ge R., Liu M., *et al.* Selective degradation of the p53-R175H oncogenic hotspot mutant by an RNA aptamer-based PROTAC. *Clin. Transl. Med.* 2023;13(2):e1191. <https://doi.org/10.1002/ctm2.1191>
42. Dey S.K., Jaffrey S.R. RIBOTACs: Small Molecules Target RNA for Degradation. *Cell Chem. Biol.* 2019;26(8):1047–1049. <https://doi.org/10.1016/j.chembiol.2019.07.015>
43. Childs-Disney J.L., Yang X., Gibaut Q.M.R., Tong Y., Batey R.T., Disney M.D. Targeting RNA structures with small molecules. *Nat. Rev. Drug Discov.* 2022;21(10):736–762. <https://doi.org/10.1038/s41573-022-00521-4>
44. Costales M.G., Suresh B., Vishnu K., Disney M.D. Targeted Degradation of a Hypoxia-Associated Non-coding RNA Enhances the Selectivity of a Small Molecule Interacting with RNA. *Cell Chem. Biol.* 2019;26(8):1180–1186.e5. <https://doi.org/10.1016/j.chembiol.2019.04.008>
45. Borgelt L., Haacke N., Lampe P., Qiu X., Gasper R., Schiller D., *et al.* Small-molecule screening of ribonuclease L binders for RNA degradation. *Biomed. Pharmacother.* 2022;154:113589. <https://doi.org/10.1016/j.biopha.2022.113589>
46. Ma S., Ji J., Tong Y., Zhu Y., Dou J., Zhang X., *et al.* Non-small molecule PROTACs (NSM-PROTACs): Protein degradation kaleidoscope. *Acta Pharm. Sin. B.* 2022;12(7):2990–3005. <https://doi.org/10.1016/j.apsb.2022.02.022>
47. Gao H., Sun X., Rao Y. PROTAC Technology: Opportunities and Challenges. *ACS Med. Chem. Lett.* 2020;11(3):237–240. <https://doi.org/10.1021/acsmchemlett.9b00597>
48. O'Brien Laramy M.N., Luthra S., Brown M.F., Bartlett D.W. Delivering on the promise of protein degraders. *Nat. Rev. Drug Discov.* 2023;22(5):410–427. <https://doi.org/10.1038/s41573-023-00652-2>
49. Cecchini C., Pannilunghi S., Tardy S., Scapozza L. From Conception to Development: Investigating PROTACs Features for Improved Cell Permeability and Successful Protein Degradation. *Front. Chem.* 2021;9:672267. <https://doi.org/10.3389/fchem.2021.672267>
50. Liu X., Zhang X., Lv D., Yuan Y., Zheng G., Zhou D. Assays and technologies for developing proteolysis targeting chimera degraders. *Future Med. Chem.* 2020;12(12):1155–1179. <https://doi.org/10.4155/fmc-2020-0073>
51. Pfaff P., Samarasinghe K.T.G., Crews C.M., Carreira E.M. Reversible Spatiotemporal Control of Induced Protein Degradation by Bistable PhotoPROTACs. *ACS Cent. Sci.* 2019;5(10):1682–1690. <https://doi.org/10.1021/acscentsci.9b00713>
52. Zeng S., Zhang H., Shen Z., Huang W. Photopharmacology of Proteolysis-Targeting Chimeras: A New Frontier for Drug Discovery. *Front. Chem.* 2021;9:639176. <https://doi.org/10.3389/fchem.2021.639176>
53. Liu J., Chen H., Liu Y., Shen Y., Meng F., Kaniskan H.U., *et al.* Cancer Selective Target Degradation by Folate-Caged PROTACs. *J. Am. Chem. Soc.* 2021;143(19):7380–7387. <https://doi.org/10.1021/jacs.1c00451>
54. Gabizon R., Shraga A., Gehrtz P., Livnah E., Shorer Y., Gurwicz N., *et al.* Efficient Targeted Degradation via Reversible and Irreversible Covalent PROTACs. *J. Am. Chem. Soc.* 2020;142(27):11734–11742. <https://doi.org/10.1021/jacs.9b13907>
55. Yuan M., Chu Y., Duan Y. Reversible Covalent PROTACs: Novel and Efficient Targeted Degradation Strategy. *Front. Chem.* 2021;9:691093. <https://doi.org/10.3389/fchem.2021.691093>
56. Jin Y., Fan J., Wang R., Wang X., Li N., You Q., *et al.* Ligation to Scavenging Strategy Enables On-Demand Termination of Targeted Protein Degradation. *J. Am. Chem. Soc.* 2023;145(13):7218–7229. <https://doi.org/10.1021/jacs.2c12809>
57. Morreale F.E., Kleine S., Leodolter J., Junker S., Hoi D.M., Ovchinnikov S., *et al.* BacPROTACs mediate targeted protein degradation in bacteria. *Cell.* 2022;185(13):2338–2353.e18. <https://doi.org/10.1016/j.cell.2022.05.009>
58. Gopal P., Dick T. Targeted protein degradation in antibacterial drug discovery? *Prog. Biophys. Mol. Biol.* 2020;152:10–14. <https://doi.org/10.1016/j.pbiomolbio.2019.11.005>
59. Sarathy J.P., Aldrich C.C., Go M.L., Dick T. PROTAC antibiotics: the time is now. *Expert Opin. Drug Discov.* 2023;18(4):363–370. <https://doi.org/10.1080/17460441.2023.2178413>
60. Venkatesan J., Murugan D., Rangasamy L. A Perspective on Newly Emerging Proteolysis-Targeting Strategies in Antimicrobial Drug Discovery. *Antibiotics (Basel).* 2022;11(12):1717. <https://doi.org/10.3390/antibiotics11121717>
61. Espinoza-Chavez R.M., Salerno A., Liuzzi A., Ilari A., Milelli A., Uliassi E., *et al.* Targeted Protein Degradation for Infectious Diseases: from Basic Biology to Drug Discovery. *ACS Bio Med. Chem. Au.* 2023;3(1):32–45. <https://doi.org/10.1021/acsbiochemau.2c00063>

62. Desantis J., Goracci L. Proteolysis targeting chimeras in antiviral research. *Future Med. Chem.* 2022;14(7):459–462. <https://doi.org/10.4155/fmc-2022-0005>
63. Ma Y., Frutos-Beltran E., Kang D., Pannecouque C., De Clercq E., Menendez-Arias L., *et al.* Medicinal chemistry strategies for discovering antivirals effective against drug-resistant viruses. *Chem. Soc. Rev.* 2021;50(7):4514–4540. <https://doi.org/10.1039/d0cs01084g>
64. Reboud-Ravaux M., El Amri C. COVID-19 Therapies: Protease Inhibitions and Novel Degradation Strategies. *Front. Drug Discov.* 2022;2. <https://doi.org/10.3389/fddsv.2022.892057>
65. Li H., Wang S., Ma W., Cheng B., Yi Y., Ma X., *et al.* Discovery of Pentacyclic Triterpenoid PROTACs as a Class of Effective Hemagglutinin Protein Degradation. *J. Med. Chem.* 2022;65(10):7154–7169. <https://doi.org/10.1021/acs.jmedchem.1c02013>
66. Li W., Yang F., Meng L., Sun J., Su Y., Shao L., *et al.* Synthesis, Structure Activity Relationship and Anti-influenza A Virus Evaluation of Oleanolic Acid-Linear Amino Derivatives. *Chem. Pharm. Bull. (Tokyo)*. 2019;67(11):1201–1207. <https://doi.org/10.1248/cpb.c19-00485>
67. Xu Z., Liu X., Ma X., Zou W., Chen Q., Chen F., *et al.* Discovery of oseltamivir-based novel PROTACs as degraders targeting neuraminidase to combat H1N1 influenza virus. *Cell Insight.* 2022;1(3):100030. <https://doi.org/10.1016/j.cellin.2022.100030>
68. De Wispelaere M., Du G., Donovan K.A., Zhang T., Eleuteri N.A., Yuan J.C., *et al.* Small molecule degraders of the hepatitis C virus protease reduce susceptibility to resistance mutations. *Nat. Commun.* 2019;10(1):3468. <https://doi.org/10.1038/s41467-019-11429-w>
69. Haniff H.S., Tong Y., Liu X., Chen J.L., Suresh B.M., Andrews R.J., *et al.* Targeting the SARS-CoV-2 RNA Genome with Small Molecule Binders and Ribonuclease Targeting Chimera (RIBOTAC) Degradation. *ACS Cent. Sci.* 2020;6(10):1713–1721. <https://doi.org/10.1021/acscentsci.0c00984>
70. Su X., Ma W., Feng D., Cheng B., Wang Q., Guo Z., *et al.* Efficient Inhibition of SARS-CoV-2 Using Chimeric Antisense Oligonucleotides through RNase L Activation. *Angew. Chem. Int. Ed. Engl.* 2021;60(40):21662–21667. <https://doi.org/10.1002/anie.202105942>
71. Zhou Y., Zheng R., Liu D., Liu S., Disoma C., Li S., *et al.* UBR5 Acts as an Antiviral Host Factor against MERS-CoV via Promoting Ubiquitination and Degradation of ORF4b. *J. Virol.* 2022;96(17):e0074122. <https://doi.org/10.1128/jvi.00741-22>
72. Zhao J., Wang J., Pang X., Liu Z., Li Q., Yi D., *et al.* An anti-influenza A virus microbial metabolite acts by degrading viral endonuclease PA. *Nat. Commun.* 2022;13(1):2079. <https://doi.org/10.1038/s41467-022-29690-x>
73. Wild M., Kicuntod J., Seyler L., Wangen C., Bertzbach L.D., Conradie A.M., *et al.* Combinatorial Drug Treatments Reveal Promising Anticytomegaloviral Profiles for Clinically Relevant Pharmaceutical Kinase Inhibitors (PKIs). *Int. J. Mol. Sci.* 2021;22(2):575. <https://doi.org/10.3390/ijms22020575>
74. Hahn F., Hamilton S.T., Wangen C., Wild M., Kicuntod J., Bruckner N., *et al.* Development of a PROTAC-Based Targeting Strategy Provides a Mechanistically Unique Mode of Anti-Cytomegalovirus Activity. *Int. J. Mol. Sci.* 2021;22(23):12858. <https://doi.org/10.3390/ijms222312858>
75. Desantis J., Mercorelli B., Celegato M., Croci F., Bazzacco A., Baroni M., *et al.* Indomethacin-based PROTACs as pan-coronavirus antiviral agents. *Eur. J. Med. Chem.* 2021;226:113814. <https://doi.org/10.1016/j.ejmech.2021.113814>
76. Zahid S., Ali Y., Rashid S. Structural-based design of HD-TAC7 PROteolysis TArgeting chimeras (PROTACs) candidate transformations to abrogate SARS-CoV-2 infection. *J. Biomol. Struct. Dyn.* 2023;41(23):14566–14581. <https://doi.org/10.1080/07391102.2023.2183037>
77. Shaheer M., Singh R., Sobhia M.E. Protein degradation: a novel computational approach to design protein degrader probes for main protease of SARS-CoV-2. *J. Biomol. Struct. Dyn.* 2022;40(21):10905–10917. <https://doi.org/10.1080/07391102.2021.1953601>

About the authors

Maria A. Zakharova, Postgraduate Student, Department of Biotechnology and Industrial Pharmacy, M.V. Lomonosov Institute of Fine Chemical Technologies, MIREA – Russian Technological University (86, Vernadskogo pr., Moscow, 119571, Russia). E-mail: zaharova_ma@mirea.ru. <https://orcid.org/0009-0004-3043-7438>

Mikhail V. Chudinov, Cand. Sci. (Chem.), Associate Professor, Department of Biotechnology and Industrial Pharmacy, M.V. Lomonosov Institute of Fine Chemical Technologies, MIREA – Russian Technological University (86, Vernadskogo pr., Moscow, 119571, Russia). E-mail: chudinov@mirea.ru. Scopus Author ID 6602589900, ResearcherID L-5728-2016, RSCI SPIN-code 3920-8067, <https://orcid.org/0000-0001-9735-9690>

Об авторах

Захарова Мария Андреевна, аспирант, кафедра биотехнологии и промышленной фармации, Институт тонких химических технологий им. М.В. Ломоносова, ФГБОУ ВО «МИРЭА – Российский технологический университет» (119571, Россия, Москва, пр-т Вернадского, д. 6). E-mail: zaharova_ma@mirea.ru. <https://orcid.org/0009-0004-3043-7438>

Чудинов Михаил Васильевич, к.х.н., доцент кафедры биотехнологии и промышленной фармации, Институт тонких химических технологий им. М.В. Ломоносова, ФГБОУ ВО «МИРЭА – Российский технологический университет» (119571, Россия, Москва, пр-т Вернадского, д. 86). E-mail: chudinov@mirea.ru. Scopus Author ID 6602589900, ResearcherID L-5728-2016, SPIN-код РИНЦ 3920-8067, <https://orcid.org/0000-0001-9735-9690>

Translated from Russian into English by H. Moshkov

Edited for English language and spelling by Dr. David Mossop

UDC 616-092+575:599.9

<https://doi.org/10.32362/2410-6593-2024-19-3-232-239>

EDN HRONBL



RESEARCH ARTICLE

Methylation of a group of microRNA genes as a marker for the diagnosis and prognosis of non-small cell lung cancer

Vitaliy I. Loginov^{1,2}, Marina S. Gubenko¹, Alexey M. Burdenny^{1,3,✉}, Irina V. Pronina^{1,4}, Pavel V. Postnikov⁴, Yulia A. Efimova⁵, Fedor V. Radus⁵, Elena S. Mochalova⁴, Tatyana P. Kazubskaya⁶

¹ Institute of General Pathology and Pathophysiology, Moscow, 125315 Russia

² Research Center for Medical Genetics, Moscow, 115522 Russia

³ Emanuel Institute for Biochemical Physics, Russian Academy of Sciences, Moscow, 119334 Russia

⁴ National Anti-Doping Laboratory (Institute), M.V. Lomonosov Moscow State University (NADL MSU), Moscow, 105005 Russia

⁵ MIREA — Russian Technological University (M.V. Lomonosov Institute of Fine Chemical Technologies), Moscow, 119571 Russia

⁶ Blokhin National Medical Research Center of Oncology, Moscow, 115478 Russia

✉ Corresponding author, e-mail: burdenny@gmail.com

Abstract

Objectives. Lung cancer, representing a difficult-to-diagnose heterogeneous malignant neoplasm, is characterized by an asymptomatic course up to late stages, a high incidence of adverse outcomes, and a high probability of metastasis. Its most common form is non-small cell lung cancer (NSCLC). Recent studies have demonstrated a significant role of non-coding RNAs—in particular, microRNAs—in the development of NSCLC. MicroRNAs, which function as post-transcriptional regulators of the expression of protein-coding genes, including those associated with oncogenesis, are involved in the processes of cell proliferation, differentiation, and apoptosis. One of the approaches for regulating the expression of microRNAs themselves is to change the methylation of the CpG island adjacent to the microRNA gene or overlapping it. It has been shown that microRNA genes are several times more likely to undergo methylation than protein-coding genes. The aim of the present work is to study changes in the level of methylation of a number of microRNA genes and compile a potential panel of markers for the diagnosis and prognosis of NSCLC.

Methods. Samples of NSCLC tumors were collected and clinically characterized at the Blokhin National Medical Research Center of Oncology, Ministry of Health of the Russian Federation, Moscow, Russia. High-molecular-weight DNA was isolated from tissues using a standard method. The level of methylation was analyzed using bisulfite conversion of DNA and quantitative methyl-specific polymerase chain reaction with real-time detection. The significance of differences between the studied groups was assessed by the nonparametric Mann–Whitney U test for independent samples. Differences were considered significant at $p < 0.05$.

Results. The analysis of methylation levels of microRNA genes revealed a significant ($p < 0.05$) increase in the methylation level of eight microRNA genes: MIR124-1/2/3, MIR125B-1, MIR129-2, MIR137, MIR375, MIR1258, and MIR339 ($p < 0.01$, false discovery rate ≤ 0.25). On the basis of receiver operating characteristic analysis, a panel of markers is proposed for the diagnosis of NSCLC according to the nature of methylation of the studied microRNA genes in the tumor and in the normal tissue.

Conclusions. Our results, which contribute to the understanding of molecular mechanisms involved in NSCLC development, can be used in the development of new diagnostic and prognostic approaches in clinical oncology.

Keywords

microRNA, methylation, panel of markers, non-small cell lung cancer

Submitted: 22.02.2024

Revised: 29.03.2024

Accepted: 15.04.2024

For citation

Loginov V.I., Gubenko M.S., Burdenny A.M., Pronina I.V., Postnikov P.V., Efimova Yu.A., Radus F.V., Mochalova E.S., Kazubskaya T.P. Methylation of a group of microRNA genes as a marker for the diagnosis and prognosis of non-small cell lung cancer. *Tonk. Khim. Tekhnol.* = *Fine Chem. Technol.* 2024;19(3):232–239. <https://doi.org/10.32362/2410-6593-2024-19-3-232-239>

НАУЧНАЯ СТАТЬЯ

Метилирование группы генов микроРНК как маркер диагностики и прогноза немелкоклеточного рака легкого

В.И. Логинов^{1,2}, М.С. Губенко¹, А.М. Бурденный^{1,3,✉}, И.В. Пронина^{1,4}, П.В. Постников⁴, Ю.А. Ефимова⁵, Ф.В. Радус⁵, Е.С. Мочалова⁴, Т.П. Казубская⁶

¹ Научно-исследовательский институт общей патологии и патофизиологии, Москва, 125315 Россия

² Медико-генетический научный центр им. академика Н.П. Бочкова, Москва, 115522, Россия

³ Институт биохимической физики им. Н.М. Эмануэля, Российская академия наук, Москва, 119334 Россия

⁴ Национальная антидопинговая лаборатория (Институт), Московский государственный университет им. М.В. Ломоносова (НАДЛ МГУ), Москва, 105005 Россия

⁵ МИРЭА — Российский технологический университет (Институт тонких химических технологий им. М.В. Ломоносова) Москва, 119571 Россия

⁶ Национальный медицинский исследовательский центр онкологии им. Н.Н. Блохина, Министерство здравоохранения Российской Федерации, Москва, 115478 Россия

✉ Автор для переписки, e-mail: burdennyu@gmail.com

Аннотация

Цели. Рак легкого представляет собой гетерогенное злокачественное новообразование с низким диагностическим потенциалом, характеризующееся бессимптомным течением вплоть до поздних стадий, высокой частотой неблагоприятных исходов и высокой вероятностью метастазирования. Его самой распространенной формой является немелкоклеточный рак легкого (НМРЛ). Последние исследования показывают значительную роль некодирующих РНК, в частности, микроРНК, в развитии НМРЛ. МикроРНК выполняют функцию пост-транскрипционных регуляторов экспрессии белок-кодирующих генов, в том числе, связанных с онкогенезом, и вовлечены в процессы пролиферации, дифференцировки и апоптоза клеток. Одним из путей регуляции экспрессии самих микроРНК является изменение метилирования CpG-островка, прилежащего к гену микроРНК или перекрывающего его. Показано, что гены микроРНК в несколько раз чаще подвергаются метилированию, чем белок-кодирующие гены. Целью настоящего исследования являлось изучение изменения уровня метилирования ряда генов микроРНК и составление потенциальной панели маркеров для диагностики и прогноза НМРЛ.

Методы. Образцы опухолей НМРЛ собраны и клинически охарактеризованы в НИИ клинической онкологии Национального медицинского исследовательского центра онкологии им. Н.Н. Блохина. Высокомолекулярную ДНК выделяли из ткани стандартным методом. Анализ уровня метилирования проводили с применением бисульфитной конверсии ДНК и количественной метилспецифичной полимеразной цепной реакцией с детекцией в реальном времени. Для оценки значимости различий между исследуемыми группами применяли непараметрический критерий Манна–Уитни для независимых выборок. Различия считали достоверными при $p < 0.05$.

Результаты. В результате анализа уровней метилирования генов микроРНК нами было показано значимое ($p < 0.05$) увеличение уровня метилирования восьми генов микроРНК: MIR124-1/2/3, MIR125B-1, MIR129-2, MIR137, MIR375, MIR1258, MIR339 ($p < 0.01$, FDR ≤ 0.25). Был проведен ROC-анализ, позволивший предложить панель маркеров для диагностики НМРЛ по характеру метилирования исследованных генов микроРНК в опухоли и норме.

Выводы. Полученные нами результаты способствуют пониманию молекулярных механизмов развития НМРЛ и могут быть использованы при разработке новых диагностических и прогностических подходов в клинической онкологии.

Ключевые слова

микроРНК, метилирование, панель маркеров, немелкоклеточный рак легкого

Поступила: 22.02.2024

Доработана: 29.03.2024

Принята в печать: 15.04.2024

Для цитирования

Логинов В.И., Губенко М.С., Бурденный А.М., Пронина И.В., Постников П.В., Ефимова Ю.А., Радус Ф.В., Мочалова Е.С., Казубская Т.П. Метилирование группы генов микроРНК как маркер диагностики и прогноза немелкоклеточного рака легкого. *Тонкие химические технологии*. 2024;19(3):232–239. <https://doi.org/10.32362/2410-6593-2024-19-3-232-239>

INTRODUCTION

Representing the most common type of lung cancer (up to 85% of cases), non-small cell lung cancer (NSCLC) is difficult to diagnose due to its heterogeneity (lung adenocarcinoma, squamous cell lung cancer, large cell lung cancer, etc.) and low detection rate in the early stages. NSCLC has a high metastatic potential. It is noted that up to 40% of detected NSCLC cases were identified as metastatic tumors. For this reason, in the diagnosis and prognosis of this type of cancer, a molecular approach is important [1].

At the moment, there is no unified system of molecular diagnostics and prognosis for determining the development of the early-stage oncological process and assessing its metastatic potential. As for any multifactorial disease, there are both genetic and epigenetic development triggers for each type of cancer [2]. One of the most significant epigenetic regulatory mechanisms, which dynamically and specifically influence processes in the cell, including gene expression, is the DNA methylation mechanism, which provokes tumor development when in an aberrant state. Aberrant methylation involves two differently directed processes: hypermethylation of tumor suppressor genes and demethylation of oncogenes. Aberrant methylation is associated with the regulation of many genes, including microRNA genes, which themselves constitute a regulatory element of the gene expression system [3].

MicroRNAs belong to the group of short non-coding RNAs, which perform a regulatory function in the body at the post-transcriptional level. MicroRNAs are involved in many cellular processes, including proliferation, differentiation, and apoptosis, whose disruption can lead to tumorigenesis [4]. Methylation/demethylation has been shown to play a much larger role in the regulation of microRNA genes than protein-coding genes. Hypermethylation leads to the switching off of the microRNA gene, while demethylation, conversely, causes its activation. Methylation and expression profiles of microRNA genes turned out to be highly specific for tumors of different locations and histological profiles [5]. NSCLC is characterized by a specific level of microRNA gene expression, which is associated with the clinical and pathological properties of a tumor. However, the methylation status of miRNA genes, which influences expression, is rarely studied. Detection of hypermethylation of a number of microRNA genes

that exhibit tumor suppressor properties in NSCLC is a priority research area due to the possibility of creating a system of diagnostic and prognostic markers based on hypermethylated microRNA genes [6].

The aim of the present work is to create a potential marker system for the diagnosis and prognosis of NSCLC based on changes in the methylation level of a number of microRNA genes in a tumor.

EXPERIMENTAL

Collection of material. The level of methylation of microRNA genes was analyzed using 70 paired samples of tumor and adjacent normal lung tissue from NSCLC patients treated at the Blokhin National Medical Research Center of Oncology, Ministry of Health of the Russian Federation, Moscow, Russia. Samples were collected during elective surgery. All tumors were classified according to the TNM classification of the International Union Against Cancer and histologically verified based on the World Health Organization classification criteria [7]. The diagnosis was carried out on the basis of histological findings. Table presents clinical data of patients.

The study included samples of NSCLC tissue from patients who had not received radiation therapy, chemotherapy, or hormone therapy before surgery. The work was carried out in compliance with the principles of voluntariness and confidentiality in accordance with the Declaration of Helsinki of the World Medical Association [8].

DNA extraction. High-molecular-weight DNA was isolated from tissue by a standard method using phenol–chloroform extraction [9]. The DNA concentration was determined by optical density using a NanoDrop ND-1000 spectrophotometer (*Thermo Fisher Scientific*, USA).

Determination of the level of methylation. The methylation of microRNA genes was analyzed using quantitative methyl-specific polymerase chain reaction with real-time detection (qMS-RT-PCR) following bisulfite conversion of DNA according to the published procedure [10]. The completeness of DNA conversion was determined using the ACTB (*ACTin Beta*) control locus using oligonucleotides specific to the unconverted template. Amplification was carried out using a qPCRmix-HS SYBR reagent kit according to

Table. Clinicopathological characteristics of the studied samples

Clinicopathological parameter		Total number, $N = 70$	%
Histologic type	Squamous cell lung cancer	39	55.7
	Lung adenocarcinoma	31	44.3
Tumor stage	I	14	20.0
	II	28	40.0
	III	20	28.6
	IV	8	11.4
Degree of differentiation	G1	6	8.6
	G2	35	50.0
	G3	29	41.4
Tumor size	T1	11	15.7
	T2	35	50.0
	T3	13	18.6
	T4	11	15.7
Lymphatic metastasis	N0	29	41.4
	N1	41	58.6
Distant metastasis	M0	62	88.6
	M1	8	11.4

the *Evrogen* (Russia) protocol in the Bio-Rad CFX96 Real-Time PCR Detection System (*Bio-Rad*, USA). Oligonucleotide sequences and PCR conditions for microRNA genes were as presented in previous work [11]. Commercial human genomic DNA #G1471 (*Promega*, USA) was used as a control for unmethylated alleles. Commercial human genomic DNA #SD1131 (*Thermo Fisher Scientific*, USA) was used as a control for 100% methylation.

Statistical processing of the results was carried out using the IBM SPSS Statistics 22 software¹. The significance of differences between the studied groups was assessed by the nonparametric Mann–Whitney U test for independent samples. Differences were considered significant at $p < 0.05$. Data were expressed

as median (Me), lower (Q1), and upper (Q3) quartiles. Correlation analysis was performed by Spearman's rank correlation method, and its significance level was calculated [12]. To compile a panel with certain sensitivity and specificity coefficients, receiver operating characteristic (ROC) analysis was performed. Differences were considered significant and reliable at $p \leq 0.05$. False discovery rate ≤ 0.25 .

RESULTS AND DISCUSSION

Using a representative statistical sample of NSCLC samples (70 tumor/normal pairs), changes in the methylation level of ten microRNA genes were studied: MIR124-1, MIR124-2, MIR124-3, MIR125B-1,

¹ <https://soware.ru/products/ibm-spss-statistics>. Accessed March 6, 2024.

MIR127, MIR129-2, MIR137, MIR375, MIR1258, and MIR339. According to the obtained results, a statistically significant ($p < 0.01$) increase in the level of their methylation (Fig. 1) in the tumor in comparison with the adjacent histologically unchanged normal tissue was found for the genes of eight out of ten microRNAs (MIR124-1/2/3, MIR127, MIR129-2, MIR137, MIR1258, and MIR339). We have previously presented convincing data for other types of cancer about the role of hypermethylation of these eight microRNAs [11, 13]. Note that, for NSCLC, a high level of methylation for the microRNA gene MIR339 was identified for the first time.

In the present work, we noted a correlation between the methylation levels of the studied microRNA genes and the clinicopathological characteristics of tumors. For example, methylation of the MIR125B-1, MIR1258,

and MIR339 genes was observed in all NSCLC tumor samples ($p < 0.05$), regardless of histological type, stage and degree of differentiation, and the presence or absence of metastases. We also noted an association between hypermethylation of the MIR124-3, MIR125B-1, MIR137, and MIR1258 genes with the presence of metastases to lymph nodes and distant metastases ($p < 0.05$). Using the ROC analysis results, we developed two potential test systems for assessing the development and progression of NSCLC, which have the potential for use in the diagnosis and prognosis of this disease (Fig. 2).

The potential diagnostic panel consists of three markers: MIR125B-1, MIR1258, and MIR339 (sensitivity $Se = 92.7$, specificity $Sp = 85.8$, area under the curve $AUC = 0.967$, $p < 10^{-5}$) (Fig. 2a). The potential prognostic panel consists of four markers: MIR124-3,

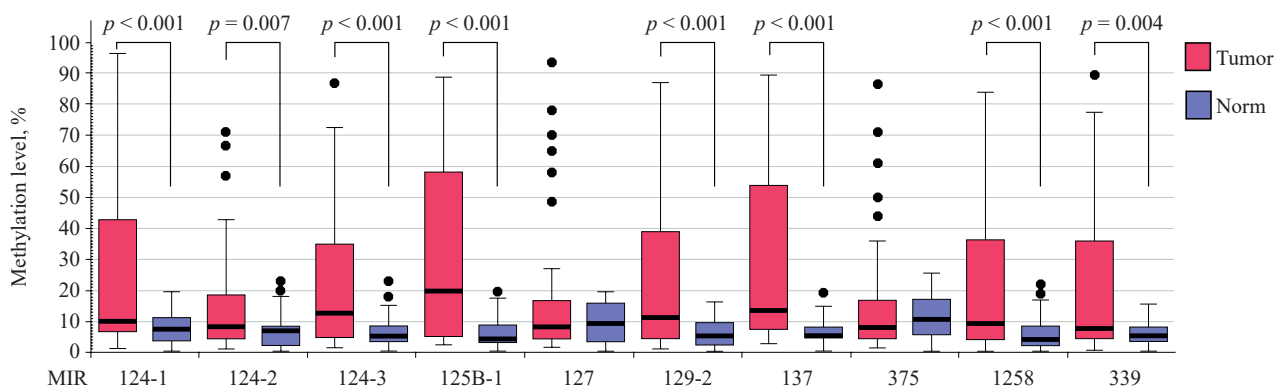


Fig. 1. Changes in the methylation level of ten microRNA genes in 70 paired tumor samples and histologically unchanged lung tissue in NSCLC

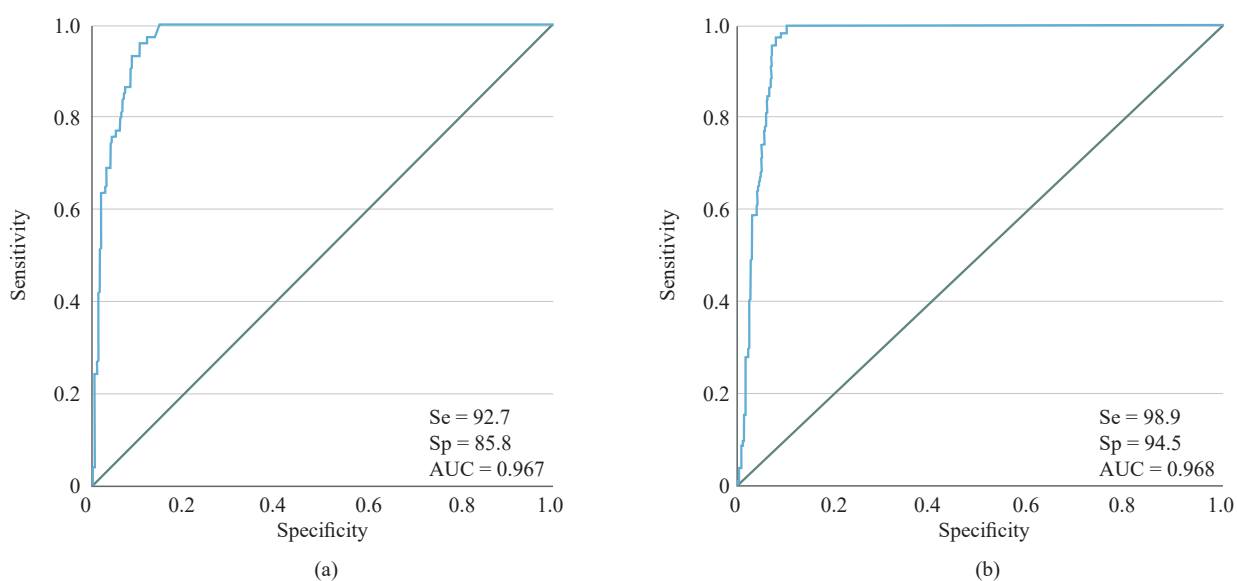


Fig. 2. ROC analysis of potential panels of markers based on assessing the methylation level of microRNA genes for the diagnosis and prognosis of NSCLC: (a) panel 1 (diagnostic): MIR125B-1, MIR1258, MIR339; (b) panel 2 (prognostic): MIR124-3, MIR125B-1, MIR1258, MIR137. Se—sensitivity; Sp—specificity; AUC—area under the curve

MIR125B-1, MIR137, and MIR1258 ($Se = 98.9$, $Sp = 94.5$, $AUC = 0.968$, $p = 1 \cdot 10^{-6}$) (Fig. 2b). The detection of hypermethylation of all microRNA genes included in the diagnostic panel suggests that the patient has NSCLC. If methylation of all genes included in the prognostic panel is detected, the patient has a high probability of developing metastatic NSCLC. Due to the high sensitivity (which exceeds 90%) and specificity of the prognostic panel of markers, their use as screening test systems with further confirmation by validated methods is justified. The detection of four hypermethylated miRNA genes of this panel may signal the need for additional monitoring of the patient for early detection and prevention of the development of metastases.

At the present stage of development of medicine, instrumental, biochemical, and histological studies of biopsy and/or resection material remain the main diagnostic methods. However, these methods are often insufficient for making a confident diagnosis. In this connection, the use of validated test systems based on molecular genetic studies could significantly change approaches to diagnosis through early detection of cell malignancy and prognosis by assessing certain tumor markers of different localizations, including NSCLC [14, 15]. The use of microRNAs as test systems for the diagnosis and prognosis of NSCLC and other types of cancer is particularly promising due to their tissue specificity, which links them to the specific course of the cancer [14].

REFERENCES

1. Araghi M., Mannani R., Heidarnejad Maleki A., Hamidi A., Rostami S., Safa S.H., Faramarzi F., Khorasani S., Alimohammadi M., Tahmasebi S., Akhavan-Sigari R. Recent advances in non-small cell lung cancer targeted therapy; an update review. *Cancer Cell Int.* 2023;23(1):162. <https://doi.org/10.1186/s12935-023-02990-y>
2. Sarhadi V.K., Armengol G. Molecular Biomarkers in Cancer. *Biomolecules.* 2022;12(8):1021. <https://doi.org/10.3390/biom12081021>
3. Li Y. Modern epigenetics methods in biological research. *Methods.* 2021;187:104–113. <https://doi.org/10.1016/j.ymeth.2020.06.022>
4. Eshkooor S.A., Ghodsian N., Akhtari-Zavare M. MicroRNAs influence and longevity. *Egypt. J. Med. Hum. Genet.* 2022;23(1):105. <https://doi.org/10.1186/s43042-022-00316-7>
5. Loginov V.I., Rykov S.V., Fridman M.V., et al. Methylation of miRNA genes and oncogenesis. *Biochemistry (Moscow).* 2015;80(2):145–162. <https://doi.org/10.1134/S0006297915020029> [Original Russian Text: Loginov V.I., Rykov S.V., Fridman M.V., Braga E.A. Methylation of miRNA genes and oncogenesis. *Biokhimiya.* 2015;80(2):184–203 (in Russ.).]
6. Liao J., Shen J., Leng Q., Qin M., Zhan M., Jiang F. MicroRNA-based biomarkers for diagnosis of non-small cell lung cancer (NSCLC). *Thorac. Cancer.* 2020;11(3):762–768. <https://doi.org/10.1111/1759-7714.13337>
7. Brierley J.D., Gospodarowicz M.K., Wittekind C. (Eds.). *TNM Classification of Malignant Tumours.* 8th ed. John Wiley & Sons; 2017. 272 p.
8. World Medical Association. World Medical Association Declaration of Helsinki: ethical principles for medical research involving human subjects. *JAMA.* 2013;310(20):2191–2194. <https://doi.org/10.1001/jama.2013.281053>
9. Loginov V.I., Burdenny A.M., Filippova E.A., et al. Aberrant Methylation of 21 MicroRNA Genes in Breast Cancer: Sets of Genes Associated with Progression and a System of Markers for Predicting Metastasis. *Bull. Exp. Biol. Med.* 2021;172(1): 67–71. <https://doi.org/10.1007/s10517-021-05333-x> [Original Russian Text: Loginov V.I., Burdenny A.M., Filippova E.A., Pronina I.V., Lukina S.S., Kazubskaya T.P., Karpukhin A.V., Khodyrev D.S., Braga E.A. Aberrant Methylation of 21 MicroRNA Genes in Breast Cancer: Sets of Genes Associated with Progression and a System of Markers for Predicting Metastasis. *Bulleten' Eksperimental'noi Biologii i Meditsiny.* 2021;172(7):81–86 (in Russ.). <https://doi.org/10.47056/0365-9615-2021-172-7-81-86>]

CONCLUSIONS

As well as contributing to an enhanced understanding of the important role played by microRNA gene methylation in the regulation of the occurrence and progression of NSCLC, the results of the study also suggest new potential biomarkers for diagnosis and prognosis, offering the possibility to develop new therapeutic targets for drug development.

Acknowledgments

The work was supported by the Scientific Research Program for 2023–2025 No. FGFU-2023-0001. The authors thank the staff of the N.N. Blokhin National Research Center of Oncology for collecting and clinico-histological characterization of samples of non-small cell lung cancer.

Authors' contributions

M.S. Gubenko, I.V. Pronina, P.V. Postnikov—responsible for experimental data.

A.M. Burdenny—concept and structure of the article.

Yu.A. Efimova, F.V. Radus, E.S. Mochalova—statistical data processing.

V.I. Loginov—bioinformatic analysis, preparation of illustrative material.

T.P. Kazubskaya—collection of clinical samples.

All co-authors have approved the final version of the article, checked the integrity of all sections of the article.

The authors declare no conflicts of interest.

10. Loginov V.I., Pronina I.V., Burdenny A.M., Filippova E.A., Kazubskaya T.P., Kushlinsky D.N., Utkin D.O., Khodyrev D.S., Kushlinskii N.E., Dmitriev A.A., Braga E.A. Novel miRNA genes deregulated by aberrant methylation in ovarian carcinoma are involved in metastasis. *Gene*. 2018;662:28–36. <https://doi.org/10.1016/j.gene.2018.04.005>
11. Klochikhina E.S., Shershov V.E., Kuznetsova V.E., Lapa S.A., Chudinov A.V. Specificities of multiprimer polymerase chain reaction optimization for the detection of infectious pneumonia agents in human. *Tonk. Khim. Tekhnol. = Fine Chem. Technol.* 2021;16(3):225–231 (Russ., Eng.). <https://doi.org/10.32362/2410-6593-2021-16-3-225-231>
12. Pronina I.V., Loginov V.I., Burdenny A.M., Fridman M.V., Senchenko V.N., Kazubskaya T.P., Kushlinskii N.E., Dmitriev A.A., Braga E.A. DNA methylation contributes to deregulation of 12 cancer-associated microRNAs and breast cancer progression. *Gene*. 2017;604:1–8. <https://doi.org/10.1016/j.gene.2016.12.018>
13. Shanebandi D., Asadi M., Seyedrezazadeh E., Zafari V., Shekari N., Akbari M., Rahbarnia L., Zarredar H. MicroRNA-Based Biomarkers in Lung Cancer: Recent Advances and Potential Applications. *Curr. Mol. Med.* 2023;23(7):648–667. <https://doi.org/10.2174/2772432817666220520085719>
14. Xu L., Huang X., Lou Y., Xie W., Zhao H. Regulation of apoptosis, autophagy and ferroptosis by non-coding RNAs in metastatic non-small cell lung cancer (Review). *Exp. Ther. Med.* 2022;23(5):352. <https://doi.org/10.3892/etm.2022.11279>

About the authors

Vitaliy I. Loginov, Cand. Sci. (Biol.), Leading Researcher, Pathogenomics and Transcriptomics Laboratory, Institute of General Pathology and Pathophysiology (8, ul. Baltiiskaya, Moscow, 125315, Russia); Senior Researcher, Laboratory of Molecular Genetics of Complex Inherited Diseases, Research Center for Medical Genetics (1, Moskvorechye ul., Moscow, 115552, Russia). E-mail: loginov7w@gmail.com. Scopus Author ID 7102884943, RSCI SPIN-code 6249-5883, <https://orcid.org/0000-0003-2668-8096>

Marina S. Gubenko, Junior Researcher, Pathogenomics and Transcriptomics Laboratory, Institute of General Pathology and Pathophysiology (8, ul. Baltiiskaya, Moscow, 125315, Russia). E-mail: art_marina@mail.ru. RSCI SPIN-code 4992-7397

Alexey M. Burdenny, Cand. Sci. (Biol.), Leading Researcher, Pathogenomics and Transcriptomics Laboratory, Institute of General Pathology and Pathophysiology (8, ul. Baltiiskaya, Moscow, 125315, Russia); Junior Researcher, Laboratory of Chemical Physics of Bioanalytical Processes, Emanuel Institute of Biochemical Physics, Russian Academy of Sciences (4, Kosygina ul., Moscow, 119334, Russia). E-mail: burdenny@gmail.com. Scopus Author ID 56049452900, RSCI SPIN-code 4429-4288, <https://orcid.org/0000-0002-9398-8075>

Irina V. Pronina, Cand. Sci. (Biol.), Main Specialist, Doping Control Department, National Anti-Doping Laboratory (Institute), Lomonosov Moscow State University (10-1, Elizavetinskii per., Moscow, 105005, Russia); Senior Researcher, Pathogenomics and Transcriptomics Laboratory, Institute of General Pathology and Pathophysiology (8, ul. Baltiiskaya, Moscow, 125315, Russia). E-mail: zolly_sten@mail.ru. Scopus Author ID 8161867200, ResearcherID G-3951-2014, ResearcherID ABD-8018-2021, RSCI SPIN-code 5706-2369, <https://orcid.org/0000-0002-0423-7801>

Pavel V. Postnikov, Cand. Sci. (Chem.), Head of the Doping Control Department, National Anti-Doping Laboratory (Institute), Lomonosov Moscow State University (10-1, Elizavetinskii per., Moscow, 105005, Russia). E-mail: postnikov@dopingtest.ru. Scopus Author ID 57021610900, RSCI SPIN-code 7251-9937, <https://orcid.org/0000-0003-3424-0582>

Yuliya A. Efimova, Cand. Sci. (Chem.), Assistant Professor, I.P. Alimarin Department of Analytical Chemistry, M.V. Lomonosov Institute of Fine Chemical Technologies, MIREA – Russian Technological University (86, Vernadskogo pr., Moscow, 119571, Russia). E-mail: efimova_yulia@bk.ru. Scopus Author ID 25228417800, <https://orcid.org/0000-0002-3582-0012>

Fedor V. Radus, Assistant, I.P. Alimarin Department of Analytical Chemistry, M.V. Lomonosov Institute of Fine Chemical Technologies, MIREA – Russian Technological University (86, Vernadskogo pr., Moscow, 119571, Russia). E-mail: radus20@mail.ru. Scopus Author ID 57890564100, <https://orcid.org/0000-0003-0938-9609>

Elena S. Mochalova, Acting Director, National Anti-Doping Laboratory (Institute), Lomonosov Moscow State University (10-1, Elizavetinskii per., Moscow, 105005, Russia). E-mail: mochalova@dopingtest.ru

Tatiana P. Kazubskaya, Dr. Sci. (Med.), Senior Scientist of Laboratory of Clinical Oncogenetics, Blokhin National Medical Research Center of Oncology (23, Kashirskoe sh., Moscow, 115478, Russia). E-mail: oncogen5@ronc.ru. Scopus Author ID 6602563950, ResearcherID F-9084-2019, RSCI SPIN-code 5224-5820, <https://orcid.org/0000-0001-5856-0017>

Об авторах

Логинов Виталий Игоревич, к.б.н., ведущий научный сотрудник лаборатории патогеномики и транскриптомики, ФГБУ «Научно-исследовательский институт общей патологии и патофизиологии» (125315, Россия, Балтийская ул., д. 8); старший научный сотрудник лаборатории молекулярной генетики сложно наследуемых заболеваний, ФГБНУ «Медико-генетический научный центр имени академика Н.П. Бочкова» (115522, Россия, Москва, ул. Москворечье, д. 1). E-mail: loginov7w@gmail.com. Scopus Author ID 7102884943, SPIN-код РИНЦ 6249-5883, <https://orcid.org/0000-0003-2668-8096>

Губенко Марина Сергеевна, младший научный сотрудник лаборатории патогеномики и транскриптомики, ФГБУ «Научно-исследовательский институт общей патологии и патофизиологии» (125315, Россия, Балтийская ул., д. 8). E-mail: artz_marina@mail.ru. SPIN-код РИНЦ 4992-7397

Бурденный Алексей Михайлович, к.б.н., ведущий научный сотрудник лаборатории патогеномики и транскриптомики, ФГБУ «Научно-исследовательский институт общей патологии и патофизиологии» (125315, Россия, Балтийская ул., д. 8); младший научный сотрудник лаборатории химической физики биоаналитических процессов, ФГБУН «Институт биохимической физики им. Н.М. Эмануэля Российской академии наук» (ИБФХ РАН) (119334, Россия, Москва, ул. Косыгина, д. 4). E-mail: burdennyu@gmail.com. Scopus Author ID 56049452900, SPIN-код РИНЦ 4429-4288, <https://orcid.org/0000-0002-9398-8075>

Пронина Ирина Валерьевна, к.б.н., главный специалист отдела допингового контроля, Национальная антидопинговая лаборатория (Институт), Московский государственный университет им. М.В. Ломоносова (105005, Россия, Москва, Елизаветинский переулок, д. 10, стр. 1); старший научный сотрудник лаборатории патогеномики и транскриптомики, ФГБУ «Научно-исследовательский институт общей патологии и патофизиологии» (125315, Россия, Балтийская ул., д. 8). E-mail: zolly_sten@mail.ru. Scopus Author ID 8161867200, ResearcherID G-3951-2014, ResearcherID ABD-8018-2021, SPIN-код РИНЦ 5706-2369, <https://orcid.org/0000-0002-0423-7801>

Постников Павел Викторович, к.х.н., начальник отдела допингового контроля, Национальная антидопинговая лаборатория (Институт), Московский государственный университет им. М.В. Ломоносова (105005, Россия, Москва, Елизаветинский переулок, д. 10, стр. 1). E-mail: postnikov@dopingtest.ru. Scopus Author ID 57021610900, SPIN-код РИНЦ 7251-9937, <https://orcid.org/0000-0003-3424-0582>

Ефимова Юлия Александровна, к.х.н., доцент кафедры аналитической химии им. И.П. Алимарина, Институт тонких химических технологий им. М.В. Ломоносова, ФГБОУ ВО «МИРЭА – Российский технологический университет» (119571, Россия, Москва, пр-т Вернадского, д. 86). E-mail: efimova_yulia@bk.ru. Scopus Author ID 25228417800, <https://orcid.org/0000-0002-3582-0012>

Радус Федор Валерьевич, ассистент кафедры аналитической химии им. И.П. Алимарина, Институт тонких химических технологий им. М.В. Ломоносова, ФГБОУ ВО «МИРЭА – Российский технологический университет» (119571, Россия, Москва, пр-т Вернадского, д. 86). E-mail: radus20@mail.ru. Scopus Author ID 57890564100, <https://orcid.org/0000-0003-0938-9609>

Мочалова Елена Сергеевна, исполняющий обязанности директора Национальной антидопинговой лаборатории (Института), Московский государственный университет им. М.В. Ломоносова (105005, Россия, Москва, Елизаветинский переулок, д. 10, стр. 1). E-mail: mochalova@dopingtest.ru.

Казубская Татьяна Павловна, д.м.н., врач-онкогенетик, старший научный сотрудник лаборатории клинической онкогенетики, ФГБУ «Национальный медицинский исследовательский центр онкологии имени Н.Н. Блохина» Министерства здравоохранения Российской Федерации (115478, Россия, Москва, Каширское шоссе, д. 23). E-mail: oncogen5@ronc.ru. Scopus Author ID 6602563950, ResearcherID F-9084-2019, SPIN-код РИНЦ 5224-5820, <https://orcid.org/0000-0001-5856-0017>

Translated from Russian into English by V. Glyanchenko

Edited for English language and spelling by Thomas A. Beavitt

UDC 60

<https://doi.org/10.32362/2410-6593-2024-19-3-240-257>

EDN JHCZWL



Development of technology for culturing a cell line producing a single-domain antibody fused with the Fc fragment of human IgG1

Dmitry S. Polyansky^{1,2,✉}, Ekaterina I. Ryabova^{1,3}, Artem A. Derkaev¹, Nikita S. Starkov¹, Irina S. Kashapova¹, Dmitry V. Shcheblyakov¹, Andrey P. Karpov¹, Ilias B. Esmagambetov¹

¹ N.F. Gamaleya National Research Center for Epidemiology and Microbiology, Ministry of Health of the Russian Federation, Moscow, 123098 Russia

² MIREA — Russian Technological University (M.V. Lomonosov Institute of Fine Chemical Technologies), Moscow, 119571 Russia

³ Moscow State Academy of Veterinary Medicine and Biotechnology — K.I. Skryabin MVA, Moscow, 109472 Russia

✉ Corresponding author; e-mail: polanskiydmityriy15@gmail.com

Abstract

Objectives. To develop an effective technology for the cultivation of Chinese hamster ovary (CHO) cells stably producing GamP2C5 antibody which is a component I of the GamCoviMab candidate drug for emergency prevention and therapy of infection caused by SARS-CoV-2 virus; to select optimal cultivation parameters and to scale this technology in production.

Methods. The study was performed on CHO GamP2C5 (clone 78) cell culture, producing a single-domain antibody fused to the Fc fragment of human IgG1 GamP2C5. Different culture media and supplements were used. Cells were cultured in Erlenmeyer flasks, Biostat[®] RM 20 wave-mixed bioreactor, Ambr[®] 250 mini bioreactors, STR 200 stirred-tank bioreactor.

Results. Using molecular-genetic and biotechnological methods, a stable clone producer of CHO GamP2C5 antibody, clone 78, was obtained. Then a technique was worked out for the cultivation of the obtained clone producer on different culture media. The most suitable cultivation regimes, culture media, and optimal supplements were selected. This technology was tested in laboratory conditions in a 10-L reactor, and then successfully scaled up for production at the *MedGamal* Branch of the Gamaleya National Research Center for Epidemiology and Microbiology.

Conclusions. This study demonstrates the fundamental feasibility of developing and scaling up a culture technology, in order to produce a drug based on a modified single-domain antibody with virus neutralizing activity against different strains of SARS-CoV-2 virus.

Keywords

monoclonal antibodies, single-domain antibodies, heavy chain antibodies, cultivation, CHO cells, bioprocess scaling

Submitted: 12.12.2023

Revised: 08.02.2024

Accepted: 17.04.2024

For citation

Polyansky D.S., Ryabova E.I., Derkaev A.A., Starkov N.S., Kashapova I.S., Shcheblyakov D.V., Karpov A.P., Esmagambetov I.B. Development of technology for culturing a cell line producing a single-domain antibody fused with the Fc fragment of human IgG1. *Tonk. Khim. Tekhnol. = Fine Chem. Technol.* 2024;19(3):240–257. <https://doi.org/10.32362/2410-6593-2024-19-3-240-257>

НАУЧНАЯ СТАТЬЯ

Разработка технологии культивирования клеточной линии, продуцирующей однодоменное антитело, слитое с Fc-фрагментом IgG1 человека

Д.М. Полянский^{1,2,✉}, Е.И. Рябова^{1,3}, А.А. Деркаев¹, Н.С. Старков¹, И.С. Кашапова¹, Д.В. Щепляков¹, А.П. Карпов¹, И.Б. Есмагамбетов¹

¹ Национальный исследовательский центр эпидемиологии и микробиологии им. Н.Ф. Гамалеи, Министерство Здравоохранения Российской Федерации, Москва, 123098 Россия

² МИРЭА — Российский технологический университет (Институт тонких химических технологий им. М.В. Ломоносова), Москва, 119571 Россия

³ Московская государственная академия ветеринарной медицины и биотехнологии — МВА им. К.И. Скрябина, Москва, 109472 Россия

✉ Автор для переписки, e-mail: polanskiydm15@gmail.com

Аннотация

Цели. Разработать эффективную технологию культивирования клеток яичников китайского хомячка (СНО), стабильно продуцирующих антитело GamP2C5, которое является компонентом I кандидатного препарата ГамКовиМаб для экстренной профилактики и терапии инфекции, вызванной вирусом SARS-CoV-2; подобрать оптимальные параметры культивирования и масштабировать данную технологию на производстве.

Методы. Исследование проводилось на культуре клеток СНО GamP2C5 (клон 78) продуцирующей однодоменное антитело, слитое с Fc-фрагментом IgG1 человека GamP2C5; были использованы различные среды для культивирования и питательные добавки. Культивирование клеток проходило в колбах Эрленмейера, биореакторе с волновым типом перемешивания Biostat[®] RM 20 basic, минибиореакторах Ambr[®] 250, биореакторе с осевым типом перемешивания STR 200.

Результаты. При помощи молекулярно-генетических и биотехнологических методов был получен стабильный клон-продуцент антитела СНО GamP2C5 (клон 78), и отработана методика культивирования полученного клона-продуцента на различных питательных средах. Были выбраны наиболее подходящие режимы культивирования, питательная среда и оптимальные подпитки. Данная технология была отработана в лабораторных условиях в 10-литровом реакторе и успешно масштабирована на производстве в филиале «Медгамал» Национального исследовательского центра эпидемиологии и микробиологии им. Н.Ф. Гамалеи.

Выводы. В данном исследовании показана принципиальная возможность разработки и масштабирования технологии культивирования для получения препарата на основе модифицированного однодоменного антитела с вируснейтрализующей активностью против различных штаммов вируса SARS-CoV-2.

Ключевые слова

моноклональные антитела, однодоменные антитела, тяжелоцепочечные антитела, культивирование, клетки СНО, масштабирование биопроцесса

Поступила: 12.12.2023

Доработана: 08.02.2024

Принята в печать: 17.04.2024

Для цитирования

Полянский Д.М., Рябова Е.И., Деркаев А.А., Старков Н.С., Кашапова И.С., Щепляков Д.В., Карпов А.П., Есмагамбетов И.Б. Разработка технологии культивирования клеточной линии, продуцирующей однодоменное антитело, слитое с Fc-фрагментом IgG1 человека. *Тонкие химические технологии*. 2024;19(3):240–257. <https://doi.org/10.32362/2410-6593-2024-19-3-240-257>

INTRODUCTION

Following the development of hybridoma technology in the mid-1970s, monoclonal antibodies [1] began to be explored as potential therapeutics for a variety of diseases [2]. Over the last decade, several dozen antibody-based drugs (Adalimumab, Pembrolizumab, Nivolumab) have been developed: some are among the top-selling drugs ranking worldwide [3]. Monoclonal antibodies are used to treat a wide range of human diseases, including various types of cancer [4]. Furthermore, therapeutic antibodies are effective in the therapy of multiple sclerosis [5], Crohn's disease [6], rheumatoid arthritis [7], and bacterial and viral infections [8].

The COVID-19 pandemic had a tremendous impact on drug and vaccine discovery and the development of strategies designed to control infectious diseases. Monoclonal antibodies represent the largest and fastest growing class of pharmaceutical compounds to have shown therapeutic potential in the treatment of viral infections, including against SARS-CoV-2 virus.

In recent years, the number of preparations based on monoclonal antibodies against viral infections, especially chronic infections [9], has increased markedly. Monoclonal antibodies can be used to suppress the spread of infection through direct viral neutralizing activity [10]. To date, several antiviral drugs with a high level of efficacy have been approved. Among them, Casirivimab/imdevimab (REGEN-COV) is the first monoclonal antibody-based drug which can be used for both treatment and emergency prevention of COVID-19 [11].

One particular case of monoclonal antibodies are the heavy chain antibodies of the camelid family. They are devoid of light chains and the variable fragments are represented by a single heavy chain domain. Furthermore, the variable fragments of the heavy chain can be used independently. Such modifications are called nanobodies, also known as single-domain antibodies or VHH [12].

Single-domain antibodies are a relatively new class of drugs. They were discovered by chance while analyzing camel serum. Due to their structure and properties, nanoantibodies are able to effectively bind to antigen epitopes which are difficult to reach for classical antibodies. They also prevent interaction of receptors with ligands, or deliver substances that perform various functions to target cells. At the same time, the disadvantages of nanoantibodies are associated with their rapid excretion by kidneys and a lack of an independent effector function due to the absence of Fc fragment. Many studies demonstrate the successful use of single-domain antibodies and their modifications for therapy and prevention of various infectious diseases

of viral and non-viral etiology [13–18]. In order to improve the pharmacokinetic and effector properties of nanoantibodies, as well as to increase their avidity due to the dimerization of the molecule, modification with the Fc fragment of human IgG is used [13, 15, 17].

A single-domain antibody fused to the Fc fragment of human immunoglobulin class, which has a broad spectrum of viral neutralizing activity against SARS-CoV-2 virus and is component I of the GamCoviMab candidate drug for therapy of COVID-19 infection, was developed in the Gamaleya National Research Center for Epidemiology and Microbiology of the Ministry of Health of the Russian Federation. The development of scalable technology for cell culture and chromatographic purification of the target antibody was beneficial to the production of this drug. This article describes our results relating to the development of a strategy to select optimal parameters for culturing processes, in order to produce a single-domain antibody fused to the Fc fragment of human immunoglobulin G class. Data is also presented on *in vitro* scale-up in a 10 L wave-mixed bioreactor and scale-up at GMP production in a 200 L stirred-tank bioreactor.

MATERIALS AND METHODS

Materials

Culture of Chinese hamster ovary (CHO) cells GamP2C5 (clone 78) producing a single-domain antibody fused to Fc fragment of human IgG1 GamP2C5 was obtained in the laboratory of immuno-biotechnology of the Gamaleya National Research Center for Epidemiology and Microbiology on the basis of CHO-K1 cells (Collection of Cultures and Tissues of the Gamaleya National Research Center for Epidemiology and Microbiology).

Cultivation media: ActiPro™ (Cytiva, USA), Fujifilm BalanCD® CHO Growth A (Irvine Scientific, USA), Cosmos (Flora Bio, Turkey), SFM4CHO (Cytiva, USA), Dynamis™ AGT™ (Thermo Fisher Scientific, USA), Capricorn (Capricorn Scientific, Germany).

Supplements: Cell Boost 6 Supplement (Cytiva, USA), Cell Boost 5 Supplement (Cytiva, USA), Cell Boost 7 A (Cytiva, USA), Cell Boost 7 B (Cytiva, USA), Cosmos Flora Bio Feed A (Flora Bio, Turkey), Cosmos Flora Bio Feed B (Flora Bio, Turkey), Capricorn's CHO Feed 1 (Capricorn Scientific, Germany), Capricorn's CHO Feed 2 (Capricorn Scientific, Germany). Protein A (ProA) Biosensors (Forte Biosciences, USA).

Culture vessels: 250 mL Erlenmeyer flasks (Corning, USA), disposable mini bioreactors for Ambr® 250 Disposable bioreactors system (Sartorius,

Germany), disposable culture bags: Flexsafe® RM 20 opt (Sartorius, Germany), Flexsafe® STR 200 (Sartorius, Germany).

Equipment

TC20 Cell Counter (Bio-Rad, USA), Celltron shaker (Infors HT, Switzerland), Biostat® RM 20 basic wave-mixed bioreactor (Sartorius, Germany), Ambr® 250 mini bioreactor (Sartorius, Germany), STR 200 stirred-tank bioreactor (Sartorius, Germany), Cedex® Bio Analyzer (Roche, Switzerland), Seven Compact S210 pH meter (METTLER TOLEDO, USA), Octet® RED96e molecular interaction analyzer (Forte Biosciences, USA).

Methods

Cell density measurement

A 20 µL suspension culture of CHO cells was taken. The obtained cell suspension was mixed with trypan blue solution (an acidic aniline dye used for counting the number of dead cells in suspension, which, unlike live cells, are stained blue) in the ratio of 1 : 1. The total volume of the stained suspension should be at least 30 µL to fill two chambers of the slide. The stained suspension was transferred by pipetting. We took 10 µL of the stained suspension with an automatic pipette and, holding the pipette at a 45° angle, gently introduced

the suspension into each of the slide chambers. Slides completely filled with stained cells were transferred to an automated TC20 Cell Counter to measure cell density.

Measurement of antibody concentration

The amount of antibodies in the samples was determined by biolayer interferometry (BLI) using Octet® RED96e system (Forte Biosciences, USA) and biosensors with immobilized protein A (Forte Biosciences, USA), according to the manufacturer's protocol. GamP2C5 antibody solutions obtained earlier by stable transfection and purified by affinity chromatography on Mabselect SuRe™ sorbent (Cytiva, USA) as previously described [13, 15, 17] were used as standard samples with known concentrations.

Measurement of residual metabolites

Concentrations of major cultures (glucose, glutamine, and glutamate) and metabolites (lactate and ammonium) in the samples were determined using a Cedex® Bio Analyzer (Roche, Switzerland) according to the manufacturer's protocol.

Cell cultivation

The cells were cultured in Erlenmeyer flasks and in wave-mixed bioreactor and stirred-tank bioreactor. Culture media in combination with supplements were used to select optimal conditions (Table 1).

Table 1. Plan of experiment

Experiment number	Media	Supplement	Containers and equipment	Volume, L
1	SFM4CHO	Cell Boost 6	Erlenmeyer flasks	0.25
2	ActiPro™	Cell Boost 7A	Erlenmeyer flasks	0.25
			Biostat® RM 20 bioreactor	10
			Ambr® 250 mini bioreactor	0.20
			Bioreactor STR 200	200
3	BalanCD®	Cell Boost 7A	Erlenmeyer flasks	0.25
		Cell Boost 7B	Biostat® RM 20 bioreactor	10
4	Cosmos	Feed A	Erlenmeyer flasks	0.25
		Feed B	Biostat® RM 20 bioreactor	10
5	Capricorn	Feed 1	Erlenmeyer flasks	0.25
		Feed 2	Biostat® RM 20 bioreactor	
6	Dynamis™ AGT™	Cell Boost 7A	Erlenmeyer flasks	0.25
		Cell Boost 7B		

Cultivation of cells in Erlenmeyer flasks

Cell suspension culture of CHO GamP2C5 (clone 78) cells was performed in Erlenmeyer flasks with a ventilated lid of 250 mL. Initial volume of cell suspension was 30 mL. Initial concentration was 0.3 mL/mL. Starting from the third day of culturing, supplements were added in the amount recommended by the manufacturer. Cultivation was performed at 37°C, 80% humidity and 5% CO₂, with a platform stirring speed of 110–130 rpm at an amplitude of 25 mm. Glucose was maintained at 4.5–5.0 g/L. If necessary, pH was maintained at 6.9–7.4 using 7.5% sodium bicarbonate solution (*Labochem International*, Germany).

Cell cultivation in a Biostat[®] RM 20 wave bioreactor

The suspension was cultured in wave-mixed bioreactor with a working volume of up to 10 L (Table 2).

The initial working volumes were 25–30% of the final volume, with a minimum concentration of 0.3 mln/mL. On the third day of cultivation, the inoculum was diluted with fresh culture medium to 65–70% of the final volume. Starting on the fifth day of culturing, supplement was added at a concentration according to the manufacturer's instructions. Furthermore, pH 6.8–7.5 was adjusted by adding sodium bicarbonate (*Labochem International*, Germany) as needed. Glucose concentration was maintained at 4.5–5.0 g/L, so glucose solution (*Merck*, USA) was used if necessary. In order to obtain the maximum content of the target product, a change in the temperature parameter and pH at the time of stationary phase of cell cultivation was applied (Table 3).

Cell cultivation in Ambr[®] 250 mini bioreactors

The suspension was cultured in mini stirred-tank bioreactors with a working volume of up to 250 mL. The initial working volumes were 25–30% of the final volume,

Table 2. Parameters of the cultivation process in the Biostat[®] RM 20 wave-mixed bioreactor

Parameter	Value
Temperature	37.0 ± 1.0°C
Dissolved oxygen, %	No lower than 40
pH	6.8–7.5
CO ₂ concentration in the gas phase, %	5.0 ± 2.0
Platform tilt angle, °	6–10
Platform swing frequency, swing/min	14–30
Volumetric flow rate of gas mixture, L/min	0.2–0.8

Table 3. Parameters of the cultivation process depending on the experiment in the Biostat[®] RM 20 wave-mixed bioreactor

Parameter	Experiment 1	Experiment 2	Experiment 3
Temperature, °C	37.0	33.0	37.0
Dissolved oxygen, %	40	40	40
pH	7.2	7.2	6.8
CO ₂ concentration in the gas phase, %	5.0	5.0	5.0
Platform tilt angle, °	7	7	7
Platform swing frequency, swing/min	15	15	15
Volumetric flow rate of gas mixture, L/min	0.5	0.5	0.5

Table 4. Parameters of the cultivation process depending on the experiment in the Ambr[®] 250 mini bioreactor

Parameter	Experiment 1	Experiment 2	Experiment 3
Temperature, °C	37.0	33.0	37.0
Dissolved oxygen, %	40	40	40
pH	7.2	7.2	6.8
CO ₂ concentration in the gas phase, %	7.0	7.0	7.0
Stirrer, rpm	300–500	300–500	300–500
Air overlay, mLpm	4	4	4
Air sparger, mL/min	4	4	4
O ₂ sparger, mLpm	0–2	0–2	0–2

and the minimum concentration was 0.6 mln/mL. On the third day of cultivation, the inoculum was diluted with fresh culture medium to 65–70% of the final volume. Starting on the fifth day of culturing, supplement was added at a concentration according to the manufacturer's instructions. The pH 6.8–7.5 was maintained by adding sodium bicarbonate (*Labochem International*, Germany) as needed. Glucose concentration was maintained at 4.5–5.0 g/L, so glucose solution (*Merck*, USA) was used if necessary. In order to obtain the maximum content of the target protein, the temperature parameter and pH were varied during cultivation (Table 4).

Cell cultivation in the STR 200 stirred-tank bioreactor

The suspension was cultured in a stirred-tank bioreactor with a working volume of 200 L. The initial working volumes were 25–30% of the final volume, and the minimum concentration was 0.5 mln/mL. On the third

day of cultivation, the inoculum was diluted with fresh culture medium to 65–70% of the final volume. Starting on the fifth day of culturing, supplement was added at a concentration according to the manufacturer's instructions. The pH 6.8–7.5 was maintained by adding sodium bicarbonate (*Labochem International*, Germany) as needed. Glucose concentration was maintained at 4.5–5.0 g/L, so glucose solution (*Merck*, USA) was used if necessary. In order to obtain the maximum content of the target antibody, the temperature parameter was changed during cultivation (Table 5).

RESULTS AND DISCUSSION

A panel of single-domain antibodies specific to the receptor-binding domain (RBD) of the S-protein of SARS-CoV-2 virus was obtained at the immunobiotechnology laboratory of the Gamaleya National Research Center for Epidemiology and

Table 5. Parameters of the cultivation process in an STR 200 stirred-tank bioreactor

Parameter	Experiment 1
Temperature, °C	37.0–33.0
Dissolved oxygen, %	40
pH	7.2
CO ₂ concentration in the gas phase, %	5.0
Stirrer, rpm	60–110
Air overlay, Lpm	10
Air sparger, L/min	10
O ₂ sparger, Lpm	0–10

Microbiology by immunization of the two-humped camel with recombinant RBD of the S-protein of SARS-CoV-2 virus and phage display technology [19]. Several of the most promising clones were selected from the obtained panel and subsequently modified by fusion with the Fc fragment of human IgG1. These forms were further investigated in detail by various *in vitro* methods, including direct viral neutralization on live SARS-CoV-2 virus. As a result, a single-domain antibody fused to the Fc fragment of human IgG1 GamP2C5 was obtained (Fig. 1).

A genetic construct was then developed, in order to allow expression of this single-domain antibody fused to the Fc fragment of human IgG1. Today, most therapeutic antibodies are produced in mammalian cells. They are best suited for the production of recombinant antibodies with the highest degree of biological similarity to antibodies produced in the human body [20]. In this study, CHO cells were used. Further, a clone stably producing this antibody was selected using cell-to-cell transfection methods and several rounds of selection. As a result, the cell line CHO GamP2C5 (clone 78) was obtained, expressing a single-domain antibody fused to the Fc fragment of human IgG1 GamP2C5.

The most important component for the development of culturing technology is the culture medium which ensures cell viability and proliferation. The composition of the culture medium directly affects the production rate and quality of biopharmaceuticals. Therefore, it is important for researchers working with cell

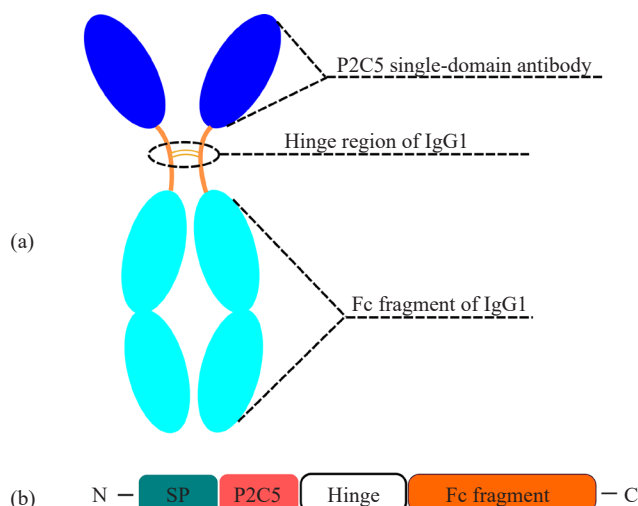


Fig. 1. (a) Schematic representation of a single-domain antibody fused with the Fc fragment of human IgG1 GamP2C5; (b) structure of a single-domain antibody fused with the Fc fragment of human IgG1 (SP—amino acid sequence of the signal peptide of the heavy chain of IgG1; P2C5—amino acid sequence of the P2C5 single-domain antibody; Hinge—amino acid sequence of the hinge region of IgG1; Fc fragment—amino acid sequence of the Fc fragment of IgG1)

cultures to select the right medium which is suitable for their purposes [21]. In order to select the optimal culture media based on availability and affordability, 6 basic culture media and 7 culture supplements were analyzed (Fig. 2).

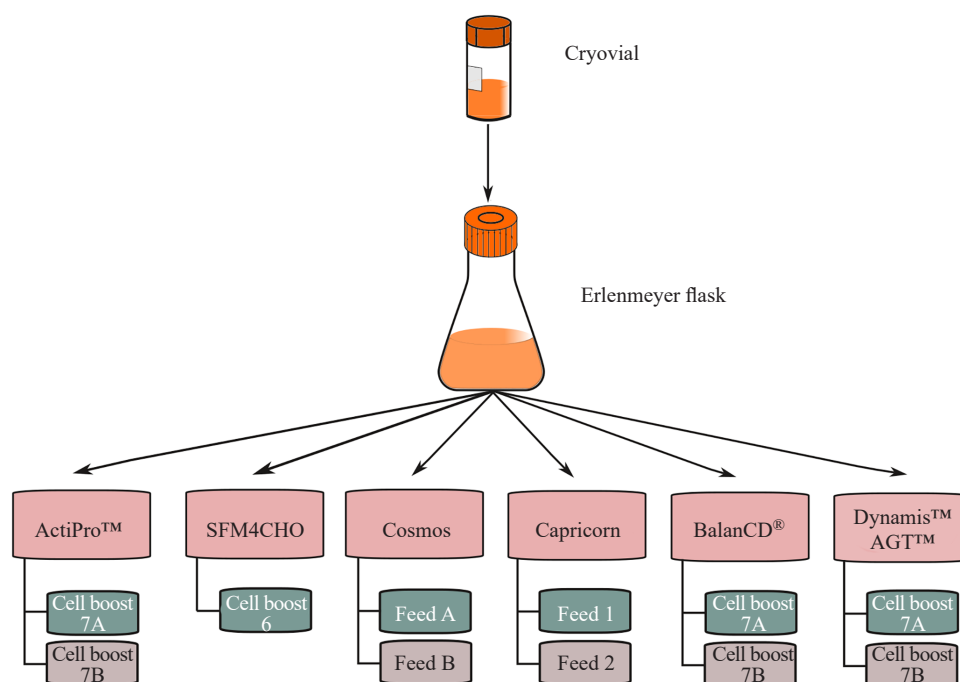


Fig. 2. Combination of culture media and supplement during the development of the cultivation process

Using these culture media and supplements, an experiment was conducted in three repetitions, aimed at developing a process for culturing the resulting clone in flasks to obtain the highest content of the target product. Cells were cultured with uniform initial parameters. The experiment was started at a cell density of 0.3 mln/mL. Cells were cultured in fed-batch mode, with glucose

and glutamine levels controlled. The survival ratios and cell culture densities at a particular day of culturing are shown in Fig. 3.

The leader in cell density was ActiPro™ medium. Cells on this medium reached a density of 10 mln/mL. Cosmos and BalanCD® media showed the best results in terms of the longest duration of cultivation. On both

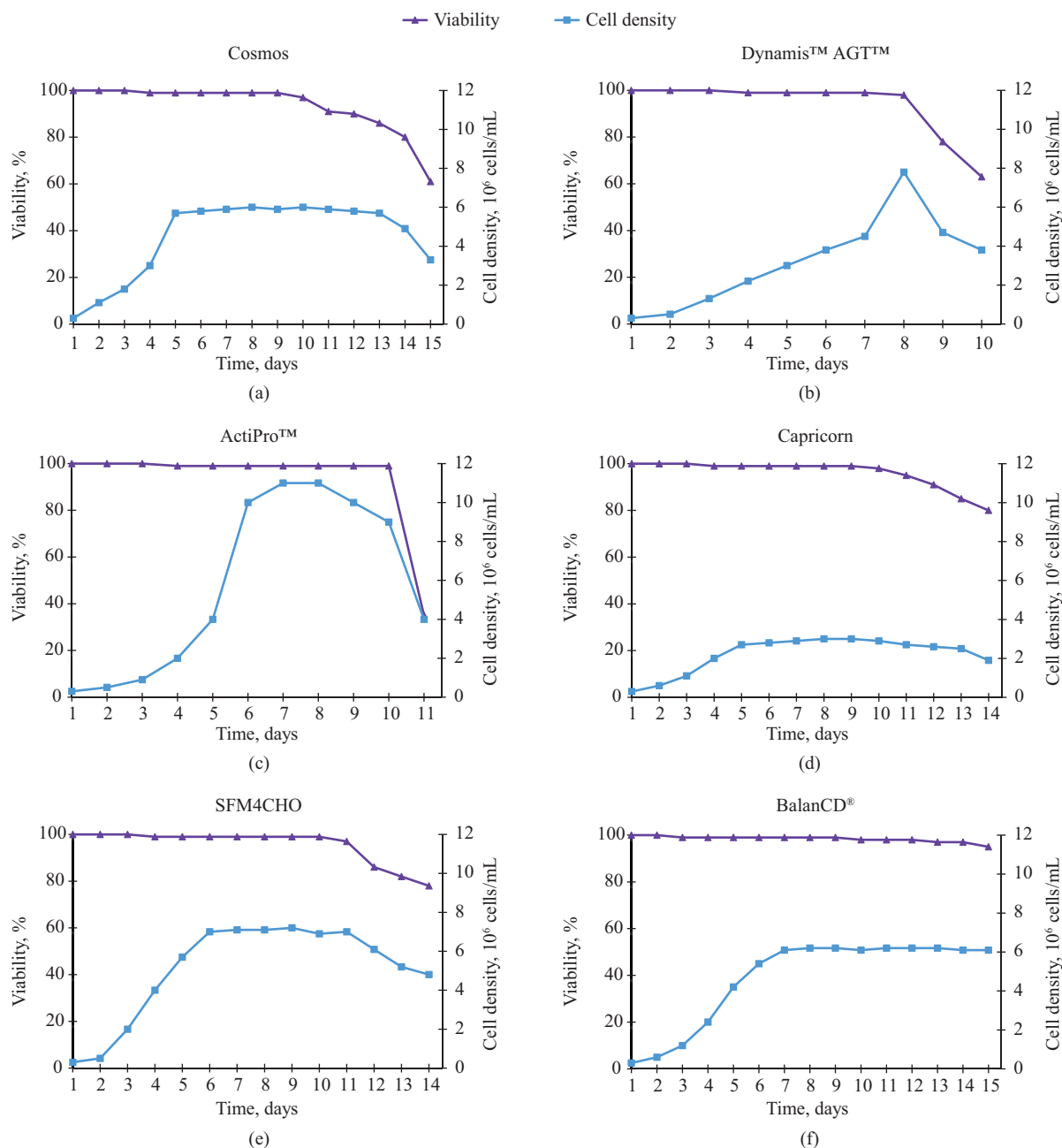


Fig. 3. The ratio of survival rate and cell culture density of CHO GamP2C5 (clone 78) in an Erlenmeyer flask when cultivated on various culture media:

- (a) Cosmos;
- (b) Dynamis™ AGT™;
- (c) ActiPro™;
- (d) Capricorn;
- (e) SFM4CHO;
- (f) BalanCD®

Table 6. Yield of the target antibody GamP2C5 determined using an Octet® RED96e system

Culture media	SFM4CHO	ActiPro™	Cosmos	BalanCD®	Dynamis™ AGT™	Capricorn
Product yield, µg/mL	364.8	671.0	478.0	580.0	284.0	220.0

media, the cell culture showed a high level of viability for 15 days. The highest content of target antibody was recorded on ActiPro™ culture medium. The content amounted to 671 µg/mL (Table 6).

Based on the growth graph of cell suspension on different culture media and based on the obtained values of final target protein content, three best culture media—ActiPro™, BalanCD®, Cosmos—were selected to develop further culturing process in wave bioreactors.

In order to study the cultivation process of the obtained clone, it was necessary to develop the cultivation process in wave bioreactors with selection of different conditions. For the purposes of this study, experiments were conducted with three best culture media. The experiments were conducted under identical conditions in a wave type stirred bioreactor with a working volume of 10 L (Fig. 4).

The initial cell density was 0.3 mln/mL. The ratio of survival and cell culture density on a particular day of cultivation is shown in Fig. 5.

In this experiment, ActiPro™ culture medium was the leader in terms of cell density, culturing time, and target protein content. Cells on this culture medium reached a density of 10 mln/mL. They were

cultured for 10 days, and the target protein content was 440 µg/mL. Comparison of GamP2C5 target antibody content depending on the culture medium is described in Table 7.

After analyzing three basic culture media, ActiPro™ medium was selected to show the maximum result in terms of target product productivity. Next, it was necessary to select the optimal cultivation conditions for further scaling of the process (Fig. 6).

In this experiment, different cultivation parameters were worked out in a wave bioreactor with a working volume of 10 L. In this part of the work, the productivity of the target protein was compared after changing the temperature parameter and pH during cultivation. The survival ratio and cell culture density on a particular day of cultivation are shown in Fig. 7.

When the temperature was lowered to 33°C, the culturing time increased, but the target protein content was lower than that at 37°C. Culturing the cells at pH 6.8 showed a lower result in target protein content compared to culturing at pH 7.2. When used on Biostat® RM 20 wave type stirred bioreactors, temperature and pH shifts did not show the expected result. The best productivity result was obtained after

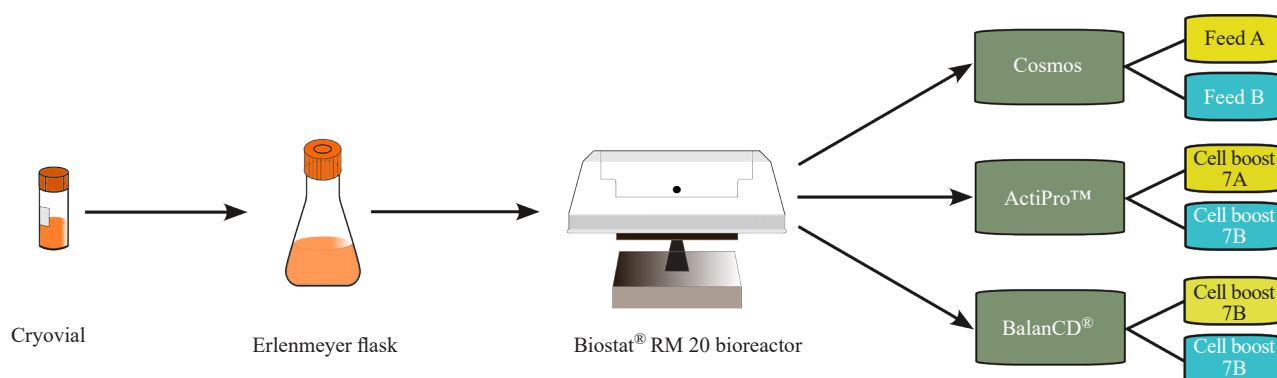


Fig. 4. Combinations of culture medium and supplement for the cultivation process in Biostat® RM 20 wave bioreactors

Table 7. Yield of the target antibody GamP2C5 determined using an Octet® RED96e system

Culture media	ActiPro™	Cosmos	BalanCD®
Product yield, µg/mL	440	250	325

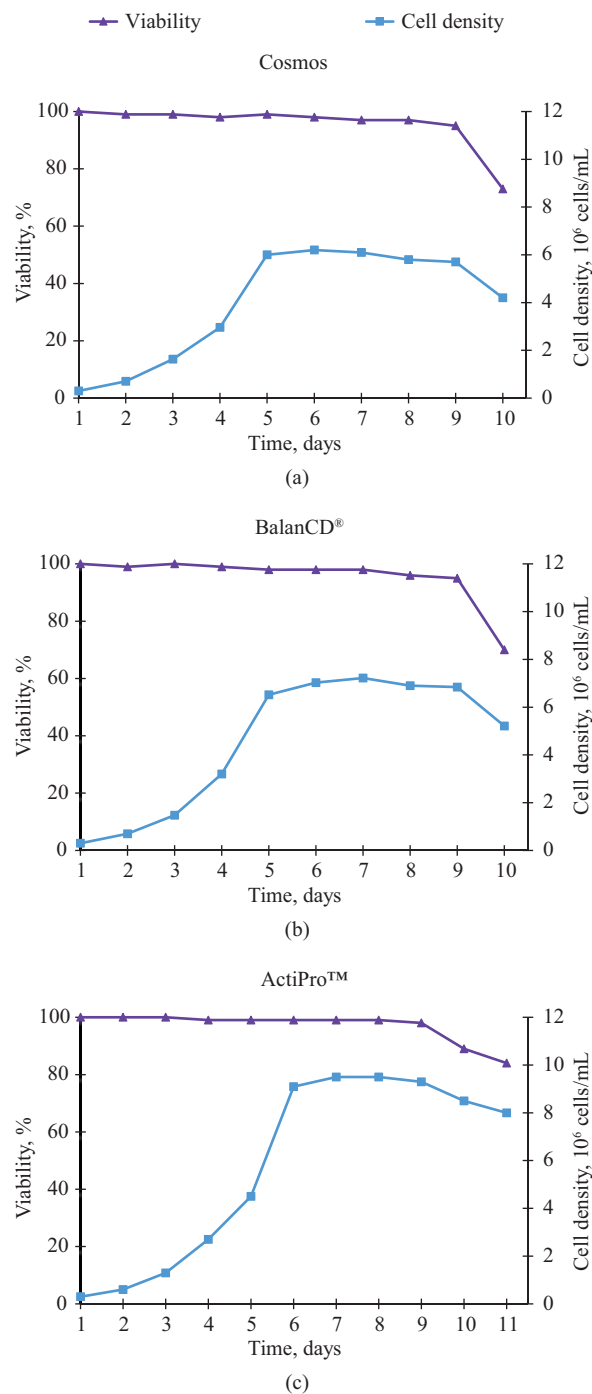


Fig. 5. The ratio of survival rate and cell culture density of CHO GamP2C5 (clone 78) in the Biostat[®] RM 20 wave bioreactor when cultivated on various culture media: (a) Cosmos; (b) BalanCD[®]; (c) ActiPro[™]

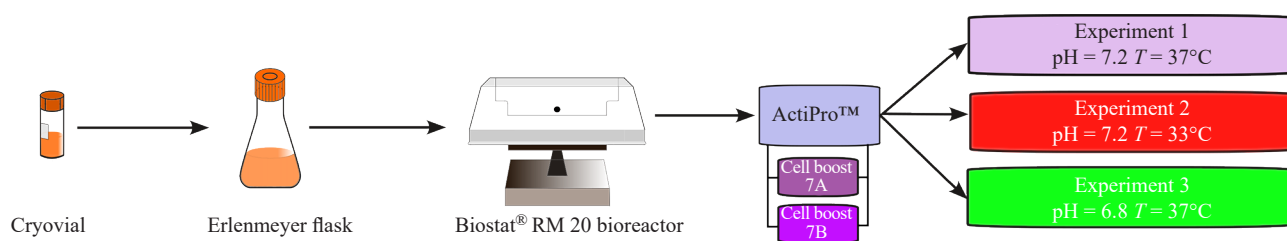


Fig. 6. Selection of optimal parameters for the cultivation process in RM 20 wave bioreactors

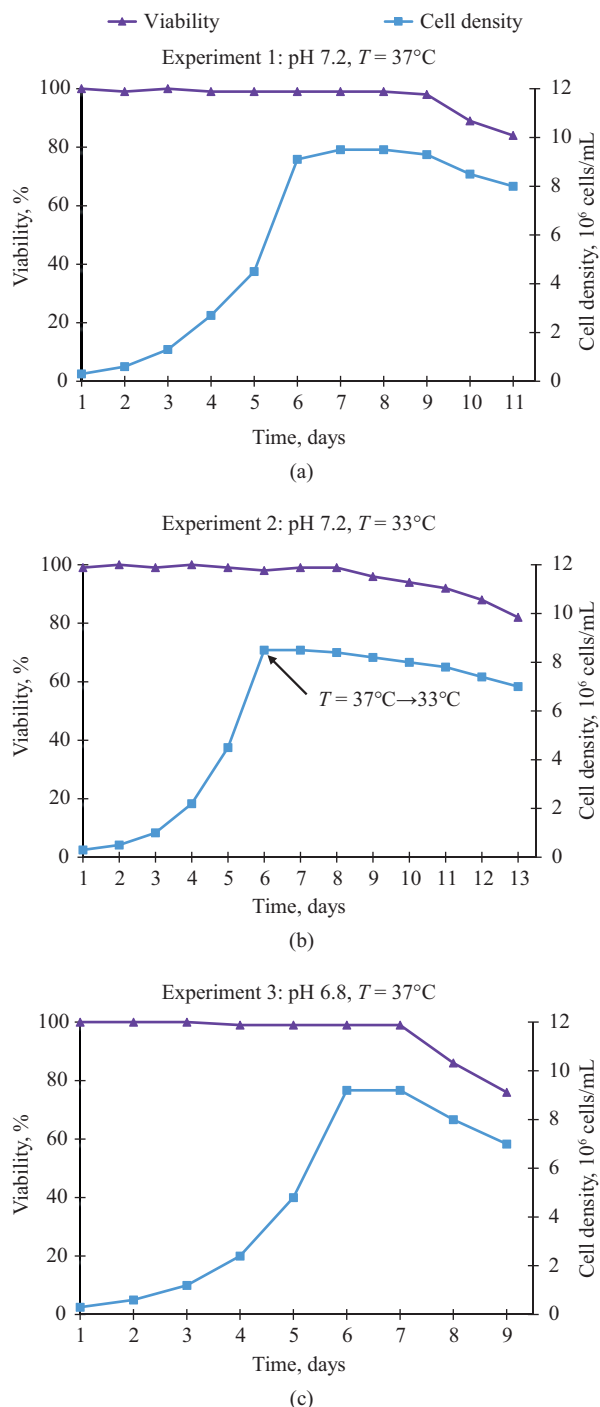


Fig. 7. Cultivation of CHO GamP2C5 (clone 78) cells under various cultivation conditions in Biostat[®] RM 20 wave bioreactor: (a) experiment 1: pH 7.2, $T = 37^\circ\text{C}$; (b) experiment 2: pH 7.2, $T = 33^\circ\text{C}$; (c) experiment 3: pH 6.8, $T = 37^\circ\text{C}$

culturing at 37°C and pH 7.2. The amount of the target antibody GamP2C5 is summarized in Table 8.

Thus, as a result of the work done at this stage, we have developed a process for culturing this clone in a laboratory-scale wave bioreactor (working volume of 10 L) with the cultivation regime indicated in Table 9.

After analyzing the process on ActiPro[™] medium with three different cultivation conditions, we selected the parameters that showed the maximum result in terms of target antibody production. Then we scaled up to a STR 200 stirred-tank bioreactor. For this process, the optimal conditions for cell cultivation had to be selected, while taking into account the change of

Table 8. Yield of the target antibody GamP2C5 determined using an Octet® RED96e system

Number of experiment	Experiment 1	Experiment 2	Experiment 3
Product yield, µg/mL	440	374	223

Table 9. Cultivation parameters for CHO cells on ActiPro™ medium in the Biostat® RM 20 wave bioreactor

Parameter	Value
Temperature, °C	37.0
Dissolved oxygen, %	40
pH	7.2
CO ₂ concentration in the gas phase, %	5.0
Platform tilt angle, °	7
Platform swing frequency, swing/min	15
Volumetric flow rate of gas mixture, L/min	0.5
Start adding supplements, day	5

stirring type. The Ambr® 250 mini bioreactor system was used for the experiments (Fig. 8).

For the processes in mini bioreactors, we used ActiPro™ culture medium in combination with supplements 7A and 7B. After the experiment in flasks, they showed the best result in terms of target antibody yield (671 µg/mL), and the highest cell density (10 mln/mL) was recorded on this medium. Furthermore, after testing the conditions on the Biostat® RM 20 bioreactor with wave-type stirring, the ActiPro™ culture medium also showed the best result in terms of target antibody content, which amounted to 440 µg/mL.

In experiments in Ambr® 250 mini bioreactors, the productivity of the target protein was compared after changing the temperature parameter and pH during

cultivation. The survival ratio and cell culture density on a certain day of cultivation are presented in Fig. 9.

In these experiments, it was found that when the temperature was lowered to 33°C, the culturing time and target protein content were longer than at 37°C. Culturing the cells at pH 6.8 showed a lower yield of target protein when compared to culturing at pH 7.2. The experiment with pH variation did not show the expected results as with the experiment in the Biostat® RM 20 wave type stirred bioreactor. However, the temperature variation in this experiment showed the best result in terms of target protein content. The amount of target antibody GamP2C5 is presented in Table 10.

Taking into account the results obtained from the experiments on Ambr® 250 mini bioreactors, process

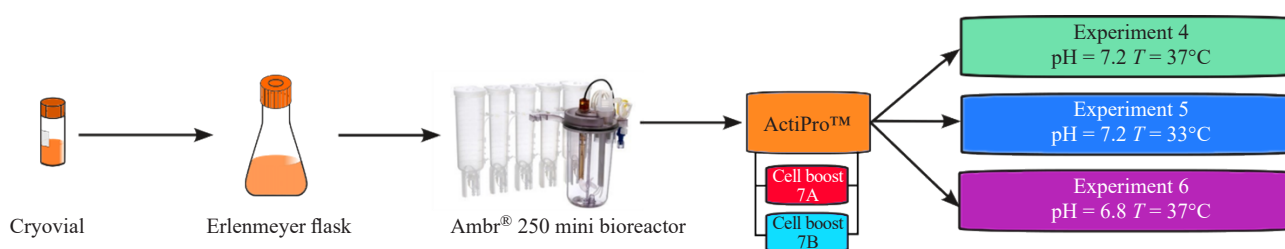


Fig. 8. Selection of optimal parameters for the cultivation process in Ambr® 250 mini bioreactors

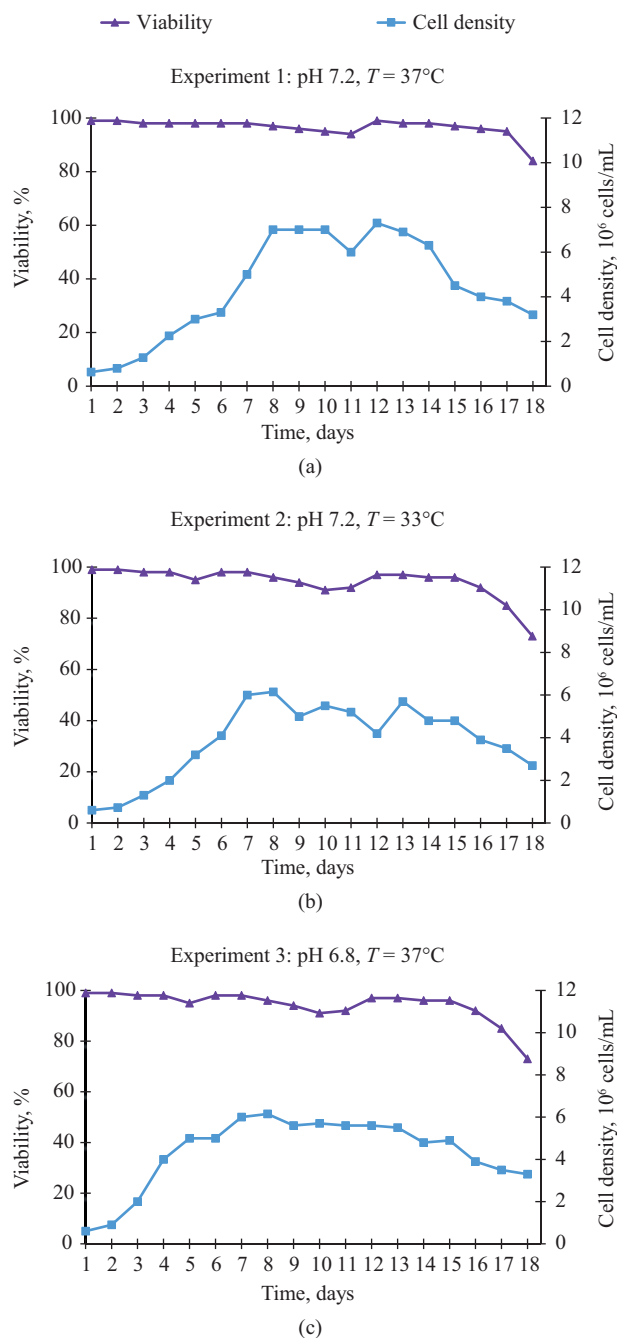


Fig. 9. Cultivation of CHO GamP2C5 (clone 78) cells under various cultivation conditions in Ambr[®] 250 mini bioreactors:
 (a) experiment 1: pH 7.2, T = 37°C;
 (b) experiment 2: pH 7.2, T = 33°C;
 (c) experiment 3: pH 6.8, T = 37°C

Table 10. Yield of the target antibody GamP2C5 determined using an Octet[®] RED96e system

Number of experiment	Experiment 4	Experiment 5	Experiment 6
Product yield, µg/mL	382	456	240

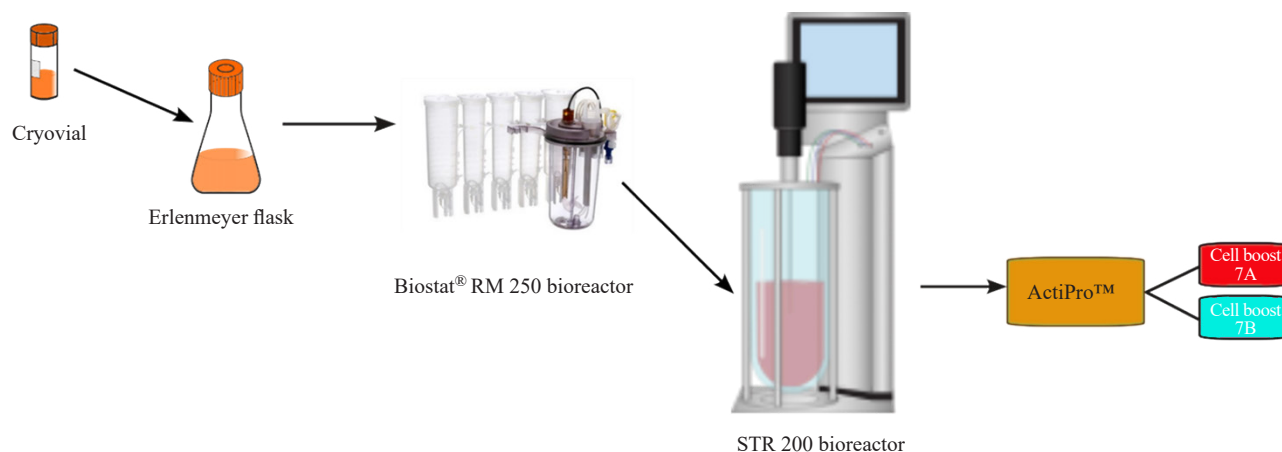


Fig. 10. Scaling diagram for the cultivation process to an STR 200 stirred-tank bioreactor with a working volume of 200 L

parameters were selected for the STR 200 stirred-tank bioreactor (Fig. 10).

After conducting a number of experiments using Ambr® 250 mini bioreactors on ActiPro™ culture medium in combination with supplements 7A and 7B, the conditions for optimal pH and temperature were selected. They showed the maximum result in terms of target antibody productivity. For the STR 200 stirred-tank bioreactor with a working volume of 200 L, the parameters obtained from the processes in the Ambr® 250 mini bioreactor were used. In order to scale the process parameters from Ambr® 250 mini bioreactors to STR 200 bioreactor, modeling was performed using Sartorius software¹. This performs the transfer of culturing process parameters from a small volume bioreactor to a larger one while maintaining mass transfer characteristics. In normal conditions, one of the dimensionless scaling factors used to scale up/down bioreactor processes is the volume flow rate (vvm , where v is the volume of air in liters, v is the volume of medium in liters, m is the time in minutes during which the exchange process (aeration) takes place) [22]. Taking this parameter into account, scaling was performed (data not presented). Furthermore, measurements on residual metabolites (glucose, glutamine, glutamate, lactate, and ammonium) were performed to ensure prolonged proliferation and block cell apoptosis during supplementation from the fifth day of culturing (Table 11).

The survival ratio and cell culture density on a particular day of cultivation are shown in Fig. 11.

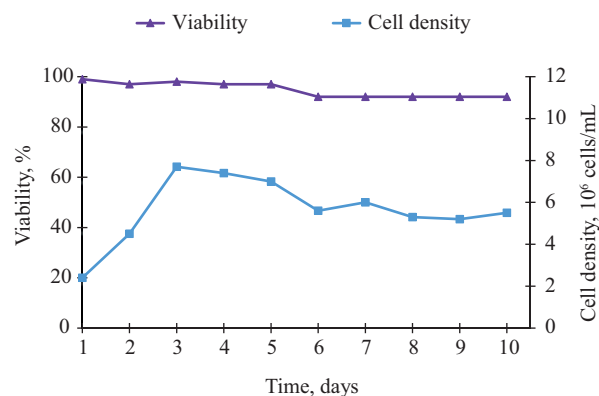


Fig. 11. Cultivation of CHO Gamp2C5 (clone 78) cells in ActiPro™ medium in an STR 200 stirred-tank bioreactor

After the process was carried out in the STR 200 stirred-tank bioreactor with cultivation modes selected using the Ambr® 250 mini bioreactor, the amount of the target antibody product Gamp2C5 amounted to 564.4 $\mu\text{g/mL}$. This value exceeds the initial value (456 $\mu\text{g/mL}$) obtained by culturing in the Ambr® 250 mini bioreactor.

CONCLUSIONS

Work was carried out to enable the selection of optimal parameters of the cultivation process for the production of component I of the GamCoviMab candidate drug. Component I of the GamCoviMab candidate drug is an antibody Gamp2C5 (CHO cell culture, clone 78). For this clone, the optimal culturing

¹ <https://www.sartogsm.ru/>. Accessed June 01, 2022.

Table 11. Data of residual metabolites according to the Cedex[®] Bio Analyzer device

Days	Glucose, mg/L	Glutamine, mM/L	Glutamate, mg/L	Lactate, mg/L	Ammonium, mM/L	Addition
5	2000.74	0.32	381.32	2345.45	7.920	1.0% 7A 0.1% 7B 1 g/L glucose
6	3343.45	0.15	598.39	1806.77	10.148	1.50% 7A 0.15% 7B 200 mM glutamine 2 g/L glucose
7	1721.22	0.48	972.53	2065.86	11.544	2.0% 7A 0.2% 7B 200 mM glutamine 3 g/L glucose
8	6158.21	1.23	1320.79	300.88	8.311	2.50% 7A 0.25% 7B
9	3891.29	0.59	1402.18	650.86	10.032	3.0% 7A 0.3% 7B
10	2191.10	0.52	1410.47	873.21	9.716	1.50% 7A 0.15% 7B
11	2272.02	0.11	584.63	727.05	3.759	2.0% 7A 0.2% 7B
12	323.82	0.21	609.07	257.12	3.258	2.50% 7A 0.25% 7B 4 g/L glucose
13	3783.16	0.21	1021.88	242.33	3.358	2 g/L glucose
14	4548.37	0.89	1101.30	323.79	8.285	–

process parameters were achieved in a stirred-tank bioreactor at pH 7.2 using temperature reduction from 37 to 33°C, with ActiPro[™] culture medium in combination with culture additives 7A and 7B, in which the CHO cell culture expressed the highest amount of the target antibody. This conclusion was based on a study of the culture conditions of CHO cells stably producing the GamP2C5 antibody (clone 78). The process of cultivation of this clone in a wave bioreactor with a working volume of 10 L is described. The optimal culture medium was selected, in order to give the maximum content of the target protein. Experiments were carried out to evaluate the effect of temperature variation during cultivation on the productivity of the target antibody. Furthermore, the pH of the culture medium was selected; something which also affects the cultivation of this clone. Then, for transfer to a production scale bioreactor (stirred-tank bioreactor), the optimal parameters were selected taking into account the change

of stirring type. The Ambr[®] 250 mini bioreactor system was used for this work, by means of which the optimal parameters in terms of temperature and pH were selected. Furthermore, the study revealed that the productivity indices for the CHO cell line stably producing the GamP2C5 antibody (clone 78) have different values in a wave-mixed and stirred-tank bioreactors. For this clone in a bioreactor with wave-type agitation (working volume 10 L), the best result in the yield of target antibody was demonstrated at $T = 37^\circ\text{C}$. When cultured in a stirred-tank bioreactor (Ambr[®] 250 mini bioreactor) the highest productivity was demonstrated at $T = 33^\circ\text{C}$. At the same time the content of target antibody in Ambr[®] 250 mini bioreactor at $T = 33^\circ\text{C}$ exceeds this index when compared with the bioreactor with wave type of agitation (working volume 10 L) at $T = 37^\circ\text{C}$. Cultivation was carried out in a stirred-tank bioreactor with a working volume of 200 L, after selecting the optimal cultivation parameters for the CHO cell line

stably producing the GamP2C5 antibody (clone 78). The parameters for this process were selected using data obtained from experiments in an Ambr[®] 250 mini bioreactor. Furthermore, supplements were added with metabolite assay/control, in order to ensure optimal culture conditions for CHO cells stably producing GamP2C5 antibody. Thus, in our study, we developed an efficient technology for culturing CHO cells stably producing GamP2C5 antibody as component I of the GamCoviMab candidate drug for emergency prevention and therapy of infection caused by SARS-CoV-2 virus.

Authors' contributions

D.S. Polyansky—conducting the experiments of cultivating CHO cells in an Ambr[®] 250 mini bioreactor, conducting the experiments of scaling the cultivation process, data collection and analysis, and writing the text of the manuscript.

E.I. Ryabova—development of CHO cell line, stably producing GamP2C5 modified single-domain antibody, conducting the

experiments of the selection of culture media in Erlenmeyer's flasks, and data collection and analysis.

A.A. Derkaev—conducting the experiments of the selection of cultural media in Erlenmeyer's flasks, measuring the concentration of the product in the culture media, and data collection and analysis.

N.S. Starkov—scaling the cultivation process in an STR 200 stirred-tank bioreactor and preparation of materials for the manuscript.

I.S. Kashapova—conducting the experiments on cultivation in Biostat[®] RM 20 wave bioreactors.

D.V. Shcheblyakov—design of a genetic construct expressing a modified single-domain antibody.

A.P. Karpov—managing the experiments on scaling the cultivation process; correcting the manuscript text, and approval of the final version of the manuscript for publication.

I.B. Esmagambetov—general management, correcting the manuscript text, and approval of the final version of the manuscript for publication.

The authors declare no conflicts of interest.

REFERENCES

1. Sun J., Yang .D., Xie X., Li L., Zeng H.Z., Gong B., Xu J.Q., Wu J.H., Qu B.B., Song G.W. Clinical application of SARS-CoV-2 antibody detection and monoclonal antibody therapies against COVID-19. *World J. Clin. Cases.* 2023;11(10): 2168–2180. <https://doi.org/10.12998/wjcc.v11.i10.2168>
2. Mitra S., Tomar P.S. Hybridoma technology; advancements, clinical significance, and future aspects. *J. Genet. Eng. Biotechnol.* 2021;19(1):159. <https://doi.org/10.1186/s43141-021-00264-6>
3. Lu R.M., Hwang Y.C., Liu I.J., Lee C.C., Tsai H.Z., LiH.J., Wu H.C. Development of therapeutic antibodies for the treatment of diseases. *J. Biomed. Sci.* 2020;27(1):1. <https://doi.org/10.1186/s12929-019-0592-z>
4. Quinteros D.A., Bermúdez J.M., Ravetti S., Cid A., Allemandi D.A., Palma S.D. Therapeutic use of monoclonal antibodies: general aspects and challenges for drug delivery. Chapter 25. In: *Nanostructures for Drug Delivery. Micro and Nano Technologies.* 2017:807–833. <https://doi.org/10.1016/B978-0-323-46143-6.00025-7>
5. Garcia J., Hurwitz H.I., Sandler A.B., Miles D., Coleman R.L., Deurloo R., Chinot O.L. Bevacizumab (Avastin[®]) in cancer treatment: a review of 15 years of clinical experience and future outlook. *Cancer Treat. Rev.* 2020;86:102017. <https://doi.org/10.1016/j.ctrv.2020.102017>
6. Chisari C.G., Sgarlata E., Arena S., Toscan S., Luca M., Patti F. Rituximab for the treatment of multiple sclerosis: a review. *J. Neurol.* 2022;269(1):159–183. <https://doi.org/10.1007/s00415-020-10362-z>
7. Hemperly A., Vande Castele N. Clinical Pharmacokinetics and Pharmacodynamics of Infliximab in the Treatment of Inflammatory Bowel Disease. *Clin. Pharmacokinet.* 2018;57(8):929–942. <https://doi.org/10.1007/s40262-017-0627-0>
8. Weinblatt M.E., Keystone E.C., Furst D.E., Kavanaugh A.F., Chartash E.K., Segurado O.G. Long term efficacy and safety of adalimumab plus methotrexate in patients with rheumatoid arthritis: ARMADA 4-year extended study. *Ann. Rheum. Dis.* 2006;65(6):753–759. <https://doi.org/10.1136/ard.2005.044404>
9. Salazar G., Zhang N., Fu T.M., An Z. Antibody therapies for the prevention and treatment of viral infections. *NPJ Vaccines.* 2017;2:19. <https://doi.org/10.1038/s41541-017-0019-3>
10. Pelegrin M., Naranjo-Gomez M., Piechaczyk M. Antiviral Monoclonal Antibodies: Can They Be More Than Simple Neutralizing Agents? *Trends Microbiol.* 2015;23(10): 653–665. <https://doi.org/10.1016/j.tim.2015.07.005>
11. Pantaleo G., Correia B., Fenwick C., Joo V.S., Perez L. Antibodies to combat viral infections: development strategies and progress. *Nat. Rev. Drug Discov.* 2022;21(9):676–696. <https://doi.org/10.1038/s41573-022-00495-3>
12. Miyazato Y., Yamamoto K., Nakaya Y., Morioka S., Takeuchi J.S., Takamatsu Y., Maeda K., Kimura M., Sugiura W., Mitsuya H., Yano M., Ohmagaria N. Successful use of casirivimab/imdevimab anti-spike monoclonal antibodies to enhance neutralizing antibodies in a woman on anti-CD20 treatment with refractory COVID-19. *J. Infect. Chemother.* 2022;28(7):991–994. <https://doi.org/10.1016/j.jiac.2022.03.002>
13. Jovčevska I., Muyldermans S. The Therapeutic Potential of Nanobodies. *BioDrugs.* 2019;34(1):11–26. <https://doi.org/10.1007/s40259-019-00392-z>
14. Esmagambetov I.B., Shcheblyakov D.V., Egorova D.A., Voronina O.L., Derkaev A.A., Voronina D.V., Popova O., Ryabova E.I., Shcherbinin D.N., Aksanova E.I., Semenov A.N., Kunda M.S., Ryzhova N.N., Zubkova O.V., Tukhvatulin A.I., Logunov D.Y., Naroditsky B.S., Borisevich S.V., Gintsburg A.L. Nanobodies Are Potential Therapeutic Agents for the Ebola Virus Infection. *Acta Naturae.* 2021;13(4):53–63. <https://doi.org/10.32607/actanaturae.11487>
15. Derkaev A.A., Ryabova E.I., Esmagambetov I.B., Shcheblyakov D.V., Godakova S.A., Vinogradova I.D., Noskov A.N., Logunov D.Y., Naroditsky B.S., Gintsburg A.L. rAAV expressing recombinant neutralizing antibody for the botulinum neurotoxin type A prophylaxis. *Front. Microbiol.* 2022;13:960937. <https://doi.org/10.3389/fmicb.2022.960937>

16. Voronina D.V., Shcheblyakov D.V., Favorskaya I.A., Esmagambetov I.B., Dzharullaeva A.S., Tukhvatulin A.I., Zubkova O.V., Popova O., Kan V.Y., Bandelyuk A.S., Shmarov M.M., Logunov D.Y., Naroditskiy B.S., Gintsburg A.L. Cross-Reactive Fc-Fused Single-Domain Antibodies to Hemagglutinin Stem Region Protect Mice from Group I Influenza a Virus Infection. *Viruses*. 2022;14(11):2485. <https://doi.org/10.3390/v14112485>
17. Panova E.A., Kleymenov D.A., Shcheblyakov D.V., Bykonia E.N., Mazunina E.P., Dzharullaeva A.S., Zolotar A.N., Derkaev A.A., Esmagambetov I.B., Sorokin I.I., Usachev E.V., Noskov A.N., Ivanov I.A., Zatsepin T.S., Dmitriev S.E., Gushchin V.A., Naroditskiy B.S., Logunov D.Y., Gintsburg A.L. Single-domain antibody delivery using an mRNA platform protects against lethal doses of botulinum neurotoxin A. *Front. Immunol.* 2023;14:1098302. <https://doi.org/10.3389/fimmu.2023.1098302>
18. Godakova S.A., Noskov A.N., Vinogradova I.D., Ugriumova G.A., Solovyev A.I., Esmagambetov I.B., Tukhvatulin A.I., Logunov D.Y., Naroditskiy B.S., Shcheblyakov D.V., Gintsburg A.L. Camelid VHHs Fused to Human Fc Fragments Provide Long Term Protection Against Botulinum Neurotoxin A in Mice. *Toxins (Basel)*. 2019;11(8):464. <https://doi.org/10.3390/toxins11080464>
19. Esmagambetov I.B., Ryabova E.I., Derkaev A.A., Shcheblyakov D.V., Dolzhikova I.V., Favorskaya I.A., Grousova D.M., Dovgiy M.A., Prokofiev V.V., Gosudarev A.I., Byrikhina D.V., Zorkov I.D., Iliukhina A.A., Kovyrshina A.V., Shelkov A.Y., Naroditskiy B.S., Logunov D.Y., Gintsburg A.L. rAAV expressing recombinant antibody for emergency prevention and long-term prophylaxis of COVID-19. *Front. Immunol.* 2023;14:1129245. <https://doi.org/10.3389/fimmu.2023.1129245>
20. Favorskaya I.A., Shcheblyakov D.V., Esmagambetov I.B., Dolzhikova I.V., Alekseeva I.A., Korobkova A.I., Voronina D.V., Ryabova E.I., Derkaev A.A., Kovyrshina A.V., *et al.* Single-Domain Antibodies Efficiently Neutralize SARS-CoV-2 Variants of Concern. *Front. Immunol.* 2022;13:822159. <https://doi.org/10.3389/fimmu.2022.822159>
21. Sedova E.S., Shcherbinin D.N., Bandelyuk A.S., Verkhovskaya L.V., Viskova N.Yu., Avdonina E.D., Prokofiev V.V., Ryabova E.I., Esmagambetov I.B., Pervoykina K.A., Bogacheva E.A., Lysenko A.A., Shmarov M.M. Method for obtaining recombinant antibodies produced by a cell line transduced with recombinant adenoviruses. *Tonk. Khim. Tekhnol. = Fine Chem. Technol.* 2023;18(1):48–64 (Russ., Eng.). <https://doi.org/10.32362/2410-6593-2023-18-1-48-64>
22. Yao T., Asayama Y. Animal-cell culture media: History, characteristics, and current issues. *Reprod. Med. Biol.* 2017;16(2):99–117. <https://doi.org/10.1002/rmb2.12024>
23. Xu P., Clark C., Ryder T., Sparks C., Zhou J., Wang M., Russell R., Scott C. Characterization of TAP Ambr 250 disposable bioreactors, as a reliable scale-down model for biologics process development. *Biotechnol. Prog.* 2017;33(2):478–489. <https://doi.org/10.1002/btpr.2417>

About the authors

Dmitry S. Polyansky, Technologist, Medgamal Branch, N.F. Gamaleya National Research Center for Epidemiology and Microbiology (The Gamaleya National Center), Ministry of Health of the Russian Federation (18, Gamaleya ul., Moscow, 123098, Russia); Assistant Professor, I.P. Alimarin Department of Analytical Chemistry, M.V. Lomonosov Institute of Fine Chemical Technologies, MIREA – Russian Technological University (86, Vernadskogo pr., Moscow, 119571, Russia). E-mail: polanskiydmityriy15@gmail.com. <https://orcid.org/0000-0003-0792-7063>

Ekaterina I. Ryabova, Junior Researcher, Laboratory of Immunobiotechnology, N.F. Gamaleya National Research Center for Epidemiology and Microbiology (The Gamaleya National Center), Ministry of Health of the Russian Federation (18, Gamaleya ul., Moscow, 123098, Russia); Postgraduate Student, K.I. Skryabin Moscow State Academy of Veterinary Medicine and Biotechnology – MVA (23, Akademika Skryabina ul., Moscow, 109472, Russia). E-mail: ryabovaei96@gmail.com. Scopus Author ID 57301278100, ResearcherID AAE-7335-2022, RSCI SPIN-code 6963-1376, <https://orcid.org/0000-0002-2687-5185>

Artem A. Derkaev, Junior Researcher, Laboratory of Immunobiotechnology, N.F. Gamaleya National Research Center for Epidemiology and Microbiology (The Gamaleya National Center), Ministry of Health of the Russian Federation (18, Gamaleya ul., Moscow, 123098, Russia). E-mail: derkaev.a@yandex.ru. Scopus Author ID 57381507000, ResearcherID AFU-7075-2022, SPIN-код РИНЦ 9339-9440, <https://orcid.org/0000-0003-3776-3856>

Nikita S. Starkov, Technologist, Medgamal Branch, N.F. Gamaleya National Research Center for Epidemiology and Microbiology (The Gamaleya National Center), Ministry of Health of the Russian Federation (18, Gamaleya ul., Moscow, 123098, Russia). E-mail: starkovns@medgamal.ru. <https://orcid.org/0009-0000-6493-5903>

Irina S. Kashapova, Researcher, Laboratory of Molecular Biotechnology, N.F. Gamaleya National Research Center for Epidemiology and Microbiology (The Gamaleya National Center), Ministry of Health of the Russian Federation (18, Gamaleya ul., Moscow, 123098, Russia). E-mail: kashapova@medgamal.com. SPIN-код РИНЦ 4860-3713, <https://orcid.org/0000-0002-5108-3841>

Dmitry V. Shcheblyakov, Cand. Sci. (Biol.), Leading Researcher, Head of the Laboratory of Immunobiotechnology, N.F. Gamaleya National Research Center for Epidemiology and Microbiology (The Gamaleya National Center), Ministry of Health of the Russian Federation (18, Gamaleya ul., Moscow, 123098, Russia). E-mail: sdmityrv@yahoo.com. Scopus Author ID 35073056900, ResearcherID E-5899-2014, SPIN-код РИНЦ 6357-2725, <https://orcid.org/0000-0002-1289-3411>

Andrey P. Karpov, Cand. Sci. (Biol.), Chief Technologist, Medgamal Branch, N.F. Gamaleya National Research Center for Epidemiology and Microbiology (The Gamaleya National Center), Ministry of Health of the Russian Federation (18, Gamaleya ul., Moscow, 123098, Russia). E-mail: ap.karpov@medgamal.ru. Scopus Author ID 22834845200

Ilias B. Esmagambetov, Cand. Sci. (Biol.), Leading Researcher, Head of the Laboratory of Stromal Regulation of Immunity, N.F. Gamaleya National Research Center for Epidemiology and Microbiology (The Gamaleya National Center), Ministry of Health of the Russian Federation (18, Gamaleya ul., Moscow, 123098, Russia). E-mail: iesmagambetov@yandex.ru. Scopus Author ID 56120429700, ResearcherID E-3327-2014, SPIN-код РИНЦ 8132-2320, <https://orcid.org/0000-0002-2063-2449>

Об авторах

Полянский Дмитрий Сергеевич, технолог, филиал «Медгамал», ФГБУ «Национальный исследовательский центр эпидемиологии и микробиологии имени почетного академика Н.Ф. Гамалеи» Министерства здравоохранения Российской Федерации (123098, Россия, Москва, ул. Гамалеи, д. 18); ассистент кафедры аналитической химии им. И.П. Алимарина, Институт тонких химических технологий им. М.В. Ломоносова, ФГБОУ ВО «МИРЭА – Российский технологический университет» (119571, Россия, Москва, пр-т Вернадского, д. 86). E-mail: polanskiydmityriy15@gmail.com. <https://orcid.org/0000-0003-0792-7063>

Рябова Екатерина Игоревна, младший научный сотрудник, лаборатория иммунобиотехнологии, ФГБУ «Национальный исследовательский центр эпидемиологии и микробиологии имени почетного академика Н.Ф. Гамалеи» Министерства здравоохранения Российской Федерации (123098, Россия, Москва, ул. Гамалеи, д. 18); аспирант, ФГБОУ ВО «Московская государственная академия ветеринарной медицины и биотехнологии – МВА имени К.И. Скрябина» (109472, Россия, Москва, ул. Академика Скрябина, д. 23). E-mail: ryabovaei96@gmail.com. Scopus Author ID 57301278100, ResearcherID AAE-7335-2022, SPIN-код РИНЦ 6963-1376, <https://orcid.org/0000-0002-2687-5185>

Деркаев Артем Алексеевич, младший научный сотрудник, лаборатория иммунобиотехнологии, ФГБУ «Национальный исследовательский центр эпидемиологии и микробиологии имени почетного академика Н.Ф. Гамалеи» Министерства здравоохранения Российской Федерации (123098, Россия, Москва, ул. Гамалеи, д. 18). E-mail: derkaev.a@yandex.ru. Scopus Author ID 57381507000, ResearcherID AFU-7075-2022, SPIN-код РИНЦ 9339-9440, <https://orcid.org/0000-0003-3776-3856>

Старков Никита Сергеевич, технолог, филиал «Медгамал», ФГБУ «Национальный исследовательский центр эпидемиологии и микробиологии имени почетного академика Н.Ф. Гамалеи» Министерства здравоохранения Российской Федерации (123098, Россия, Москва, ул. Гамалеи, д. 18). E-mail: starkovns@medgamal.ru. <https://orcid.org/0009-0000-6493-5903>

Кашапова Ирина Сергеевна, научный сотрудник, лаборатория клеточной микробиологии, ФГБУ «Национальный исследовательский центр эпидемиологии и микробиологии имени почетного академика Н.Ф. Гамалеи» Министерства здравоохранения Российской Федерации (123098, Россия, Москва, ул. Гамалеи, д. 18). E-mail: kashapova@medgamal.com. SPIN-код РИНЦ 4860-3713, <https://orcid.org/0000-0002-5108-3841>

Щебляков Дмитрий Викторович, к.б.н., ведущий научный сотрудник, заведующий лабораторией иммунобиотехнологии, ФГБУ «Национальный исследовательский центр эпидемиологии и микробиологии имени почетного академика Н.Ф. Гамалеи» Министерства здравоохранения Российской Федерации (123098, Россия, Москва, ул. Гамалеи, д. 18). E-mail: sdmitryv@yahoo.com. Scopus Author ID 35073056900, ResearcherID E-5899-2014, SPIN-код РИНЦ 6357-2725, <https://orcid.org/0000-0002-1289-3411>

Карпов Андрей Павлович, к.б.н., главный технолог, филиал «Медгамал», ФГБУ «Национальный исследовательский центр эпидемиологии и микробиологии имени почетного академика Н.Ф. Гамалеи» Министерства здравоохранения Российской Федерации (123098, Россия, Москва, ул. Гамалеи, д. 18). E-mail: ap.karpov@medgamal.ru. Scopus Author ID 22834845200

Есмагамбетов Ильяс Булатович, к.б.н., ведущий научный сотрудник, заведующий лабораторией стромальной регуляции иммунитета, ФГБУ «Национальный исследовательский центр эпидемиологии и микробиологии имени почетного академика Н.Ф. Гамалеи» Министерства здравоохранения Российской Федерации (123098, Россия, Москва, ул. Гамалеи, д. 18). E-mail: iesmagambetov@yandex.ru. Scopus Author ID 56120429700, ResearcherID E-3327-2014, SPIN-код РИНЦ 8132-2320, <https://orcid.org/0000-0002-2063-2449>

Translated from Russian into English by H. Moshkov

Edited for English language and spelling by Dr. David Mossop

Chemistry and technology of inorganic materials
Химия и технология неорганических материалов

UDC 54.061

<https://doi.org/10.32362/2410-6593-2024-19-3-258-266>

EDN KYWKWJ



Solid solutions in disulfide systems $\text{Re(IV)S}_2\text{-Ti(IV)S}_2$, $\text{Re(IV)S}_2\text{-Mo(IV)S}_2$, and $\text{Re(IV)S}_2\text{-W(IV)S}_2$

Ekaterina I. Efremova, Mikhail A. Lazov, Mikhail R. Kobrin✉, Valery V. Fomichev

MIREA — Russian Technological University (M.V. Lomonosov Institute of Fine Chemical Technologies), Moscow, 119571 Russia

✉ Corresponding author, e-mail: kobrin92@ya.ru

Abstract

Objectives. Chalcogenides of transition elements with low oxidation states, as well as their substituted derivatives, remain a poorly studied class of chemical compounds. Rhenium disulfide has many distinctive features and great application potential as a new two-dimensional semiconductor. This is due to its unusual structure and unique anisotropic properties. The presence of weak interlayer bonding and a unique distorted octahedral (1T) structure suggests the possibility of creating new phases on its basis. The aim of this work is to obtain and study phases in systems $\text{Re(IV)S}_2\text{-Ti(IV)S}_2$, $\text{Re(IV)S}_2\text{-Mo(IV)S}_2$, and $\text{Re(IV)S}_2\text{-W(IV)S}_2$.

Methods. The samples were obtained by high-temperature solid-phase ampoule synthesis in a vacuum. The study was carried out using X-ray phase analysis and X-ray photoelectron spectroscopy.

Results. The regions of existence of solid solutions, intercalates and two-phase regions in the resulting systems were established. Diffraction patterns were obtained for the new phases and the crystal lattice parameters were calculated. Based on data relating to the binding energies of core electrons with the nucleus, the study showed the valence states of the elements after synthesis. The study also confirmed that all phases obtained as a result of synthesis contain transition elements in the oxidation state (IV).

Conclusions. Intercalated solid solutions are formed in areas rich in rhenium, while in areas close to titanium and molybdenum disulfides, intercalated phases are attained. In the $\text{ReS}_2\text{-WS}_2$ system there is a region of solid solutions, including 30, 50, and 70 mol % rhenium disulfide. Their structure is a polymorphic modification of the structure of the original components. The presence of rhenium, molybdenum, and tungsten in these phases in the oxidation state (+IV) was confirmed. The data obtained on phase formation in dichalcogenide systems can be practically used in the creation of materials with unique electronic, magnetic, and optical properties with a wide range of applications.

Keywords

solid solutions, intercalates, transition metal disulfides, phase formation, crystal lattice, binding energies

Submitted: 07.11.2023

Revised: 08.12.2023

Accepted: 11.04.2024

For citation

Efremova E.I., Lazov M.A., Kobrin M.R., Fomichev V.V. Solid solutions in disulfide systems $\text{Re(IV)S}_2\text{-Ti(IV)S}_2$, $\text{Re(IV)S}_2\text{-Mo(IV)S}_2$, and $\text{Re(IV)S}_2\text{-W(IV)S}_2$. *Tonk. Khim. Tekhnol. = Fine Chem. Technol.* 2024;19(3):258–266. <https://doi.org/10.32362/2410-6593-2024-19-3-258-266>

НАУЧНАЯ СТАТЬЯ

Твердые растворы в системах дисульфидов Re(IV)S₂-Ti(IV)S₂, Re(IV)S₂-Mo(IV)S₂ и Re(IV)S₂-W(IV)S₂

Е.И. Ефремова, М.А. Лазов, М.Р. Кобрин✉, В.В. Фомичев

МИРЭА — Российский технологический университет (Институт тонких химических технологий
им. М.В. Ломоносова), Москва, 119571 Россия

✉ Автор для переписки, e-mail: kobrin92@ya.ru

Аннотация

Цели. Халькогениды переходных элементов с низкой степенью окисления, а также их замещенные производные до сих пор являются малоизученным классом химических соединений. В качестве нового двумерного полупроводника дисульфид рения имеет множество отличительных особенностей и обладает большим потенциалом для применения благодаря своей необычной структуре и уникальным анизотропным свойствам, а наличие у данного соединения слабой межслойной связи и уникальной искаженной октаэдрической (1T) структуры позволяет предположить возможность создания новых фаз на его основе. Цель данной работы — получение и исследование фаз в системах Re(IV)S₂-Ti(IV)S₂, Re(IV)S₂-Mo(IV)S₂ и Re(IV)S₂-W(IV)S₂.

Методы. Образцы были получены методом высокотемпературного твердофазного ампульного синтеза в вакууме. Исследование проводили методами рентгенофазового анализа и рентгеновской фотоэлектронной спектроскопии.

Результаты. Установлены области существования твердых растворов, интеркалатов и двухфазных областей в полученных системах. Для новых фаз получены дифрактограммы и рассчитаны параметры кристаллической решетки. По данным энергий связи основных электронов с ядром показано, в каких валентных состояниях находятся элементы после синтеза, подтверждено, что все полученные в результате синтеза фазы содержат переходные элементы в степени окисления (IV).

Выводы. В богатых рением областях образуются твердые растворы по типу внедрения, в то время как в областях, близких к дисульфидам титана и молибдена, реализуются интеркалированные фазы. В системе ReS₂-WS₂ существует область твердых растворов, включающая 30, 50 и 70 мол. % дисульфида рения, структура которых является полиморфной модификацией структуры исходных компонентов. Подтверждено присутствие рения, молибдена и вольфрама в этих фазах в степени окисления (+IV). Полученные данные о фазообразовании в системах дихалькогенидов могут быть практически использованы при создании материалов, обладающих уникальными электронными, магнитными и оптическими свойствами с обширной областью применения.

Ключевые слова

твердые растворы, интеркалаты, дисульфиды переходных металлов, фазообразование, кристаллическая решетка, энергии связи

Поступила: 07.11.2023

Доработана: 08.12.2023

Принята в печать: 11.04.2024

Для цитирования

Ефремова Е.И., Лазов М.А., Кобрин М.Р., Фомичев В.В. Твердые растворы в системах дисульфидов Re(IV)S₂-Ti(IV)S₂, Re(IV)S₂-Mo(IV)S₂ и Re(IV)S₂-W(IV)S₂. *Тонкие химические технологии*. 2024;19(3):258–266. <https://doi.org/10.32362/2410-6593-2024-19-3-258-266>

INTRODUCTION

Layered transition metal dichalcogenides are a relevant area of numerous scientific studies. This is due to the variety of physical and physicochemical properties of materials based on these compounds [1–3]. However, transition element chalcogenides with low oxidation degree, as well as their substituted derivatives, are still an understudied class of chemical compounds [4].

Transition element dichalcogenides are of interest due to their layered structure and a wide range of electrical properties from semiconducting in group 4 (d0) to metallic in group 5 (d1), then back to semiconducting in group 6 (d2). Here d0, d1, and d2 are the number of free valence electrons which remain after bond formation

in dichalcogenides [5]. Dichalcogenides can also act as superconductors [6]. Furthermore, dichalcogenides are known for their segmentoelectric, catalytic and optical properties, and also have a forbidden zone of tunable widths [7].

Solid solutions and doped compounds of transition metal disulfides are important objects of research in chemical technology (materials science). This is due to the variety of electronic, magnetic and optical properties for which they are used in electronics (second harmonic generators, field-effect transistors), catalysis and in power engineering (solar cells) [2]. The combination of different properties (e.g., semiconductor and dielectric properties) can lead

to interesting results and promising applications of the materials [9, 10]. Transition metals and their sulfides can be used as additives designed to improve the properties of the original layered materials. For example, rhenium sulfide is used as an additive to a photocatalyst for hydrogen evolution, or to cadmium sulfide, in order to increase the speed of this process. In the future this will allow us to completely move away from catalysts based on noble metals [11–13].

Rhenium disulfide (ReS₂) forms two-dimensional (2D) layered crystals [14]. As a novel 2D semiconductor, rhenium disulfide has many distinctive features. It also has great potential for applications due to its unusual structure and unique anisotropic properties [15]. Due also to its crystal structure, rhenium disulfide has many distinctive characteristics when compared with titanium, molybdenum and tungsten dichalcogenides: it has weak interlayer bonding and a unique distorted octahedral structure (structure type 1T). Due to such distinctive characteristics, bulk and monolayer ReS₂ have almost identical zone structures, and both of them belong to direct-gap semiconductors [16, 17]¹.

Combination of the properties of 4th and 6th groups of disulfides (titanium, molybdenum, tungsten) with the properties of rhenium disulfide in a single structured phase of the host-guest type, can be assumed to result in a change in their properties.

The aim of the present work is the synthesis of new phases: solid solutions in the Re(IV)S₂-Ti(IV)S₂, Re(IV)S₂-Mo(IV)S₂, and Re(IV)S₂-W(IV)S₂ systems.

MATERIALS AND METHODS

The following initial substances were used in the work: rhenium—metal powder with the content of the main component not less than 99.9% of rhenium (GOST 25278.16-87²), titanium—metal powder, chemically pure (Company Standard Technical Specification KOMP 3-272-10), tungsten—metal powder, chemically pure (Company Standard Technical Specification KOMP 3-684-13), elemental sulfur, especially pure (*Component-Reactive*, Russia, TU 3-304-10), and molybdenum disulfide (*Spets Metal Master*, Russia, TU 48-19-133-90). Other dichalcogenides were obtained by direct interaction of powders of corresponding metals (titanium, tungsten, and rhenium) and elemental sulfur.

The synthesis of rhenium disulfide was carried out by the method described above [4]. The suspensions of metallic rhenium and elemental sulfur were placed in a quartz ampoule, vacuumized (pressure 10⁻⁵ atm), sealed, and placed in a muffle furnace. Synthesis was carried out in the following mode. Over a period of 5 h the ampoule with the reaction mixture was gradually heated to a temperature of 1000°C and kept at this temperature for 20 h. Then the ampoule with the sample was cooled in the furnace for a day. The yield of the product by sulfur is stoichiometric. Titanium and tungsten disulfides were prepared by a similar method.

The synthesis of samples in the double disulfide systems Re(IV)S₂-Ti(IV)S₂, Re(IV)S₂-Mo(IV)S₂, and Re(IV)S₂-W(IV)S₂ was carried out in the following way. The disulfides were mixed in stoichiometric amounts. Then the resulting charge was homogenized in a ball mill for 30 min and then sealed in a vacuum-quartz ampoule. The synthesis was carried out in a muffle furnace and heated to 1100°C for 10 h. It was then kept at this temperature for 48 h, and then spontaneously cooled. Samples of double sulfides were prepared with the ratio of the main component from 0 to 100%.

X-ray studies were performed on a XRD-6000 diffractometer (*Shimadzu*, Japan) (Cu-K_α radiation, 2θ = 10°–60°, imaging step 0.2 deg/min, exposure 10 s). A ICDD-JCPDS³ card index was used to identify the phases (rhenium disulfide (card 89-0341), trigonal crystal lattice; titanium disulfide (card 15-853), hexagonal crystal lattice; molybdenum disulfide (card 17-744), hexagonal crystal lattice; tungsten disulfide (card 8-237), hexagonal crystal lattice).

Studies of the electronic structure and composition by X-ray photoelectron spectroscopy were carried out on a Kratos AXIS Ultra DLD electron spectrometer (*Kratos Analytical*, United Kingdom) with a monochromatized X-ray source Al K_α (*hν* = 1486.6 eV, energy resolution 0.5 eV).

RESULTS AND DISCUSSION

Phase formation in the ReS₂-TiS₂ system

Diffractograms of some samples of the system in the titanium-rich region are shown in Fig. 1. The calculated unit cell parameters of these phases are presented in Table 1. It should be noted that the nature of the X-ray

¹ BE Lookup Table for Signals from Elements and Common Chemical Species. URL: https://xpslibrary.com/wp-content/uploads/2019/07/BE_Lookup_table.pdf. Accessed October 18, 2022.

² GOST 25278.16-87. State Standard of the USSR. Alloys and foundry alloys of rare metals. Methods for determination of rhenium. Moscow: Izdatel'stvo standartov; 1998.

³ International Center for Diffraction Data (former name—Joint Committee on Powder Diffraction Standards). <https://www.icdd.com/>. Accessed December 28, 2023.

diffraction patterns of the initial components, namely the insufficient number of reflexes (for example, the number of reflexes is four for rhenium disulfide according to the ICDD-JCPDS card catalog), may lead to an error in the calculation of lattice parameters of solid solutions. However, this does not affect the determination of phase formation of the synthesized samples. The results of X-ray phase analysis established the invariability of lattice parameters in this region of rhenium disulfide concentrations, allowing us to speak about the formation of solid solutions of Re_xTi_(1-x)S₂ composition in the range $0 < x \leq 0.04$. With increasing Re content, the existence of a two-phase region with the presence of TiS₂ was noted.

Analysis of Fig. 2 shows that compositions with rhenium disulfide content of 50% have two phases, and with a content of 60% and more—one phase. Thus, solid solutions are established in a wide region rich in rhenium. It can also be seen that in compositions with rhenium content of 60% and 70%, the reflexes 34° and 57.7° are present. These belong to the rhenium disulfide phase which is consistent with the data obtained from the JCPDS database (card 89-0341). Calculation of lattice parameters was performed for the solid solutions obtained (Table 1). When analyzing the results, it should be borne in mind that the ionic radii of all transition elements in the oxidation degree (IV), considered in this work, are approximately equal and are ~0.6 Å [18]. In this case, the consistency of the lattice parameters may indicate the formation of solid substitution solutions based on both titanium disulfide and rhenium disulfide. At the same time, it can be assumed that the changes observed in the *c* parameter indicate the formation of intercalated compounds based on rhenium disulfide. This is natural if we assume that the layers in the structure

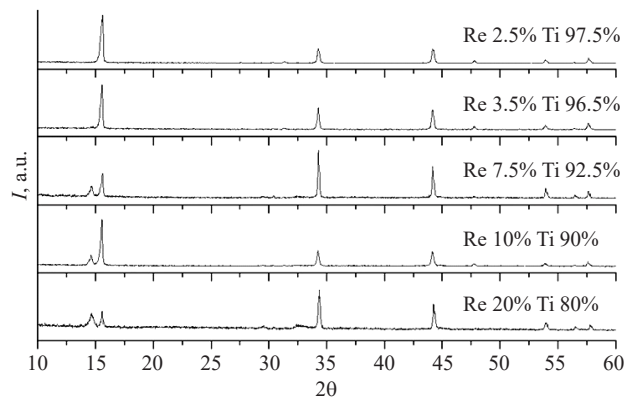


Fig. 1. Diffraction patterns of some samples of the system ReS₂-TiS₂, including solid solutions of composition substitution Re_{1-x}Ti_xS₂ (2.5 and 3.5% Re)

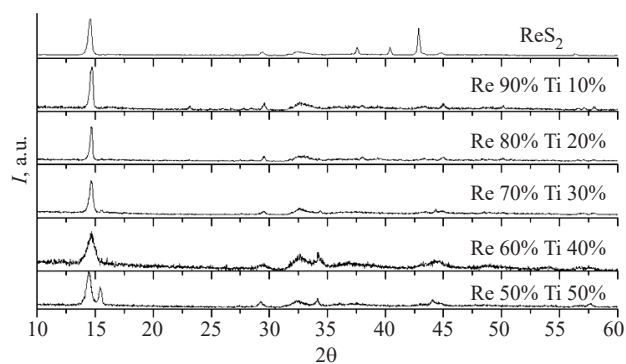


Fig. 2. Diffraction patterns of the original ReS₂ and solid solutions synthesized from it with the nominal composition Re_{1-x}Ti_xS₂

of rhenium disulfide are weakly connected and that the interlayer distance of rhenium disulfide is larger than that of titanium disulfide. Noticeable changes caused by the intercalation of rhenium in TiS₂ include the broadening

Table 1. Crystal lattice parameters and bond energies of some phases Re_xTi_(1-x)S₂

Composition	<i>a</i> , Å	<i>c</i> , Å	<i>V</i> , Å ³	Re bond energy, eV	Ti bond energy, eV
ReS ₂ , trigonal crystal lattice	6.35(5)	12.78(15)	434.49	41.00	—
ReS ₂ 95%	6.39(5)	12.23(15)	432.39	42.06	—
ReS ₂ 90%	6.41(5)	12.27(15)	436.21	—	—
ReS ₂ 80%	6.55(5)	12.76(15)	474.91	—	—
ReS ₂ 70%	6.41(5)	12.28(15)	437.66	—	—
ReS ₂ 3.5%	3.40(4)	5.69(6)	56.93	40.92	456.09
TiS ₂ , hexagonal crystal lattice	3.40(4)	5.69(6)	57.14	—	457.20

Note: *a* and *c* are lattice measurements, *V* is unit cell volume.

of the diffraction maxima (compared to the original ones) and a decrease in their relative intensity. This effect may be due to the appearance of microstresses in the host lattice or a decrease in the crystallite size.

X-ray photoelectron spectra were measured for titanium(IV) sulfide and samples of three compositions: Re_{0.035}Ti_{0.965}S₂, Re_{0.95}Ti_{0.05}S₂, and a sample from the two-phase region with rhenium(IV) sulfide content of 20% (Table 1). The Ti 2p line has an energy of 457.2 eV, corresponding to tetravalent titanium in the sulfides. In samples Re_{0.035}Ti_{0.965}S₂ and Re_{0.95}Ti_{0.05}S₂ both peaks of titanium were shifted. This suggests the formation of solid solutions in the considered systems. Other forms of rhenium in the samples were not observed.

Phase formation in the ReS₂-MoS₂ system

Figure 3 shows the diffractograms of samples of the rhenium disulfide-molybdenum disulfide system with a different ratio of components (from 20 to 90%). The results of calculation of crystal lattice parameters are presented in Table 2. The table shows that the parameters of samples with different sulfide content differ from those of pure metal disulfides.

Analysis of the X-ray diffraction patterns enables two regions of solid solutions to be defined: on the basis of ReS₂—up to 35 mol % MoS₂, and on the basis of MoS₂—up to 20 mol % ReS₂. In the concentration range from 20 to 65 mol % MoS₂ a two-phase region is observed in the system. The MoS₂ based solid solutions show a change in both lattice parameters as the rhenium content increases. This may indicate the formation of a solid solution introduction. On the rhenium disulfide side, there is a sharp change in the *a* and *V* parameters for the phase containing 20 mol % MoS₂. This may suggest the formation of a solid solution of introduction on the basis of rhenium disulfide. Given weak interaction between ReS₂ layers, the introduction of molybdenum

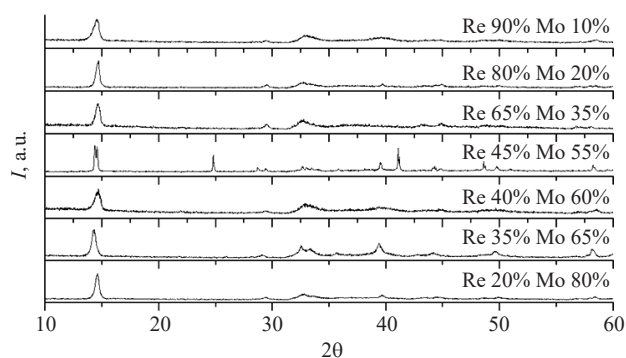


Fig. 3. Diffraction patterns of the ReS₂-MoS₂ system

into the layer structure will naturally affect mainly the *a* parameter, while the *c* parameter may remain unchanged.

Phase formation in the ReS₂-WS₂ system

According to the X-ray diffraction patterns of samples of ReS₂-WS₂ system (Fig. 4) and calculated parameters of crystal lattices (Table 3), a conclusion can be drawn about the formation of solid solutions in the region with the content of rhenium disulfide from 30 to 70%. Figure 4 shows that X-ray diffraction patterns of samples with rhenium disulfide content of 70, 50, and 30% are characterized by additional reflections. This may indicate polymorphism in this part of the double system. Since the presence of polymorphic modifications in this system is characteristic only for tungsten disulfide, it can be assumed that polymorphism refers to this sulfide [19] specifically. The decrease in the values of the crystal lattice parameters of solid solutions compared to those of rhenium disulfide can be related to the strengthening of interlayer interaction during the introduction of WS₂ into the layers and the alignment of their wavy structure.

Table 2. Crystal lattice parameters and bond energies of solid solutions formed in the ReS₂-MoS₂ system

ReS ₂ composition	<i>a</i> , Å	<i>c</i> , Å	<i>V</i> , Å ³	Re bond energy, eV	Mo bond energy, eV
MoS ₂ , hexagonal crystal lattice	3.161(18)	12.290(4)	106.43	–	229.50
ReS ₂ 20%	3.165(25)	12.254(87)	106.30	42.67	227.21
ReS ₂ 35%	3.173(46)	12.328(16)	107.50	41.15	226.31
ReS ₂ 80%	6.749(03)	12.727(5)	501.99	41.61	226.32
ReS ₂ , trigonal crystal lattice	6.352(52)	12.779(44)	434.49	41.00	–

X-ray photoelectron spectra of some synthesized samples of double systems (Tables 1–3, Fig. 5) show the presence of transition elements (titanium, molybdenum, tungsten, and rhenium) in oxidation degrees (IV). Pure disulfides of rhenium, molybdenum, tungsten, and titanium were used as reference compounds in analyzing the spectra. This concurs well with the literature date (see Footnote 1). Certain changes in the binding energy of the backbone electrons of these elements are due to the formation of solid solutions. This is natural, bearing in mind that in individual disulfides the metal-to-metal interatomic distances are small and comparable to the interatomic distances in metals.

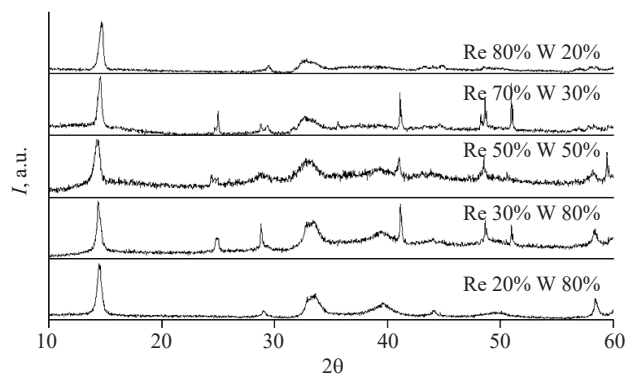


Fig. 4. Diffraction patterns of solid solutions in the ReS₂-WS₂ system

Table 3. Crystal lattice parameters and bond energies of solid solutions formed in the ReS₂-WS₂ system

ReS ₂ composition	<i>a</i> , Å	<i>c</i> , Å	<i>V</i> , Å ³	Re bond energy, eV	W bond energy, eV
WS ₂ , hexagonal crystal lattice	3.15(6)	12.31(54)	153.76	–	32.00
ReS ₂ 20%	3.29(7)	12.4(87)	169.05	42.11	33.88
ReS ₂ 30%	5.75(62)	12.45(33)	519.29	41.27	32.97
ReS ₂ 70%	5.39(7)	12.64(56)	462.59	40.34	32.01
ReS ₂ 80%	5.71(98)	12.69(12)	521.08	42.62	34.67
ReS ₂ , trigonal crystal lattice	6.35(21)	12.78(65)	649.67	41.00	–

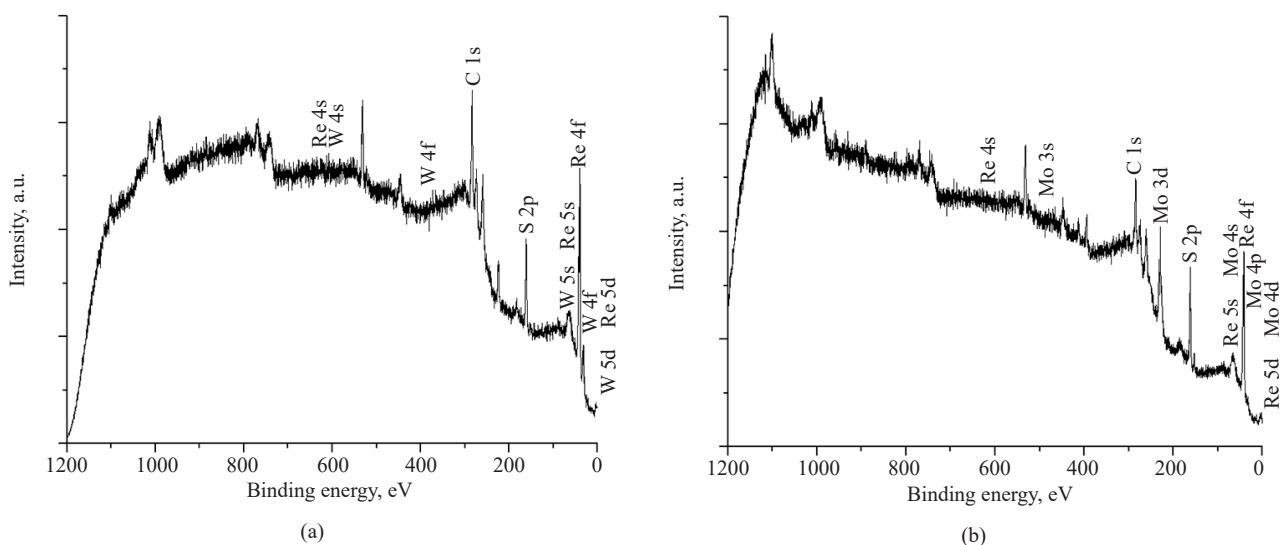


Fig. 5. Survey spectrum of the ReS₂ 35%–WS₂ 65% solid solution (a) and the ReS₂ 80%–MoS₂ 20% solid solution (b)

Analysis of the chemical state of atoms (rhenium, molybdenum, and sulfur) on the surface of solid solution sulfides Re_{0.8}Mo_{0.2}S₂ consisted in a detailed study of the spectra of the electronic levels of Re 4f, Mo 3d, and S 2p. This enabled us to quantitatively characterize the binding energies of the backbone electrons with the nucleus.

In the X-ray photoelectron spectrum of Re 4f spin-orbit splitting of the peak occurs, in all samples the element is characterized by the presence of two lines. This is consistent with the literature data (see Footnote 1). In samples containing molybdenum, the binding energies of both peaks shifted, possibly indicating the formation of solid solutions in the systems under consideration. Other forms of rhenium in the samples were not observed.

Molybdenum is present in the spectrum of solid solution with a rhenium content of 20% in two lines, and in three lines in the rest of the samples. This suggests the possible formation of the oxide form with Mo(IV) along with disulfide, as well as the presence of trace amounts of molybdenum in higher degrees of oxidation. The presence of these peaks prevents us from accurately determining the atomic ratio of elements in the samples obtained. Conclusions on energy redistribution were made only on the bonding energy. This corresponds to molybdenum in disulfide (Table 2). In the samples containing molybdenum and tungsten, the bond energies of both peaks shifted, possibly indicating the formation of solid solutions in the systems under consideration.

In all samples tungsten is represented by one line corresponding to the energy of the sulfide of the element with valence (IV). The samples show a change in the binding energy of the backbone electrons to the nucleus (Table 3), indicating redistribution of energy during the formation of solid solutions.

For the Re(IV)S₂-Ti(IV)S₂ system, the photoelectron spectra of three samples were investigated: intercalate of composition Re_{0.035}Ti_{0.965}S₂, solid solution of

composition Re_{0.95}Ti_{0.05}S₂ and two-phase region with the content of rhenium(IV) sulfide 20%. The change of bonding energy allows us to judge about its redistribution, i.e. about the formation of solid solutions and intercalate compounds.

For titanium, the samples with rhenium also show doublets, one peak of which corresponds to titanium sulfide with changed value of binding energy. The second peak, absent in the pure titanium sulfide sample, may correspond to a more oxidized form of titanium which bonds to rhenium in a particular way. This data needs to be investigated in more detail. Conclusions on the energy redistribution were drawn only from the binding energy, corresponding to titanium in the disulfide.

CONCLUSIONS

The paper presents the results of the study of phase formation in the systems Re(IV)S₂-Ti(IV)S₂, Re(IV)S₂-Mo(IV)S₂, and Re(IV)S₂-W(IV)S₂. X-ray phase and X-ray photoelectron spectroscopic study of the isolated phases were carried out. Areas of existence of solid solutions in the systems were established. It was shown that in rhenium-rich areas, solid solutions of the embedding type are formed, while in areas close to titanium and molybdenum disulfides intercalated phases are attained. In the ReS₂-WS₂ system, there is a region of solid solutions including 30, 50, and 70 mol % of rhenium disulfide. The structure represents a polymorphic modification of the structure of the initial components (structural type CdI₂). The presence of rhenium, molybdenum and tungsten in these phases in oxidation degree (IV) was also confirmed.

Authors' contribution

All authors equally contributed to the research work.

The authors declare no conflicts of interest.

REFERENCES

1. Zhang E., Jin Y., Yuan X., Wang W., Zhang C., Tang L., Liu S., Zhou P., Hu W., Xiu F. ReS₂-Based Field-Effect Transistors and Photodetectors. *Adv. Funct. Mater.* 2015;25(26): 4076–4082. <https://doi.org/10.1002/adfm.201500969>
2. Al-Dulaimi N., Lewis D.J., Zhong X.L., Malik M.A., O'Brien P. Chemical Vapour Deposition of Rhenium Disulfide and Rhenium-Doped Molybdenum Disulfide Thin Films Using Single-Source Precursors. *J. Mater. Chem.* 2016;4(12):2312–2318. <https://doi.org/10.1039/C6TC00489J>
3. Lemme M.C., Akinwande D., Huyghebaert C. 2D materials for future heterogeneous electronics. *Nat. Commun.* 2022;13(1):1392. <https://doi.org/10.1038/s41467-022-29001-4>
4. Ionov A.M., Kobrin M.R., Mozchil R.N., Sigov A.S., Syrov Yu.V., Fomichev V.V. Synthesis and study of rhenium(IV) disulphide. *Fine Chem. Technol.* 2017;12(6): 83–90 (in Russ.). <https://doi.org/10.32362/2410-6593-2017-12-6-83-90>
5. Dalmatova S.A., Fedorenko A.D., Mazalov L.N., Asanov I.P., Ledneva A.Y., Tarasenko M.S., Enyashin A.N., Zaikovskii V.I., Fedorov V.E. XPS experimental and DFT investigations on solid solutions of Mo_{1-x}Re_xS₂ (0 < x < 0.20). *Nanoscale.* 2018;10(21):10232–10240. <https://doi.org/10.1039/c8nr01661e>
6. Liu C.X. Unconventional Superconductivity in Bilayer Transition Metal Dichalcogenides. *Phys. Rev. Lett.* 2017;118(8):087001. <https://doi.org/10.1103/PhysRevLett.118.087001>

- Huang J., Li X., Jin X., Wang L., Deng Y. High-efficiency and stable photocatalytic hydrogen evolution of rhenium sulfide co-catalyst on Zn_{0.3}Cd_{0.7}S. *Mater. Adv.* 2020;1(3):363–370. <https://doi.org/10.1039/D0MA00187B>
- Chen R., Ma M., Luo Y., Qian L., Wan S., Xu S., She X. Fabrication of Ce-ReS₂ by Molten Salt for Electrochemical Hydrogen Evolution. *Trans. Tianjin University.* 2022;28(60):440–445. <http://doi.org/10.1007/s12209-022-00314-1>
- Ponomarenko V.P., Popov V.S., Popov S.V., Chepurinov E.L. Photo- and nanoelectronics based on two-dimensional 2D-materials (a review) (Part I. 2D-materials: properties and synthesis). *Uspekhi Prikladnoi Fiziki = Advances in Applied Physics.* 2019;7(1):10–48 (in Russ.).
- Azizar G.A.B., Hong J.W. Optimizing intrinsic cocatalyst activity and light absorption efficiency for efficient hydrogen evolution of 1D/2D ReS₂-CdS photocatalysts via control of ReS₂ nanosheet layer growth. *J. Mater. Sci. Technol.* 2023;168:103–113. <https://doi.org/10.1016/j.jmst.2023.05.035>
- Su N., Bai Y., Shi Z., Li J. ReS₂ Cocatalyst Improves the Hydrogen Production Performance of the CdS/ZnS Photocatalyst. *ACS Omega.* 2023;8(6):6059–6066. <https://doi.org/10.1021/acsomega.2c08110>
- Wang N., Li Y., Wang L., Yu X. Photocatalytic Applications of ReS₂-Based Heterostructures. *Molecules.* 2023;28(6):2627. <http://doi.org/10.3390/molecules28062627>
- Rahman M., Davey K., Qiao S. Advent of 2D Rhenium Disulfide (ReS₂): Fundamentals to Applications. *Adv. Functional Mater.* 2017;27(10). <https://doi.org/10.1002/adfm.201606129>
- Satheesh P.P., Jang H-S., Pandit B., Chandramohan S., Heo K. 2D Rhenium Dichalcogenides: From Fundamental Properties to Recent Advances in Photodetector Technology. *Adv. Functional Mater.* 2023;33(16). <https://doi.org/10.1002/adfm.202212167>
- Hart L., Dale S., Hoye S., Webb J.L., Wolverson D. Rhenium dichalcogenides: layered semiconductors with two vertical orientations. *Nano Lett.* 2016;16(2):1381–1386. <https://doi.org/10.1021/acs.nanolett.5b04838>
- Wolverson D., Hart L.S. Lattice dynamics of the rhenium and technetium dichalcogenides. *Nanoscale Res. Lett.* 2016;11(1):250. <https://doi.org/10.1186/s11671-016-1459-9>
- Wolverson D., Crampin S., Kazemi A.S., Ilie A., Bending S.J. Raman spectra of monolayer, few-layer, and bulk ReSe₂: an anisotropic layered semiconductor. *ACS Nano.* 2014;8(11):11154–11164. <https://doi.org/10.1021/nn5053926>
- Shannon R.D., Prewitt C.T. Revised values of effective ionic radii. *Acta Cryst.* 1970;B26(7):1046–1048. <https://doi.org/10.1107/S0567740870003576>
- Golub A.S., Zubavichus Ya.V., Slovokhotov Yu.L., Novikov Yu.N. Single-layer dispersions of transition metal dichalcogenides in the synthesis of intercalation compounds. *Russ. Chem. Rev.* 2003;72(2):123–141. <https://doi.org/10.1070/RC2003v072n02ABEH000789> [Original Russian Text: Golub A.S., Zubavichus Ya.V., Slovokhotov Yu.L., Novikov Yu.N. Single-layer dispersions of transition metal dichalcogenides in the synthesis of intercalation compounds. *Uspekhi khimii.* 2003;72(2):138–158 (in Russ.).]

About the authors

Ekaterina I. Efremova, Cand. Sci. (Chem.), Assistant Professor, A.N. Reformatskii Department of Inorganic Chemistry, M.V. Lomonosov Institute of Fine Chemical Technologies, MIREA – Russian Technological University (86, Vernadskogo pr., Moscow, 119571, Russia). E-mail: katifeefremova@yandex.ru. Scopus Author ID 56506855800, RSCI SPIN-code 8228-8730, <https://orcid.org/0009-0005-1088-7308>

Mikhail A. Lazov, Cand. Sci. (Chem.), Assistant Professor, I.P. Alimarin Department of Analytical Chemistry, M.V. Lomonosov Institute of Fine Chemical Technologies, MIREA – Russian Technological University (86, Vernadskogo pr., Moscow, 119571, Russia). E-mail: lazovm@gmail.com. Scopus Author ID 56466030700, RSCI SPIN-code 9661-9280, <https://orcid.org/0000-0001-8578-1683>

Mikhail R. Kobrin, Lecturer, A.N. Reformatskii Department of Inorganic Chemistry, M.V. Lomonosov Institute of Fine Chemical Technologies, MIREA – Russian Technological University (86, Vernadskogo pr., Moscow, 119571, Russia). E-mail: kobrin92@ya.ru. RSCI SPIN-code 9071-5240, <https://orcid.org/0000-0002-8744-3028>

Valery V. Fomichev, Dr. Sci. (Chem.), Professor, K.A. Bolshakov Department of Chemistry and Technology of Rare Elements, M.V. Lomonosov Institute of Fine Chemical Technologies, MIREA – Russian Technological University (86, Vernadskogo pr., Moscow, 119571, Russia). E-mail: valeryfom@rambler.ru. Scopus Author ID 57196028937, ResearcherID P-9883-2017, RSCI SPIN-code 8950-0895, <https://orcid.org/0000-0003-4840-0655>

Об авторах

Ефремова Екатерина Игоревна, к.х.н., доцент кафедры неорганической химии им. А.Н. Реформатского, Институт тонких химических технологий им. М.В. Ломоносова, ФГБОУ ВО «МИРЭА – Российский технологический университет» (119571, Россия, Москва, пр-т Вернадского, д. 86). E-mail: katifeefremova@yandex.ru. Scopus Author ID 56506855800, SPIN-код РИНЦ 8228-8730, <https://orcid.org/0009-0005-1088-7308>

Лазов Михаил Александрович, к.х.н., ассистент, кафедра аналитической химии им. И.П. Алимарина, Институт тонких химических технологий им. М.В. Ломоносова, ФГБОУ ВО «МИРЭА – Российский технологический университет» (119571, Россия, Москва, пр-т Вернадского, д. 86). E-mail: lazovm@gmail.com. Scopus Author ID 56466030700, SPIN-код РИНЦ 9661-9280, <https://orcid.org/0000-0001-8578-1683>

Кобрин Михаил Романович, преподаватель, кафедра неорганической химии им. А.Н. Реформатского, Институт тонких химических технологий им. М.В. Ломоносова, ФГБОУ ВО «МИРЭА – Российский технологический университет» (119571, Россия, Москва, пр-т Вернадского, д. 86). E-mail: kobrin92@ya.ru. SPIN-код РИНЦ 9071-5240, <https://orcid.org/0000-0002-8744-3028>

Фомичев Валерий Вячеславович, д.х.н., профессор кафедры химии и технологии редких элементов им. Большакова К.А., Институт тонких химических технологий им. М.В. Ломоносова, ФГБОУ ВО «МИРЭА – Российский технологический университет» (119571, Россия, Москва, пр-т Вернадского, д. 86). E-mail: valeryfom@rambler.ru. Scopus Author ID 57196028937, ResearcherID P-9883-2017, SPIN-код РИНЦ 8950-0895, <https://orcid.org/0000-0003-4840-0655>

Translated from Russian into English by H. Moshkov

Edited for English language and spelling by Dr. David Mossop

